



SIMILARITY LAWS FOR TRANSPIRED TURBULENT FLOWS SUBJECTED TO PRESSURE GRADIENTS, SEPARATION AND WALL HEAT TRANSFER

Mateus Carvalho Guimaraes

Dissertação de Mestrado apresentada ao Programa de Pós-graduação em Engenharia Mecânica, COPPE, da Universidade Federal do Rio de Janeiro, como parte dos requisitos necessários à obtenção do título de Mestre em Engenharia Mecânica.

Orientador: Daniel Onofre Almeida Cruz

Rio de Janeiro
Fevereiro de 2018

SIMILARITY LAWS FOR TRANSPIRED TURBULENT FLOWS SUBJECTED
TO PRESSURE GRADIENTS, SEPARATION AND WALL HEAT TRANSFER

Mateus Carvalho Guimaraes

DISSERTAÇÃO SUBMETIDA AO CORPO DOCENTE DO INSTITUTO
ALBERTO LUIZ COIMBRA DE PÓS-GRADUAÇÃO E PESQUISA DE
ENGENHARIA (COPPE) DA UNIVERSIDADE FEDERAL DO RIO DE
JANEIRO COMO PARTE DOS REQUISITOS NECESSÁRIOS PARA A
OBTENÇÃO DO GRAU DE MESTRE EM CIÊNCIAS EM ENGENHARIA
MECÂNICA.

Examinada por:

Prof. Daniel Onofre Almeida Cruz, D.Sc.

Prof. Atila Pantaleão Silva Freire, Ph.D.

Prof. Fabio Antonio Tavares Ramos, D.Sc.

Prof. Luca Roberto Augusto Moriconi, D.Sc.

RIO DE JANEIRO, RJ – BRASIL
FEVEREIRO DE 2018

Guimaraes, Mateus Carvalho

Similarity laws for transpired turbulent flows subjected to pressure gradients, separation and wall heat transfer/Mateus Carvalho Guimaraes. – Rio de Janeiro: UFRJ/COPPE, 2018.

IX, 249 p. 29,7cm.

Orientador: Daniel Onofre Almeida Cruz

Dissertação (mestrado) – UFRJ/COPPE/Programa de Engenharia Mecânica, 2018.

Referências Bibliográficas: p. 89 – 115.

1. Turbulence. 2. Flow separation. 3. Wall transpiration. 4. Wall heat transfer. I. Cruz, Daniel Onofre Almeida. II. Universidade Federal do Rio de Janeiro, COPPE, Programa de Engenharia Mecânica. III. Título.

*I would like to dedicate this work
to my brother Lao.*

Acknowledgments

I'm profoundly grateful to many people for their help in the preparation of this work. For his guidance and brilliant advises I thank Professor Daniel Cruz. The many discussions with Professor Atila Silva Freire and interesting suggestions from Professors Fabio Ramos, Carlos Da Silva, Luca Moriconi and Klaus Gersten are highly appreciated. I would like to thank, also, many professors for kindly providing me their experimental or DNS data as well as many of their publications. They are, in alphabetical ordering, Ayse Gungor, Doug McLean, George Mellor, Hiroyuki Abe, Jens Fransson, John Eaton, Juliana Loureiro, Klaus Gersten, Marco Ferro, Martin Oberlack, Martin Skote, Roney Thompson, Uzak Zhapbasbayev, Yvan Maciel and the U.S. Defense Technical Information Center (DTIC) Reference team. I would like to acknowledge Coordenação de Aperfeiçoamento de Pessoal de Nível Superior (CAPES) and Fundação de Amparo à Pesquisa do Estado do Rio de Janeiro (FAPERJ) for the financial support during the course of this work. Above all, I wish to thank my mom, Márcia, my brother, Lao, and all my friends and professors.

Resumo da Dissertação apresentada à COPPE/UFRJ como parte dos requisitos necessários para a obtenção do grau de Mestre em Ciências (M.Sc.)

LEIS DE SIMILARIDADE PARA ESCOAMENTOS TURBULENTOS
TRANSPIRADOS COM GRADIENTES DE PRESSÃO, SEPARAÇÃO E
TRANSFERÊNCIA DE CALOR NA PAREDE

Mateus Carvalho Guimaraes

Fevereiro/2018

Orientador: Daniel Onofre Almeida Cruz

Programa: Engenharia Mecânica

Novas leis de escala para escoamentos turbulentos transpirados com gradientes de pressão não nulos e transferência de calor na parede são propostas. A nova lei de parede é a primeira na literatura a considerar os efeitos combinados da transpiração e gradiente de pressão, incluindo o fenômeno da separação do escoamento. A questão da similaridade dos perfis de velocidade e temperatura média na região próxima a parede é estudada e encontra-se que perfis provenientes de escoamentos com diferentes taxas de transpiração são similares quando escalados por novas expressões para a velocidade e temperatura características do escoamento, respectivamente, deduzidas neste trabalho a partir de uma análise de ordens de grandeza da equação aproximada do movimento. O domínio de validade das leis de parede é estendido, para incluir a região externa da camada limite, utilizando o caráter intermitente do escoamento nesta região. A nova formulação é comparada com mais de 200 perfis de velocidade e temperatura média provenientes de diversas bases de dados de escoamentos turbulentos e também com diferentes modelos de turbulência disponíveis na literatura mostrando que, para a maioria dos perfis analisados, a teoria proposta se ajusta melhor aos dados.

Abstract of Dissertation presented to COPPE/UFRJ as a partial fulfillment of the requirements for the degree of Master of Science (M.Sc.)

SIMILARITY LAWS FOR TRANSPIRED TURBULENT FLOWS SUBJECTED TO PRESSURE GRADIENTS, SEPARATION AND WALL HEAT TRANSFER

Mateus Carvalho Guimaraes

February/2018

Advisor: Daniel Onofre Almeida Cruz

Department: Mechanical Engineering

New scaling laws for transpired turbulent flows with non-zero pressure gradients and wall heat transfer are derived. The new wall laws are the first presented in literature that consider flow transpiration and separation. It emerges from the proposed scaling that mean velocity and temperature profiles are self-similar with respect to the transpiration rate in the whole near wall region of the flow. The domains of validity of the wall laws are extended, to include the outer region of the boundary layer, using the intermittent character of the flow in that region. It is found that the *intermittency factor* used in the model is a universal function of the wall normal direction scaled by the boundary layer thickness. The new theory is compared to over 200 experimental and DNS mean velocity and temperature profiles from several turbulence databases and with other turbulence models as well showing that, for most of the profiles analyzed, the new formulation gives a better fit to the data.

Contents

1	Introduction	1
2	Brief review of the present state of the art	3
2.1	Zero pressure gradient and internal non-transpired flows	4
2.2	Zero pressure gradient and internal flows with wall transpiration . . .	13
2.3	Non-zero pressure gradient flows with zero wall transpiration	24
2.4	Non-zero pressure gradient flows with wall transpiration	27
3	Proposed theory	30
3.1	Characteristic scales of the flow	30
3.1.1	Zero pressure gradient flows with wall transpiration	30
3.1.2	Non-zero pressure gradient flows with wall transpiration . . .	33
3.2	New wall functions	34
3.2.1	Zero pressure gradient flows with wall transpiration	34
3.2.2	Non zero pressure gradient flows with zero wall transpiration .	40
3.2.3	Non zero pressure gradient flows with wall transpiration . . .	50
3.3	Description of the outer layer	57
4	Comparisons with other theories and datasets	65
4.1	Assessment of the data	65
4.2	Mean velocity profiles	74
4.3	Mean temperature profiles	75
4.4	Mixing length profiles	79
4.5	Thermal mixing length profiles	85
5	Discussion and Conclusion	88
	Bibliography	89
A	Some demonstrations	116

B	Comparisons with other theories and databases	118
B.1	Zero pressure gradient and confined flows with wall transpiration . . .	119
B.2	Non-zero pressure gradient flows	184

Chapter 1

Introduction

Transpired turbulent flows are wall bounded flows where injection or suction (transpiration) of fluid is applied through a porous wall. This kind of flow occurs frequently in nature and in the industry and practical examples are drag reduction and boundary layer control (GAD-EL HAK, 2000), film cooling technique in turbine blades, aircraft surfaces, rocket thrust chambers or any surface in general (GOLDSTEIN, 1971), production or filtration of oil in horizontal wells (CLEMO *et al.*, 2006), atmospheric flows over vegetation canopies (FINNIGAN, 2000), geophysical flows in natural channels and rivers with permeable beds (seepage flows) (LU *et al.*, 2008), coastal protection structures (MANES *et al.*, 2011) and so on. While most theoretical studies of turbulent flows with wall transpiration focus on the zero pressure gradient case, it is expected that in real applications the pressure gradients are non-zero. In fact, one important application of wall transpiration is flow separation control— suction can suppress flow separation, while blowing has the opposite effect.

In this work, a phenomenological study of transpired turbulent flows with non-zero pressure gradients and separation is presented. New expressions for the characteristic velocity and temperature scales of the flow u_c and T_c —a crucial concept in turbulence modeling— are derived and new scaling laws for the near wall mean velocity and temperature profiles are proposed. Analytical studies of such a complex flow have proven elusive. To the present author's knowledge, the new near wall laws are the first in the literature to describe the combined effects of wall transpiration and flow separation. When experimental data and direct numerical simulations (DNS) of mean velocity and temperature profiles are scaled with u_c and T_c , they collapse onto one single curve in the near-wall region, suggesting that they can be made self-similar with respect to the transpiration rate when properly scaled. This contrasts with the classical theories for transpired flows. In the proposed formulation, all free parameters are constants that do not vary with the transpiration rate, the pressure gradient parameter or any other flow variable and, differently from

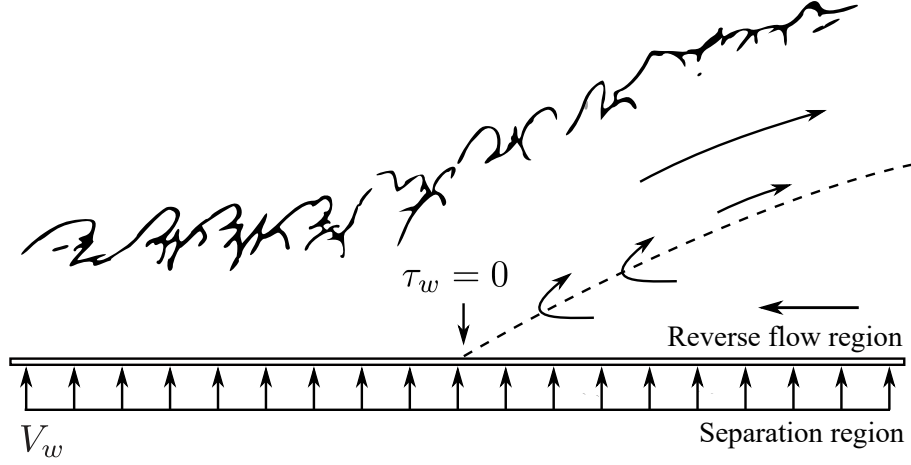


Figure 1.1: The separated turbulent boundary layer with wall transpiration. Adapted from SIMPSON (1981).

some other wall law formulations available in the literature, no empirical corrections to the Von Karman constant and the y -axis intercept were used. As the use of wall functions as boundary conditions in high Reynolds number turbulence models (e.g. the $\kappa - \epsilon$ model) can drastically improve their accuracy and reduce computational costs, the new near wall laws can be of great utility in practical applications, but they are also of extreme interest from a purely theoretical viewpoint.

The domains of validity of the wall laws is extended, to include the outer region of the boundary layer, using the intermittent character of the flow in that region. Comparisons with the data show that the *intermittency factor* used in this work is a universal function independent of the transpiration rate or the pressure gradient parameter. This representation of the mean velocity profile can provide the basis for an integral method of predicting flows with wall transpiration and non-zero pressure gradients. Figure 1.1 shows a sketch of the flow studied in this work.

The present text is structured as follows. Chapter 2 offers a brief literature review on the topic. The new theory and main contributions of this work are described in chapter 3. Comparisons between the data and the theory are also presented in chapter 3. The aim of chapter 4 is to discuss which theories best fit the data. Discussion and conclusions are made in chapter 5.

Chapter 2

Brief review of the present state of the art

One of the milestones in modern fluid mechanics is Prandtl's boundary layer theory. Another key contribution, made by Von Karman and considered by many one of the greatest accomplishments in turbulence theory, is the *logarithmic law of the wall* for the inner region of wall bounded turbulent flows. Due to its huge importance in a vast number of applications, there have been considerable efforts to extend the domain of validity of such theories to other non-canonical flows. Here, a quick review of more than one century of turbulence research highlights the major contributions. There are more than 300 references cited in this work.

Many theoretical works regarding near wall turbulent flows focus on obtaining expressions for the stream-wise mean velocity and temperature profiles close to the wall in the form of the so called *wall laws* and *defect laws*. The law of the wall is valid in a thin region close to the wall, while the defect law describes the flow in the outer part of the boundary layer. The thin inner region is subdivided into a viscous/conductive sub-layer, where mean viscous/diffusion effects are predominant, and a fully turbulent region, where turbulence dominates the flow¹ (figure 2.1). The outer 90% (approximately) region of the boundary layer is dominated essentially by inertia effects. Another important characteristic of the viscous sub-layer and the outer region is the highly intermittent character of the flow in those regions.

The near wall laws are of great importance since equations to evaluate the mean friction factor and Stanton number—parameters of crucial importance in engineering applications—can be obtained from them (CLAUSER, 1956). The near wall laws can also be used as boundary conditions in more sophisticated turbulence models (e.g. in high Reynolds number turbulence models), so better wall laws would improve the accuracy of those models (LAUNDER & SPALDING, 1974). Experimental

¹Some authors also include a region between the viscous sub-layer and the fully turbulent region called the buffer layer, where both turbulence and viscous effect are important.

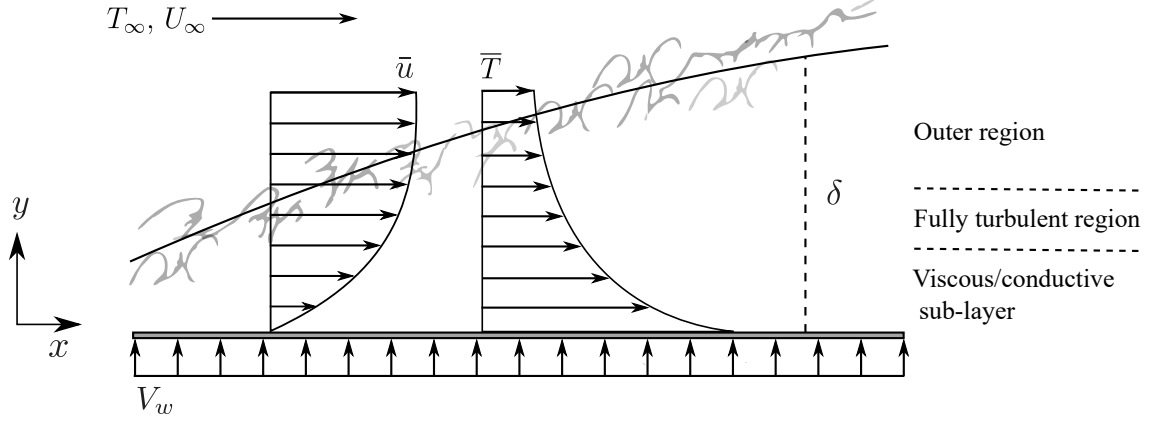


Figure 2.1: The structure of the turbulent boundary layer—with wall injection, far from separation.

techniques used to obtain the mean wall shear stress can also benefit from the use of wall laws (e.g. the Preston tube, the Stanton tube and Clauser charts).

In Section 2.1 the different wall laws to describe zero pressure gradient boundary layers, pipe and channel flows over solid impervious walls are presented. The classic theories that include the effects of wall transpiration are described in Section 2.2 and those who consider non-zero pressure gradients are described in Section 2.3. Section 2.4 reviews some formulations proposed in the past to describe turbulent flows with the combined effects of pressure gradients and wall transpiration.

2.1 Zero pressure gradient and internal non-transpired flows

One of the first studies of turbulent flows in pipes were carried out by DARCY (1858), who obtained on the basis of careful measurements, a formula to calculate the stream-wise direction mean velocity profile \bar{u} given by, with a slightly different notation,

$$U_{\max} - \bar{u} = 11.3 \left(\frac{r}{R} \right)^{3/2} \sqrt{\frac{i}{R}}, \quad (2.1)$$

where r is the distance from the conduit of radius R centerline, U_{\max} is the value of \bar{u} at $r = 0$ and i is, in Darcy's words, *la charge par mètre* which can be translated in the present nomenclature as the flow driven force $-\partial \bar{P} \pi R^2$ per unity of the fluid's density ρ and per unity of the distance ∂x where the pressure difference $\partial \bar{P}$ is computed. In a pipe flow with a constant circular cross section the square root of this quantity per unity of R is, apart from a multiplicative constant, equal to the

friction velocity u_τ , defined as

$$u_\tau = \text{sgn}(\tau_w) \sqrt{\frac{|\tau_w|}{\rho}}, \quad (2.2)$$

where τ_w is the mean wall shear stress, which allows equation 2.1 to be written in the form

$$\frac{U_{max} - \bar{u}}{u_\tau} = f\left(\frac{r}{R}\right). \quad (2.3)$$

Nowadays the above expression is called the *velocity defect law*. It was discovered originally for turbulent pipe flows but it was also used for channel flows (VON KARMAN, 1930), boundary layers (SHULTZ-GRUNOW, 1940) and, more recently, it could be derived from purely theoretical arguments, using the method of linear stability analysis (MALKUS, 1979).

Moving forward on the time-line, some authors developed semi-empirical techniques—rather than pure curve fitting of data—to obtain expressions for the mean velocity profile where assumptions of many types have been made. Considering the so-called Boussinesq hypothesis, which has its roots in the works of BOUSSINESQ (1870, 1877), and in the present state of knowledge can be written as

$$-\rho \overline{u'v'} = \rho \nu_t \frac{\partial \bar{u}}{\partial y}, \quad (2.4)$$

where $-\rho \overline{u'v'}$ is the turbulent shear stress (u and v are the instantaneous stream wise and wall normal direction velocity components, a prime denotes their fluctuations with respect to their means and a bar denotes a statistic mean) and ν_t is the kinematic eddy viscosity, TAYLOR (1915) (for transfer of vorticity) and PRANDTL (1925) (for transfer of momentum) noticed that ν_t has the dimension of a product including a velocity and a length scale. An analogy with Maxwell kinetic theory of gases lead Prandtl to formulate his famous mixing length formulas²,

$$\nu_t = \ell^2 \left| \frac{\partial \bar{u}}{\partial y} \right|, \quad (2.5)$$

where ℓ is called the mixing length and,

$$-\rho \overline{u'v'} = \rho \ell^2 \frac{\partial \bar{u}}{\partial y} \left| \frac{\partial \bar{u}}{\partial y} \right|. \quad (2.6)$$

²In fact, these ideas were conceded much earlier by BOUSSINESQ (1870) himself, who performed an average of the Navier-Stokes equations (before the work of REYNOLDS (1894)!) and a closure model using an analogy to the kinetic theory of gases with an eddy viscosity given by $\nu_t = \tilde{A} u_o r$, where \tilde{A} is a dimensionless constant depending on wall roughness, u_o the speed of the liquid near the wall and r is the pipe radius (see FRISCH (1995) and also SCHMITT (2007)).

Using expression 2.6 with a constant mixing length ℓ and assuming a linear stress distribution, PRANDTL (1925) was able to deduce the 3/2 power law for the velocity profile first introduced by Darcy. Using PRANDTL (1925) mixing length formula (eq. 2.6) with a mixing length given by

$$\ell = \varkappa \left| \frac{\partial \bar{u} / \partial y}{\partial^2 \bar{u} / \partial y^2} \right|, \quad (2.7)$$

where \varkappa is an universal constant³—the Von Karman constant—and assuming a linear stress distribution, VON KARMAN (1930) derived one of the firsts logarithmic formulas to calculate the velocity profile in a closed channel flow,

$$\frac{U_{max} - \bar{u}}{u_\tau} = -\frac{1}{\varkappa} \left[\ln \left(1 - \sqrt{\frac{y}{h}} \right) + \sqrt{\frac{y}{h}} \right], \quad (2.8)$$

where h is the channel half width. VON KARMAN (1930) and PRANDTL (1932) also deduced a logarithmic velocity profile assuming that near the wall there is a region of constant shear stress (the fully turbulent region in figure 2.1) and that the mixing length in that region, being a characteristic length scale of the dominant eddies, should be limited in size by the solid wall so it bears to be proportional to the distance from the wall,

$$\ell = \varkappa y. \quad (2.9)$$

With those assumptions they obtained

$$\frac{\bar{u}}{u_\tau} = \frac{1}{\varkappa} \ln \left(\frac{y u_\tau}{\nu} \right) + C, \quad (2.10)$$

where ν is the fluid kinematic viscosity and C is a constant of integration. Equation 2.10 is the celebrated *logarithmic law of the wall*. The original values of the constants were set as $\varkappa = 0.38$ and $C = 4.82$ but, most probably because of COLES's (1968) work, they were, for a long time, assumed to be approximately $\varkappa = 0.41$ and $C = 5$ however, recent estimations place them as low as $\varkappa = 0.384$ and $C = 4.127$ (NAGIB *et al.*, 2006) and as high as $\varkappa = 0.436$ and $C = 6.15$ (ZAGAROLA & SMITS, 1998). There are also evidences that for low Reynolds number flows the constants are actually functions of the Reynolds number (SIMPSON, 1970). In this work, the values of $\varkappa = 0.41$ and $C = 5$ are used.

The Boussinesq hypothesis and Prandtl mixing length theory have been subjected to a lot of criticism in the past (BERNARD & WALLACE, 2002; POPE, 2000; SCHMITT, 2007; TENNEKES & LUMLEY, 1972; THOMPSON *et al.*, 2010). But in fact, the *logarithmic law of the wall* could be derived by many authors using

³Universal in the sense that it should be Reynolds number and flow geometry independent.

completely different approaches. Among them, dimensional analysis and matching⁴ of inner and outer expansions (ISAKSON (1937); MILLIKAN (1938); CLAUSER (1954); YAJNIK (1970); MELLOR (1972), SYCHEV & SYCHEV (1987), etc.), assumptions of local equilibrium between the production and dissipation of turbulent energy (TOWNSEND, 1961) and Lie-group analysis of the Reynolds-averaged Navier-Stokes equations (OBERLACK, 2001). However, these approaches also include assumptions of various types that can also be questioned (BARENBLATT *et al.*, 1997; FREWER *et al.*, 2014; GEORGE, 2007; LONG & CHEN, 1981; MALKUS, 1979; MORRISON, 2007; PANTON, 2005; SPALART, 2011). Of course, as the *log-law* is already well-established in the literature since a long time, the different techniques could be developed specifically targeting it as a final result. In that light, the *log-law* can be considered just an *à posteriori* justification of experimental evidence—with the appropriate choice of the constants κ and C it provides a good fit to the data, so it can be regarded as a very useful tool in engineering applications.

The principal contender of the *logarithmic law of the wall* has been the power law,

$$\frac{\bar{u}}{u_\tau} = C_1(Re) \left(\frac{yu_\tau}{\nu} \right)^{\xi(Re)}, \quad (2.11)$$

where $C_1(Re)$ and $\xi(Re)$ are functions of the Reynolds number Re , usually based on the momentum thickness θ and the free stream velocity. Sometimes yu_τ/ν is replaced by $yu_\tau/\nu + a^+$ to satisfy Galilean invariance (a^+ being an arbitrary constant). Some examples of empirically obtained power law formulas are the 3/2th law (DARCY, 1858; PRANDTL, 1925), the 2th law for the outer layer (BAZIN, 1865; KEULEGAN, 1938; LAUFER, 1954) and the 1/7th law for the inner layer (KEULEGAN, 1938; NIKURADSE, 1933; SARMA *et al.*, 1983; SCHLICHTING, 1968).

Recently, the power law could be derived using theoretical arguments as rigorous as those used to obtain the *logarithmic law* including Millikan’s matching of inner and outer expansions (AFZAL, 2001; MILLIKAN, 1938), *intermediate asymptotics* and *incomplete similarity* assumptions⁵ (BARENBLATT & MONIN, 1979; BARENBLATT *et al.*, 1997; GEORGE *et al.*, 1997; LONG & CHEN, 1981). Accordingly to BARENBLATT (1993), incomplete similarity was used to obtain important results in areas as diverse as quantum field theory, flame propagation theory, fluid mechanics and biology. The power law exponent $\xi(Re)$ can be obtained from theory, and in recent formulations it varies with the inverse of the Reynolds number logarithmic but the functional form of the coefficient $C_1(Re)$ is usually obtained from

⁴Pre-1960s works present different versions of what can be called Millikan’s matching, while latter works usually make use of a more sophisticated method that might be referred to as Kaplan limits matching, which is discussed in detail in the book of VAN DYKE (1975).

⁵Intermediate asymptotics because the theory is developed for very large, but finite Reynolds number and incomplete similarity because the resulted scalings are Reynolds number dependent.

curve fitting procedures of experimental data (see AFZAL (2001) for a review in this topic).

In terms of accuracy, both the *log-law* and the *power law* perform equally well when compared to experimental data (BUSCHMANN & GAD-EL HAK, 2007). It is interesting to note that, with the appropriate choice of parameters $\xi(Re)$, $C_1(Re)$ and a^+ , the *power law* and the *log-law* are mathematically identical in the limit of infinite Reynolds number, so the *power law* contains the *log-law* as a particular case. Other velocity profile formulas that appear in the literature involve hyperbolic tangents and powers (RANNIE, 1956; ZAGUSTIN & ZAGUSTIN, 1969), and also logarithmic and powers (AFZAL, 1976; BUSCHMANN & GAD-EL HAK, 2003).

Turning the attention to the outer part of the turbulent boundary layer, several procedures to calculate the mean flow in that region have been proposed in the past by different authors. The first model to be presented, still in the spirit of the Boussinesq hypothesis, considers a constant kinematic eddy viscosity in the outer region of the layer,

$$\nu_t \propto U_\infty \delta^*, \quad (2.12)$$

where $\delta^* = \int_0^\infty (U_\infty - \bar{u}) dy / U_\infty$ is the displacement thickness. Its physical interpretation due to CLAUSER (1956) is that the turbulent boundary layer structure resembles a situation of a laminar boundary layer with a very thin sublayer of a different fluid with a much lower viscosity. In that scenario the (turbulent) outer mean velocity profile would be given by the solution of the Blasius equation with the kinematic viscosity given by equation 2.12 and a boundary condition of a non-zero slip velocity. This solution should be matched with the inner layer solution (e.g. the *log-law*) in an arbitrary point inside the boundary layer (BARONTI *et al.*, 1964; CEBECI, 2004; TOWNSEND, 1956). This procedure gives quite accurate results but it has to be implemented numerically.

Two different approaches that avoid a direct confrontation with the non-linear inertia terms in the Reynolds-averaged Navier-Stokes equations are SARNECKI (1959) intermittency hypothesis and COLES (1956) law of the wake. The former will be discussed here in some detail because, as it will be shown later, it can be successfully applied to flows with wall transpiration and pressure gradients.

In all turbulent flows with a free boundary, it has been reported that, as the free stream is approached the turbulence becomes intermittent, that is, for only a fraction γ_s of the time is the flow turbulent (KLEBANOFF, 1955). In such flows, it can be observed the presence of a sharp, well-defined boundary whose shape and position vary continuously with time, that separates turbulent to non-turbulent fluid—the turbulent/non-turbulent (T/NT) interface. The term “non-turbulent” is used in preference to “laminar” because the flow in question is not completely free

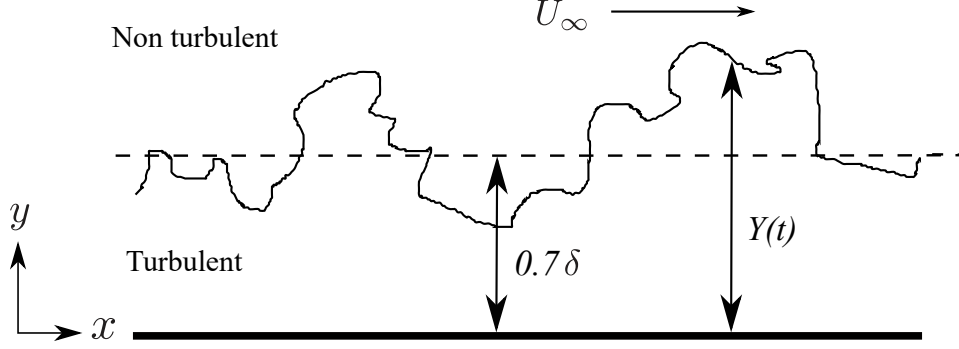


Figure 2.2: A sketch of the Turbulent/Non-Turbulent interface. The increase in $\delta(x)$ cannot be seen because the extension in the stream-wise direction is small.

from turbulence, but its turbulence level is much lower than that of the contiguous turbulent flow. In fact, the distinction made between turbulent and non-turbulent flow can be on the basis of presence or absence, respectively, of random vorticity fluctuations (CORRSIN & KISTLER, 1955). From the vorticity equation, obtained by taking the curl of the Navier-Stokes equations, and given by

$$\frac{D\vec{\omega}}{Dt} = \nu \nabla^2 \vec{\omega} + \vec{\omega} \cdot \nabla \vec{u}, \quad (2.13)$$

it is clear that the only way vorticity can depart from zero is by molecular diffusion—where the vorticity vector $\vec{\omega}$ is zero, also is the vortex-stretching term $\vec{\omega} \cdot \nabla \vec{u}$ —and, at the high Reynolds numbers of turbulent flows, viscous effects can be significant only if gradients are very steep, the T/NT interface should be actually a thin layer where viscosity has a dominant influence (POPE, 2000). For that reason, the T/NT interface is also called the viscous super-layer. It turns that this is indeed the case and theoretical reasoning can show that its thickness scales with the Kolmogorov length scale, the Taylor micro-scale or the friction length scale depending on the flow type (CHAUHAN *et al.*, 2014; DA SILVA & TAVEIRA, 2010; DA SILVA & DOS REIS, 2011). A good review in the topic of interfacial layers can be found in DA SILVA *et al.* (2014). The functional form of the intermittency factor $\gamma_s(\vec{x})$ can be obtained in the following manner. Defining $Y(t)$ as the location of the T/NT interface for any fixed x -station (see figure 2.2), $\gamma_s(y)$ is given by one minus the cumulative distribution of $Y(t)$,

$$\gamma_s(y) = \text{prob}[y \leq Y(t)] = 1 - \text{CDF}_{Y(t)}(y), \quad (2.14)$$

where the operator $\text{prob}[A]$ gives the probability of the event A and $\text{CDF}_{Y(t)}(y)$ is the cumulative distribution function of the random variable $Y(t)$. Experimental data from several authors (CHAUHAN *et al.*, 2014; CORRSIN & KISTLER, 1955; DE SILVA *et al.*, 2017; KLEBANOFF, 1955) shows that $Y(t)$ has, in a very accurate

approximation, a Gaussian distribution with mean μ and standard deviation σ , so $\gamma_s(y)$ can be written as,

$$\gamma_s(y) = 1 - \frac{1}{2} \left[1 + \operatorname{erf} \left(\frac{y - \mu}{\sqrt{2}\sigma} \right) \right]. \quad (2.15)$$

The average position of the T/NT interface is proportional to the width length scale of the flow $\mu \approx 0.7\delta$ and the parameter σ/δ gives an index of the activity of entrainment at the interface (TOWNSEND, 1976).

The intermittency factor can be used in turbulence modeling in a variety of manners. For example, it can be introduced in equation 2.12 to improve the constant eddy viscosity formulation (TENNEKES & LUMLEY, 1972). Another possibility is known as SARNECKI (1959) intermittency hypothesis. Sarnecki postulates that the mean velocity profile in the outer region of the turbulent boundary layer can be represented by,

$$\bar{u} = \gamma_s u_{\text{turb}} + (1 - \gamma_s) u_{\text{pot}}, \quad (2.16)$$

where u_{turb} and u_{pot} are the mean velocities over the time the flow is turbulent and potential (or non-turbulent) respectively. He then assumes that $u_{\text{pot}} = U_\infty$, in accordance with CORRSIN & KISTLER (1955) theory, and also that u_{turb} could be obtained from the law of the wall. These assumptions demand that there will be a discontinuous velocity jump at the interface. However, in the real, situation the velocity and all other fields vary smoothly across the layer but as its thickness is very thin compared with the flow width, this misconception should not represent a major problem to the model. This point is discussed further in Section 3.3.

Another way to extend the domain of validity of the wall laws to the outer region of the layer is simply to sum a function in the velocity profile formula that would do the job of eliminate the discrepancy that appears between the wall law and the data in that region,

$$\frac{\bar{u}}{u_\tau} = f \left(\frac{yu_\tau}{\nu} \right) + W(x, y), \quad (2.17)$$

where $f(yu_\tau/\nu)$ is the wall function (e.g. the *log-law* or *the power law*) and $W(x, y)$ is the deviation of $f(yu_\tau/\nu)$ to \bar{u} in the outer layer. The origin of that idea is difficult to trace—(COLES (1968) cite the work of HUDIMOTO (1935)— but COLES (1956) was perhaps the first who did an extensive experimental campaign to evaluate $W(x, y)$. Coles then wrote,

$$W(x, y) = \frac{\Pi(x)}{\varkappa} \mathcal{W} \left(\frac{y}{\delta} \right), \quad (2.18)$$

where the wake function $\mathcal{W}(y/\delta)$ was found to be a universal function and the wake

parameter $\Pi(x)$ was found to have a constant value⁶ for equilibrium layers (see Section 2.3) and to be a function of the stream-wise direction x for non-equilibrium flows. From the point of view of matched asymptotic expansions theory in singular perturbation problems, equation 2.17 can be viewed as the first two terms of a composite expansion, but the functional form of $W(x, y)$ has always been obtained empirically. Table 2.1 shows some wake functions that have been proposed by several authors in the past⁷. CORNISH (1960) was the first to notice that with COLES (1956) version of the wake function the velocity profile formula doesn't satisfy the condition of zero wall normal direction derivative at the edge of the boundary layer. NELSON (1964) was the first to formulate an analytical expression (instead of giving the wake function in a table format) that satisfies this condition. The other functions were formulated simply to give a better fit to experimental data and the most accurate one is probably CHAUHAN *et al.* (2007) version.

The semi-empirical techniques developed to describe the mean velocity profile can be successfully applied to predict the behavior of other fields as well. One of particular interest in many industrial applications, and subject of study in this work, is the mean temperature field \bar{T} . The near wall mean temperature profile in a turbulent flow with heat transfer at the wall can be obtained using a thermal version of the BOUSSINESQ (1870) hypothesis,

$$\bar{q} = \rho c_p \overline{v'T'} = -\rho c_p \alpha_t \frac{\partial \bar{T}}{\partial y}, \quad (2.19)$$

where \bar{q} is the turbulent heat flux in the wall normal direction, c_p is the specific heat at constant pressure and α_t is a turbulent thermal diffusivity. Defining a quantity called the turbulent Prandtl number as

$$Pr_t = \frac{\nu_t}{\alpha_t}, \quad (2.20)$$

with $\nu_t = \ell^2 \partial \bar{u} / \partial y$ obtained from the mixing length theory gives

$$\bar{q} = -\rho c_p \frac{\ell^2}{Pr_t} \frac{\partial \bar{u}}{\partial y} \frac{\partial \bar{T}}{\partial y}. \quad (2.21)$$

Assuming a constant turbulent Prandtl number and a constant turbulent heat flux in the near wall region leads to, after integration in the wall normal direction, the *thermal logarithmic law of the wall*

$$\frac{T_w - \bar{T}}{T^*} = \frac{1}{\kappa_r} \ln \left(\frac{y u_\tau}{\nu} \right) + C(Pr), \quad (2.22)$$

⁶In CEBECI (2004) the wake parameter Π is actually a function of the Reynolds number.

⁷The author obtained the parameter A in NELSON's (1964) formula in order to force $\mathcal{W}(1) = 2$.

Table 2.1: Various proposals for the wake function.

Author	$\mathcal{W}(\eta)$
ROTTA (1950, 1953)	$(A\eta)\varkappa/\Pi$, A being an unspecified constant
ROSS & ROBERTSON (1951)	some linear function of η
COLES (1956)	tabulated
HINZE (1959)	$1 + \sin[(2\eta - 1)\pi/2]$, or equivalently, $1 - \cos(\pi\eta)$
CORNISH (1960)	tabulated
NELSON (1964)	$\{A\eta^{2.5} - [1/2.75 + 2.5A/2.75]\eta^{2.75}\}/\Pi$, $A = (1 + 5.5\Pi)/0.25$
MOSES (1964)	$6\eta^2 - 4\eta^3$
FINLEY <i>et al.</i> (1966)	$\eta^2(1 - \eta)/\Pi + g\eta^2(3 - 2\eta)$, where $g = 0.55$ for pipe $g = 2.5$ for flat plate and $g = 1.25$ for thin water layer flow.
COLES (1968), and also SPALDING (1965)	$2\sin^2(\eta\pi/2)$
BULL (1969)	$0, \eta \leq 0.08$ $1 - \cos[\pi(\eta - 0.08)/(1 - 0.08)], 0.08 \leq \eta \leq 1$
ALLAN (1970)	$[1 - \cos(\alpha\eta)]/(1 - \cos\alpha)$ α is the solution of $\alpha \sin \alpha / (1 - \cos \alpha) = -1/\Pi$
ROTTA (1970)	$2\sin^2(\eta\pi/2) + \eta^5(1 - \eta)(4\eta - 3)/\Pi$
WHITE (1974)	$0.6\varkappa\alpha Re_\tau\eta/\Pi$, $\alpha = (2/C_f)^{3/2}d(U_{ref}/U_\infty)/d(x/l)/Re$
GRANVILLE (1987, 1976) and also DEAN (1976)	$\eta^2(6 - 4\eta) + \eta^2(1 - \eta)/\Pi$
LEWKOWICZ (1982)	$\eta^2(6 - 4\eta) - \eta^2(1 - 3\eta + 2\eta^2)/\Pi$
AFZAL (1996)	$\eta^2(6 - 4\eta) - \eta^2(3 - 8\eta + 5\eta^2)/(2\Pi)$
GUO & JULIEN (2001)	$2\sin^2(\pi\eta/2) - \eta/\Pi$
GUO & JULIEN (2003)	$2\varkappa\sin^2(\pi\eta/2)/\Pi - \eta^3/(3\Pi)$
CHAUHAN <i>et al.</i> (2007)	$2\{1 - \exp[-(5a_2 + 6a_3 + 7a_4)\eta^4/4 + a_2\eta^5 + a_3\eta^6 + a_4\eta^7]\} \times$ $\times [1 - \ln(\eta)/(2\Pi)] / \{1 - \exp[-(a_2 + 2a_3 + 3a_4)/4]\}$, $a_2 = 132.841, a_3 = -166.2041$ and $a_4 = 71.9114$.
QINGYANG (2009)	$2\ln(1 - \eta) + 8\ln[1/\cos(\pi\eta/2) + \tan(\pi\eta/2)]/\pi$

where T_w is the mean wall temperature, $T^* = q_w/(\rho c_P u_\tau)$ is the friction temperature, q_w is the mean wall heat flux, $\kappa_\tau = \kappa/Pr_t = 0.482$ is the thermal Karman constant, Pr is the molecular Prandtl number and $C(Pr)$ is a function of Pr . The functional form of this parameter has been obtained essentially by a curve fit of data (KADER, 1981; SCHLICHTING & GERSTEN, 2017) but it can be obtained using theory. For water and air flows where $Pr \approx 0.7$, the parameter $C(Pr)$ assumes a value of approximately 3.8. The constant turbulent Prandtl number model is known as some form of the Reynolds analogy. A good review of it can be found in KAYS (1994). The experimental data of BLACKWELL *et al.* (1972) suggests that near the wall Pr_t is fairly independent of wall transpiration, what is in disagreement with the data of ELENA (1977) and VÉROLLET (1972), and that the presence of an adverse pressure gradient decreases its value as the pressure gradient increases.

Similarly to the mean velocity profile, the logarithmic behavior of the mean temperature profile can also be obtained using matching arguments with a temperature defect law together with a thermal version of the law of the wall (ELENA, 1977; SCHLICHTING & GERSTEN, 2017). There are also some authors who claim the presence of a power law profile instead (WANG *et al.*, 2008).

The validity of the thermal wall laws can be extended to include the outer region of the flow empirically, adapting COLES (1956) idea of the wake function to the thermal problem (KADER, 1991; WANG *et al.*, 2008).

An important assumption made in the heat transfer models described in this text is that the temperature difference between the wall and the free stream (or the pipe/channel centerline), $T_w - T_\infty$, is small enough so the assumption of constant fluid properties—especially viscosity—can be justified.

2.2 Zero pressure gradient and internal flows with wall transpiration

The firsts experimental studies of turbulent boundary layers with wall transpiration started in the late 1940s at MIT under the supervision of professor H. S. Mickley and co-workers. Experimental campaigns of the Heat and Mass Transfer group at Stanford University and of the Cambridge University group are also very important. A great collection of references to these works can be found in KENDALL *et al.* (1964), SQUIRE (1980) and MOFFAT & KAYS (1984). In addition to these references, it can be cited the experimental works from TENNEKES (1964), TORII *et al.* (1966), ROTTA (1970), MIRONOV & LUGOVSKOI (1972), BAKER & LAUNDER (1974b), SENDA *et al.* (1981), JARŽA (1988) for boundary layers in a flat plate and the works from STEVENSON (1964a) and JONSSON & SCOTT (1965) for

boundary layers over an axial circular cylinder. Recent experimental studies of the turbulent boundary layer with blowing were conducted by YOSHIOKA & ALFREDSSON (2006), SCHWEIKERT *et al.* (2013), KORNILOV & BOIKO (2014, 2016) and FERRO (2017), and with suction by TRIP & FRANSSON (2014) and FERRO *et al.* (2017); FERRO (2017). A large amount of experimental work dealing with steep changes in the wall boundary condition, e.g. application of wall injection (WOOLDRIDGE & MUZZY, 1965, 1966) or suction (DUTTON, 1960; FAVRE *et al.*, 1966; FULACHIER *et al.*, 1977, 1987; SANO & HIRAYAMA, 1984; VEROLLET, 1977) after long impervious lengths, application of localized suction or blowing through porous strips or slots (AGRAWAL *et al.*, 2010; ANTONIA *et al.*, 1988; ANTONIA & FULACHIER, 1989; BELLETTRE, 1998; SANO, 1992) and pipe flow with wall suction (ELENA, 1977; SCHILDKNECHT *et al.*, 1979) has also been done in the Institut de Mécanique Statistique de la Turbulence (IMST) and elsewhere. Fewer experiments for a closed channel with wall transpiration (ERSHIN *et al.*, 1991; ZHAPBASBAEV & ISAKHANOVA, 1998; ZHAPBASBAYEV & YERSHIN, 2003), an open channel with wall transpiration (NAKAGAWA & NEZU, 1979; NEZU, 1977) and for pipes with wall injection (OLSON & ECKERT, 1966) were also carried out.

Direct numerical simulation (DNS) of the Navier-Stokes equations has proven to be a useful tool in the understanding and modeling of turbulence phenomena. The first DNS of a flow with wall transpiration was conducted by MARIANI *et al.* (1993), who simulated the asymptotic suction boundary layer. Recently, the asymptotic layer was studied using DNS and large eddy simulations (LES) by SCHLATTER & ÖRLÜ (2011), BOBKE *et al.* (2016) and KHAPKO *et al.* (2016). A turbulent channel flow where injection is applied at one wall and suction at the other (at the same rate) was simulated by SUMITANI & KASAGI (1995), NIKITIN & PAVELEV (1998), CHUNG & SUNG (2001) and AVSARKISOV *et al.* (2014). DNS of a spatially developing turbulent boundary layer with uniform blowing and uniform suction was performed by KAMETANI & FUKAGATA (2011) and of a Couette flow with wall transpiration by KRAHEBERGER *et al.* (2018, 2017). There are also many works where DNS were used to explore the effects of unconventional distributions of the transpiration velocity or the surface permeability in flow control and drag reduction schemes (CHOI *et al.*, 1994; GÓMEZ *et al.*, 2016; JIMÉNEZ *et al.*, 2001; MIN *et al.*, 2006; QUADRIO *et al.*, 2007; ROSTI *et al.*, 2015).

To derive the near wall laws for transpired flows, the approximation that is usually assumed for the mean shear stress profile close to the wall is,

$$\tau = \rho V_w \bar{u} + \tau_w, \quad (2.23)$$

where τ is the mean shear stress (the sum of the turbulent shear stress $-\overline{\rho u'v'}$ and viscous shear stress $\rho\nu\partial\bar{u}/\partial y$) and V_w is the value of the mean wall normal direction velocity component \bar{v} at the wall, i.e., the transpiration velocity. V_w is positive in the case of wall injection (blowing) and negative in the case of wall suction. Equation 2.23 was used in the fully turbulent region of the boundary layer for the first time by KAY (1948), who considered the asymptotic suction boundary layer. For this layer, the growth due to skin friction is exactly compensated by suction, so that its thickness remains constant and all derivatives with respect to x vanish (TENNEKES, 1965a). The flow in question is extremely difficult to realize experimentally, and usually is reached approximately by applying suction after a long stretch of solid surface (DUTTON, 1960; FAVRE *et al.*, 1966). For flows with wall injection or sucked flows far from the asymptotic condition equation 2.23 should be viewed as an approximation, obtained from a linearization of the equation of motion, that gives a fair representation of the data in the near wall region (see ANDERSEN *et al.* (1972) for example).

Using equation 2.23 together with PRANDTL (1925) mixing length formula or assumptions of local equilibrium between the production and dissipation of turbulent energy, many authors derived an expression to calculate the stream-wise direction mean velocity profile close to the wall, \bar{u} , that when written explicitly has a logarithmic squared term so that it has been labeled the “bi-logarithmic law of the wall” (BLACK & SARNECKI, 1958; BRADSHAW, 1967; CLARKE *et al.*, 1955; DORRANCE, 1956; DORRANCE & DORE, 1954; KAY, 1948; KORNILOV, 2015; LIN & KARUNARATHNA, 2006; MICKLEY & DAVIS, 1957; NAYAK & BARDEN, 1972; RUBESIN, 1954; SILVA-FREIRE, 1988; SIMPSON, 1967; STEVENSON, 1963a; TORII *et al.*, 1966; TOWNSEND, 1961; VAN-DRIEST, 1957; VIGDOROVICH, 2016; WILCOX & TRACI, 1976). The most famous version of the *bi-log* law reads, after STEVENSON (1963a),

$$\frac{2u_\tau}{V_w} \left\{ \left(1 + \frac{V_w \bar{u}}{u_\tau^2} \right)^{1/2} - 1 \right\} = \frac{1}{\varkappa} \ln \left(\frac{yu_\tau}{\nu} \right) + 5 + f(V_w^+), \quad (2.24)$$

where $f(V_w^+)$ is a function of the non-dimensional transpiration velocity, $V_w^+ = V_w/u_\tau$, with the property $f(0) = 0$ to guarantee that equation 2.24 approaches the *logarithmic law of the wall* in the limit $V_w \rightarrow 0$. STEVENSON (1963a) argue that $f(V_w^+)$ is zero but comparisons with different datasets shows that it varies considerable with V_w^+ (figure 2.3). The functional form of $f(V_w^+)$ has been derived essentially by an empirical fit of experimental data (BRADSHAW, 1967; KORNILOV, 2015; LIN & KARUNARATHNA, 2006; SILVA-FREIRE, 1988; WILCOX & TRACI, 1976) or using the intersection point between the viscous sub-layer solu-

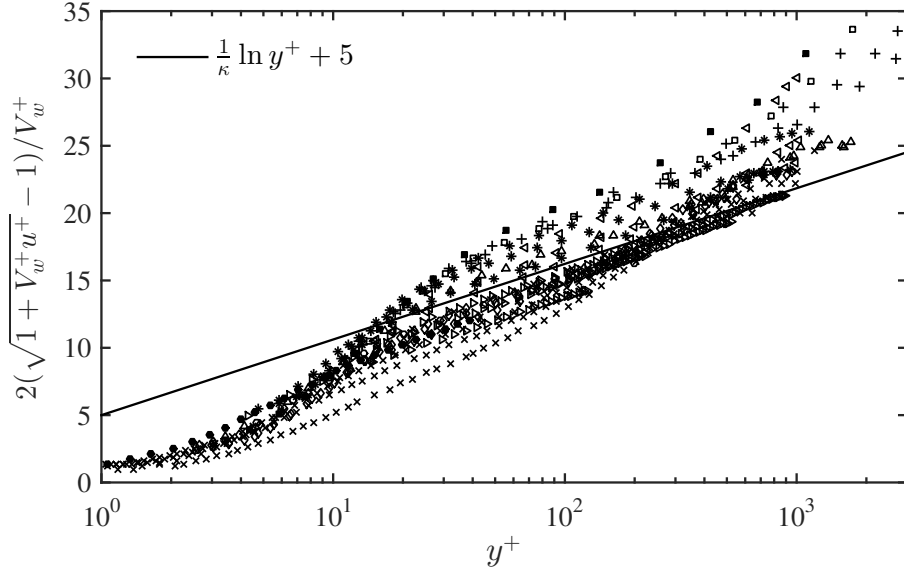


Figure 2.3: Experimental and DNS mean velocity profiles plotted in the bi-logarithmic coordinates. Dimensionless variables with the superscript + are scaled with u_τ and ν/u_τ . Symbols as in figure 3.2.

tion (SCHLICHTING, 1942)

$$\frac{V_w \bar{u}}{u_\tau^2} = \exp\left(\frac{V_w y}{\nu}\right) - 1, \quad (2.25)$$

and the bi-log formula, the point (y_a, u_a) . If equation 2.24 is evaluated at this position the following expression is obtained,

$$f(V_w^+) = \frac{2}{V_w^+} \left\{ \left(1 + V_w^+ u_a^+ \right)^{1/2} - 1 \right\} - \frac{1}{\kappa} \ln(y_a^+) - 5, \quad (2.26)$$

where dimensionless variables with the superscript + are scaled with u_τ and ν/u_τ . Equation 2.26 is useful once two more independent equations to calculate u_a^+ and y_a^+ are known. One equation comes from the viscous sub-layer solution but some assumption needs to be made in order to determine the other. RUBESIN (1954) and BLACK & SARNECKI (1958) assumed that u_a^+ doesn't vary with wall transpiration so its value can be obtained from the non-transpired case, while VAN-DRIEST (1957) and MICKLEY & DAVIS (1957) proposed different empirical expressions to correlate u_a^+ and y_a^+ . SIMPSON (1967) assumed that the values of both y_a^+ and u_a^+ can be obtained from the non-transpired case, i.e. $u_a^+ = y_a^+ = 10.8$, but this condition is inconsistent with the viscous sub-layer solution. To calculate $f(V_w)$, VIGDOROVICH (2016) proposes a two term Taylor series expansion for small V_w^+ and estimates the values of its coefficients using SPALDING (1961) empirical formula for the composite mean velocity profile from non-transpired flows.

CLARKE *et al.* (1955) formulation is interesting because it doesn't have any

free parameter to improve the fit between theory and the data but comparisons with many databases show that his version of the *bi-log law* is the one who provides the best fit to the data for most of the profiles analyzed by the author. His equation reads,

$$\frac{\bar{u}}{u_\tau} = \frac{1}{\kappa} \ln \left(\frac{yu_\tau}{\nu} \right) + 5 + \frac{V_w}{4\kappa^2 u_\tau} \ln^2 \left(\frac{yu_\tau}{\nu} \right). \quad (2.27)$$

TORII *et al.* (1966) wrote the *bi-log law* with a slightly different form than Stevenson's version and the parameter $f(V_w^+)$ was obtained from unspecified origins. MARXMAN & GILBERT (1963) extended the $1/7^{\text{th}}$ power law formula to the case of a flow with wall transpiration while TURCOTTE (1960) proposed an exponential of an hyperbolic tangent function for \bar{u} based on RANNIE (1956) theory. Both KAY (1948) and NAYAK & BARDEN (1972) assumed a linear distribution for the mixing length throughout the whole boundary layer and applied different boundary conditions at the edge of the layer to obtain slightly different expression that do not contain the classic *log-law* as a particular case.

The *bi-logarithmic law* was obtained by SILVA-FREIRE (1988) in a more general form with three free parameters using the method of matched asymptotic expansions together with mixing length theory. Assuming that Stevenson's law provide good theoretical predictions, Silva-Freire obtained these parameters so his expression coincides with equation 2.24 and obtained the functional form of $f(V_w^+)$ by curve fitting procedures of ANDERSEN *et al.* (1972) experimental data.

The other approach that has been taken by some authors to obtain the near wall laws is an extension of MILLIKAN (1938) phenomenological theory of turbulence. Based fundamentally in simple dimensional analysis and similarity arguments this theory predicts a logarithmic dependence in the law of the wall. In a region close to the wall, it's assumed that the mean velocity profile has the form of the law of the wall,

$$\frac{\bar{u}}{u_c} = F\left(\frac{y}{y_c}\right), \quad (2.28)$$

and the profile in the outer layer has the form of the defect law (DARCY, 1858; MALKUS, 1979; SHULTZ-GRUNOW, 1940; VON KARMAN, 1930),

$$\frac{U_\infty - \bar{u}}{u_c} = g\left(\frac{y}{\delta}\right), \quad (2.29)$$

where u_c and y_c are characteristic velocity and length scales of the flow close to the wall and δ is a characteristic length scale in the outer portion of the flow. If there is an intermediate region where these two laws are to be valid (the “overlap” region), matching of the mean velocity gradients in both expressions gives the so-

called “semi-logarithmic” law of the wall,

$$\frac{\bar{u}}{u_c} = C \ln \left(\frac{y}{y_c} \right) + B, \quad (2.30)$$

where C and B are parameters that usually depends on the value of the transpiration velocity, surface roughness and so on. Several authors have proposed different expressions for u_c and y_c (AFZAL, 1976; ANDERSEN *et al.*, 1972; AVSARKISOV *et al.*, 2014; COLES, 1972; FERRO *et al.*, 2017; KAY, 1948; NAKAGAWA & NEZU, 1979; TENNEKES, 1964) but in all formulations the collapse of mean velocity profiles from flows with different values of V_w^+ has not been obtained.

TENNEKES (1965a) argues that the *bi-logarithmic law* is unacceptable as it conflicts with the concept of related similarity laws for the inner and outer region of a turbulent boundary layer. In TENNEKES’s (1965a) view, similarity laws in the form of the law of the wall for the inner region and the defect law for the outer region also exist for the asymptotic suction boundary layer—this is confirmed by the data in the works of TENNEKES (1965a) and FERRO (2017)—so there must be an intermediary region where these two laws overlap. According to Tennekes, an overlap region is only possible if the mean velocity profile has a logarithmic behavior in that region.

To obtain expressions for the characteristic velocity and length scales, TENNEKES (1965a) invokes the concept of the turbulent asymptotic suction boundary layer, where equation 2.23 is also valid in the outer portion of the flow and integration from the outer edge inwards (viscous stress neglected) gives,

$$V_w \frac{\bar{u} - U_\infty}{u_\tau^2} = \frac{-\overline{u'v'}}{u_\tau^2}. \quad (2.31)$$

Based on this equation and in the laminar sub-layer solution, equation 2.25, Tennekes proposed that the characteristic velocity scale is given by,

$$u_c^{\text{Tennekes}} = -0.06 u_\tau^2 / V_w, \quad (2.32)$$

where the minus sign appears because $V_w < 0$ for suction and the factor 0.06 was obtained empirically. FERRO *et al.* (2017) recent experimental study of the asymptotic layer gives strength to this result. This expression has obvious complications in the limit $V_w \rightarrow 0$, so Tennekes restricted its applications for the cases with “moderate suction rates”, i.e., in Tennekes definition, $0.04 < -V_w/u_\tau < 0.1$. For flows with arbitrary suction or blowing rates, asymptotic or not, Tennekes proposed, based on

purely empirical grounds, a provisional velocity scale given by

$$u_c^{\text{Tennekes}} = u_\tau + 9V_w. \quad (2.33)$$

When scaled by u_c^{Tennekes} , experimental velocity profiles have a constant slope but the y -axis intercept varies with the transpiration velocity V_w^+ and the functional form of this parameter was obtained by curve fitting procedures of experimental data.

COLES (1972) also criticized the *bi-log law* arguing that some conceptual complications appear in two limiting cases, the asymptotic layer and the blow-off condition. The blow-off condition is defined by the boundary condition $\tau_w = 0$, and it might be obtained if sufficient high injection is applied ($V_w/U_\infty > 0.01$ or $V_w/U_\infty > 0.035$ accordingly to MOFFAT & KAYS (1984) and COLES (1972) respectively), even in the case of a zero pressure gradient flow. For the asymptotic layer, COLES (1972) estimates that an imaginary value might appear in the bi-logarithmic expression. In the blow-off condition, the *bi-log law* with COLES (1968) \sin^2 wake function gives a \sin^4 relation to the velocity profile and accordingly to COLES (1972), the experimental data from MUGALEV (1959) shows that the profile varies with a \sin^2 and not a \sin^4 . In COLES (1972) version of the *semi-logarithmic law*, the characteristic scales u_c and ν/u_c are obtained from a characteristic stress τ_c based on a integral mean inside the viscous sublayer,

$$\rho(u_c^{\text{Coles}})^2 = \tau_c = \frac{1}{y_a} \int_0^{y_a} \tau dy. \quad (2.34)$$

Inside the viscous sub-layer, the shear stress is given by $\rho\nu\partial\bar{u}/\partial y$, so equation 2.34 gives

$$(u_c^{\text{Coles}}) = \sqrt{\nu \frac{u_a}{y_a}}. \quad (2.35)$$

The position of the intercept point (y_a, u_a) can be obtained for a particular value of V_w^+ solving (numerically) the sub-layer solution, equation 2.25, together with the *semi-logarithmic law*, equation 2.30. The values of the constants C and B were obtained from the non-transpired case.

AFZAL (1975) derived the semi-logarithmic formula using the method of matched asymptotic expansions with COLES (1972) expressions for the characteristic velocity and length scales while NEZU (1977), NAKAGAWA & NEZU (1979) and WATTS (1972) proposed that the *logarithmic law of the wall* is still valid for transpired flows if empirical corrections are applied to the Von Karman constant and y -axis intercept. A similar approach was carried out by other authors but with the *log-law* constants being functions of the surface permeability instead of the

transpiration velocity (BREUGEM *et al.*, 2006; MANES *et al.*, 2011; SUGA *et al.*, 2010).

AVSARKISOV *et al.* (2013) expression for u_c is based on a mean value of the friction velocities in both walls of a transpired channel flow, $u_c^{\text{Avsarkisov}} = \sqrt{(u_{\tau b}^2 + u_{\tau s}^2)/2}$, where $u_{\tau b}$ and $u_{\tau s}$ are the friction velocities at the wall where blowing and suction is applied respectively. This expression is a measure of the pressure gradient in the flow but it conflicts with the concept that near a wall the flow is governed by local conditions only (ROTTA, 1962). An empirical fit was made to determine the y -axis intercept as a function of the transpiration velocity.

Now turning the attentions to the outer portion of the layer, in the case of a flow with zero wall transpiration the combination of the *log-law* with Coles law of the wake (equations 2.10, 2.17 and 2.18) and the velocity defect law (equation 2.29) gives, for equilibrium flows,

$$\frac{U_\infty - \bar{u}}{u_\tau} = -\frac{1}{\kappa} \ln\left(\frac{y}{\delta}\right) + \frac{\Pi(x)}{\kappa} \left[2 - \mathcal{W}\left(\frac{y}{\delta}\right)\right] = g\left(\frac{y}{\delta}\right). \quad (2.36)$$

For a flow with wall injection, MICKLEY & SMITH (1963) argue that the above relation is still valid if one changes the friction velocity u_τ by a characteristic velocity given by the maximum value of the total shear stress in the layer, $u_c^{\text{Mickley}} = \sqrt{\tau_{\text{max}}/\rho}$. This relation breaks down for suction, where the maximum value of the total shear stress occurs at the wall. BLACK & SARNECKI (1958) argue that the velocity defect law cannot overlap the *bi-log law*, so they proposed the following extension of Coles composite profile to the case of a flow with wall transpiration,

$$\bar{u} = u_\tau f(y^+)_{\text{Bilog}} + u_c^{\text{Black}} \left[\frac{\Pi(x)}{\kappa} \mathcal{W}\left(\frac{y}{\delta}\right) \right], \quad (2.37)$$

where $f(y^+)_{\text{Bilog}}$ is BLACK & SARNECKI (1958) version of the *bi-log law* and,

$$u_c^{\text{Black}} = \sqrt{u_\tau^2 + V_w u_\tau f(y^+)_{\text{Bilog}}}. \quad (2.38)$$

STEVENSON (1963b, 1964b) proposed a modified velocity defect law in the form

$$\frac{2u_\tau}{V_w} \left\{ \left(1 + \frac{V_w U_\infty}{u_\tau^2}\right)^{\frac{1}{2}} - \left(1 + \frac{V_w \bar{u}}{u_\tau^2}\right)^{\frac{1}{2}} \right\} = g\left(\frac{y}{\delta}\right), \quad (2.39)$$

where $g(y/\delta)$ is the same universal function from the non-transpired case, while TENNEKES (1964, 1965b) modified velocity defect law reads,

$$\frac{U_\infty - \bar{u}}{u_c^{\text{Tennekes}}} = g_2\left(\frac{y}{\delta}\right), \quad (2.40)$$

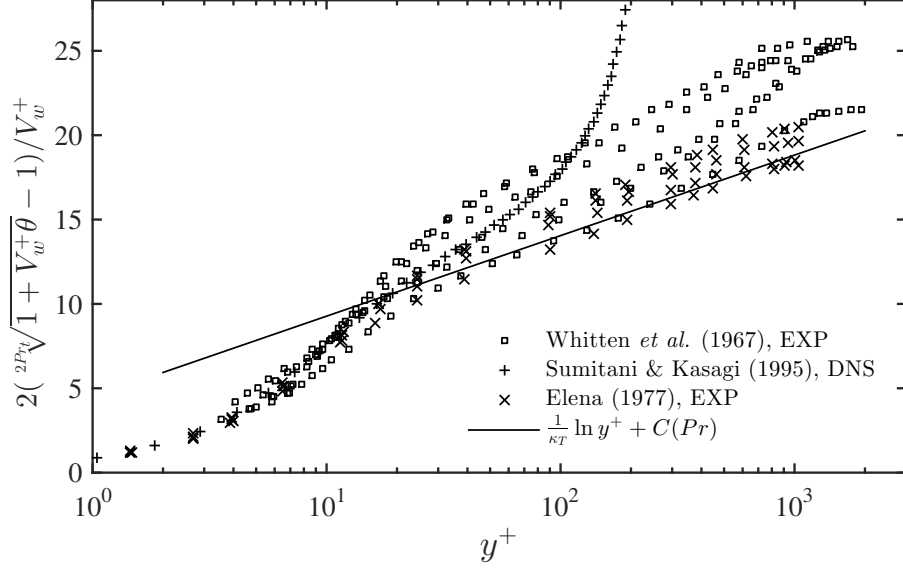


Figure 2.4: Experimental and DNS mean temperature profiles plotted in the bi-logarithmic coordinates. Dimensionless variables with the superscript + are scaled with T^* and ν/u_τ .

where $g_2(y/\delta)$ is not the same function from the non-transpired case, but matching with Tennekes inner layer solution shows that it is also logarithmic. Tennekes argue that this relation should be valid if, in addition to CLAUSER (1954) equilibrium parameter (Section 2.3), an extra equilibrium parameter defined by $\Lambda = V_w U_\infty / u_\tau^2$ should be constant—as in the laminar case. The works from COLES (1972) and NAYAK & BARDEN (1972) follow similar lines. SILVA-FREIRE (1988) extended the *bi-log law* domain of validity to the outer region of the flow using a modified wake parameter that takes into consideration the effects of wall transpiration. The functional form of this parameter was obtained empirically.

MCQUAID (1968) assumed SARNECKI (1959) intermittency hypothesis with STEVENSON (1963a) version of the *bi-logarithmic law* and an intermittency factor independent of wall transpiration. His formulation compared well with STEVENSON (1964a), MICKLEY & DAVIS (1957) and his own data for turbulent layers with blowing but the values of the friction velocities were chosen to give the best fit between the data and his theory. THOMPSON (1969a,b) formulation is similar to MCQUAID (1968) but he preferred to use BLACK & SARNECKI (1958) version of the *bi-logarithmic law* instead of Stevenson's and the analysis was done for suction.

Table 2.2 shows, in chronological order, the different formulations that have been proposed in the past to describe the near wall behavior of the mean velocity profile in transpired turbulent flows and also the parameters used in each formulation, when applicable.

The derivation techniques used to obtain the thermal law of the wall for transpired flows are similar to those used to obtain the mean velocity profile formula.

The approximation that is usually employed for the mean heat flux near the wall \bar{q} , exact for the asymptotic layer, is given by

$$\bar{q} = q_w + \rho c_P V_w (T_w - \bar{T}). \quad (2.41)$$

Assuming the constant turbulent Prandtl number model with the mixing length theory gives, after some algebraic manipulations similar to those performed by STEVENSON (1963a) for the mean velocity profile, the thermal *bi logarithmic law* of the wall

$$2Pr_t \frac{u_\tau}{V_w} \left\{ \left(1 + \frac{V_w}{u_\tau} \theta \right)^{1/(2Pr_t)} - 1 \right\} = \frac{1}{\varkappa_T} \ln \left(\frac{y u_\tau}{\nu} \right) + C(Pr) + f_T(V_w^+), \quad (2.42)$$

where

$$\theta = \frac{T_w - \bar{T}}{T^*}, \quad (2.43)$$

and $f_T(V_w^+)$ is a function of the non dimensional transpiration velocity V_w^+ with the property $f_T(0) = 0$. The thermal *bi-log law* was derived for the first time by TORII *et al.* (1966), but it was presented in a rather incomplete format. A more complete derivation was presented in VÉROLLET (1972) and FULACHIER (1972), who assumed $f_T(V_w^+) = 0$. From figure 2.4 it can be seen clearly that $f_T(V_w^+) \neq 0$, as mean temperature profiles are not self similar when plotted in the thermal *bi-log law* coordinates using T^* and ν/u_τ as the scaling parameters. The functional form of $f_T(V_w^+)$ was derived in FARACO-MEDEIROS & SILVA-FREIRE (1992) using the intersection point between the conductive sub layer solution and the thermal *bi-log law* in a similar way RUBESIN (1954) did for the mean velocity profile. A slightly different version of the thermal *bi-log law* also appears in VIGDOROVICH (2004), but he didn't obtain an expression to evaluate the parameter $f_T(V_w^+)$.

To describe the behavior of the mean temperature profile in the outer region of the flow, VÉROLLET (1972) and FULACHIER (1972) proposed a modified temperature defect law that is similar to Stevenson's defect law for the mean velocity profile. FARACO-MEDEIROS & SILVA-FREIRE (1992) extended the domain of validity of thermal *bi-log law* to the outer region using a thermal wake function, with the wake parameter being a function of the transpiration rate and the functional form of it was obtained empirically.

Table 2.2: Parameters in the different wall law formulations for transpired turbulent flows.

Author	$f(V_w^+)$, B , \varkappa_V , etc.
KAY (1948)	n.a.
DORRANCE & DORE (1954)	$-2/V_w^+$
RUBESIN (1954)	$2[(1 + 13.1V_w^+)^{1/2} - 1]/V_w^+ +$ $+ \ln[V_w^+ / \ln(1 + 13.1V_w^+)]/\varkappa - 5$
CLARKE <i>et al.</i> (1955)	eq. 2.27
DORRANCE (1956)	$2[(1 + 13.1V_w^+)^{1/2} - 1]/V_w^+ +$ $+ \ln[V_w^+ / \ln(1 + 13.1V_w^+)]/\varkappa - 5$
VAN-DRIEST (1957)	$(y_a/\nu)(\tau_a/\rho)^{1/2} = (y_a u_\tau/\nu)_0$
MICKLEY & DAVIS (1957)	$u_a^+ y_a^+ = 195 + 2.5(10^4)(V_w/U_\infty)$
BLACK & SARNECKI (1958)	$2[(1 + 13.1V_w^+)^{1/2} - 1]/V_w^+ +$ $+ \ln[V_w^+ / \ln(1 + 13.1V_w^+)]/\varkappa - 5$
TURCOTTE (1960)	$(1/2)(1 + u_{\tau 0}/u_\tau)$
TOWNSEND (1961)	n.a.
MARXMAN & GILBERT (1963)	n.a.
STEVENSON (1963a)	0
TENNEKES (1964, 1965a)	$-11V_w^+ + 0.19$
TORII <i>et al.</i> (1966)	$2(-1 + \zeta_2)(1 - 0.2/\varkappa)/V_w^+ +$ $+ 0.2\{2(-1 + \zeta_1)/V_w^+ - \ln[2\ln(\zeta_1)/V_w^+]/0.2\}/\varkappa$
SIMPSON (1967)	$2[(1 + 11V_w^+)^{1/2} - 1]/V_w^+ - \ln(11)/\varkappa - 5$
BRADSHAW (1967)	$1375(V_w^+)^2$
WATTS (1972)	$\varkappa_V = \varkappa/(1 - 390F),$ $B = 7.5 + 5.5 \arctan[2.2(-F/0.0014 - 1)]/\pi$
COLES (1972)	5
ANDERSEN <i>et al.</i> (1972)	$5 + 14(u_\tau/u_c^{\text{Andersen}} - 1)$
NAYAK & BARDEN (1972)	n.a.
AFZAL (1975)	5
WILCOX & TRACI (1976)	$\varkappa_V = \varkappa/\{1 + V_w^+[3.36 + \ln(y^+)/(4\varkappa)]\}$
NEZU (1977)	$\varkappa_V = \varkappa/(1 + 9.2V_w^+)$, $B = 5(1 - 5V_w^+)$
SILVA-FREIRE (1988)	$-512V_w/U_\infty$
LIN & KARUNARATHNA (2006)	n.a.
AVSARKISOV <i>et al.</i> (2014)	$-90.62(V_w^+)^{1.188}$
KORNILOV (2015)	$9.6V_w^+$
VIGDOROVICH (2016)	$-3.51V_w^+/\varkappa$
FERRO <i>et al.</i> (2017)	0.993

2.3 Non-zero pressure gradient flows with zero wall transpiration

A large number of experimental works have been devoted to study turbulent flows with non-zero pressure gradients. In internal flows such as pipes and channels with constant cross sections the flow is usually subjected to a relatively low favorable pressure gradient, so its influence in the near wall laws is small⁸. Furthermore, for highly accelerated boundary layers the flow is usually in a state of reversal to laminar flow. This makes most part of the attention turn for high adverse pressure gradient flows (APG), specially those where flow separation may occur. A great number of references to experimental works dealing with such flows can be found in SIMPSON (1985, 1989) and MACIEL *et al.* (2006). More recent experimental studies of high APG boundary layers include the works from LOUREIRO *et al.* (2007), KNOPP *et al.* (2015), WILLERT (2015), ATKINSON *et al.* (2016) and CUVIER *et al.* (2017). High adverse pressure gradient flows were also studied extensively using DNS (COLEMAN *et al.*, 2015; KITSIOS *et al.*, 2016; LEE & SUNG, 2008, 2009; SKOTE, 2001; SKOTE *et al.*, 1998; SPALART & LEONARD, 1987; SPALART & WATMUFF, 1993). The same can be said to flows with boundary layer separation (ABE *et al.*, 2012, 2013; GUNGOR *et al.*, 2016; MANHART & FRIEDRICH, 2002; NA & MOIN, 1998; SKOTE & HENNINGSON, 2002; SPALART & COLEMAN, 1997; SPALART & LEONARD, 1987).

There are many theoretical works that deal with the question of scaling and equilibrium in the outer part of the flow (CASTILLO & GEORGE, 2001; CLAUSER, 1954; DURBIN & BELCHER, 1992; MELLOR & GIBSON, 1966; PERRY & SCHOFIELD, 1973; ROTTA, 1950; SKOTE, 2001; YAGLOM, 1979; ZAGAROLA & SMITS, 1998). Equilibrium means similarity of the mean velocity profiles when properly scaled in defect law coordinates and is usually associated with equilibrium in the production and dissipation of turbulent kinetic energy. In CLAUSER's (1954) classical analysis, the flow is said to be in equilibrium if the Clauser equilibrium parameter,

$$\beta_{\text{Clauser}} = \frac{\delta d\bar{P}/dx}{\tau_w}, \quad (2.44)$$

is held constant through the flow. The physical interpretation of this result is that there are only two forces that act in the boundary layer, the normal force (per unit of area) caused by the pressure gradient $\delta d\bar{P}/dx$ and a shear force caused by the wall shear stress τ_w , and the flow should be in equilibrium when these two forces

⁸This might not be the case in a confined flow with wall injection, as when V_w/U_b increases the pressure gradient increases while the wall shear stress decreases so the absolute value of the pressure gradient parameter $|P^+|$ can assume values as high as those from separated flows. For instance, in AVSARKISOV *et al.* (2014) flow with the highest injection rate $|P^+| = 2.8$.

preserve a constant ratio along the flow.

In the thin inner region close to the wall, one important non-dimensional parameter that quantifies the strength of the pressure gradient is the pressure gradient parameter, defined as

$$P^+ = \frac{\rho dP_w/dx}{\nu u_\tau^3}, \quad (2.45)$$

where ρ is the fluid density and dP_w/dx is the stream-wise direction mean pressure gradient at the wall. Many investigators suggest that the extent of validity of the logarithmic law of the wall in APG flows can be quantified by a threshold value of P^+ between 0.01 and 0.05 (ALVING & FERNHOLZ, 1995; BROWN & JOUBERT, 1969; DRIVER, 1991; SAMUEL & JOUBERT, 1974; SPALART & LEONARD, 1987) and that the influence of the pressure gradient is visible at the outer region of the flow only (table 2.3). Other authors argue that the log-law is still valid in APG flows if the Von Karman constant and the y -axis intercept are replaced by empirically determined functions of P^+ (DIXIT & RAMESH, 2009; NAGIB & CHAUHAN, 2008; NICKELS, 2004). SIMPSON *et al.* (1977, 1981) suggest that the log-law is no longer valid when instantaneous reverse flow first appears near the wall. Close to the detachment/reattachment points where $\tau_w \rightarrow 0$ the log-law cannot be valid. In that region of the flow, many authors proposed that the near wall behavior of the mean velocity profile can be described by the *half-power law*, (AFZAL, 1983; KADER & YAGLOM, 1978; PERRY, 1966; PERRY *et al.*, 1966; SPALART & LEONARD, 1987; SPALDING, 1967; STRATFORD, 1959; TELBANY & REYNOLDS, 1980),

$$\frac{\bar{u}}{u_p} = \frac{2}{K(x)} \left(\frac{y u_p}{\nu} \right)^{1/2} + B(x), \quad (2.46)$$

where $u_p = (\nu dP_w/dx/\rho)^{1/3}$. The parameters $K(x)$ and $B(x)$ vary with the stream-wise direction and there is no agreement in the scientific community with respect to their correct functional forms or the values that they assume at the detachment/reattachment points. A more general formula that contain the *half-power law* and the *log-law* as particular cases was derived by several authors (AFZAL, 2008; BERNARD *et al.*, 2003; CRUZ & FREIRE, 1998, 2002; GERSTEN, 1998; GERSTEN *et al.*, 1993; KIEL, 1995; MCDONALD, 1969; MELLOR, 1966; NAKAYAMA & KOYAMAT, 1984; PATEL, 1965, 1973; PERRY *et al.*, 1966; SKOTE & HENNINGSON, 2002; SZABLEWSKI, 1972; TOWNSEND, 1961, 1976; VIETH, 1997). This formula contains a combination of square root and logarithmic terms so it has been labeled the *half-power-log law* by some authors. The original version derived

by TOWNSEND (1961) reads

$$\bar{u} = \frac{\sqrt{\tau_w/\rho}}{K(x)} \left\{ \ln \left(\frac{4\tau_w^{3/2}}{\rho^{1/2}\nu \frac{dP_w}{dx}} \times \frac{(\tau_w + \frac{dP_w}{dx}y)^{1/2} - \tau_w^{1/2}}{(\tau_w + \frac{dP_w}{dx}y)^{1/2} + \tau_w^{1/2}} \right) + B(x)K(x) + \right. \\ \left. - 2(1 - 0.2 \operatorname{sgn} \frac{dP_w}{dx}) \right\} + \frac{2(1 - 0.2 \operatorname{sgn} \frac{dP_w}{dx})}{K(x)} \left(\frac{\tau_w}{\rho} + \frac{1}{\rho} \frac{dP_w}{dx} y \right)^{1/2}. \quad (2.47)$$

Equations 2.46 and 2.47 could be derived by a variety of methods including Prandtl momentum transfer theory, assumptions of local equilibrium between the production and dissipation of turbulent energy, asymptotic methods and so on. TOWNSEND (1961) considers that the parameters $K(x)$ and $B(x)$ are constants and equal to their values from the zero pressure gradient case, i.e. $K(x) = \varkappa$ and $B(x) = 5$ approximately, but in other versions of the *half-power-log law* these parameters vary in the stream wise direction and their functional forms have been obtained by an empirical fit of experimental data. Using matching arguments as those described in Section 2.4, TENNEKES & LUMLEY (1972) obtained a *semi-logarithmic* formula for the mean velocity profile in the region of the flow with vanishing shear stress,

$$\frac{\bar{u}}{u_p} = 5.3 \ln \left(\frac{yu_p}{\nu} \right) + 8. \quad (2.48)$$

A more general formula that contains the above equation and the log-law as particular cases was derived by SHIH *et al.* (1999) and a slightly different version of it was presented later in SHIH *et al.* (2003). SIMPSON (1983) argue that in the back-flow region the mean velocity profile can be described by a combination of a logarithm and a linear term,

$$\frac{\bar{u}}{|U_N|} = A_{\text{simp}} \left(\frac{y}{N} - \log \frac{y}{N} - 1 \right) - 1, \quad (2.49)$$

where $A_{\text{simp}} \approx 0.3$ and N is the distance from the wall where the reverse flow speed reach its maximum value, U_N . Simpson's expression was compared to his own experimental data showing good agreement, but other authors found that the coefficient A_{simp} vary considerably for each profile (DEVENPORT & SUTTON, 1991; DIANAT & CASTRO, 1989; LE *et al.*, 1997; SKOTE & HENNINGSON, 2002). WILCOX (1989) also proposed an expression for the mean velocity profile that contain a combination of logarithmic and linear terms,

$$\frac{\bar{u}}{u_\tau} = \frac{1}{\varkappa} \ln \left(\frac{yu_\tau}{\nu} \right) + 5 - 1.13P^+ \left(\frac{yu_\tau}{\nu} \right) + O(P^{+2}), \quad (2.50)$$

but the validity of his formula was restricted to flows with small values of the pressure gradient parameter P^+ .

The thermal law of the wall for non-zero pressure gradients flows is usually de-

rived using dimensional analysis and matching arguments. In the region of vanishing shear stress, many authors derived an *inverse-half-power law* for the mean temperature profile given by (AFZAL, 1982, 1999; CRUZ & FREIRE, 1998, 2002; KADER, 1991; KIEL, 1995; PERRY *et al.*, 1966; SZABLEWSKI, 1972; VIETH, 1997),

$$\frac{T_w - \bar{T}}{T_p} = \frac{-2}{K_T(x)} \left(\frac{yu_p}{\nu} \right)^{-1/2} + B_T(x), \quad (2.51)$$

where $T_p = q_w/(\rho c_P u_p)$ and the parameters $K_T(x)$ and $B_T(x)$ vary in the stream wise direction x , but assume constant values at the point where $\tau_w = 0$. These values are different from the thermal Karman constant κ_T and y -axis intercept $C(Pr)$ from the zero pressure gradient case. Those authors could also derive an expression that contain both the *inverse half-power law* and the *log law* as particular cases. KIEL (1995) version reads,

$$\frac{T_w - \bar{T}}{T_p} = 2 \frac{P^+}{K_T(x)} \ln \left| \frac{\sqrt{yu_p/\nu + P^{+2/3}} - P^{+1/3}}{\sqrt{yu_p/\nu}} \frac{2}{\sqrt{|P^+|}} \right| + |P^+|^{1/3} B_T(x). \quad (2.52)$$

In the above expression and in the other *inverse-half-power-log law* formulations the functional forms of the parameters $K_T(x)$ and $B_T(x)$ are obtained by empirical fits of experimental data.

2.4 Non-zero pressure gradient flows with wall transpiration

The number of experimental works dealing with transpired turbulent boundary layers with a non-zero pressure gradient is scarce. Some of these works were reviewed in SQUIRE (1980) and MOFFAT & KAYS (1984). It can also be cited the studies from BAKER & LAUNDER (1974a) and SANO & HIRAYAMA (1984). The effects of wall transpiration in turbulent flows that separate over complex geometries such the backward facing step (SANO *et al.*, 2009; URUBA *et al.*, 2007; YANG *et al.*, 1994) or a two-dimensional hump (POSTL & FASEL, 2006; RUMSEY *et al.*, 2004) were also studied by experiments and DNS.

There is no law of the wall formulation in the literature that predicts separated or high APG flows with wall transpiration and the simplest turbulence models that deals with such flows are extensions of VAN DRIEST (1956) model with modified damping functions for the mixing length (see ANDERSEN *et al.*, 1972). MCQUAID (1968) argues that the bi-log law is still valid in non-zero pressure gradient transpired flows provided that a modified pressure gradient parameter that includes the effects

Table 2.3: Correlations to calculate the Cole’s wake parameter Π as function of Clauser equilibrium parameter β , the Reynolds number R_θ or the wall transpiration parameter $F = V_w/U_\infty$.

Author	Proposed correlation
MELLOR & GIBSON (1966)	$\Pi + \ln[\varkappa/(1 + \Pi)] = \varkappa[-2.6775 - 0.275\beta + 4.082(\beta + 0.5)^{3/4}]/2$
WHITE (1974)	$\beta = (1.25\Pi)^{4/3} - 0.5$
DAS & WHITE (1986)	$\beta = 0.76\Pi + 0.42\Pi^2, d\bar{P}/dx > 0$ $\beta = -5.5 + 2.5\Pi + 0.09\Pi^2, \tau_w \approx 0$ $\beta = 0.6\Pi - 0.33, d\bar{P}/dx < 0$
DAS (1987)	$\beta = -0.4 + 0.76\Pi + 0.41\Pi^2$
SILVA-FREIRE (1988)	$\Pi_{v_w} = \Pi + V_w^+[-1.95 \ln(V_w/U_\infty) - 3.1]$
SUCEC & OLJACA (1995)	$\beta = -0.5 + 0.76\Pi + 0.41\Pi^2$
WILCOX <i>et al.</i> (1998)	$\Pi = 0.6 + 0.51\beta - 0.01\beta^2$
CEBECI (2004)	$\Pi = 0.55\{1 - \exp[-0.243(R_\theta/425 - 1)^{1/2} - 0.298(R_\theta/425 - 1)]\}, R_\theta < 6000,$ $\Pi = 0.55, R_\theta > 6000$
DURBIN & REIF (2011)	$\Pi = 0.8(\beta + 0.5)^{3/4}$

of wall transpiration is small,

$$-0.004 < \frac{\nu}{\rho(u_\tau^2 + V_w \bar{U})^{3/2}} \frac{d\bar{P}}{dx} < 0.006. \quad (2.53)$$

THOMPSON (1969a) work follow similar lines but he preferred not to give a range of validity as equation 2.53 because, accordingly to him, no reliable method to measure the wall shear stress was available. ANDERSEN *et al.* (1972) version of the semi-logarithmic law of the wall, equation 2.30, relies on a characteristic velocity scale given by a characteristic stress inside the boundary layer,

$$u_c^{\text{Andersen}} = \sqrt{\frac{\tau_c^{\text{Andersen}}}{\rho}}, \quad (2.54)$$

where τ_c^{Andersen} is the total shear stress evaluated at a characteristic distance from the wall, y_c^{Andersen} , given by approximately three times the VAN DRIEST (1956) length scale A_{Van} . In Van Driest turbulence model, it is assumed the BOUSSINESQ (1870) hypothesis together with PRANDTL (1925) momentum transfer theory with

a mixing length given by,

$$\ell = \varkappa y \left[1 - \exp \left(- \frac{y^+}{A_{\text{Van}}^+} \right) \right], \quad (2.55)$$

where the parameter A_{Van}^+ is a measure of the sub-layer thickness. Van driest expression for ℓ comes from an analogy with the Stokes problem of a plate that executes oscillations parallel to itself. For zero-pressure gradients non-transpired flows, $A_{\text{Van}}^+ \approx 26$, but ANDERSEN *et al.* (1972) found from their experimental data that A_{Van}^+ is a function of the transpiration velocity and pressure gradient. For a given flow condition, the value of this parameter can be determined using a solver that numerically integrate the boundary layer equations with the Van Driest closure and a value of A_{Van} that forces the solution to give a good fit to the data. In a semi-log plot, ANDERSEN *et al.* (1972) formula has a constant slope of $1/\varkappa$ but the y -axis intercept varies with the transpiration velocity and pressure gradient and the functional form of this parameter was obtained by an empirical fit of experimental data.

Chapter 3

Proposed theory

3.1 Characteristic scales of the flow

3.1.1 Zero pressure gradient flows with wall transpiration

In most theoretical investigations of turbulent flows it is of crucial importance to determine the relevant scales of the flow. For zero pressure gradient non-transpired flows a velocity scale is naturally chosen as the friction velocity u_τ . However, in a flow subjected to wall transpiration, when mean velocity profiles are scaled with u_τ and ν/u_τ they do not collapse onto one single curve in the near wall region (figure 2.3). Furthermore, in the blow-off condition the friction velocity is effectively zero suggesting, from the present point of view, that in such flows the friction velocity is no longer the proper velocity scale of the flow. This question was already addressed by other authors, who also advocate a velocity scale different than u_τ (ANDERSEN *et al.*, 1972; AVSARKISOV *et al.*, 2013; COLES, 1972; FERRO *et al.*, 2017; MICKLEY & SMITH, 1963; TENNEKES, 1964). A new expression for the characteristic velocity scale u_c , will be derived here through some order of magnitude considerations—in this work, the physically intuitive concept of order of magnitude will be used rather than the mathematically rigorous definition as given in MEYER (1967) for example. At the bottom of the fully turbulent region, the approximated x -momentum equation can be cast as

$$V_w \bar{u} = \nu \frac{\partial \bar{u}}{\partial y} - \overline{u'v'} - u_\tau^2, \quad (3.1)$$

where $-\overline{\rho u'v'}$ is the turbulent shear stress. In this region, it is assumed that the mean velocity and the turbulent fluctuations are of the order of the characteristic velocity scale,

$$O(\bar{u}) = O(u') = O(v') = O(u_c), \quad (3.2)$$

which allows the following estimations for the inertia and turbulent terms in equation 3.1,

$$O(V_w \bar{u}) = O(V_w u_c), \quad O(-\overline{u'v'}) = O(u_c^2). \quad (3.3)$$

Considering that the viscous term can be approximated by,

$$O\left(\nu \frac{\partial \bar{u}}{\partial y}\right) = O\left(\frac{\tau_w}{\rho}\right), \quad (3.4)$$

it results from simple order of magnitude arguments—equations 3.3, 3.4 and 3.1—that the characteristic velocity can be estimated from the algebraic equation,

$$u_c^2 - \alpha V_w u_c - u_\tau^2 = 0, \quad (3.5)$$

where α is a proportionality coefficient of unity order. Equation 3.5 has a positive real root given by

$$u_c = \frac{\alpha V_w + \sqrt{\alpha^2 V_w^2 + 4u_\tau^2}}{2}. \quad (3.6)$$

In the blow-off condition, where $u_\tau = 0$ and $V_w > 0$, expression 3.6 gives a non-zero velocity scale, $u_c = \alpha V_w$, and when the transpiration velocity is zero it reduces to $u_c = u_\tau$, the proper velocity scale for non-transpired flows. Now it is shown that when two asymptotic cases are considered the velocity scale given by equation 3.6 recovers the expressions obtained by TENNEKES (1965a). Considering the case with “arbitrary suction or blowing rates” first, it is convenient to write equation 3.6 in the following non-dimensional form,

$$\frac{u_c}{u_\tau} = \frac{\alpha V_w / u_\tau + 2 \sqrt{\alpha^2 V_w^2 / (4u_\tau^2) + 1}}{2}. \quad (3.7)$$

Expanding the square root term in equation 3.7 in a two terms Taylor series for small values of V_w / u_τ gives,

$$\sqrt{\alpha^2 V_w^2 / (4u_\tau^2) + 1} = 1 + \frac{\alpha^2}{8} \left(\frac{V_w}{u_\tau}\right)^2 + O\left(\frac{V_w}{u_\tau}\right)^3, \quad (3.8)$$

which enables equation 3.7 to be re-written as

$$\frac{u_c}{u_\tau} = 1 + \frac{\alpha}{2} \left(\frac{V_w}{u_\tau}\right) + \frac{\alpha^2}{8} \left(\frac{V_w}{u_\tau}\right)^2 + O\left(\frac{V_w}{u_\tau}\right)^3. \quad (3.9)$$

Considering cases where the values of V_w / u_τ are small enough so that the Taylor series expansion given by equation 3.8 is justified but not too small so it makes sense to retain the term $\alpha V_w / (2u_\tau)$ in equation 3.9—the influence of V_w / u_τ is of second order in the Taylor series expansion but of first order in the equation for

u_c/u_τ —for example when $V_w/u_\tau \sim 0.1$, allows equation 3.9 to be re-written in an approximated, dimensional form given by

$$u_c = u_\tau + \frac{\alpha}{2}V_w, \quad (3.10)$$

recovering Tennekes’s velocity scale for “arbitrary suction or blowing” rates.

Considering now the case of a flow with “moderate suction rates”, it is useful to write equation 3.6 as

$$u_c = \frac{\alpha V_w - \alpha V_w \sqrt{1 + 4u_\tau^2/(\alpha^2 V_w^2)}}{2}, \quad (3.11)$$

where the minus sign before the square root appears because $V_w < 0$ for suction—so $\sqrt{V_w^2} = -V_w$. Expanding the square root term in equation 3.11 in a two terms Taylor series for small u_τ/V_w leads to

$$u_c \approx \frac{\alpha V_w - \alpha V_w [1 + 2u_\tau^2/(\alpha^2 V_w^2)]}{2} = -\left(\frac{1}{\alpha}\right) \frac{u_\tau^2}{V_w}, \quad (3.12)$$

recovering Tennekes’s velocity scale for flows with “moderate suction” rates. The above expression was deduced for sucked flows with $-V_w \gg u_\tau$, where it is expected that the flow might be in a state of reversal to laminar—for example, in KHAPKO’s *et al.* (2016) simulation with $-V_w/u_\tau \sim 0.06$ the flow is already in the verge of relaminarization. If this is the case, equation 3.12 is consistent with the laminar sub-layer solution, where mean velocity profiles are self similar when scaled by u_τ^2/V_w (TENNEKES, 1964).

When $-V_w/u_\tau \gg 1$ the values of the characteristic velocity scale obtained from equation 3.12 are much smaller than the friction velocity so it is reasonable to question if, in a situation with very high suction rates, the value of $-V_w/u_\tau$ would be so large that equation 3.12 would give the nonphysical result of a zero characteristic velocity scale. However, as an increase in the suction velocity is always followed by an increase in the friction velocity, it is difficult to believe that this would be the case in any real situation.

Here a curious result is noticed if one sets the value of $\alpha = 18$. In this case even the numeric coefficients in equations 3.10 and 3.12 are approximately the same obtained by Tennekes, i.e., $\alpha/2 = 9$ and $-1/\alpha = -0.06$. However, these values were obtained by Tennekes in order to fit his semi-logarithmic formula for the mean velocity profile to the experimental data so, in the present formulation, a different value will be given to the constant α (see section 3.2.1).

3.1.2 Non-zero pressure gradient flows with wall transpiration

Strong APGs can lead to flow separation, where points with zero wall shear stress are present in the flow so the friction velocity u_τ is no longer the proper velocity scale. In many studies, a parameter with dimension of a velocity based on the pressure gradient at the wall, $u_p = (\nu(dP_w/dx)/\rho)^{1/3}$, is defined as the relevant velocity scale but, far from the separation region or in the particular case of a zero pressure gradient flow u_p is not the proper velocity scale. An expression that contain both u_τ and u_p as particular cases will be derived here in a similar fashion to CRUZ & FREIRE (1998) analysis.

Considering a flow with zero wall transpiration, at the bottom of the fully turbulent region a balance between the turbulent and viscous stresses occurs so that the approximated x -momentum equation can be cast as,

$$\frac{1}{\rho} \frac{dP_w}{dx} y = \nu \frac{\partial \bar{u}}{\partial y} - \overline{u'v'} - u_\tau^2. \quad (3.13)$$

Assuming that the turbulent fluctuations are of the order of the characteristic velocity scale,

$$O(u') = O(v') = O(u_{cp}), \quad (3.14)$$

where u_{cp} is the characteristic velocity scale in the non-transpired case, and that the distance from the wall is of the order of the characteristic length scale

$$O(y) = O(\nu/u_{cp}), \quad (3.15)$$

allows the orders of magnitude of the pressure and turbulent terms in equation 3.13 to be estimated as,

$$O\left(\frac{1}{\rho} \frac{dP_w}{dx} y\right) = O\left(\frac{1}{\rho} \frac{dP_w}{dx} \frac{\nu}{u_{cp}}\right) = O\left(\frac{u_p^3}{u_{cp}}\right), \quad (3.16)$$

and

$$O(-\overline{u'v'}) = O(u_{cp}^2). \quad (3.17)$$

With these considerations and from simple order of magnitude arguments similar to those used in section 3.1.1, the characteristic velocity scale of the flow can be estimated from the highest real root of the algebraic equation,

$$u_{cp}^3 - u_\tau^2 u_{cp} - (\gamma u_p)^3 = 0, \quad (3.18)$$

where γ is a proportionality coefficient of order one. In the limit $\tau_w \rightarrow 0$, expression

3.18 gives $u_{cp} \rightarrow \gamma u_p$, recovering the characteristic velocity scale for the near detachment/reattachment point region originally proposed by STRATFORD (1959) and when the pressure gradient is zero expression 3.18 gives $u_{cp} = u_\tau$.

Considering a non-zero pressure gradient flow with wall transpiration, the analysis is the natural extension of the previous ones presented in this section. In such flows, the characteristic velocity scale is estimated from the highest real root of the algebraic equation,

$$u_c^3 - \alpha u_c^2 V_w - u_\tau^2 u_c - (\gamma u_p)^3 = 0. \quad (3.19)$$

3.2 New wall functions

3.2.1 Zero pressure gradient flows with wall transpiration

To derive an expression for the stream-wise mean velocity profile in the fully turbulent region close to the wall, some considerations with respect to the mean shear stress τ in that region will be done first. If the viscous contribution can be neglected, it will be considered that τ is affected essentially by two distinct mechanisms. One is momentum transport induced by eddies associated with the turbulence of the flow. The other represents the bulk influence of V_w in τ and it acts as an enhancement mechanism to the turbulent stresses when the flow is subjected to wall injection and as a suppression mechanism when suction is applied. With these considerations, it is assumed that τ can be written as the sum of two components, τ_e and τ_{v_w} , associated with these two mechanisms respectively,

$$\tau = \tau_e + \tau_{v_w}, \quad (3.20)$$

where the subscript e refers to eddy, and v_w to wall transpiration. Similar decompositions of the turbulent shear stress have been proposed in the past by different authors (MANES *et al.*, 2012; MENDOZA & ZHOU, 1992). Furthermore, in the expression for the turbulent stress, obtained from an integration of the approximated x -momentum equation, exact for the asymptotic suction boundary layer, given by

$$\tau = \tau_w + \rho V_w \bar{u}, \quad (3.21)$$

the turbulent stress is written as the sum of two components, where the influence of wall transpiration appears explicitly in the second one, $\rho V_w \bar{u}$, suggesting that, in the closure expression, the turbulent stress should also be written as the sum of two components, as in equation 3.20.

An expression for τ_e can be obtained assuming the Boussinesq hypothesis (BOUSSINESQ, 1870) and an analogy with Maxwell kinetic theory of gases (POPE,

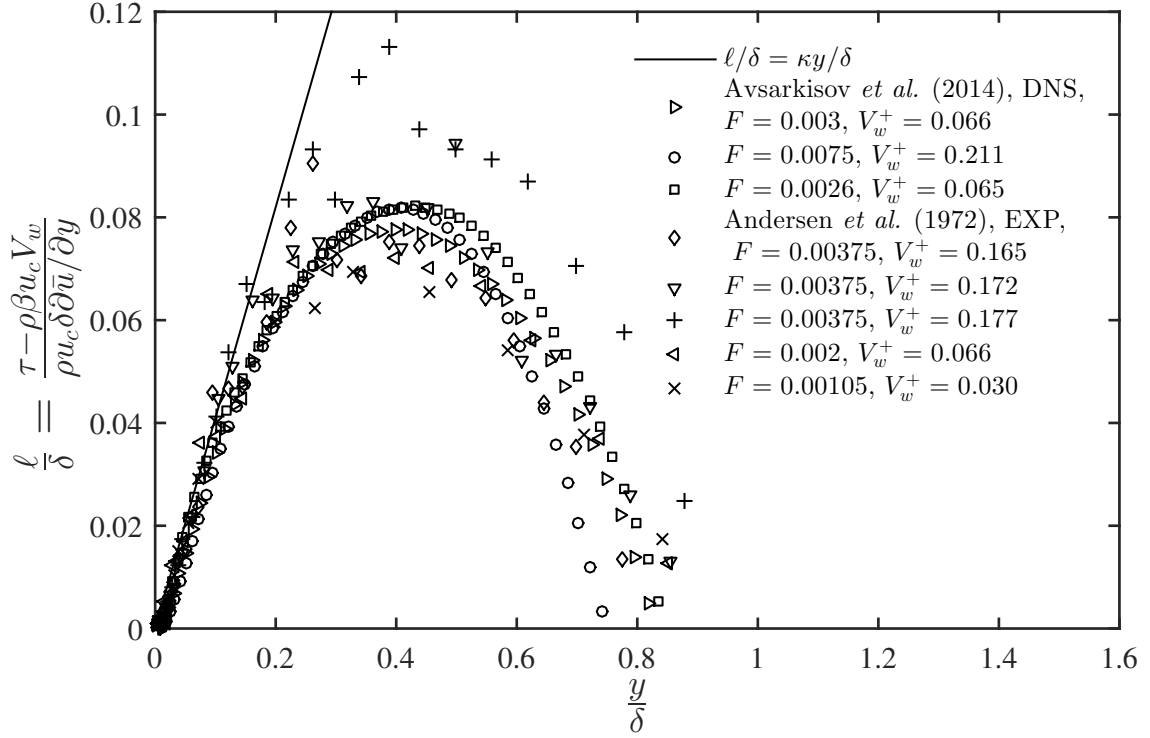


Figure 3.1: Experimental and DNS mixing length profiles accordingly with the proposed theory with $\alpha = 3.15$, $A = 0.35$ and $\kappa = 0.41$. $F = V_w/U_\infty$ is the dimensionless transpiration parameter.

2000; TENNEKES & LUMLEY, 1972),

$$\tau_e = \rho u_c \ell \frac{\partial \bar{u}}{\partial y}, \quad (3.22)$$

where $\ell = \kappa y$ is the mixing length. To write an expression for the component of the turbulent shear stress associated with the extra momentum transport caused by the wall transpiration, τ_{vw} , a cruder assumption will be made. This component must be zero in the case of a flow with zero wall transpiration. Furthermore, in accordance with well-known empirical information (ANDERSEN *et al.*, 1972), it should be positive in the case of blowing and negative in the case of suction. It should also be somehow related to the characteristic velocity of the flow, u_c . With that considerations in mind, one of the simplest assumption that one can make is that τ_{vw} is proportional to the transpiration velocity V_w and the characteristic velocity u_c ,

$$\tau_{vw} = \rho \beta u_c V_w, \quad (3.23)$$

where β is a proportionality constant of unity order. Figure 3.1 shows that equations 3.20 to 3.23 provide reasonable agreement with the data in the 15% (approximately) inner region of transpired flows with zero or negligible small pressure gradients. In section 4.4, it is shown that the proposed expression for the turbulent shear stress

gives an equivalent good fit to the data when compared to the classical expression obtained from the mixing length theory, i.e. when compared to $\tau = \rho \ell^2 (\partial \bar{u} / \partial y)^2$. The advantage of the new model is that it allows an analytical solution in the more general case of a transpired flow with non-zero pressure gradients.

With the assumptions made hitherto, the order of magnitude of the turbulent shear stress (per unit of ρ) is given by $O(\overline{u'v'}) = O(u_c^2) + O(u_c V_w)$. In a first glance, this seems to be inconsistent with the assumption made on section 3.1 that $O(\overline{u'v'}) = O(u_c^2)$. However, it can be shown that in the fully turbulent region of the flow where the turbulent stress is never negligibly small compared to the other terms in the equation of motion, $O(\overline{u'v'}) = O(u_c^2) + O(u_c V_w) = O(u_c^2)$, so no inconsistency is being made in this regard (see Appendix A).

Integrating expressions 3.20 to 3.23 and writing the result in an appropriate non-dimensional form yields,

$$\frac{\bar{u}}{u_c} = \frac{u_\tau^2}{u_c V_w} \left\{ \left(A \frac{y u_c}{\nu} \right)^{\frac{V_w}{\varkappa u_c}} - 1 \right\} + \beta, \quad (3.24)$$

where A is a constant of integration. Equation 3.24 is the new law of the wall for transpired turbulent flows with zero pressure gradients. Now it will be shown that in the particular case of a flow with zero wall transpiration, i.e. in the limit $V_w \rightarrow 0$, equation 3.24 reduces to the classic logarithmic-law of the wall. To evaluate equation 3.24 in that limit, it is useful to use the following property of the logarithms,

$$\ln z = \lim_{w \rightarrow 0} \frac{1}{w} (z^w - 1), \quad (3.25)$$

with $z = A y u_c / \nu$ and $w = V_w / (\varkappa u_c)$. In the limit $V_w \rightarrow 0$ equation 3.6 for the characteristic velocity scale of the flow gives $u_c = u_\tau$, so the new law of the wall evaluated at this limit gives,

$$\frac{\bar{u}}{u_\tau} = \frac{1}{\varkappa} \ln(A y^+) + \beta. \quad (3.26)$$

From equation 3.26 its clear that the classical logarithmic-law of the wall is recovered if the following equality is satisfied,

$$\frac{1}{\varkappa} \ln(A) + \beta = 5, \quad (3.27)$$

giving a formula to express the constant A as a function of β or vice versa. With equation 3.27, the new law of the wall has two constants that could not be obtained from theory and must be calibrated in order to give a good fit to the data. Convenient values was found to be $A = 0.35$ and $\alpha = 3.15$. In the author's opinion, a

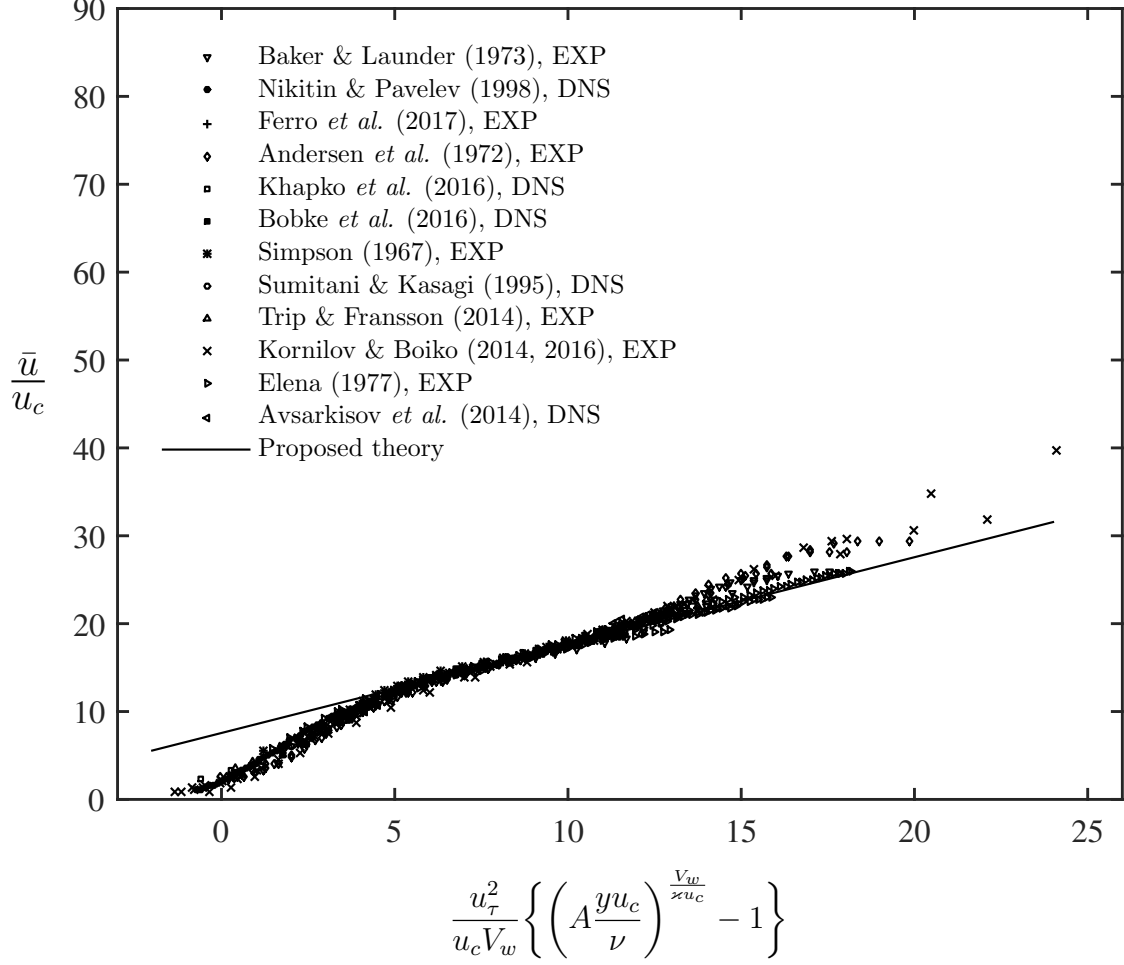


Figure 3.2: Thirty two (32) experimental (EXP) and DNS mean velocity profiles plotted with similarity coordinates. The values of the transpiration parameters are in the range $-0.00345 \leq F \leq 0.0164$, $-0.065 \leq V_w^+ \leq 0.87$ and are described in detail on table 3.1. The proposed theory is plotted with $A = 0.35$ and $\alpha = 3.15$.

theory that contain empirically calibrated constants are superior, in some sense, to a theory that contain empirical functions. From this viewpoint, the present formulation has an advantage over most versions of the bi-logarithmic or semi-logarithmic formulas. When plotted in non-dimensional coordinates suggested from the new law of the wall, experimental and DNS mean velocity profiles from several databases collapse onto one single curve in the whole near wall region of the flow (figure 3.2). The excellent collapse of the profiles suggests that there is self-similarity with respect to the transpiration velocity—a key result obtained in this study. The data shown in figure 3.2 include boundary layer flows with wall injection (ANDERSEN *et al.*, 1972; BAKER & LAUNDER, 1974b; KORNILOV & BOIKO, 2014, 2016) and suction (BOBKE *et al.*, 2016; FERRO *et al.*, 2017; KHAPKO *et al.*, 2016; SIMPSON, 1967; TRIP & FRANSSON, 2014), pipe flow with wall suction (ELENA, 1977) and closed channel flows with wall injection (AVSARKISOV *et al.*, 2014; NIKITIN &

Table 3.1: List of databases including the values of the non-dimensional transpiration parameters for each mean velocity profile shown in figure 3.2.

Database	F	V_w^+
SIMPSON (1967), EXP	-0.0011, -0.00238, -0.00251	-0.0022, -0.0044, -0.0044
ANDERSEN <i>et al.</i> (1972), EXP	0.001, 0.002, 0.00376	0.03, 0.067, 0.182
BAKER & LAUNDER (1974b), EXP	0.0011, 0.0021	0.029, 0.06
ELENA (1977), EXP	-0.00083, -0.00197, -0.0032	-0.014, -0.032, -0.049
SUMITANI & KASAGI (1995), DNS	0.00344	0.061
NIKITIN & PAVELEV (1998), DNS	0.01	0.221
TRIP & FRANSSON (2014), EXP	-0.0008, -0.001, -0.0014	-0.018, -0.021 -0.028
KORNILOV & BOIKO (2014), EXP	0.0015, 0.0029, 0.0043,	0.046, 0.108, 0.194
AVSARKISOV <i>et al.</i> (2014), DNS	0.0026, 0.003, 0.0069, 0.0075, 0.0164, 0.016	0.065, 0.066, 0.16 0.211, 0.681, 0.871
KORNILOV & BOIKO (2016), EXP	0.00395	0.239
BOBKE <i>et al.</i> (2016), DNS	-0.003	-0.055
KHAPKO <i>et al.</i> (2016), DNS	-0.00345	-0.059
FERRO (2017), EXP	-0.00258, -0.00283, -0.00309, -0.00327	-0.051, -0.053 -0.056, -0.058

PAVELEV, 1998; SUMITANI & KASAGI, 1995). Assessment of the data is provided at section 4.1.

The thermal law of the wall can be obtained from an analogy with the fluid dynamic model in the following manner. It is assumed that the turbulent heat flux can be written as the sum of two components,

$$\bar{q} = q_e + q_{v_w}, \quad (3.28)$$

where q_e is associated with the larger, turbulent-energy-carrying eddies and q_{v_w} represents the bulk influence of transpiration in \bar{q} . The first term on the right-hand side of equation 3.28, q_e , will be modeled with a thermal version of the Boussinesq hypothesis given by,

$$q_e = -\rho c_p u_c \ell_T \frac{\partial \bar{T}}{\partial y}, \quad (3.29)$$

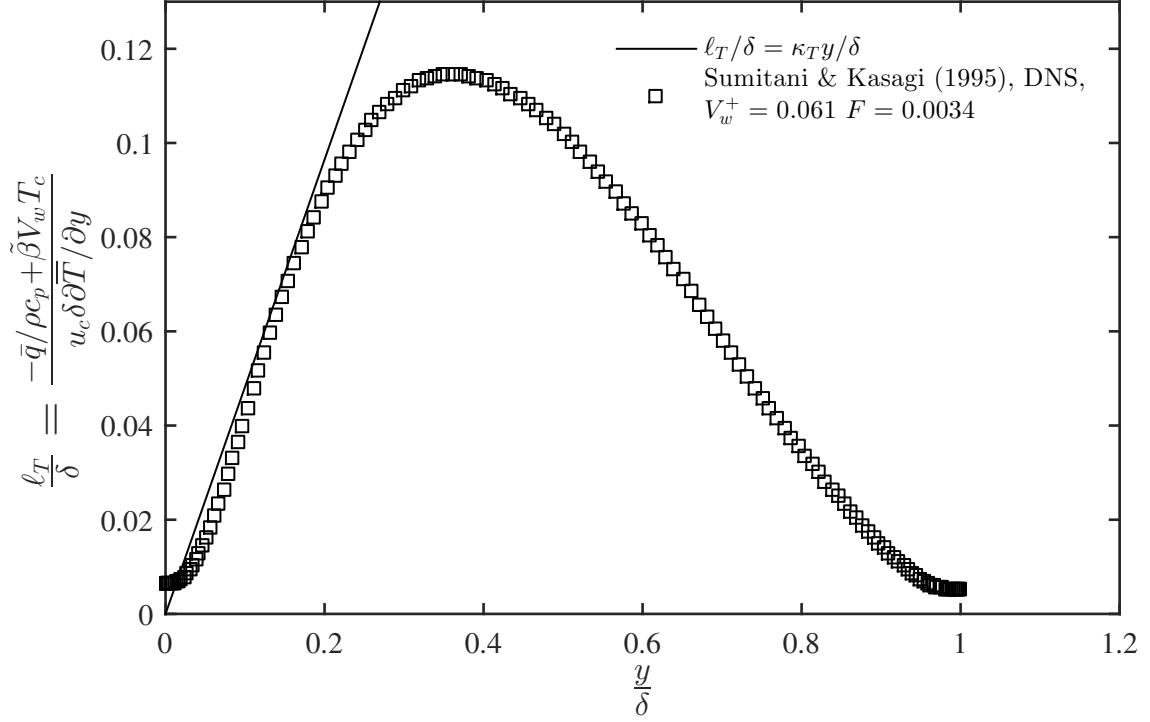


Figure 3.3: DNS thermal mixing length profiles compared to the proposed theory with $\alpha = 3.15$, $A_T = 0.6$ and $\kappa_T = 0.482$.

where $\ell_T = \kappa_T y$ is the thermal mixing length. The second term will be modeled using simple dimensional analysis,

$$q_{vw} = \rho c_p \tilde{\beta} V_w T_c, \quad (3.30)$$

where $\tilde{\beta}$ is a proportionality factor of order one and T_c is a characteristic temperature scale given by

$$T_c = \frac{q_w}{\rho c_p u_c}, \quad (3.31)$$

obtained from an analogy with the friction temperature scale, $T^* = q_w/(\rho c_p u_\tau)$, but with u_τ replaced by u_c . The validity of these assumptions is tested against the DNS data from SUMITANI & KASAGI (1995) in figure 3.3 (with $\tilde{\beta}$ obtained from equation 3.34). As it can be seen from the figure, good agreement between theory and the data is obtained in the near wall region of the flow. Integrating equations 3.29 to 3.31 with the approximated governing equation,

$$\bar{q} = q_w + \rho c_p V_w (T_w - \bar{T}), \quad (3.32)$$

and writing the result in a proper non dimensional form gives,

$$\frac{T_w - \bar{T}}{T_c} = \frac{u_c}{V_w} \left\{ \left(A_T \frac{y u_c}{\nu} \right)^{\frac{V_w}{\kappa_T u_c}} - 1 \right\} + \tilde{\beta}, \quad (3.33)$$

Table 3.2: List of databases including the values of the non-dimensional transpiration parameters for each mean temperature profile shown in figure 3.4.

Database	F	V_w^+
WHITTEN (1967), EXP	$-0.00251, -0.00238,$	$-0.043, -0.044$
	$-0.0011, 0.00096$	$-0.022, 0.026$
	$0.00186, 0.00378$	$0.056, 0.16$
SUMITANI & KASAGI (1995), DNS	0.00344	0.061

where A_T is a constant of integration. An expression for $\tilde{\beta}$ is obtained when the new thermal law of the wall is evaluated in the limit $V_w \rightarrow 0$,

$$\tilde{\beta} = C(Pr) - \frac{1}{\varkappa_T} \ln(A_T), \quad (3.34)$$

where $C(Pr)$ is the y -axis intercept in the thermal logarithmic law of the wall for non transpired flows.

When non dimensional mean temperature profiles from flows with different values of the transpiration rate are plotted with coordinates suggested from the new thermal law of the wall, scaled by T_c and ν/u_c , an excellent collapse is obtained in the near wall region of the flow (figure 3.4). The new theory with $A_T = 0.6$ and $\alpha = 3.15$ gives an excellent fit to the boundary layer flow with injection or suction data from WHITTEN (1967) and the channel flow data from SUMITANI & KASAGI (1995) (injection side) but not to the pipe flow with suction data from ELENA (1977). A possible explanation for this fact is that in the latter there is considerable deceleration of the flow caused by wall suction. This deceleration is not present in the boundary layer or in the channel flow simulated by SUMITANI & KASAGI (1995). A good fit to ELENA (1977) data can be obtained with $A_T = 3.2$ instead (figure 3.5), indicating that, unfortunately, this constant is flow geometry dependent.

3.2.2 Non zero pressure gradient flows with zero wall transpiration

Considering the case of a flow with non-zero pressure gradients but zero wall transpiration, the turbulent shear stress will be modeled using the BOUSSINESQ (1870) hypothesis and the—modified—mixing length concept;

$$\tau = \rho u_{cp} \ell \frac{\partial \bar{u}}{\partial y}, \quad (3.35)$$

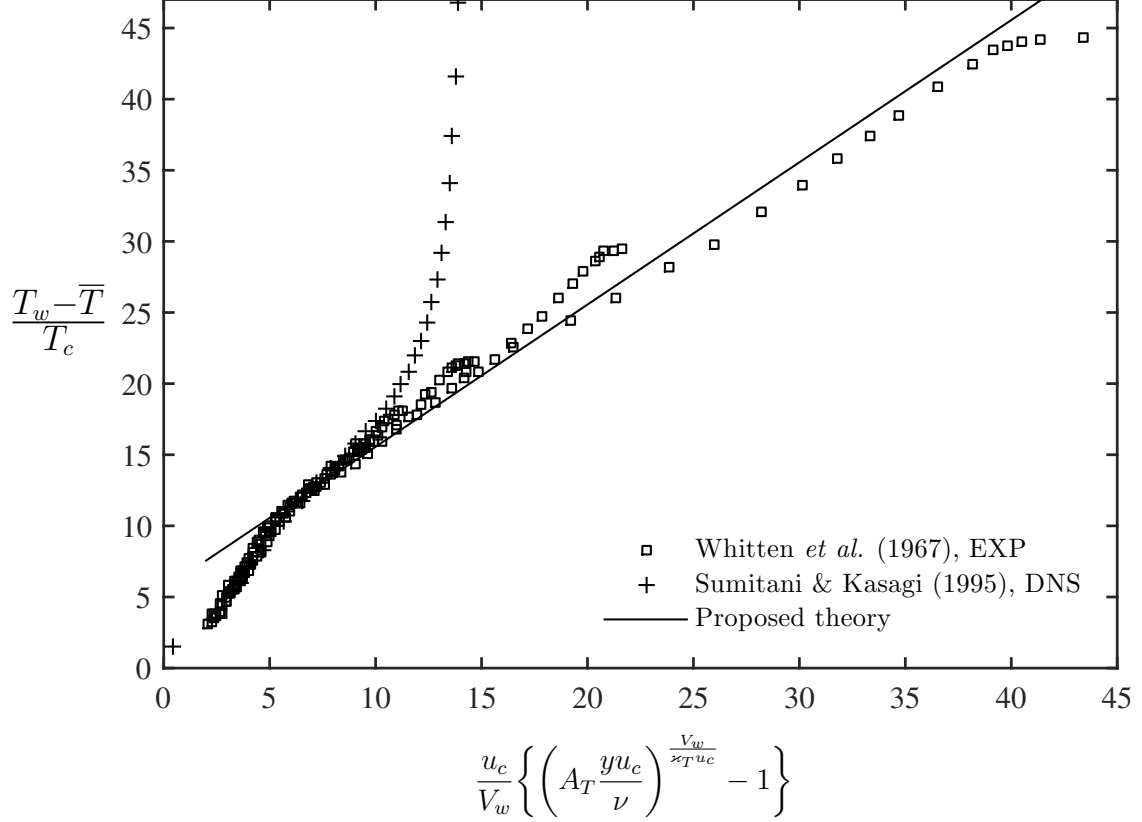


Figure 3.4: Eight EXP and DNS mean temperature profiles plotted with similarity coordinates. The values of the transpiration parameters are in the range $-0.00251 \leq F \leq 0.00378$, $-0.044 \leq V_w^+ \leq 0.16$ and are described in detail on table 3.2. The proposed theory is plotted with $A_T = 0.6$ and $\alpha = 3.15$.

where u_{cp} is the characteristic velocity scale of the flow. In this simplified analysis, the recommendation made by SIMPSON (1989) that near separation the turbulent stress should not be modeled using the mean velocity gradient has been ignored—in the separation region there are points where the mean velocity gradient is zero but the turbulent stresses don't. However, comparisons with experimental and DNS results from different databases (DENGEL & FERNHOLZ, 1990; GUNGOR *et al.*, 2016; MACIEL *et al.*, 2006; MARUŠIĆ & PERRY, 1995; SKOTE & HENNINGSON, 2002) show that in the near wall region of the flow this approximation is of fair accuracy for the present proposes (figure 3.6 and section 4.4).

It is well-known that the usual two terms Taylor series approximation (or Couette flow approximation) for the mean shear stress,

$$\tau = \tau_w + \frac{dP_w}{dx} y, \quad (3.36)$$

is very inaccurate even for boundary layer flows with a small pressure gradient parameter P^+ . The reason for this is that the stress gradient $\partial\tau/\partial y$ is considerable different from its value at the wall, $\partial P_w/\partial x$, even in the region close to the wall

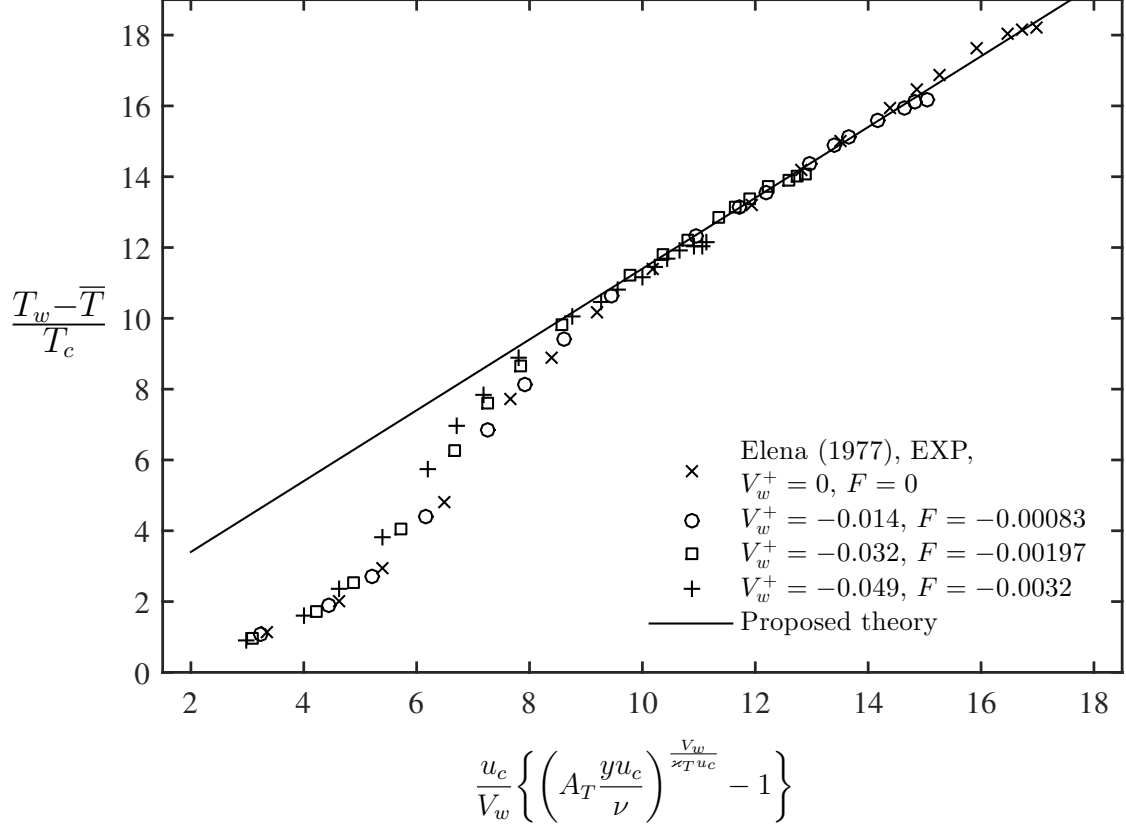


Figure 3.5: Pipe flow with wall suction EXP mean temperature profiles plotted with similarity coordinates. The proposed theory is plotted with $A_T = 3.2$ and $\alpha = 3.15$.

just outside of the viscous sub-layer. The introduction of higher order terms in the Taylor series would only worsen the situation as the series rapidly diverge. A more accurate approximation can be obtained if a non-dimensional coefficient λ is introduced in order to reduce the influence of the pressure gradient,

$$\tau = \tau_w + \lambda \frac{dP_w}{dx} y. \quad (3.37)$$

In the light of MCDONALD's (1969) work, λ is the ratio of stress to pressure gradient and is caused by the influence of the inertia terms near the wall. Analyzing NEWMAN (1951) data, MCDONALD (1969) found that the value of λ dropped lower than $1/3$ as separation was approached, but he concluded that $\lambda = 0.7$ was a good approximation for most datasets that he analyzed. PERRY *et al.* (1966) proposed a varying λ from 0.65 to 0.9, while GRANVILLE (1989) set $\lambda = 0.9$. KNOPP *et al.* (2015) obtained a value of $\lambda = 0.6$ for their own data and $\lambda = 0.9$ for SKÅRE & KROGSTAD (1994) data. Comparing equation 3.37 to experimental and DNS results from many databases the author found that $\lambda < 1$ is a better approximation than $\lambda = 1$ for most of the profiles but its precise value do vary. For the sake of simplicity, λ will be considered here as a calibration parameter with a

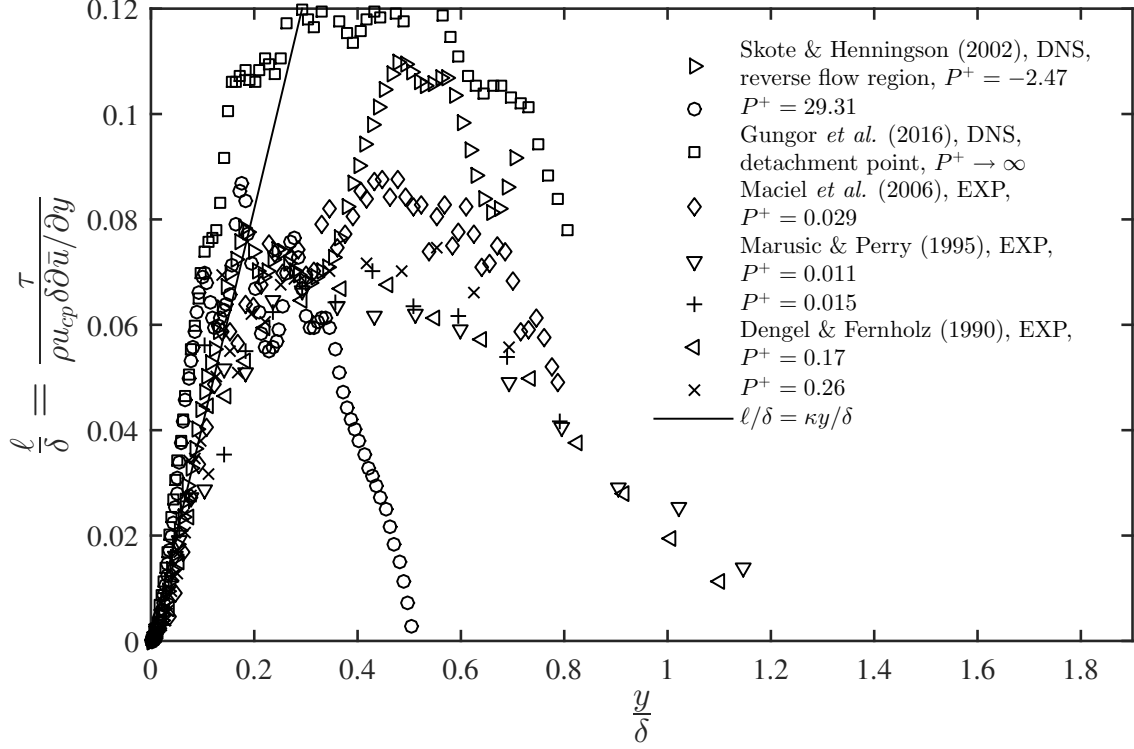


Figure 3.6: EXP and DNS mixing length profiles from high APG and separated flows compared with the proposed theory with $\gamma = 3.4$ and $\kappa = 0.41$.

constant value that will be chosen to give a good fit between the proposed model and the velocity profiles data. A convenient value was found to be $\lambda = 0.45$. Integrating equation 3.35 with 3.37 in the wall normal direction and writing the result in the non-dimensional form leads to,

$$\frac{\bar{u}}{u_{cp}} = \frac{u_\tau^2}{\varkappa u_{cp}^2} \ln \left(\frac{y u_{cp}}{\nu} \right) + \lambda \frac{u_p^3}{\varkappa u_{cp}^3} \left(\frac{y u_{cp}}{\nu} \right) + f(x), \quad (3.38)$$

where $f(x)$ is a constant (in $y u_c / \nu$) of integration. Equation 3.38 has a similar form to those proposed by other authors (SIMPSON, 1983; WILCOX, 1989); in particular, it contains a combination of logarithmic and linear terms. When experimental and DNS mean velocity profiles are plotted with coordinates \bar{u}/u_{cp} versus the right-hand side of equation 3.38 without $f(x)$, they look like straight lines with a unity slope but, unfortunately, they do not collapse onto one single curve. This means that $f(x)$ is a function of the stream-wise direction, x . The functional form of $f(x)$ will be derived here analytically, using the blending region between the sub-layer and the fully turbulent layer. Evaluating equation 3.38 at the point where it intercepts with the sub-layer solution, the point (y_a, u_a) , leads to

$$f(x) = \frac{u_a}{u_{cp}} - \frac{u_\tau^2}{\varkappa u_{cp}^2} \ln \left(\frac{y_a u_{cp}}{\nu} \right) - \lambda \frac{u_p^3}{\varkappa u_{cp}^3} \left(\frac{y_a u_{cp}}{\nu} \right). \quad (3.39)$$

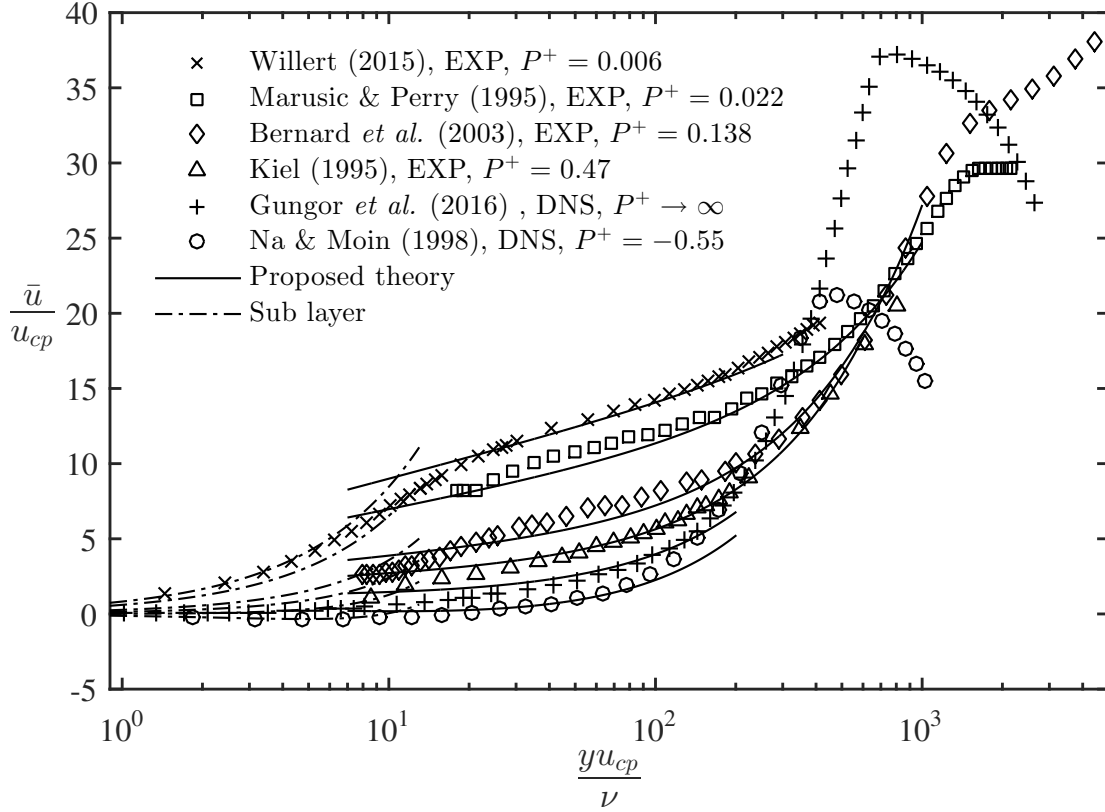


Figure 3.7: Experimental and DNS mean velocity profiles from non-zero pressure gradient flows compared to the proposed theory with $\gamma = 3.4$ and $\lambda = 0.45$.

The problem now is to determine y_a and u_a , so two more independent equations are needed. One equation is the viscous sub-layer solution,

$$\frac{\bar{u}}{u_\tau} = \frac{yu_\tau}{\nu} + \frac{1}{2} \left(\frac{u_p}{u_\tau} \right)^3 \left(\frac{yu_\tau}{\nu} \right)^2, \quad (3.40)$$

that can be used to express u_a in terms of y_a . The second equation is obtained in the limit $\partial \bar{P}/\partial x \rightarrow 0$. It is known that, in the zero pressure gradient case, $y_a u_\tau/\nu$ assumes a constant value of approximately 10.8. This is certainly not the case in a non-zero pressure gradient flow—recall that u_τ can be zero. In the limit $\partial \bar{P}/\partial x \rightarrow 0$, the characteristic velocity scale is given by $u_{cp} \rightarrow u_\tau$ so, the simplest expression for $y_a u_{cp}/\nu$ that have the correct asymptotic behavior is,

$$\frac{y_a u_{cp}}{\nu} = 10.8. \quad (3.41)$$

In other words, $f(x) \rightarrow 5$ when $\partial \bar{P}/\partial x \rightarrow 0$ if $y_a u_{cp}/\nu = 10.8$, and the logarithmic law of the wall for zero pressure gradient flows is recovered. Figure 3.7 shows the new law of the wall with $\lambda = 0.45$ and $\gamma = 3.4$ and the viscous sub-layer solution for different values of the pressure gradient parameter, P^+ , including profiles in the separation zone. It can be viewed that the intercept between these two solutions

is always at $y_a u_{cp}/\nu = 10.8$. Some data from different authors (BERNARD *et al.*, 2003; GUNGOR *et al.*, 2016; KIEL, 1995; MARUŠIĆ & PERRY, 1995; NA & MOIN, 1998; WILLERT, 2015) is also shown in the figure. The new formulation gives an excellent fit to the data, specially considering that these are not the curves that best fit the data, they were all plotted with the same values of λ and γ and these parameters were not re-calibrated for each profile.

The new scaling proposed in this work also allows some interesting results from the zero pressure gradient case to be extrapolated to the non-zero case. For example, if an estimation of the viscous sub-layer thickness in the zero pressure gradient case is given by $\delta_{\text{sub}} = 5.5\nu/u_\tau$, in the non-zero pressure gradient case is given by $\delta_{\text{sub}} = 5.5\nu/u_{cp}$.

In the thin region around the detachment/reattachment points, where $\tau_w \rightarrow 0$ and $P^+ \rightarrow \infty$, the new law of the wall assumes the form of a linear function,

$$\frac{\bar{u}}{u_p} = \frac{\lambda}{\varkappa\gamma} \left(\frac{yu_p}{\nu} \right) + \frac{10.8^2}{2\gamma^2} - \frac{10.8\lambda}{\varkappa\gamma^2}. \quad (3.42)$$

This result doesn't agree with the well-established *half power law*, proposed first by STRATFORD (1959) based on the mixing length formula, but when mean velocity profiles are plotted with a non-dimensional linear coordinates system, a linear portion appears in the near wall region of the flow (figure 3.8a). Furthermore, as it is shown in figure 3.8b, in that region a linear power law gives an equivalent fit to the data when compared to the half power law—the small disagreement between this two laws can be attenuated with small changes in their calibration parameters or it can be argued that it is within the interval of experimental uncertainties. Figure 3.8b also shows that the domains of validity of these two laws are, approximately, in the range $5 \leq yu_p/\nu \leq 30$.

To derive an expression for the near wall mean temperature profile no analogy between the thermal and the mechanical problem was attempted. The reason for that becomes evident when one compares the momentum and the energy equations (with respective boundary conditions) in the case of a non-zero pressure gradient flow—there are no mathematical similarities between them. Furthermore, the experimental data from BLACKWELL *et al.* (1972) and PAK (1999) suggest that the turbulent Prandtl number near the wall is a function of the pressure gradient parameter, indicating the break down of the Reynolds analogy in such flows. In this light new hypothesis regarding the turbulent fluctuations will be done in order to derive a new turbulence closure model for the governing equation. Assuming that

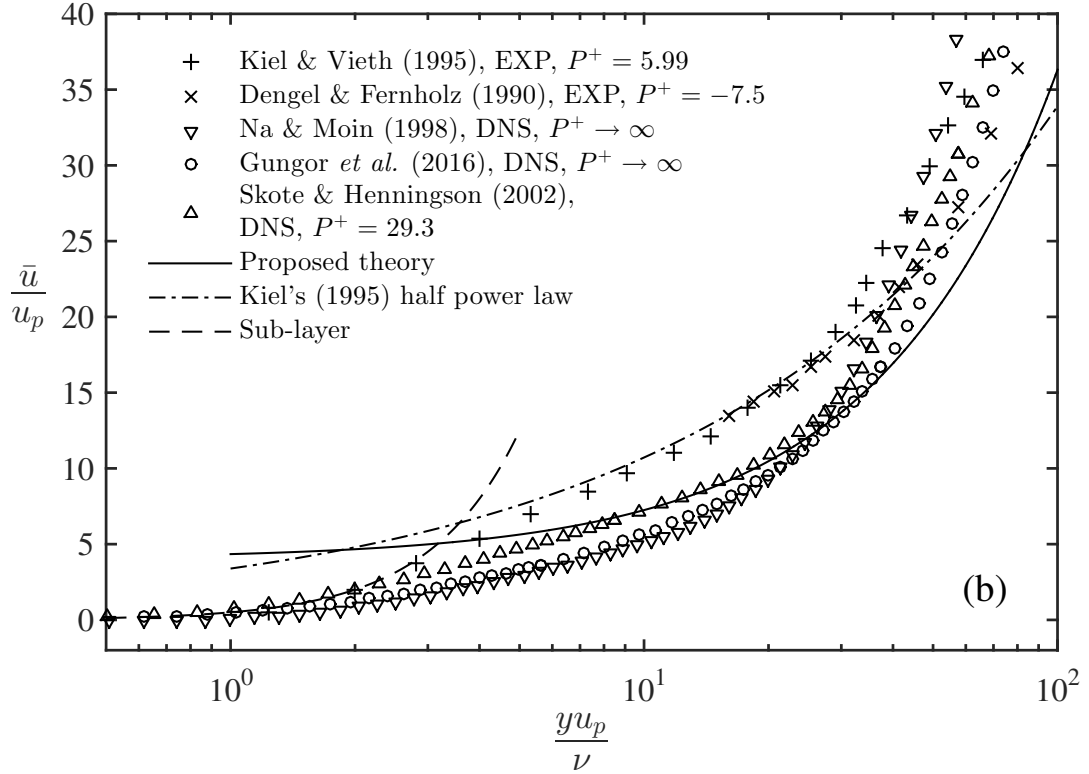
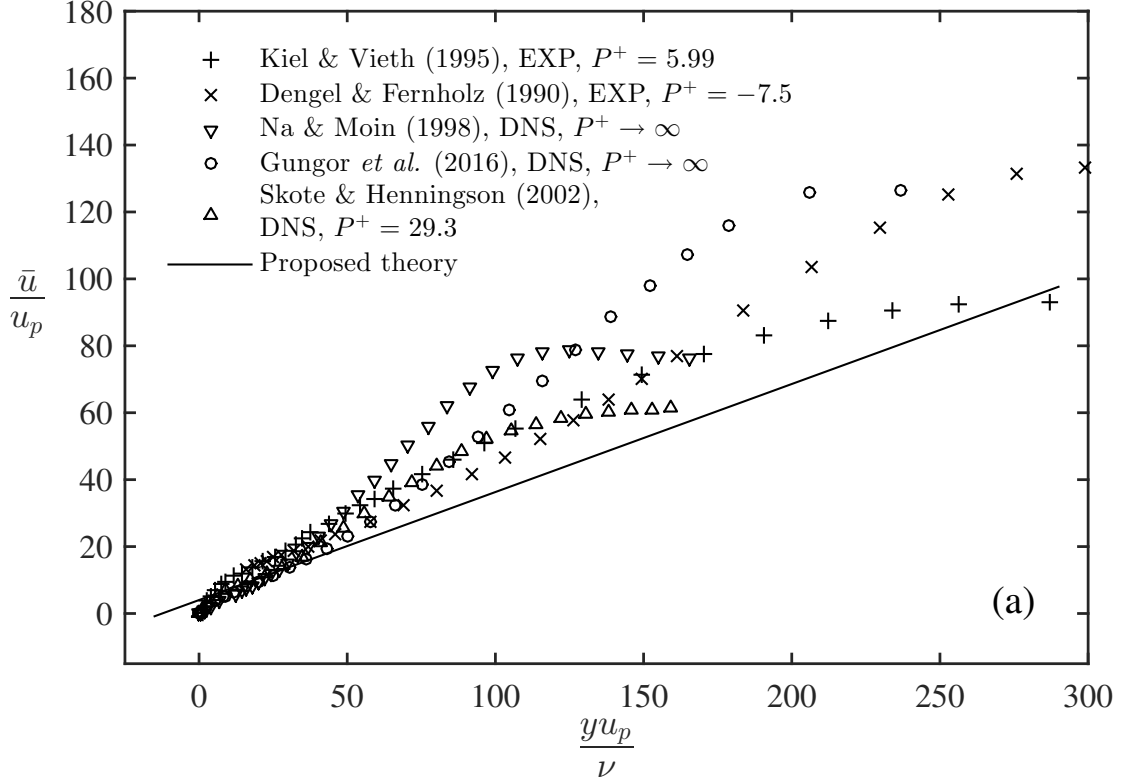


Figure 3.8: EXP and DNS mean velocity profiles at the detachment/reattachment point of flat plate boundary layer flows compared to the proposed theory with $\gamma = 3.4$ and $\lambda = 0.45$; (a) a view of the complete profiles; (b) a zoom in the near wall region.

v' and T' scale accordingly to the following expressions,

$$v' \sim \sqrt{u'v'} = \sqrt{\kappa y u_c \frac{\partial \bar{u}}{\partial y}} = \sqrt{\frac{\tau_w}{\rho} + \frac{1}{\rho} \frac{dP_w}{dx}} y, \quad (3.43)$$

and equivalently for T' ,

$$T' \sim \sqrt{-\kappa_T y T_c \frac{\partial \bar{T}}{\partial y}}, \quad (3.44)$$

suggests that the turbulent heat flux can be modeled accordingly to,

$$\bar{q} = \rho c_p \sqrt{\frac{\tau_w}{\rho} + \frac{1}{\rho} \frac{dP_w}{dx}} y \sqrt{-\kappa_T y T_c \frac{\partial \bar{T}}{\partial y}}. \quad (3.45)$$

In order to have at least one free parameter to calibrate the model, the above expression will be calculated with u_c from equation 3.18 and a thermal proportionality constant $\gamma_T = 3.1$ instead of $\gamma = 3.4$ used for the mean velocity profile. When compared to BLACKWELL *et al.* (1972) and ORLANDO *et al.* (1974) experimental data, equation 3.45 with $\gamma_T = 3.1$ shows a good agreement in the near wall region of the layer (figure 3.9). In section 4.5, it is shown that the proposed expression for the turbulent heat flux gives an equivalent good fit to the data when compared to the classical expression obtained from mixing length theory, i.e. when compared to $q = \rho c_p \ell \partial \bar{u} / \partial y \ell_T \bar{T} / \partial y$. The advantage of the new model is that it allows an analytical solution in the more general case of a transpired flow with non-zero pressure gradients.

The second hypothesis to be done is the classical one that near the wall the turbulent heat flux is approximately constant,

$$\bar{q} = q_w. \quad (3.46)$$

In the author knowledge there is no experimental justification for this approximation in the separation region of the flow but, for attached layers with adverse pressure gradients as strong as $P^+ \sim 0.04$, the data from BLACKWELL *et al.* (1972) and ORLANDO *et al.* (1974) compares well with it.

Integrating equations 3.46 with 3.45 in the wall normal direction leads to,

$$\frac{T_w - \bar{T}}{T_c} = \frac{1}{\kappa_T} \frac{u_c^2}{u_\tau^2} \left\{ \ln \left(\frac{y u_c}{\nu} \right) - \ln \left(\frac{u_\tau^2}{u_c^2} + \frac{u_p^3 y u_c}{u_c^3 \nu} \right) \right\} + \tilde{C}, \quad (3.47)$$

where the constant of integration \tilde{C} should be determined in order to guarantee boundedness when $u_\tau \rightarrow 0$ and the correct asymptotic behavior when $\partial P_w / \partial x \rightarrow 0$. One of the simplest expression with that properties was found by inspection and is

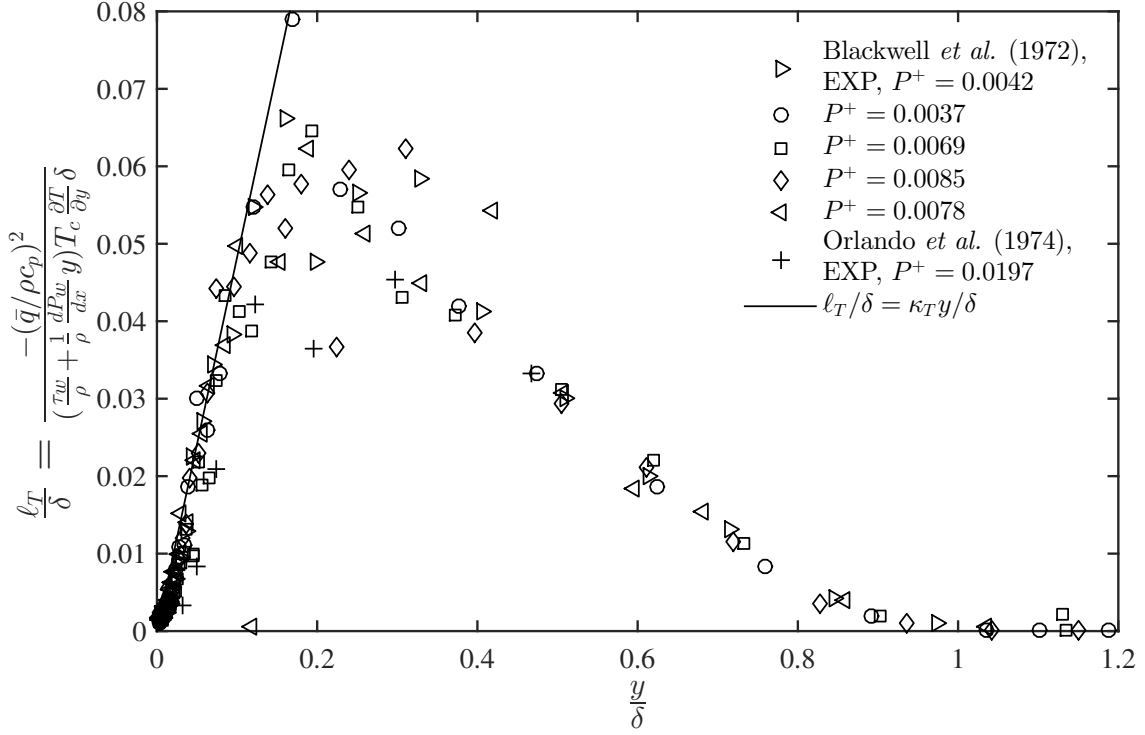


Figure 3.9: EXP thermal mixing length profiles compared to the proposed theory with $\gamma_T = 3.1$ and $\kappa_T = \varkappa_T = 0.482$.

given by,

$$\tilde{C} = \frac{1}{\varkappa_T} \frac{u_c^2}{u_\tau^2} \ln(\gamma_T^{-3}) - \frac{1}{\varkappa_T} \frac{u_\tau}{u_c} \ln(\gamma_T^{-3}) + C(Pr), \quad (3.48)$$

where $C(Pr)$ is the y -axis intercept in the thermal logarithmic law of the wall for zero pressure gradient flows. As $u_p^3/u_c^3 \rightarrow \gamma_T^{-3}$ when $u_\tau \rightarrow 0$, the first term in the right hand side (r.h.s) of equation 3.48 guarantees boundedness in that limit and as $u_c/u_\tau \rightarrow 1$ when $\partial P_w/\partial x \rightarrow 0$ the last two terms make the new thermal law of the wall correct for zero pressure gradient flows, but the factor u_τ/u_c has a rather empirical flavor—the vanishing of this term close to separation gives a better fit to VOGEL (1984) data. Equation 3.48 allows the new thermal law of the wall to be written as,

$$\frac{T_w - \bar{T}}{T_c} = \frac{1}{\varkappa_T} \ln \left\{ \frac{\left(\frac{yu_c}{\nu} \gamma_T^{-3} \right)^{\frac{u_c^2}{u_\tau^2} \gamma_T^{\frac{3u_\tau}{u_c}}}}{\left(\frac{u_\tau^2}{u_c^2} + \frac{u_p^3}{u_c^3} \frac{yu_c}{\nu} \right)^{\frac{u_c^2}{u_\tau^2}}} \right\} + C(Pr), \quad (3.49)$$

suggesting that mean temperature profiles should be plotted with coordinates as those shown in figure 3.10. As it can be seen from that figure, the profiles from ORLANDO *et al.* (1974) data do not collapse with those from BLACKWELL *et al.* (1972) data in the whole near wall region but, in an intermediary region of the layer the proposed theory gives an excellent fit to both data sets.

In the region of vanishing wall shear stress the new thermal law of the wall

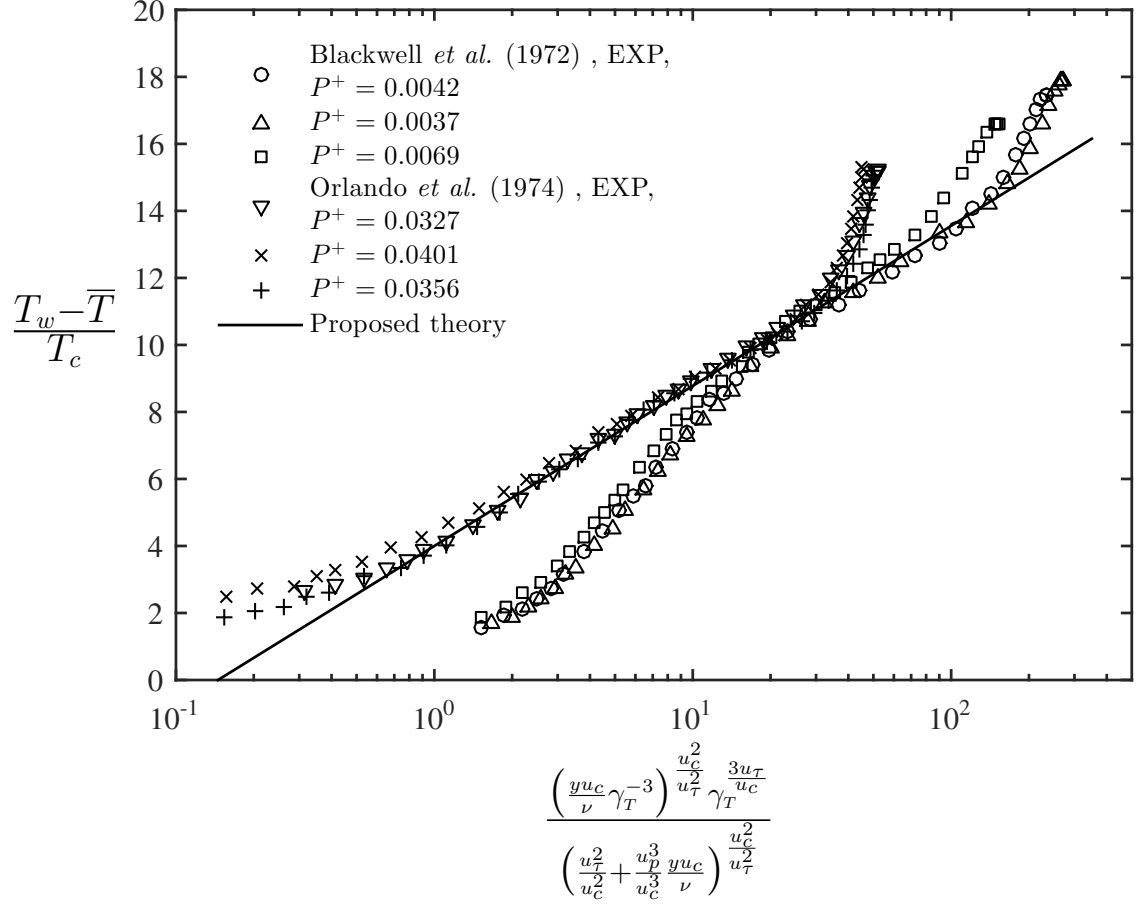


Figure 3.10: EXP mean temperature profiles from strong and mild APG boundary layer flows compared to the proposed theory with $\gamma_T = 3.1$.

assumes the form of an *inverse linear power law* given by,

$$\frac{T_w - \bar{T}}{T_p} = -\frac{\gamma_T}{\varkappa_T} \left(\frac{yu_p}{\nu} \right)^{-1} + \frac{C(Pr)}{\gamma_T} + \frac{1}{\gamma_T \varkappa_T}. \quad (3.50)$$

When this equation is compared to VOGEL (1984) data of a backward-facing step flow, good agreement is obtained in the near wall region (figure 3.11).

The performance of the model is considerably good considering that it has only one calibration constant, $\gamma_T = 3.1$, that do not vary with P^+ while in other models both the thermal Karman constant and y -axis intercept are empirically calibrated functions of P^+ . Another advantages of the proposed formulation over the classical models is the far superior fit that it gives to the data (see section 4.3) and that its domain of validity can be extended, to include the effects of wall transpiration and pressure gradients (see section 3.2.3).

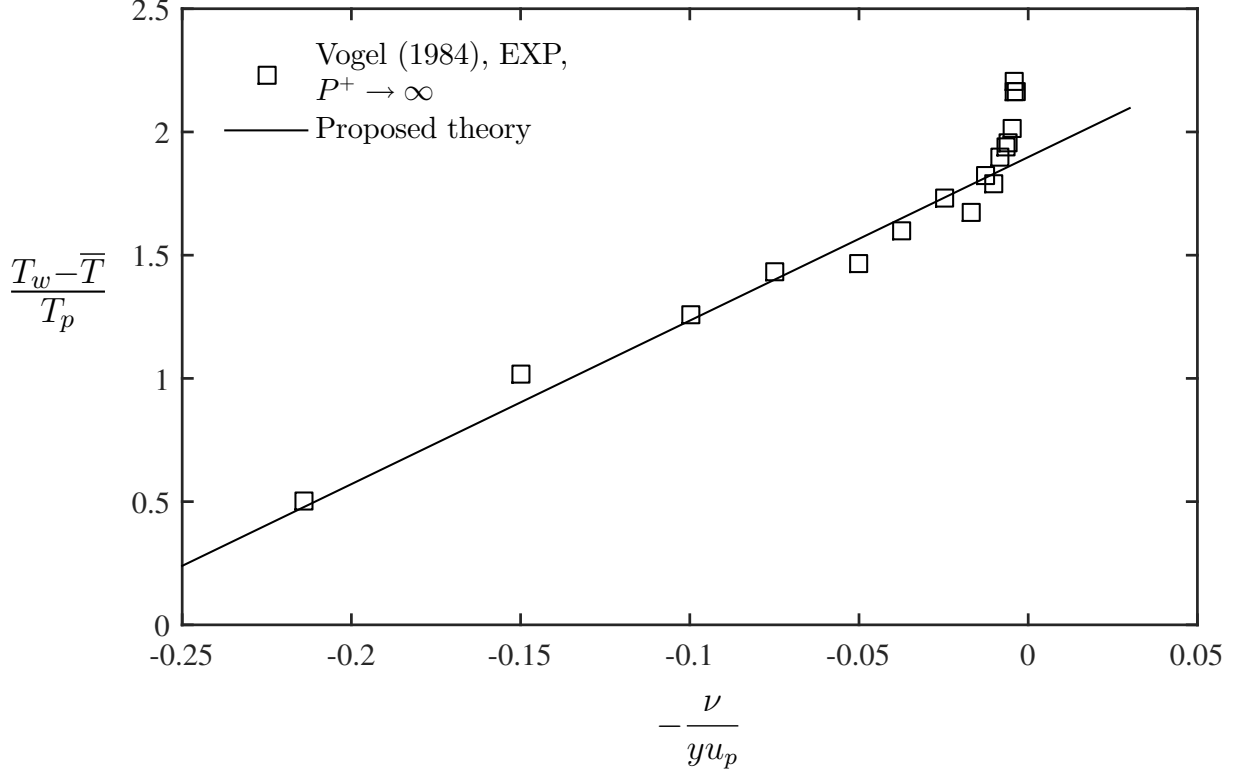


Figure 3.11: EXP mean temperature profile from a separated flow compared to the proposed theory with $\gamma_T = 3.1$.

3.2.3 Non zero pressure gradient flows with wall transpiration

An important application of wall transpiration is flow separation control. While suction can suppress flow separation, blowing has the opposite effect. Here, new wall laws for turbulent flows with the combined effects of wall transpiration and pressure gradient, including flow separation, will be derived. As wall functions for this kind of flows are not available in the literature, it is the author's opinion that this might be one of the main contributions of this work.

Considering first the mean velocity profile, the derivation procedure is an extension of those presented in the last sections. The two equations to be solved are the approximated equation of motion

$$\tau = \tau_w + \lambda \frac{dP_w}{dx} y + \rho V_w \bar{u}, \quad (3.51)$$

with a turbulence closure given by

$$\tau = \rho u_c \kappa y \frac{\partial \bar{u}}{\partial y} + \beta \rho u_c V_w, \quad (3.52)$$

where u_c is obtained from the solution of the cubic equation 3.19. Equation 3.52

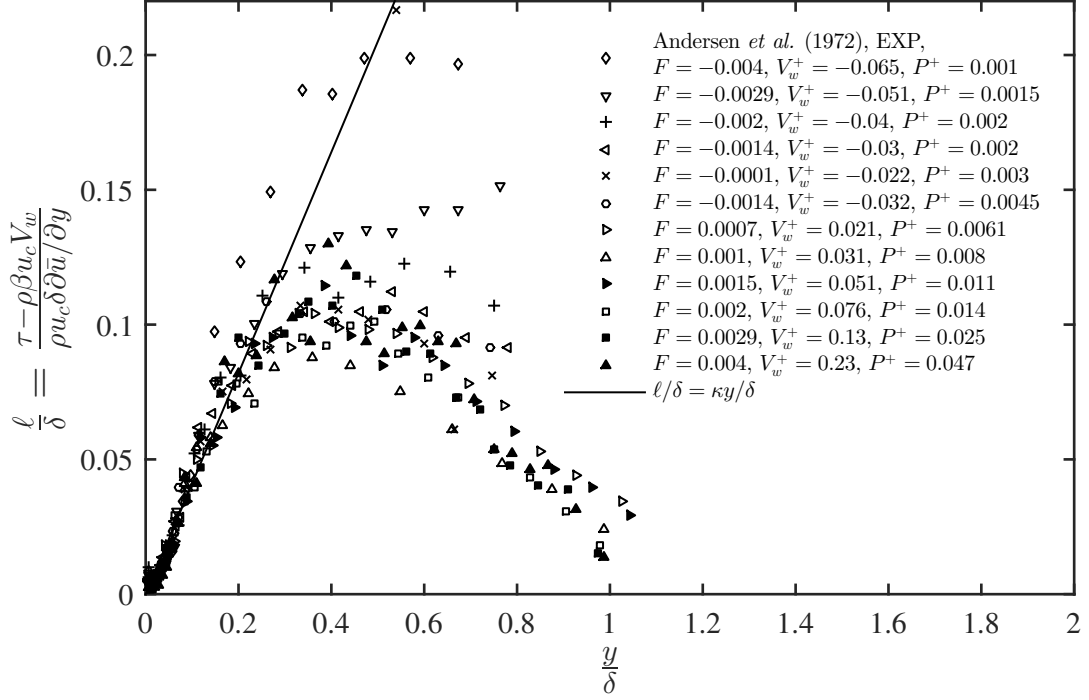


Figure 3.12: Mixing length profiles from high APG boundary layer flows with wall transpiration compared to the proposed theory with $\alpha = 3.15$, $A = 0.35$, $\gamma = 3.4$, $\lambda = 0.45$ and $\kappa = 0.41$.

is compared with the experimental data from ANDERSEN *et al.* (1972) in figure 3.12, in the form of mixing length profiles, showing good agreement in the near wall region of the flow. One of the beauties of the model proposed in this work is that it allows a simple analytical solution, where conventional mixing length models don't. Integrating equations 3.51 with 3.52 in the wall normal direction and writing the result in an appropriate non-dimensional form yields,

$$\frac{\bar{u}}{u_c} = \frac{u_\tau^2}{u_c V_w} \left\{ \left(A \frac{y u_c}{\nu} \right)^{\frac{V_w}{\kappa u_c}} - 1 \right\} + \lambda \frac{u_p^3}{\kappa u_c^3 - u_c^2 V_w} \left(\frac{y u_c}{\nu} \right) - \frac{u_\tau^2}{\kappa u_{cp}^2} \ln(A) + f(x), \quad (3.53)$$

where $f(x)$ is given by equation 3.39 and is re-written explicitly here,

$$f(x) = \frac{1}{2} \left(\frac{u_p}{u_{cp}} \right)^3 10.8^2 + \left(\frac{u_\tau}{u_{cp}} \right)^2 10.8 - \left(\frac{u_\tau}{u_{cp}} \right)^2 \frac{\ln(10.8)}{\kappa} - \lambda \left(\frac{u_p^3}{\kappa u_{cp}^3} \right) 10.8. \quad (3.54)$$

In the derivation of equation 3.53 the integration constant was chosen to force the new law of the wall to have the correct asymptotic behavior in the limits $V_w \rightarrow 0$ and $P^+ \rightarrow 0$, i.e. to have equations 3.24 and 3.38 as particular cases.

The new law of the wall, equation 3.53, has four empirically calibrated constants, $A = 0.35$, $\alpha = 3.15$, $\lambda = 0.45$ and $\gamma = 3.4$, so it's acknowledged that it may suffer from over-fitting. However, these values were calibrated with data from two limiting cases and were not re-calibrated for the case where the combined effects

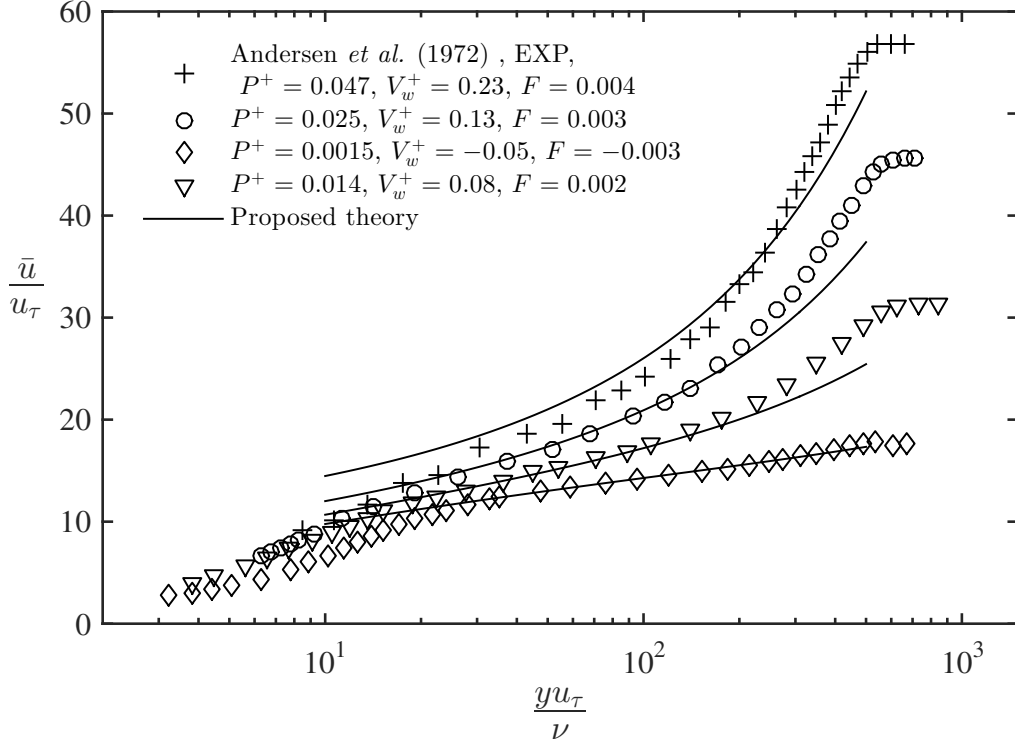


Figure 3.13: Experimental mean velocity profiles from mild and strong APG boundary layer flows with wall transpiration compared to the proposed theory with $\alpha = 3.15$, $A = 0.35$, $\gamma = 3.4$ and $\lambda = 0.45$.

of pressure gradient and wall transpiration are present. Furthermore, a comparison with ANDERSEN's *et al.* (1972), BLACKWELL's *et al.* (1972) and ORLANDO's *et al.* (1974) data of turbulent boundary layer flows over the flat plate with wall transpiration and mild or strong adverse pressure gradients shows that the new law of the wall gives an excellent fit to the data in the near wall region (figures 3.13 and 3.14). ANDERSEN's *et al.* (1972) and BLACKWELL's *et al.* (1972) flows are similar and ORLANDO's *et al.* (1974) has a much stronger pressure gradient—for the same value of the suction rate F , ORLANDO's *et al.* (1974) flow has a pressure gradient parameter P^+ approximately three times higher than those in ANDERSEN's *et al.* (1972) and BLACKWELL's *et al.* (1972) flows.

Evaluating equation 3.53 close to the detachment/reattachment points where the wall shear stress vanishes, i.e. in the limit $\tau_w \rightarrow 0$, leads to

$$\frac{\bar{u}}{u_c} = \frac{\lambda u_p^3}{\kappa u_c^3 - u_c^2 V_w} \left(\frac{y u_c}{\nu} \right) + \frac{10.8^2}{2\gamma^3} - \frac{10.8\lambda}{\kappa\gamma^3}. \quad (3.55)$$

The author emphasizes that the above equation is the first scaling law in the literature that considers the effects of wall transpiration in the region of the flow with vanishing wall shear stress.

The only data of a turbulent separated flow with transpiration of fluid homoge-

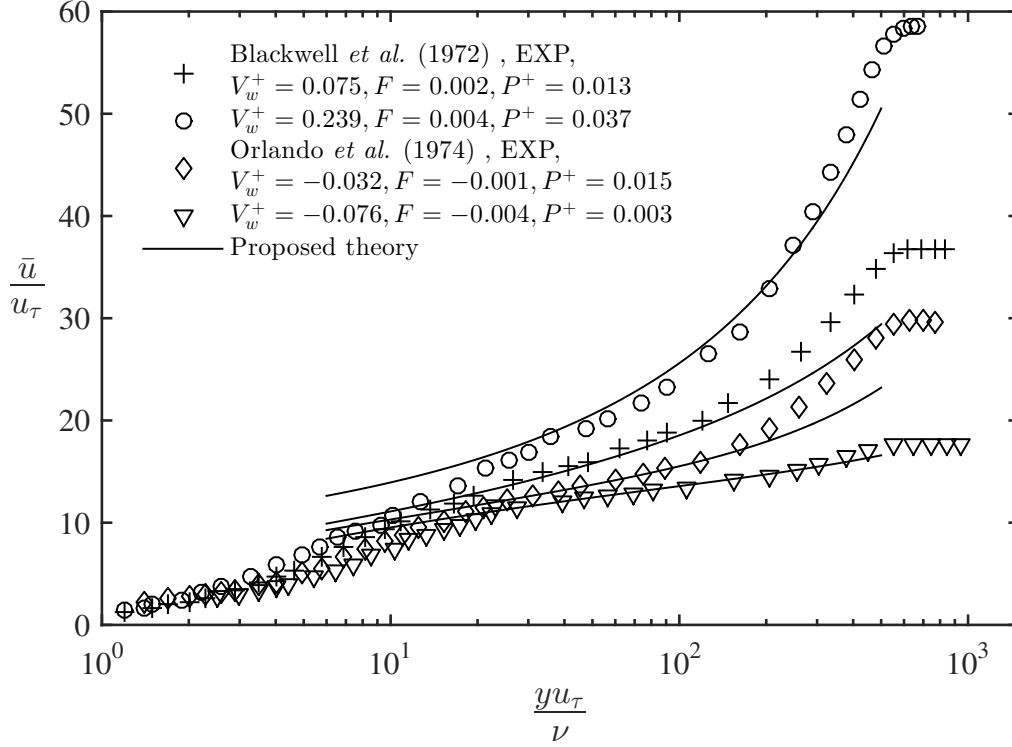


Figure 3.14: Experimental mean velocity profiles from mild and strong APG boundary layer flows with wall transpiration compared to the proposed theory with $\alpha = 3.15$, $A = 0.35$, $\gamma = 3.4$ and $\lambda = 0.45$.

neously distributed through the wall available to the author is from YANG *et al.* (1994), who studied experimentally the influence of wall injection in a flow over the backward facing step. Before analyze YANG's *et al.* (1994) data is wise to consider the simpler case of a backward facing step flow with zero wall transpiration¹. Comparing the backward facing step data from several works (DRIVER & SEEGMILLER, 1985; JOVIC & DRIVER, 1994; LE *et al.*, 1997; YANG *et al.*, 1994) the author found that when mean velocity profiles at the reattachment points are scaled by the velocity scale proposed by STRATFORD (1959) and TOWNSEND (1961), $u_p = (\nu(dP_w/dx)/\rho)^{1/3}$, they do collapse approximately onto one single curve in the near wall region but this curve is not the same where the profiles from a separated boundary layer flow over the flat plate collapse (see figure B.1 in Appendix B). Of course, as the flow in question is very complex, it can be argued that the disagreement is within the interval of experimental uncertainties but in order to maximize the agreement with the data one would have to consider that the calibration constants in the classical *half-power law* or the new *linear power law* are flow geometry dependent. In the proposed model, a good fit to the data could be obtained by re-calibrating the value of only one constant, $\gamma = 5.2$.

When YANG's *et al.* (1994) velocity profiles from flows with different injection

¹The backward facing step flow with zero wall transpiration is already very complex!

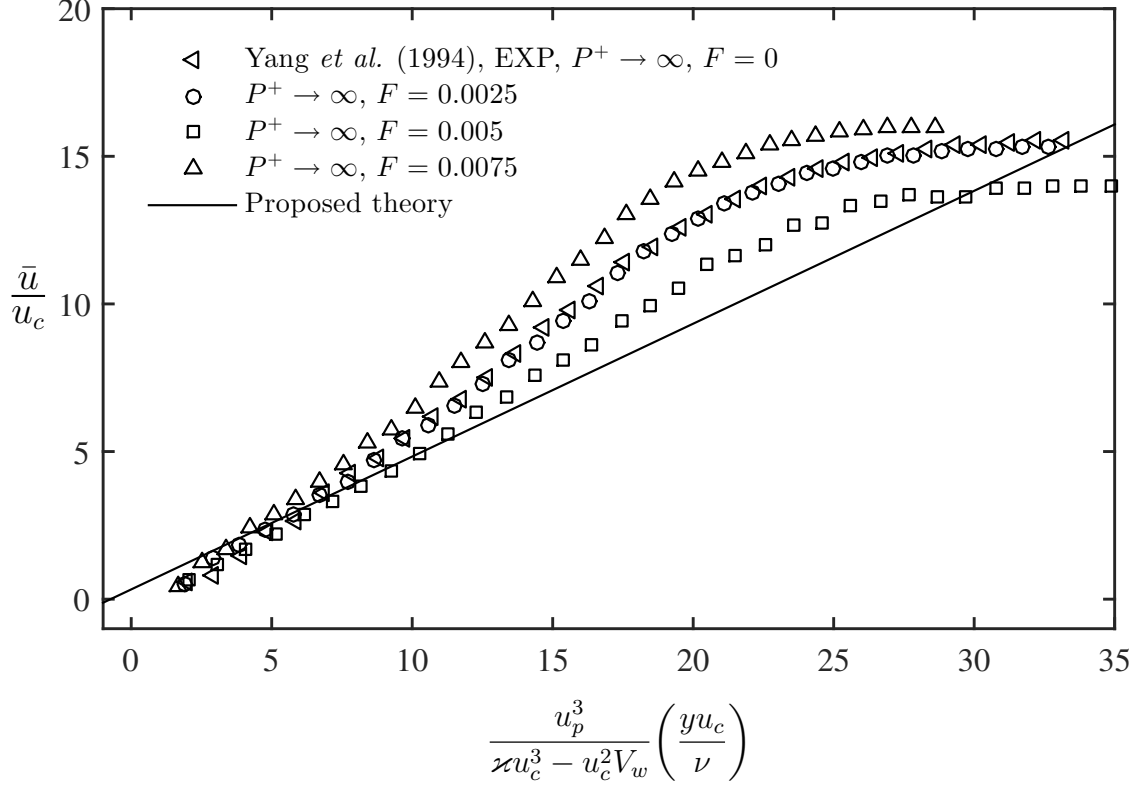


Figure 3.15: Experimental mean velocity profiles in the reattachment point of backward facing step flows with wall injection plotted with similarity coordinates. The proposed theory is plotted with $\alpha = 3.15$, $\gamma = 5.2$ and $\lambda = 0.45$.

rates are plotted with non-dimensional coordinates suggested from the model, they collapse onto one single curve in the near wall region suggesting that the profiles are self-similar with respect to the transpiration velocity, as in the zero pressure gradient case, and that u_c is a proper velocity scale (figure 3.15). The proposed theory gives a good qualitative agreement to the data in a rather thin region close to the wall (figure 3.15).

Considering now the heat transfer problem, an equation for the near wall mean temperature profile can be obtained once an appropriate closure assumption for the turbulent heat flux is made. An analysis of the model presented in section 3.2.2 for non-transpired flows reveals that the same result for the mean temperature profile (equation 3.49) can be derived if a different closure expression given by

$$\bar{q} = -\rho c_p u_c \ell_T \left(\frac{\tau_w + \frac{\partial P_w}{\partial x} y}{\rho u_{cp}^2} \right) \frac{\partial \bar{T}}{\partial y}, \quad V_w \rightarrow 0, \quad (3.56)$$

is used instead. Comparing the above equation and the expression for \bar{q} in the zero pressure gradient case (equations 3.28 to 3.31), suggests that in a more general flow where non-zero pressure gradients and wall transpiration are present the turbulent

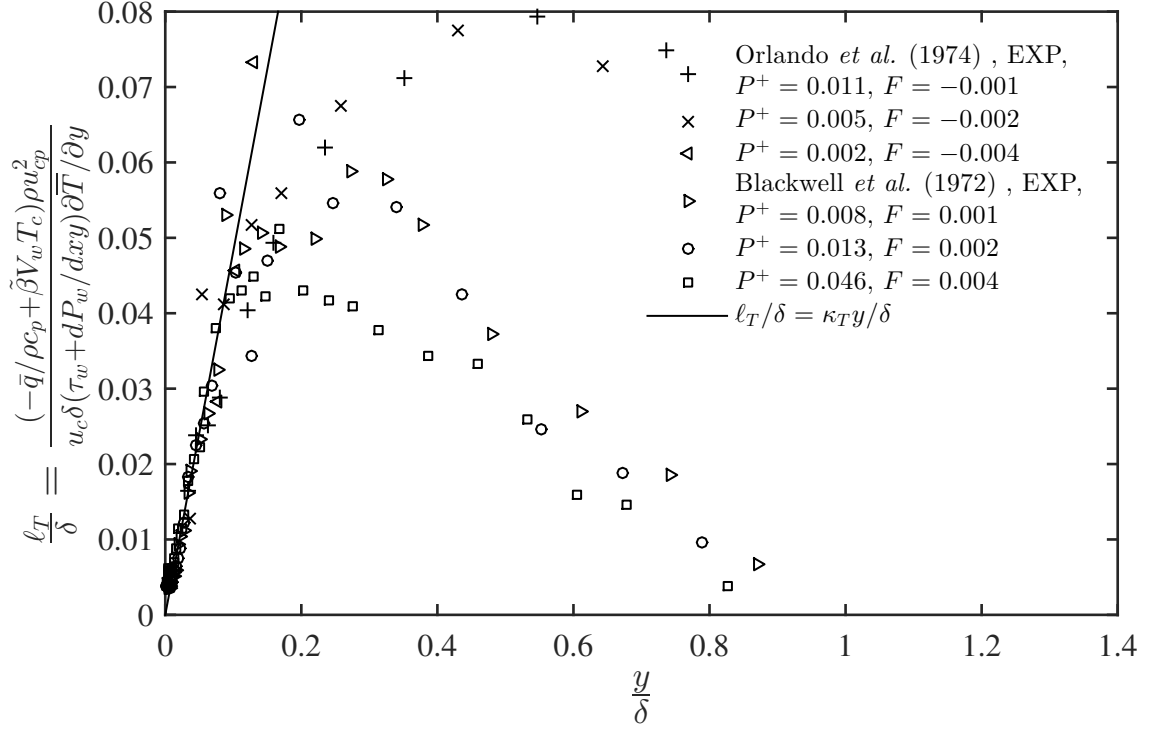


Figure 3.16: EXP thermal mixing length profiles compared to the proposed theory with $\gamma_T = 3.1$, $\alpha = 3.15$, $A_T = 0.6$ and $\kappa_T = 0.482$.

heat flux can be modeled by the following expression,

$$\bar{q} = -\rho c_p u_c \ell_T \left(\frac{\tau_w + \frac{\partial P_w}{\partial x} y}{\rho u_{cp}^2} \right) \frac{\partial \bar{T}}{\partial y} + \tilde{\beta} \rho c_p V_w T_c. \quad (3.57)$$

When equation 3.57 is compared with the experimental data from BLACKWELL *et al.* (1972) and ORLANDO *et al.* (1974) in the form of mixing length profiles (with $\tilde{\beta}$ obtained from equation 3.34), a good agreement is obtained in the near wall region of the layer (figure 3.16). Integrating expression 3.57 together with the approximated governing equation,

$$\bar{q} = q_w + \rho c_p V_w (T_w - \bar{T}), \quad (3.58)$$

in the y direction and writing the result in a non-dimensional form leads to

$$\frac{T_w - \bar{T}}{T_c} = \frac{u_c}{V_w} \left\{ \left(\bar{C} \frac{\frac{y u_c}{\nu}}{\frac{u_{cp}^2}{u_{cp}^2} + \frac{u_p^3}{u_{cp}^2 u_c} \frac{y u_c}{\nu}} \right)^{\frac{u_{cp}^2 V_w}{\kappa_T u_c u_{cp}^2}} - 1 \right\} + \tilde{\beta}, \quad (3.59)$$

where the constant of integration \bar{C} should be determined to guarantee boundedness when $u_\tau \rightarrow 0$ with $V_w \neq 0$ and the correct asymptotic behaviors when $dP_w/dx \rightarrow 0$ with $V_w \neq 0$ and when $V_w \rightarrow 0$ with $dP_w/dx \neq 0$. One of the simplest expressions

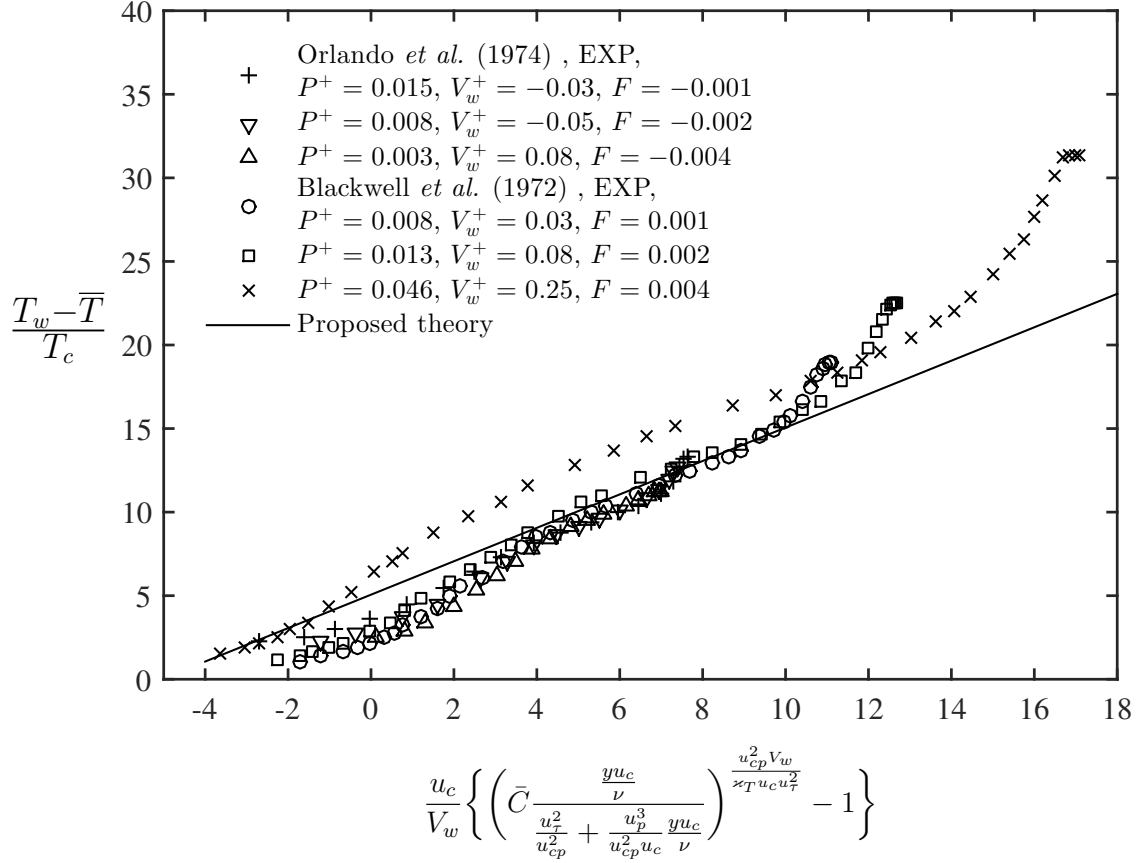


Figure 3.17: EXP mean temperature profiles from strong and mild APG boundary layer flows with wall transpiration compared to the proposed theory with $\gamma_T = 3.1$, $\alpha = 3.15$ and $A_T = 0.6$.

with that properties was found by inspection and is given by

$$\bar{C} = A_T \frac{u_\tau^2 / u_{cp}^2}{\gamma_T} 3(u_\tau^3 / u_{cp}^3 - 1). \quad (3.60)$$

The new thermal law of the wall is compared with BLACKWELL's *et al.* (1972) and ORLANDO's *et al.* (1974) experimental data from strong and mild APG boundary layers with wall injection and suction, respectively, in figure 3.17. The proposed theory gives a good fit to the data except for the case with the higher injection rate, where the slope of the profile seems to be accurately predicted but the intercept is a little underestimated. As is discussed in section 4.1, the experimental values of the friction factor obtained in flows with higher injection rates are subjected to larger errors so it can be argued that the small discrepancy between the theory and the data for the profile in question is within the interval of experimental uncertainties.

The author emphasizes that equation 3.59 is the first scaling law presented in literature that considers the effects of wall transpiration and non-zero pressure gradients in the near wall behavior of the mean temperature profile. As \bar{C} and $\tilde{\beta}$ can

be calculated from equations 3.60 and 3.34, respectively, the new thermal law of the wall has three calibration constants, $\gamma_T = 3.1$, $\alpha = 3.15$ and $A_T = 0.6$. The values of these parameters were obtained from two limiting cases, $V_w = 0$ with $dP_w/dx \neq 0$ and $dP_w/dx = 0$ with $V_w \neq 0$, and they were not re-calibrated in the more general case of a flow with $V_w \neq 0$ and $dP_w/dx \neq 0$.

To evaluate equation 3.59 in the region of vanishing wall shear stress, it is useful to use the following formula

$$\exp(z) = \lim_{w \rightarrow \infty} \left(1 - \frac{z}{w}\right)^{-w}, \quad (3.61)$$

with $z = -u_{cp}^3 V_w / (\kappa_T u_p^3 u_c y u_c / \nu)$ and $w = u_{cp}^2 V_w / (\kappa_T u_c u_\tau^2)$. With the above expressions it can be shown that when $u_\tau \rightarrow 0$ the new thermal law of the wall assumes the form of an exponential function given by,

$$\frac{T_w - \bar{T}}{T_c} = \frac{u_c}{V_w} \left\{ \left[\exp \left(1 - \gamma_T^3 \frac{\nu}{y u_c} + \ln A_T \right) \right]^{\frac{V_w}{\kappa_T u_c}} - 1 \right\} + \tilde{\beta}. \quad (3.62)$$

Unfortunately, there was no data to test the validity of equation 3.62 available to the author.

3.3 Description of the outer layer

The domain of validity of the wall laws will be extended, to include the outer region of the layer, using the intermittent character of the flow in that region². The physical picture and mathematical tools were explored in some detail in section 2.1. Assuming SARNECKI (1959) intermittency hypothesis,

$$\bar{u} = \gamma_s u_{\text{turb}} + (1 - \gamma_s) U_\infty, \quad (3.63)$$

with u_{turb} obtained from the new law of the wall (multiplying both sides of equation 3.53 by u_c) and using an intermittency factor given by an error function (resulted from a Gaussian integral),

$$\gamma_s(y/\delta) = \frac{1}{2} \left[1 - \operatorname{erf} \left(\frac{y/\delta - \mu/\delta}{\sqrt{2}\sigma/\delta} \right) \right], \quad (3.64)$$

leads to the new formula for the mean velocity profile. Comparisons between this expression and the data reveal a happy circumstance—the parameters μ/δ and σ/δ are constants that do not vary with the transpiration velocity or the pressure gradient

²The author gratefully acknowledge a contribution made by Professor Carlos B. Da Silva, who suggested that the outer region of the layer could be described using the T/NT interface.

parameter and the intermittency factor γ_s is a universal function of y/δ . Recall that μ and σ are the mean and standard deviation in a Gaussian distribution of the PDF of $Y(t)$, the position of the turbulent/non-turbulent (T/NT) interface. Their values are given by $\mu/\delta = 0.78$ and $\sigma/\delta = 0.14$ in KLEBANOFF (1955) and $\mu/\delta = 0.66$ and $\sigma/\delta = 0.11$ in CHAUHAN *et al.* (2014). In figures 3.19, 3.20, 3.21 and 3.18 all profiles were plotted with $\mu/\delta = 0.66$ and $\sigma/\delta = 0.23$. The theory gives an excellent fit to the data through the whole layer, including the near wall region ($y/\delta < 0.1$ approximately). The profiles in the reverse flow region are particularly difficult to predict in turbulence modeling, specially the small portion of the layer where \bar{u} assumes negative values, so it's quite surprising how this simplistic approach can predict even those profiles so well. The value of σ/δ used here is considerably different from those reported in KLEBANOFF (1955) and CHAUHAN *et al.* (2014). SARNECKI (1959), and also THOMPSON (1967) and MCQUAID (1968) argue that as the intermittency hypothesis assumes a discontinuous velocity jump (from u_{turb} to U_∞) at the T/NT interface, the intermittency factor used in the model is expected to be different to the actually measured γ_s (using a vorticity probe, the kurtosis or skewness of the PDF of a hot-wire signal, etc.). In fact, those authors didn't use expression 3.64 for γ_s but a rather empirical one given in a graphic format. In KRUG *et al.* (2017), equations 3.63 and 3.64 are used with different values of μ/δ and σ/δ for the zero pressure gradient boundary layer and for confined flows, where the physical interpretation of the model is difficult because there is no intermittency. The authors argue that the interface where the jump takes place is not the T/NT interface, and that the model could be explained physically using a recent concept of interfacial shear layers that separates uniform momentum zones reported in other works. It is the author's opinion that the present formulation has a richer physical ground compared to the purely empirical descriptions available in the literature for the wake profile.

Now turning the attentions to the heat transfer problem in the outer region of the flow, an original expression for the mean temperature profile is proposed here based on a simple analogy with the fluid-dynamical problem. It is proposed that the temperature difference $T_w - \bar{T}$ can be expressed by the following equation,

$$T_w - \bar{T} = \varphi(T_w - T_{\text{turb}}) + (1 - \varphi)(T_w - T_\infty), \quad (3.65)$$

where $T_w - T_{\text{turb}}$ is obtained from the new thermal law of the wall (multiplying both sides of equation 3.59 by T_c) and φ is a thermal intermittency factor. Equation 3.65 will be referred to as the *thermal intermittency hypothesis*. Assuming that φ varies

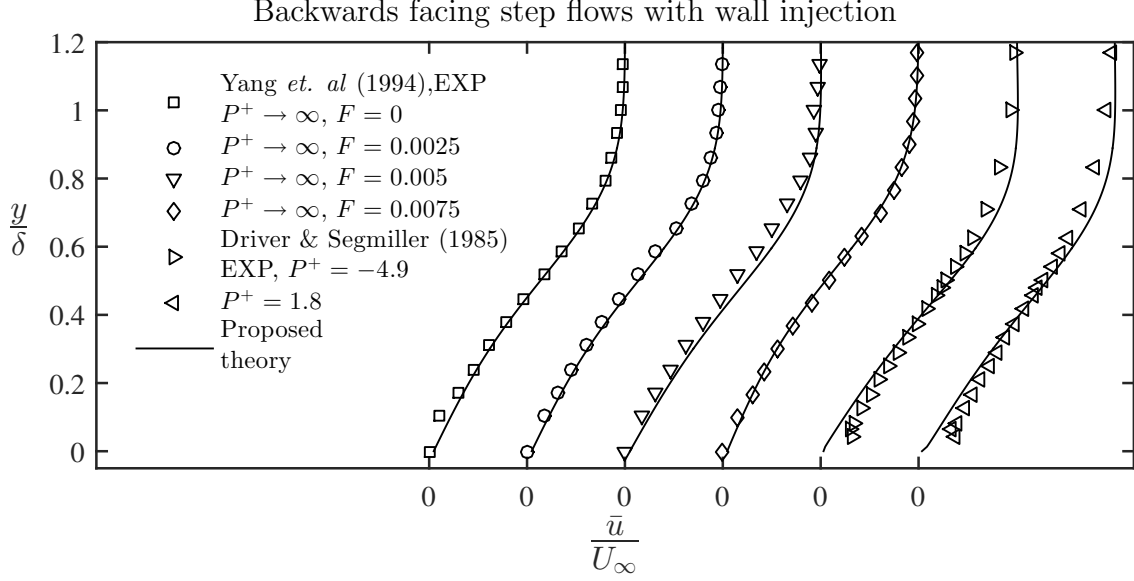


Figure 3.18: Mean velocity profiles plotted in outer coordinates.

with y/δ in a similar form γ_s does allows one to write,

$$\varphi(y/\delta) = \frac{1}{2} \left[1 - \operatorname{erf} \left(\frac{y/\delta - \mu_T/\delta}{\sqrt{2}\sigma_T/\delta} \right) \right], \quad (3.66)$$

where μ_T and σ_T meanings are analogous to μ and σ but they are associated with the transfer of energy/heat (instead of momentum) problem. If the values of the former parameters are taken to be different from the latter the connection made between the model and the classical T/NT interface, based on the transfer of vorticity, is loosened in some way but, in fact, it is sound that the thermal intermittency hypothesis model should be linked to a different interface with a more thermal-like structure—as the scalar or the scalar gradient T/NT interface (SILVA & DA SILVA (2017) and references within).

Figure 3.22 and 3.23 show some comparisons between mean temperature profiles obtained from the thermal intermittency hypothesis with $\mu_T = 0.6$ and $\sigma_T = 0.3$ and the experimental data from several authors (BLACKWELL *et al.*, 1972; ORLANDO *et al.*, 1974; VOGEL, 1984; WHITTEN, 1967), plotted in outer non-dimensional coordinates. An excellent agreement between the theory and the data is obtained for almost all profiles shown so φ can be considered a universal function of y/δ —it does not depend on the transpiration rate, pressure gradient parameter or Reynolds number.

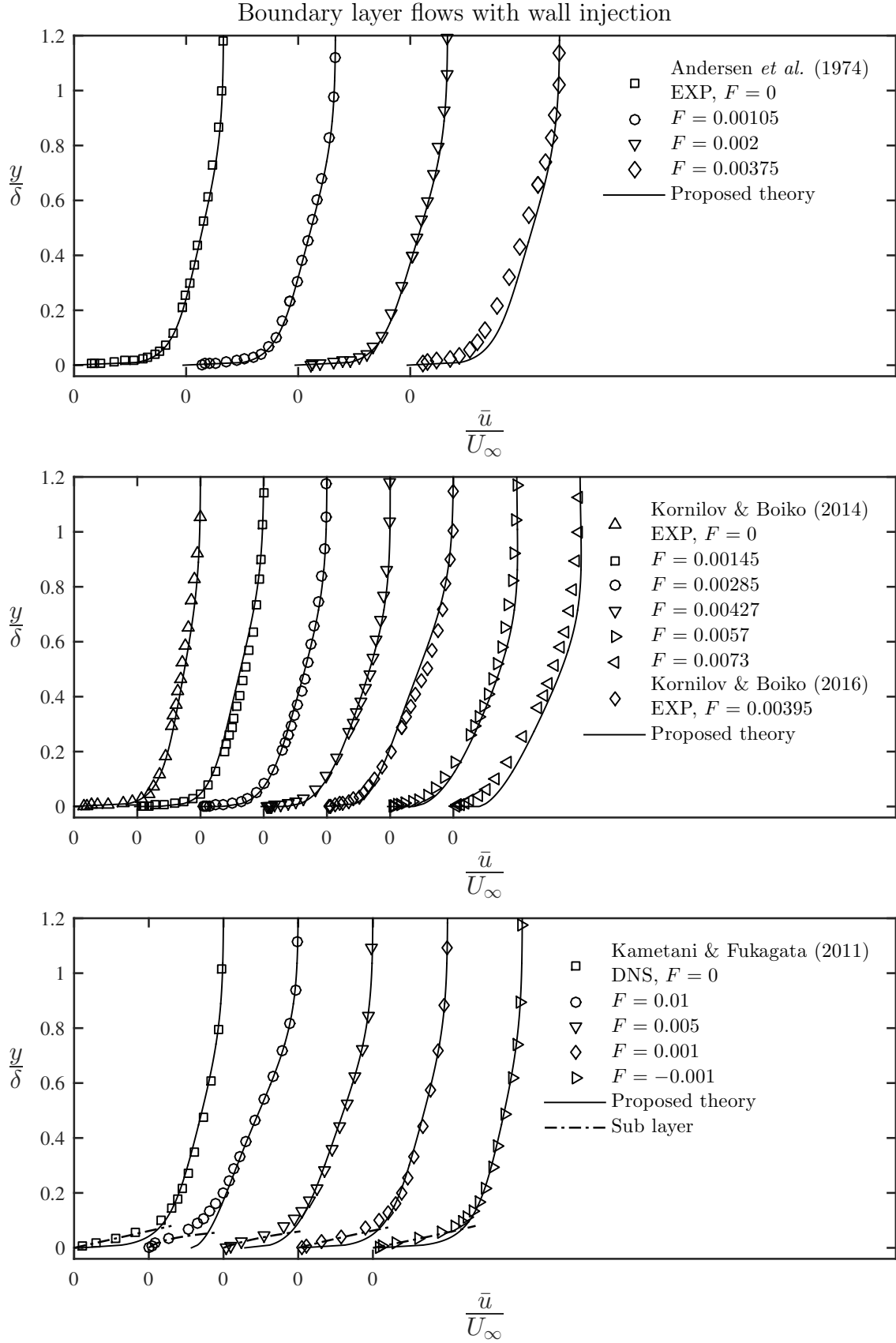


Figure 3.19: Mean velocity profiles plotted in outer coordinates.

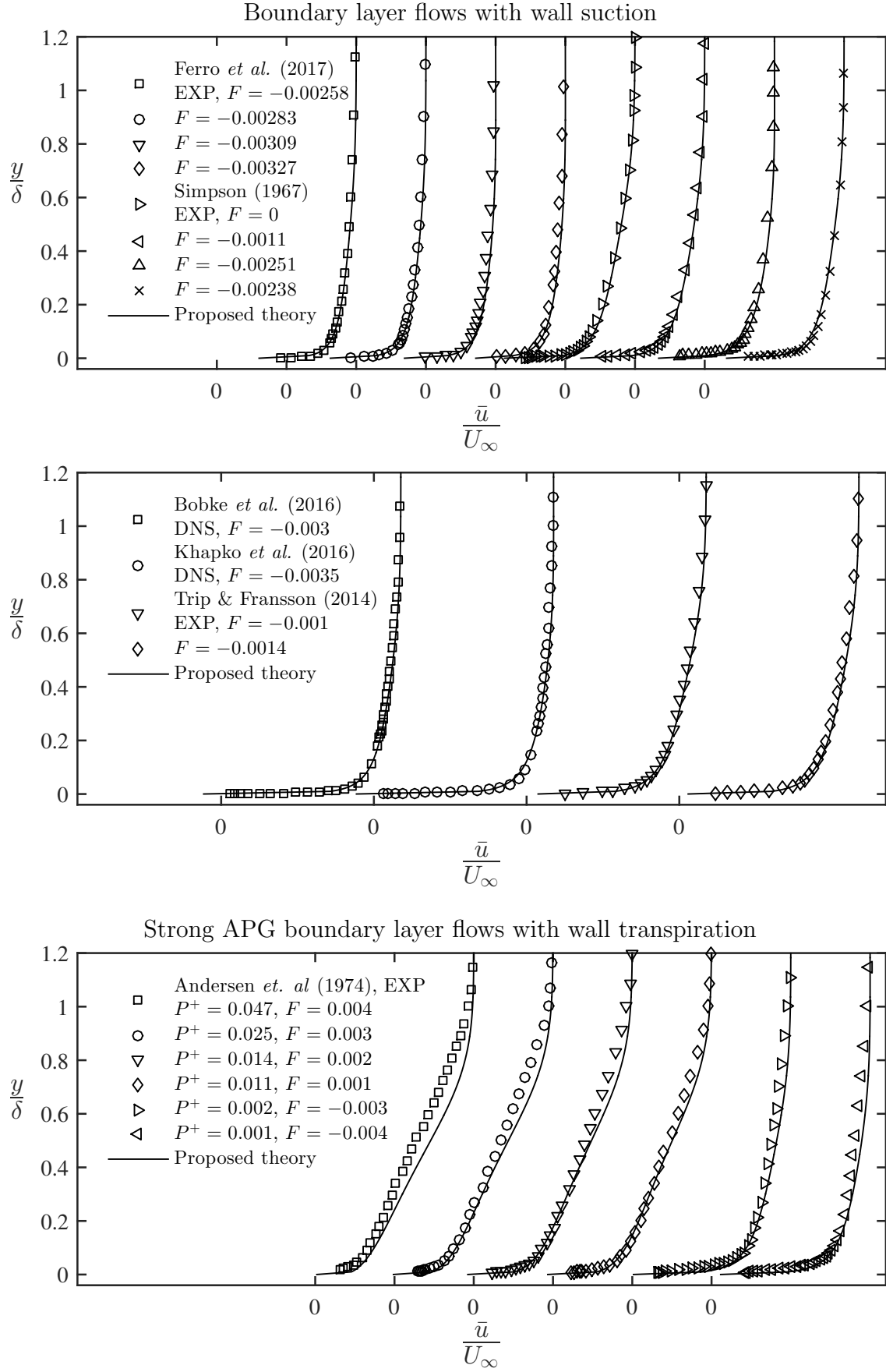


Figure 3.20: Mean velocity profiles plotted in outer coordinates.

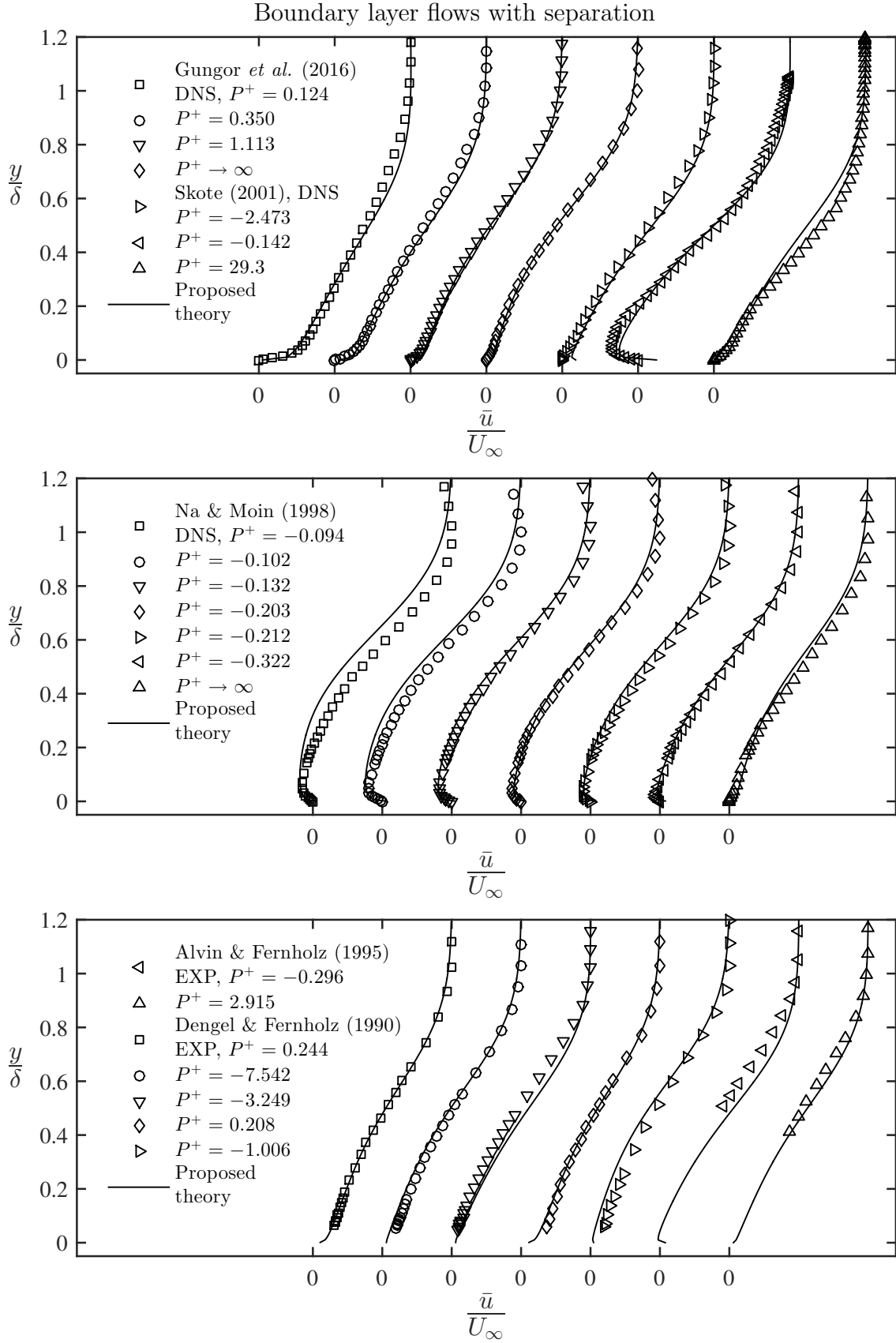


Figure 3.21: Mean velocity profiles plotted in outer coordinates.

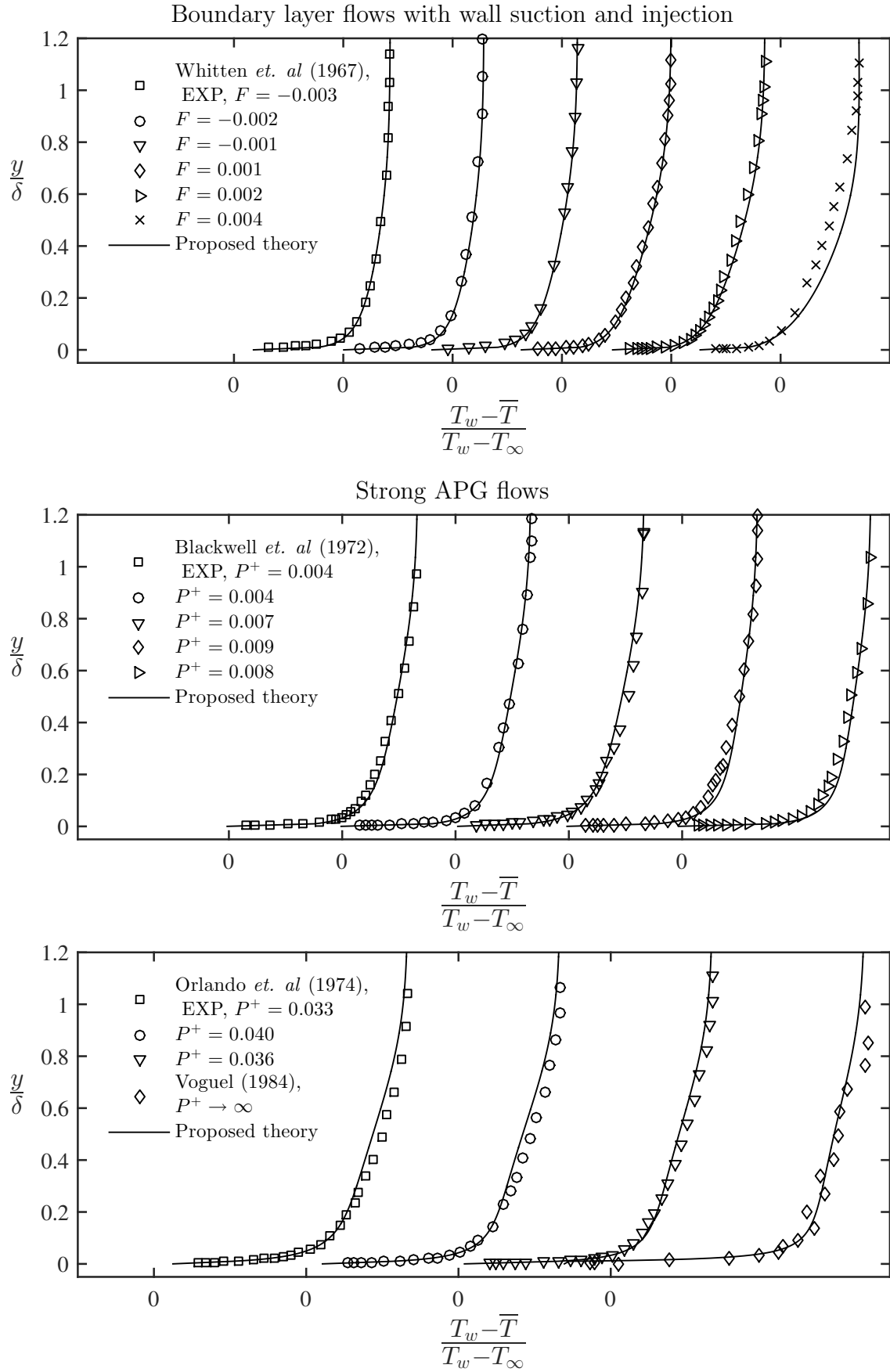


Figure 3.22: Mean temperature profiles plotted in outer coordinates.

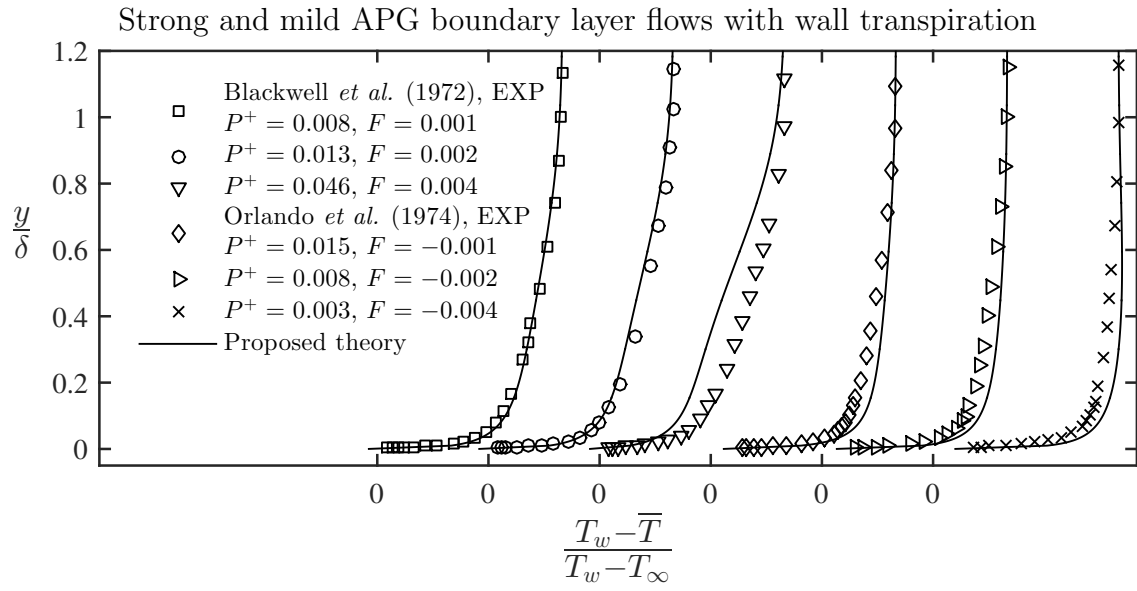


Figure 3.23: Mean temperature profiles plotted in outer coordinates.

Chapter 4

Comparisons with other theories and datasets

4.1 Assessment of the data

A critical survey is made of available data on transpired turbulent flows with the intent to provide an estimation of the quality and repeatability of the data. Special attention is given for two undesirable circumstances that should be avoided when comparing different scaling laws with the data; flows in the *relaminarization* regime when high suction rates are considered and cases where large errors in the experimental skin friction coefficient are possibly present when flows with high injection rates are considered. Being these two conditions briefly discussed, experimental and DNS data from different databases are carefully examined to check matchability.

Being the process of flow reversal from turbulent to laminar of very complex nature, it is quite surprising how it can be quantified by a single threshold value of the suction rate F_{sst} , below which no self-sustained turbulence is observed. While earlier works suggested $F_{\text{sst}} \approx -0.01$ (DUTTON, 1960; TENNEKES, 1965a), recent—and better—estimations place it as $F_{\text{sst}} \approx -0.0036$ (FERRO, 2017; KHAPKO *et al.*, 2016; WATTS, 1972). The numerical work from KHAPKO *et al.* (2016) is probably the most thorough with that respect. In the present study all experimental and DNS profiles used in the comparisons, except for one case only, are from flows with $F > -0.0036$ so it is believed that they are in the fully turbulent regime.

To test the validity of the wall law formulas with experimental data, it is desirable that the value of the wall shear stress be known accurately. This is quite a challenging task to accomplish for the experimentalist when the flow is subjected to wall injection. In many works, the experimental skin friction coefficient has been obtained from some form of the momentum-integral equation. For zero pressure

gradients flows this equation is given by

$$\frac{C_f}{2} = \frac{d\theta}{dx} - \frac{V_w}{U_\infty}. \quad (4.1)$$

As the blowing rate increases, the gradient in the momentum thickness approaches the blowing-rate parameter and the calculated friction factor is the result of a small difference in two large numbers, each with some error (KENDALL *et al.*, 1964). The opposite is true for sucked flows, making the suction experimental data particularly valuable for testing new theories for transpired turbulent layers. DAHM & KENDALL (1968) estimate that in a flow with a blowing rate of $V_w/U_\infty = 0.005$ a $\pm 1\%$ uncertainty in both $d\theta/dx$ and V_w/U_∞ admits to about $\pm 32\%$ uncertainty in friction factor! Although any experimental method of evaluation can be subjected to criticism, it was decided to show only data from authors who did not rely solely on equation 4.1. In that regard, SQUIRE (1980)¹ made an extensive analysis of many data sets and recommended the zero pressure gradient boundary layer flow with wall injection as measured by ANDERSEN *et al.* (1972) with blowing rates up to $F = 0.004$, which was considered to be a moderate injection rate. SQUIRE (1980) argues that the layers with $F > 0.004$ are not two-dimensional.

It is important to check how well experimental and DNS profiles obtained from different databases agree with each other. When scaled by the friction velocity and length scales, there is self-similarity of the mean velocity profiles with respect to the Reynolds number Re —based on the free stream velocity and momentum thickness for boundary layer flows, the bulk velocity and channel half width for channel flows and the bulk velocity and pipe radius for pipe flows—in the whole near wall region of the flow so profiles with the same value of the transpiration parameter V_w^+ would collapse into one single curve in that region when plotted in classical wall coordinates. For that reason, it was decided to compare profiles with similar values of V_w^+ with coordinates \bar{u}/u_τ versus yu_τ/ν and a logarithmic scale on the abscissa, so the near wall region can be seen in detail. This is done in figures 4.1 to 4.8 and the results are described below.

Considering flows with wall suction first, the data chosen for the analysis are the boundary layers measured by SIMPSON (1967), TRIP & FRANSSON (2014), FERRO *et al.* (2017) and simulated by BOBKE *et al.* (2016), KHAPKO *et al.* (2016), KAMETANI & FUKAGATA (2011) and the pipe flow measurements from ELENA (1977). As it can be seen from figures 4.1 and 4.2 there is an excellent agreement between profiles with similar values of V_w^+ , which is a good indicator of the reliability of the data.

¹SQUIRE (1980) work was presented in the 1980-81 Stanford Conference of Complex Turbulent Flows, where ANDERSEN *et al.* (1972) data was considered a “trustworthy” test case for comparisons with computations (KLINE *et al.*, 1980).

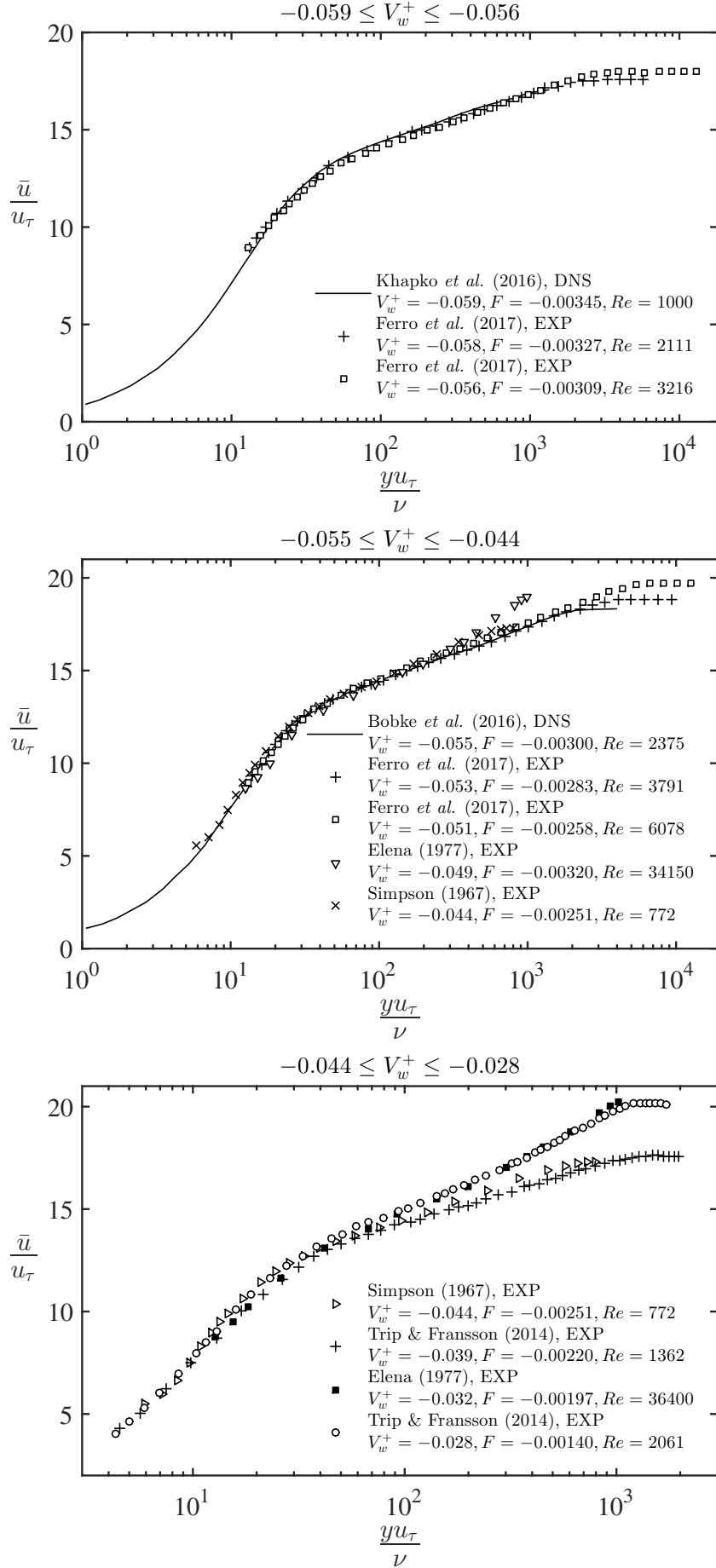


Figure 4.1: Comparisons between data from different research groups.

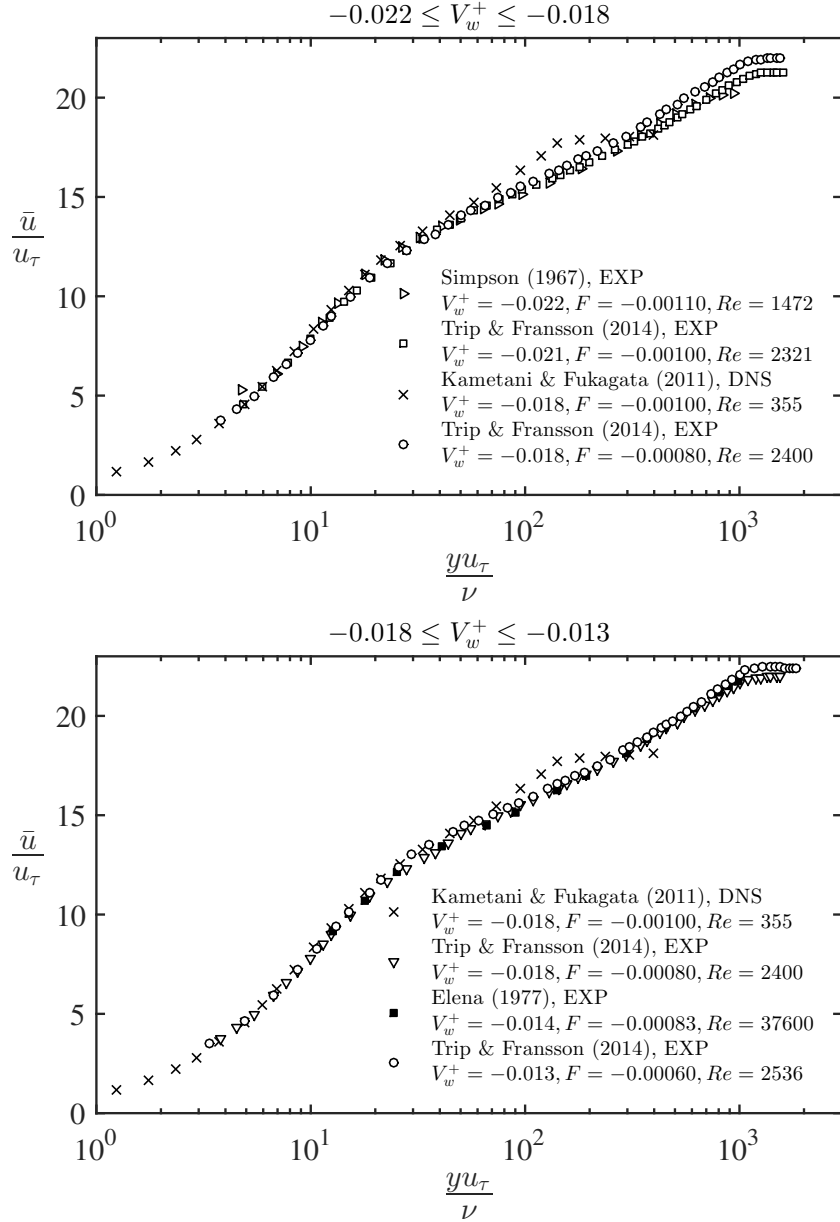


Figure 4.2: Comparisons between data from different research groups.

To study the effects of wall injection in the mean velocity profiles, the data selected are the boundary layer measurements from ANDERSEN *et al.* (1972), ROTTA (1970), BAKER & LAUNDER (1974b), KORNILOV & BOIKO (2014), KORNILOV & BOIKO (2016) and simulations from KAMETANI & FUKAGATA (2011) and the channel flow measurements from NEZU (1977) and simulations from SUMITANI & KASAGI (1995), NIKITIN & PAVELEV (1998) and AVSARKISOV *et al.* (2014). Contrasting with the case where suction is applied, there are some disagreements between the results from different databases, specially when higher injection rates are considered. The author speculates that the disagreements are caused by large errors in the experimental mean wall shear stress values—the possi-

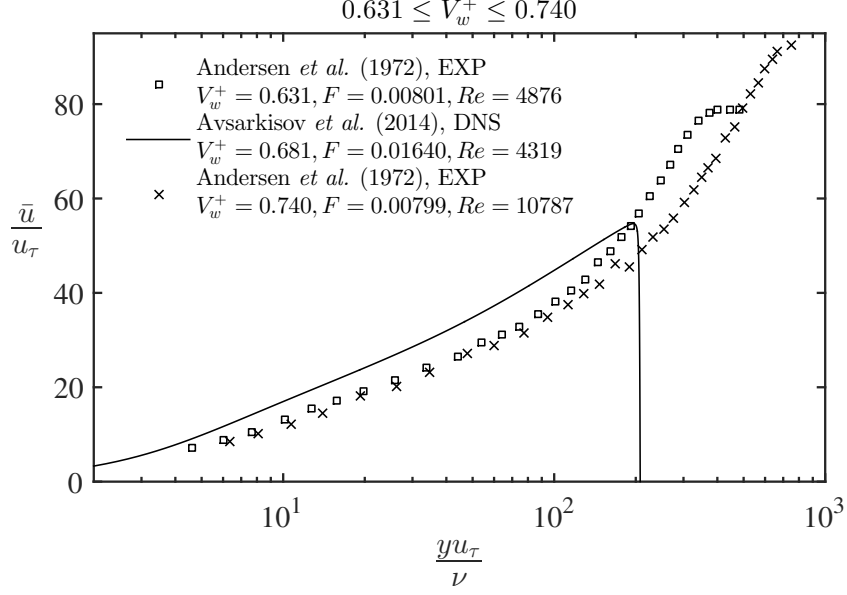


Figure 4.3: Comparisons between profiles from different databases.

bility of three-dimensional effects and poor judgment in the choice of tripping devices are also not discarded. The justification for such assertion is as follows. Considering the DNS data, where it is relatively easy to compute the values of the wall shear stress with some accuracy, there is an excellent agreement between profiles from different databases for injection rates as high as $V_w^+ \sim 0.5$ and $F \sim 0.01$ (figures 4.4b, 4.5b, 4.5c, 4.6a, 4.6c and 4.7b). The experimental profiles that do not agree with each other or with the DNS do have approximately the same slope so changing the values of u_τ it is possible to make them collapse—remember that in a plot with classical wall coordinates changes in u_τ cause only an upward or downward shift in the profiles without changing their slopes (figures 4.3 and 4.4a). Nevertheless, there are some experimental profiles from different databases that agree very well with each other and with the DNSs as well (figures 4.5c, 4.7a, 4.7c and 4.8). Summing up, for high injection rates with $V_w^+ \sim 0.5$ and $F \sim 0.01$ there is an excellent agreement between the DNSs but not with the experimental profiles—except perhaps for some of Andersen’s profiles (figures 4.4a and b). For moderate injection rates with $V_w^+ \sim 0.2$ and $F \sim 0.004$ the agreement is very good between the experimental data from ANDERSEN *et al.* (1972), KORNILOV & BOIKO (2014), NEZU (1977) and the DNSs. ROTTA (1970) and BAKER & LAUNDER (1974b) experiments only agree with other databases for flows with low injection rates with $V_w^+ \sim 0.06$ and $F \sim 0.002$ (figures 4.6b, 4.7a, 4.7b and 4.8).

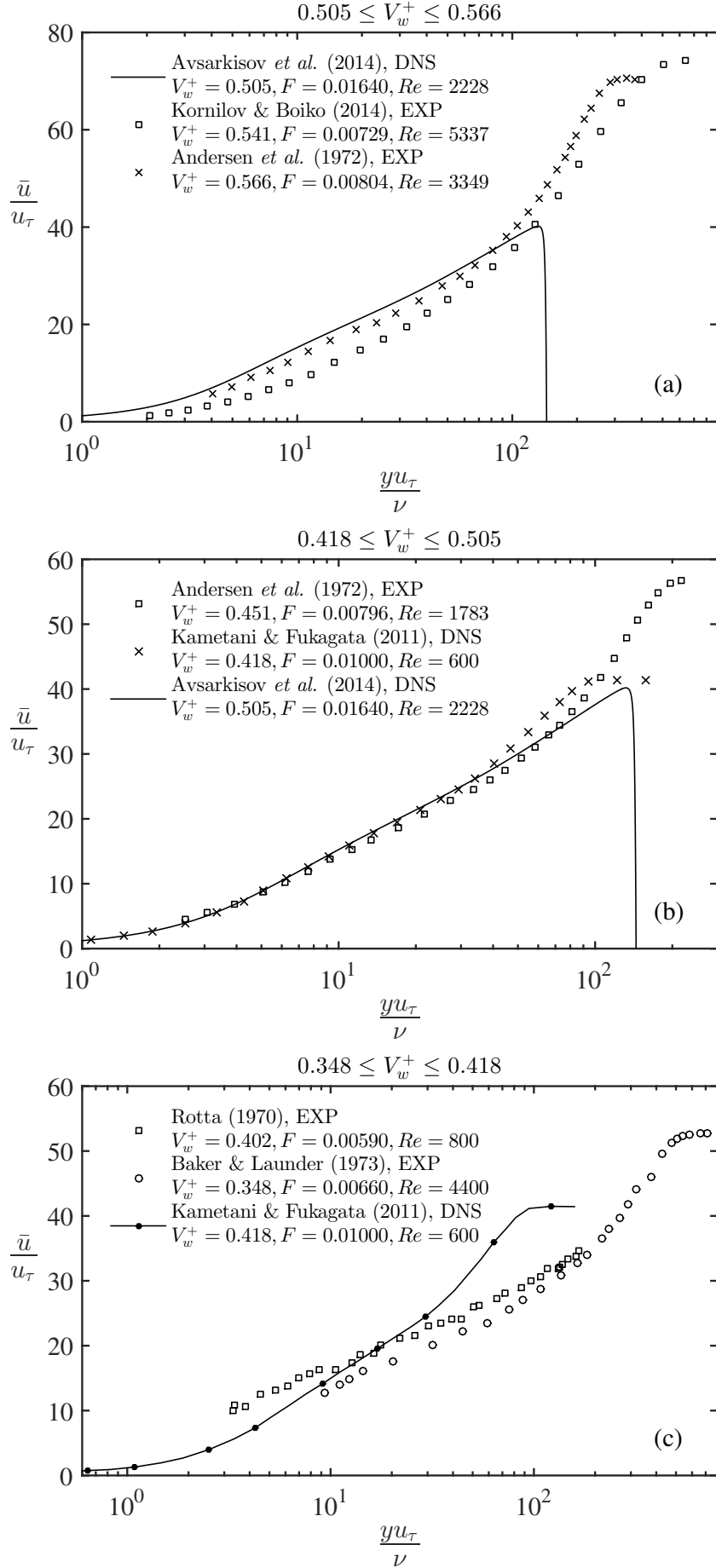


Figure 4.4: Comparisons between profiles from different databases.

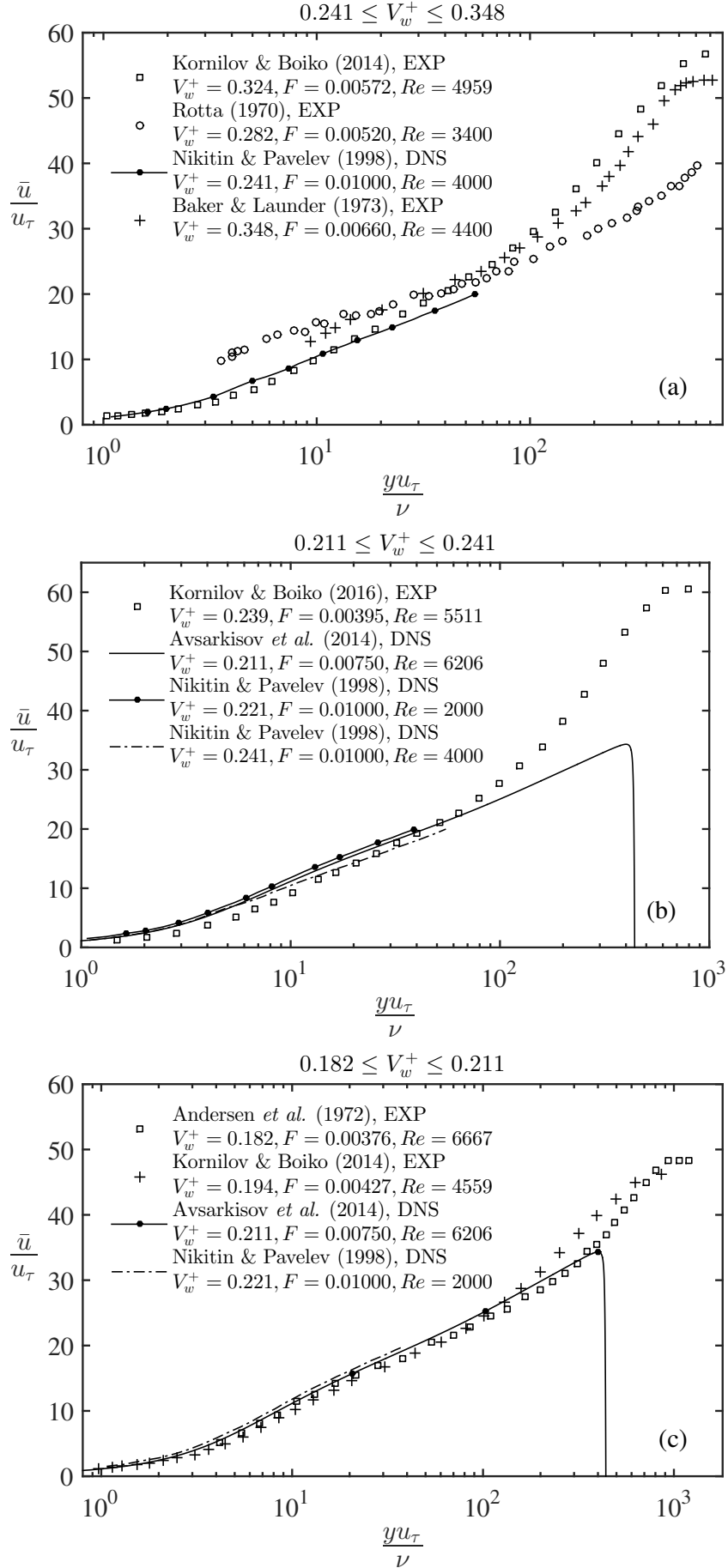


Figure 4.5: Comparisons between profiles from different databases.

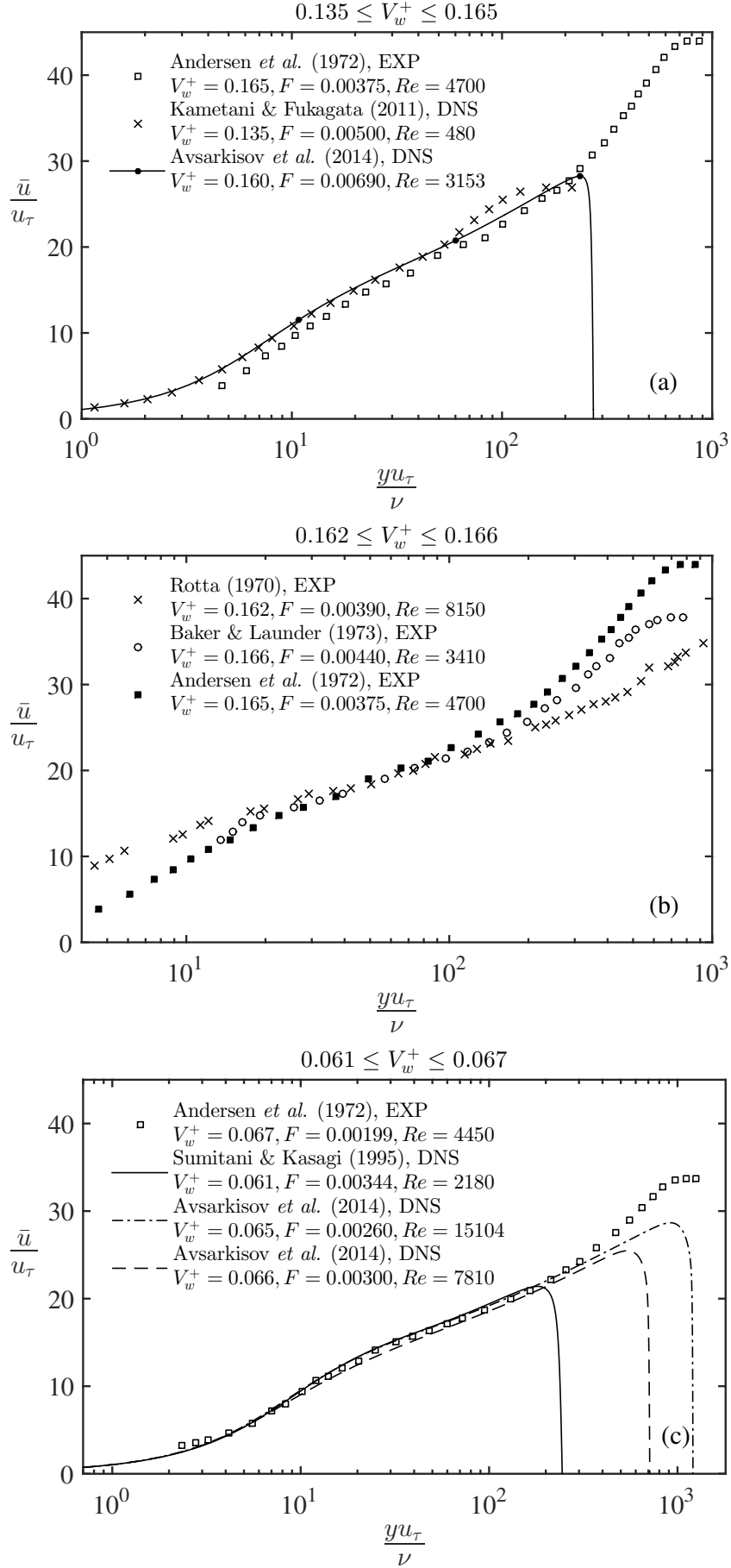


Figure 4.6: Comparisons between profiles from different databases.

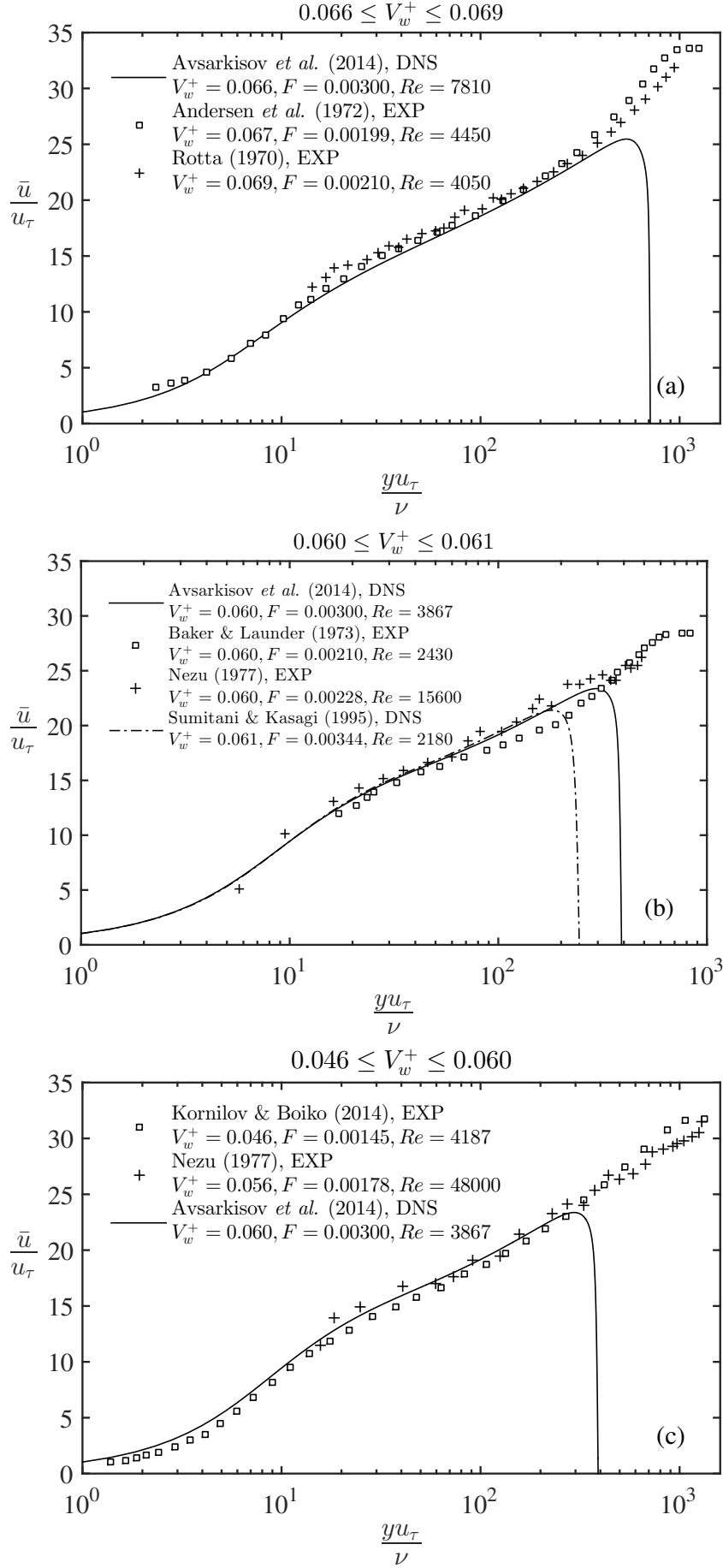


Figure 4.7: Comparisons between profiles from different databases.

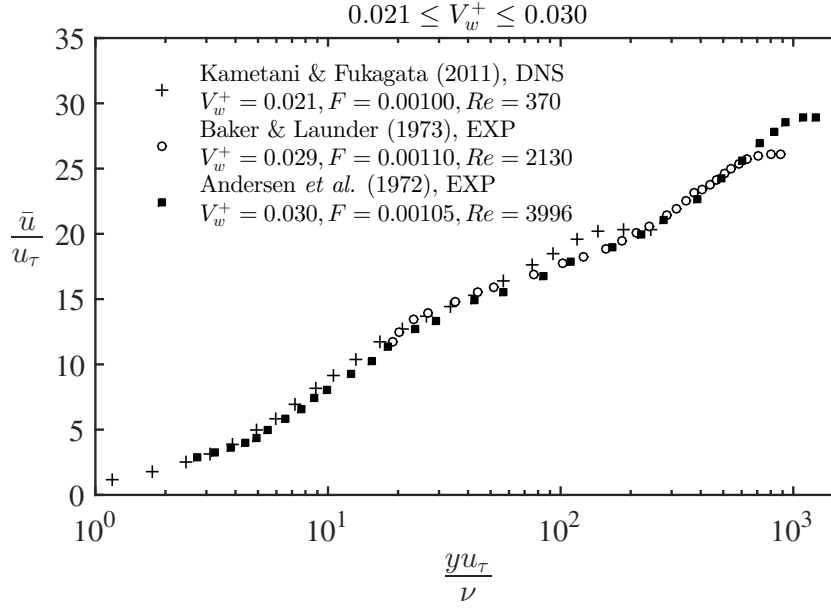


Figure 4.8: Comparisons between profiles from different databases.

4.2 Mean velocity profiles

Figure 4.9 shows a comparison between four different formulations and some data from transpired flows with zero (or negligible small) pressure gradients. CLARKE *et al.* (1955) and COLES (1972) expressions were chosen to represent the bi-log law and the semi-log law, respectively, because when compared to other versions of these formulations, they are the ones who provide the best fit to the data in most of the profiles analyzed by the author. The numerical solution of CEBECI (1970) turbulence model is also shown. While Clarke's formulation gives a very good fit to the data, Coles formula doesn't predict the correct slope of the profiles very accurately and Cebeci's solution gives a worst fit to the sucked flows data. For all profiles shown, the proposed theory seems to fit the data slightly better than the other formulations do, but it can be argued that the improvement is within the experimental uncertainties.

Figures 4.10 and 4.11 show some comparisons between data from non-transpired flows with strong adverse pressure gradients, including profiles in the separation region, and different formulations of the problem. KIEL (1995) version of the half-power-log law provides a great fit to the data but in his formulation both the Von Karman constant and the y -axis intercept vary with P^+ and the functional forms of these parameters were obtained empirically. AFZAL (2008) formula with $\varkappa = 0.41$ gives a good fit to the data except for the profiles at the reverse flow region ².

²AFZAL (2008) also gives an empirical formula to calculate the Karman constant as a function

The numerical solution of CEBECI (1970) turbulence model does not fit the data very well when the pressure gradient parameter P^+ is high and the flow is far from equilibrium. This result was also obtained by other authors (JOHNSON & KING, 1984; SIMPSON, 1985). SHIH *et al.* (2003) version of the semi-logarithmic law of the wall doesn't perform as well as KIEL (1995) version of the half-power-log law, but his formula does not contain empirically calibrated functions and its free parameters are all constants. The proposed theory gives an excellent fit to the data for all profiles shown but, considering the experimental uncertainties, one can't tell if it gives a better fit compared to KIEL (1995) formula.

In figure 4.11, some data from flows with wall transpiration and strong adverse pressure gradients are compared to the proposed theory and CEBECI (1970) model. The proposed theory gives an excellent fit to the profiles while Cebeci's model doesn't perform very well when the pressure gradient parameter P^+ is very high.

Figures 4.9 to 4.11 show the viscous sub-layer solution, which is given by

$$u^+ = \frac{P^+ \exp(V_w^+ y^+) - P^+ V_w^+ y^+ - P^+ + V_w^+ \exp(V_w^+ y^+) - V_w^+}{V_w^{+2}}, \quad (4.2)$$

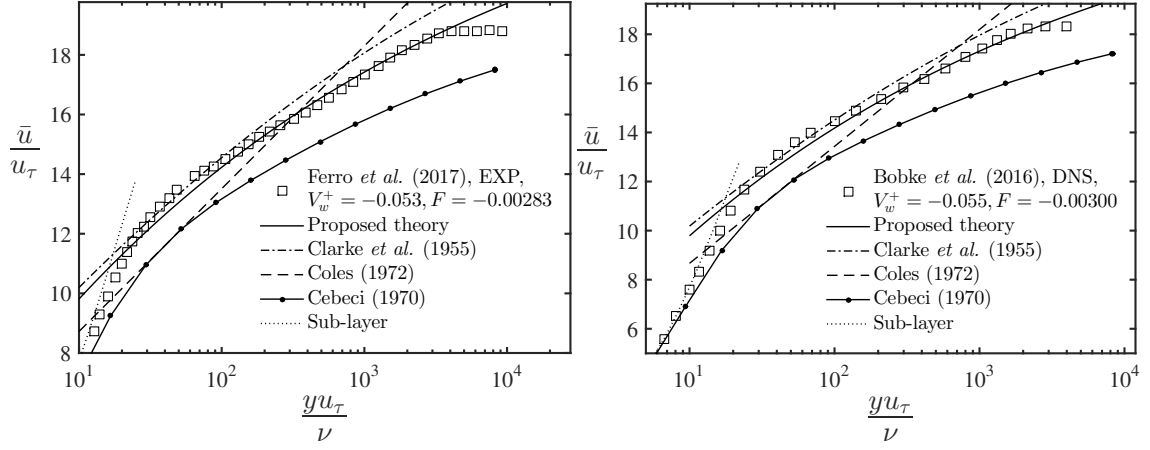
and in some cases it is re-written as $\bar{u}/u_p = f(yu_p/\nu)$. A more complete comparison between different theories and about 200 EXP and DNS mean velocity profiles from several flow developments can be found in Appendix B.

4.3 Mean temperature profiles

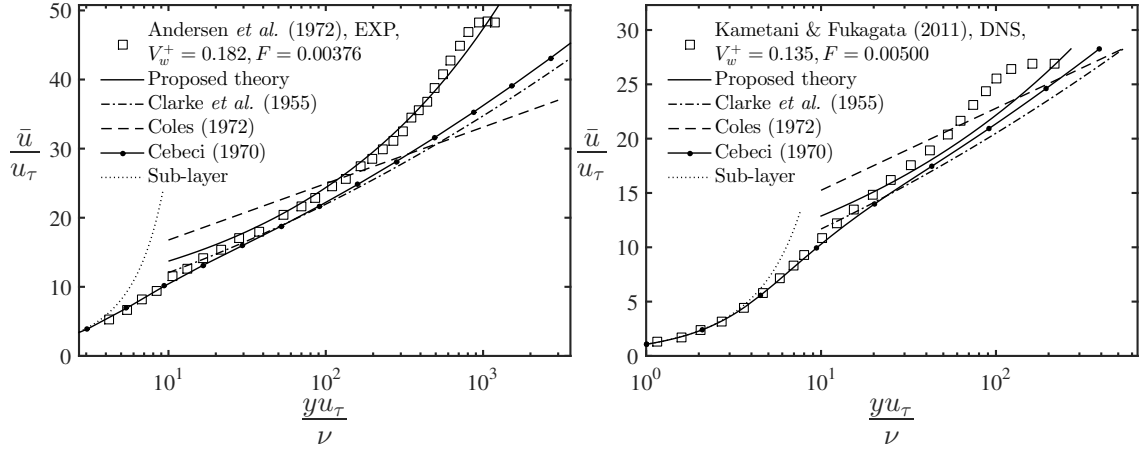
Figure 4.12 shows some comparisons between the proposed theory, FARACO-MEDEIROS & SILVA-FREIRE (1992) and VÉROLLET (1972) formulations with some data from transpired flows with zero (or negligible small) pressure gradients. VÉROLLET (1972) formula clearly overpredict the correct behavior of the mean velocity profile for all profiles shown. Considering the boundary layer flow EXP data from WHITTEN (1967) and the channel flow DNS data from SUMITANI & KASAGI (1995) (injection side), both the proposed theory and FARACO-MEDEIROS & SILVA-FREIRE (1992) model give an excellent fit to the data, except for the flow with the lowest suction rate where the proposed theory performs better. It could be argued that FARACO-MEDEIROS & SILVA-FREIRE (1992) formulation is superior to the proposed theory, as the former doesn't have any free parameter to improve the fitting with the data, while the latter has two calibration constants. But in the present work it was found a coordinate system—the similarity coordinates— where mean temperature profiles are self-similar in the whole wall

of P^+ but when $P^+ \rightarrow 0$, his version of the half power log law with that function does not reduce to the classic logarithmic law of the wall.

Boundary layer flow with wall suction



Boundary layer flow with wall injection



Pipe flow with wall suction and channel flow with wall injection

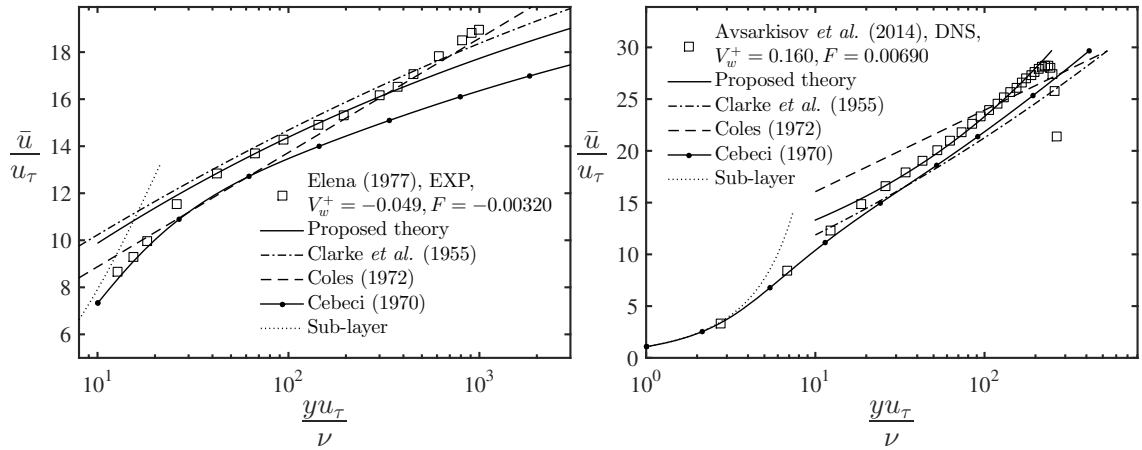
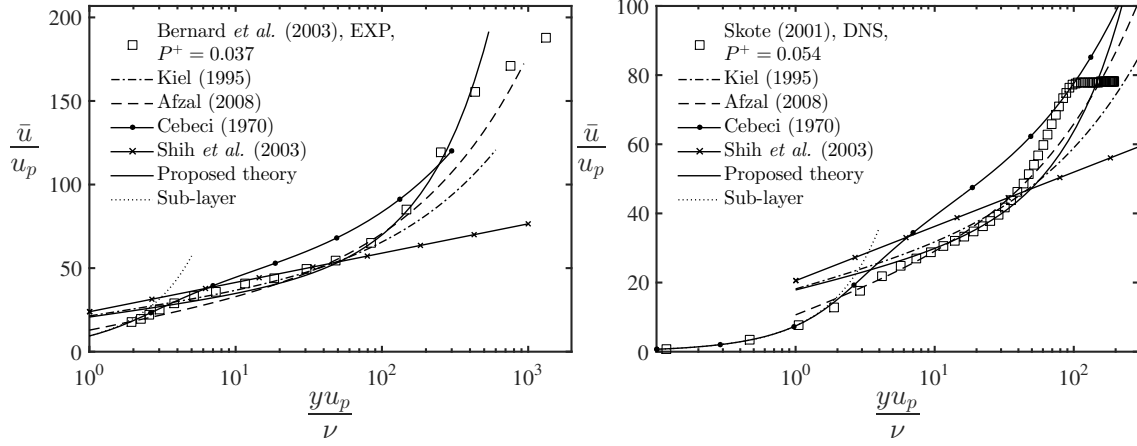


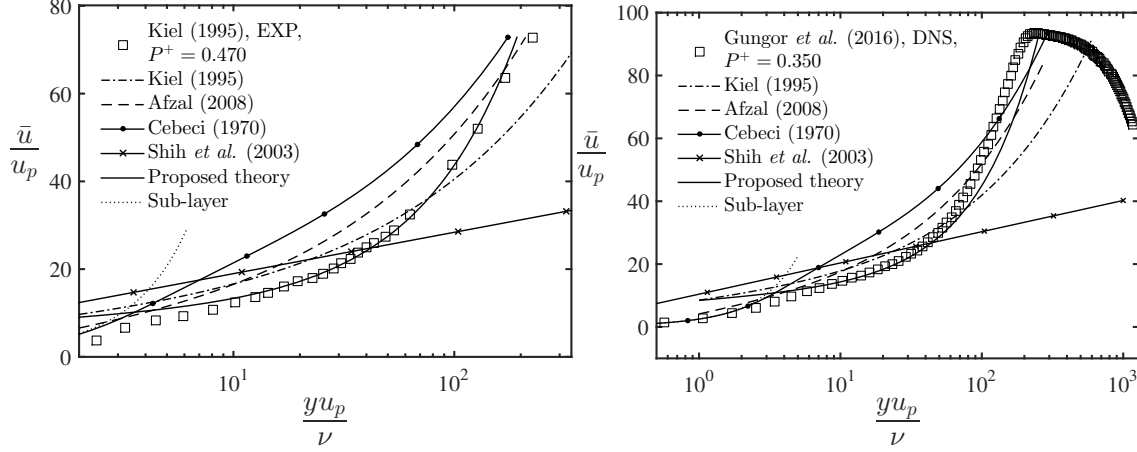
Figure 4.9: Comparisons between different theories and the data.

region, while in FARACO-MEDEIROS & SILVA-FREIRE (1992) model there is no collapse of the profiles very close to the wall. Furthermore, the present formulation

Strong APG boundary layers



Very strong APG boundary layers



Profiles close to the detachment point

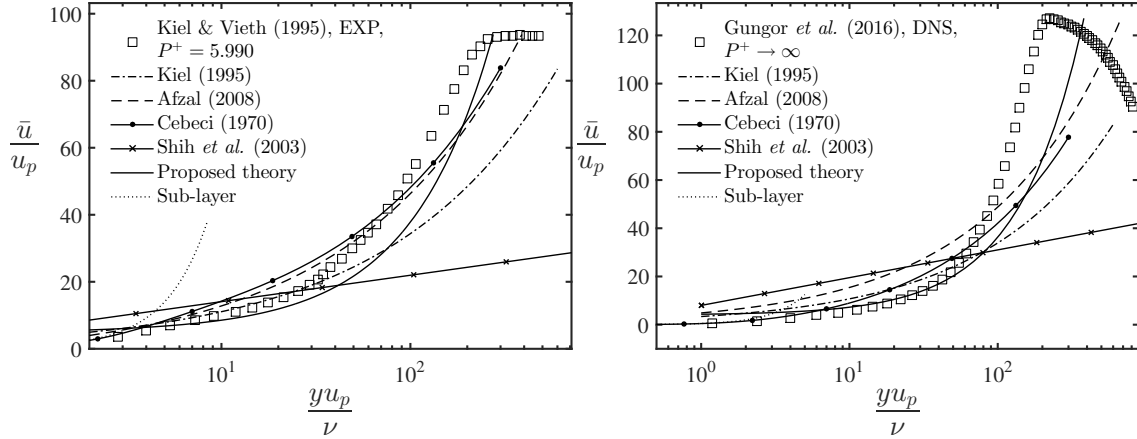
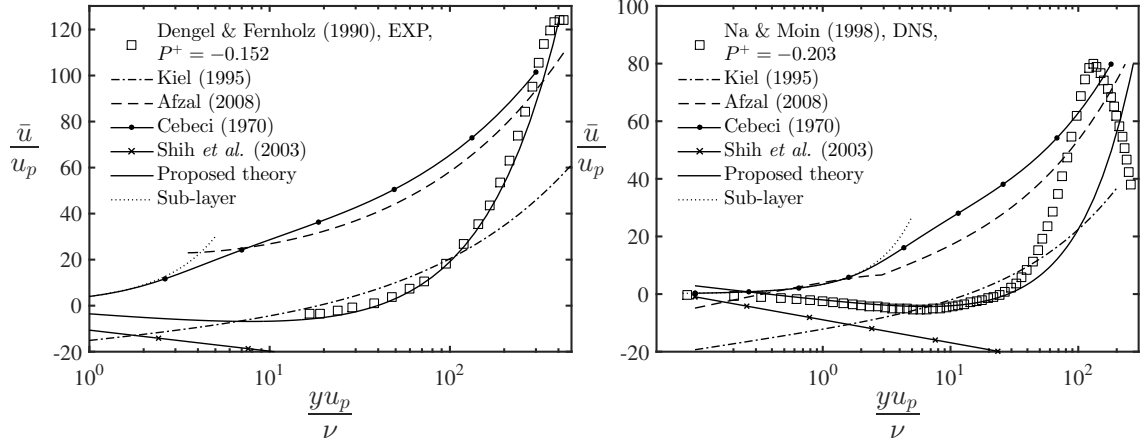


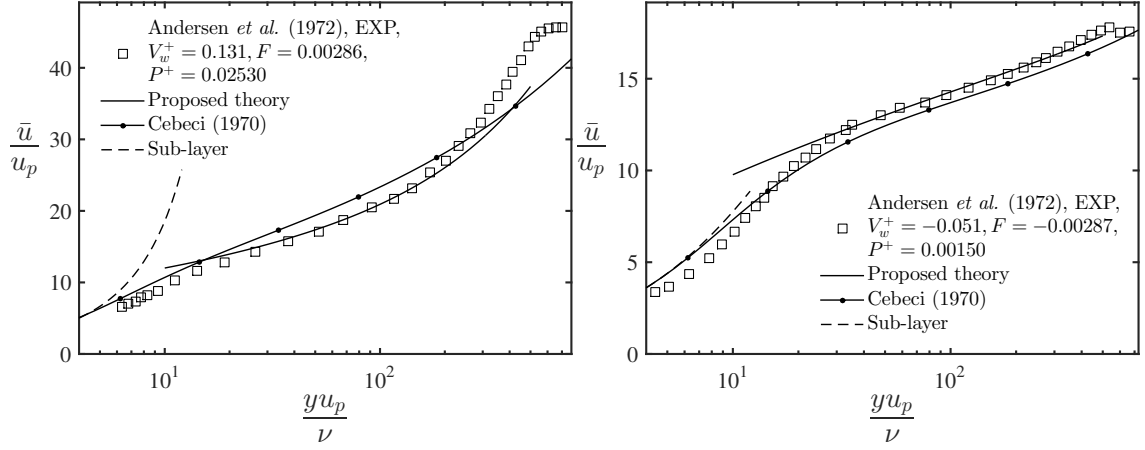
Figure 4.10: Comparisons between different theories and the data.

considers the effects of strong APGs, including flow separation, while FARACO-MEDEIROS & SILVA-FREIRE (1992) model doesn't. Considering now the pipe

Profiles in the reverse flow region



Strong APG boundary layer flow with wall transpiration



Backward facing step flow with wall injection

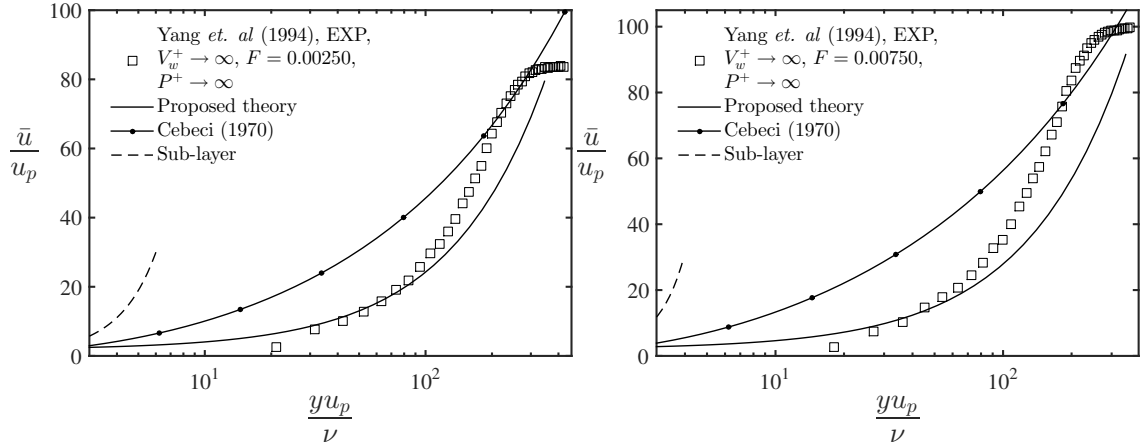


Figure 4.11: Comparisons between different theories and the data.

flow with suction EXP data from ELENA (1977), the proposed theory performs much better than the other formulations. This is no surprise as one of the constants

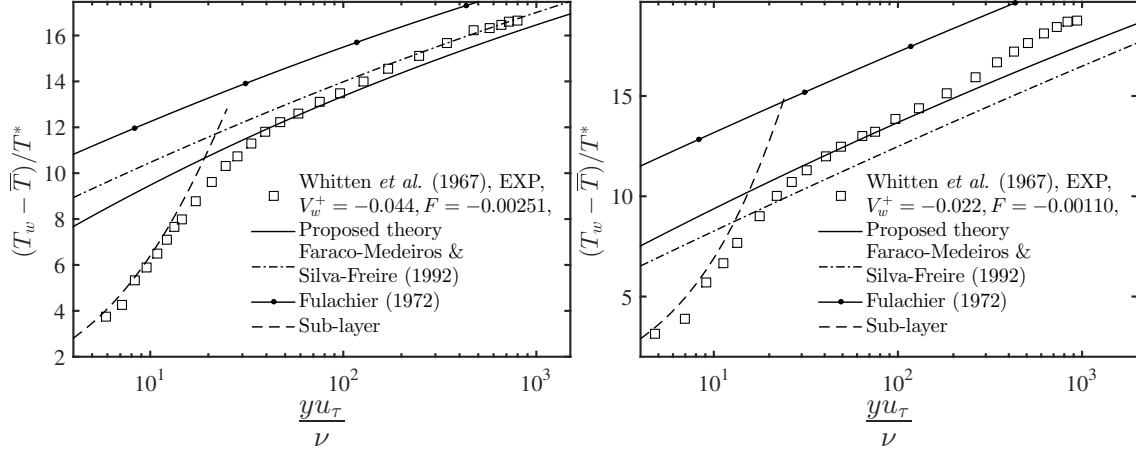
in the model was re-calibrated to fit ELENA (1977) data.

Figure 4.13 shows some comparisons between the proposed theory, KIEL (1995) version of the inverse half-power-log-law and AFZAL (1982) version of the inverse half-power law. AFZAL (1999) formulation, which has the same form of SZABLEWSKI (1972), is not shown because, although it contains the inverse half-power-law and the log-law as particular cases, it has an additive constant that tends to infinity when $\tau_w \rightarrow 0$. PERRY *et al.* (1966) and KADER (1991) versions of the inverse half-power-law also give $\bar{T} \rightarrow \infty$ as $\tau_w \rightarrow 0$ and to evaluate \bar{T} with CRUZ & FREIRE (2002) formula the EXP mean shear stress profile should be known and this quantity is only available in BLACKWELL *et al.* (1972) data. From figure 4.13 is clear that the proposed formulation has a much better performance when compared to the other models, giving an excellent fit to the data for all profiles analyzed. Considering BLACKWELL *et al.* (1972) boundary layer flows with mild APGs, both KIEL (1995) and AFZAL (1982) formulation overpredict the value of the additive constant. Their performance is improved for ORLANDO *et al.* (1974) boundary layer flows with strong APGs but for the backward-facing step flow from VOGEL (1984) they also give a poor fit to the data.

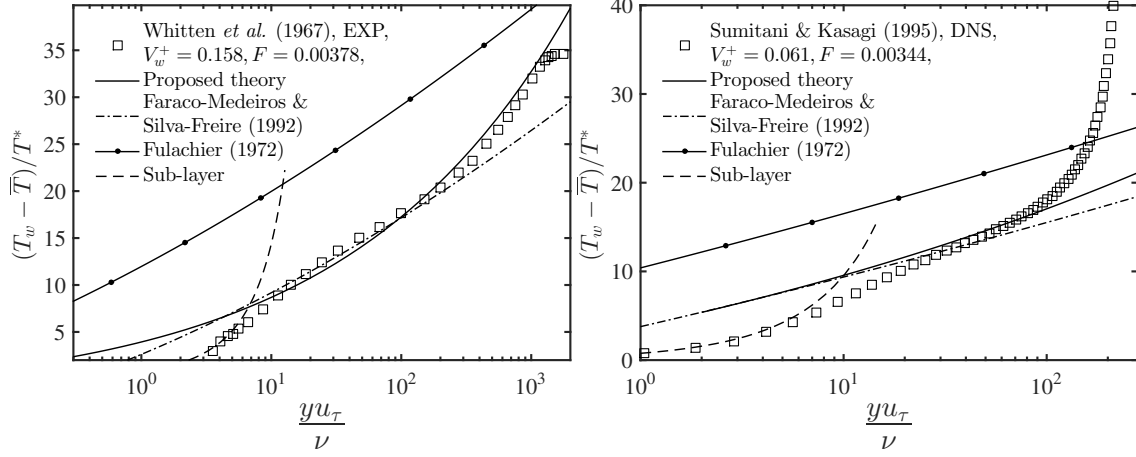
4.4 Mixing length profiles

Figures 4.14, 4.15 and 4.16 show experimental mixing length profiles from several flow developments accordingly to the proposed theory and to the classic mixing length formulation with a logarithmic scale on the abscissa so the near wall region can be seen in detail. As it can be seen from those figures, these formulations give an equivalent fit to the data in the $y/\delta < 0.15$ inner region of the boundary layer. The advantage of the new theory in relation to the classical one is that the new theory allows an analytical solution for the mean velocity profile in the case of a flow with wall transpiration and non-zero pressure gradients.

Boundary layer flow with wall suction



Boundary layer and channel flow with wall injection



Pipe flow with wall suction

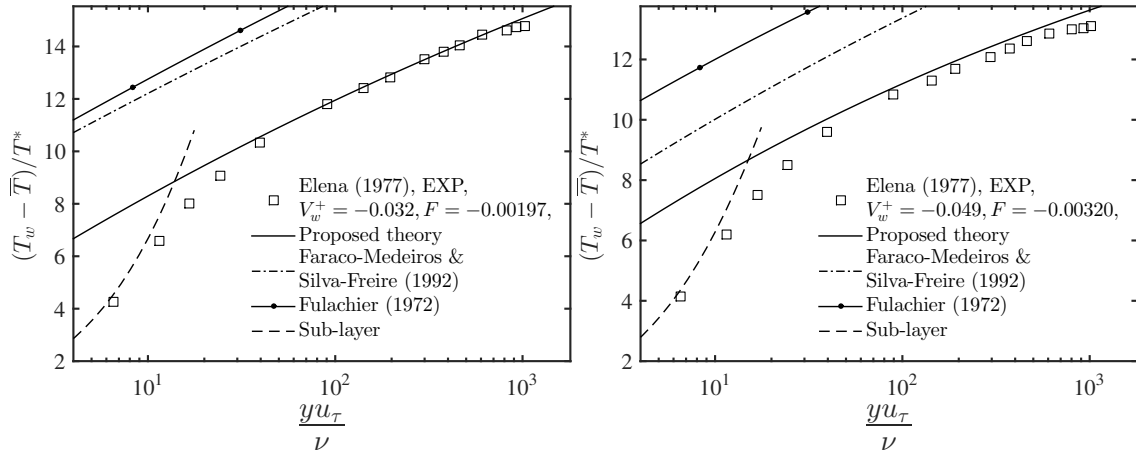
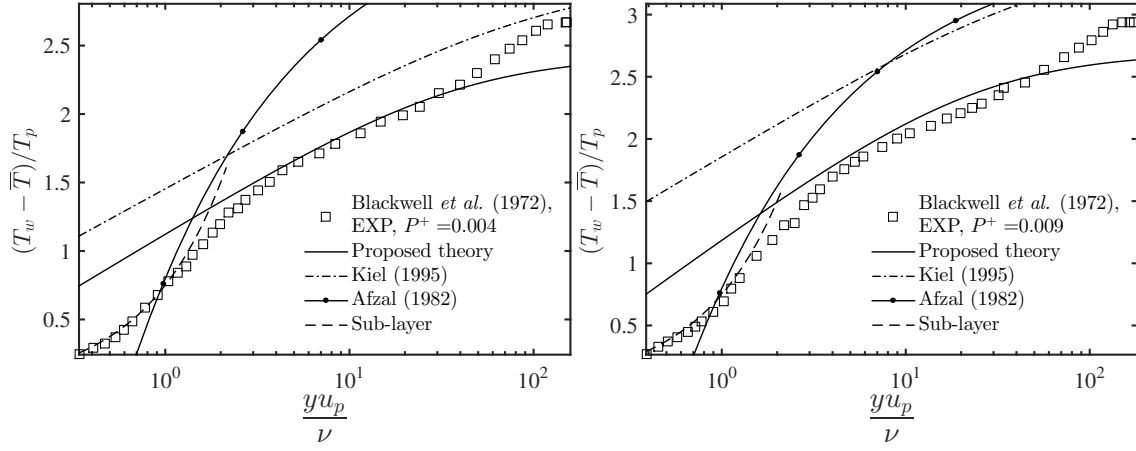
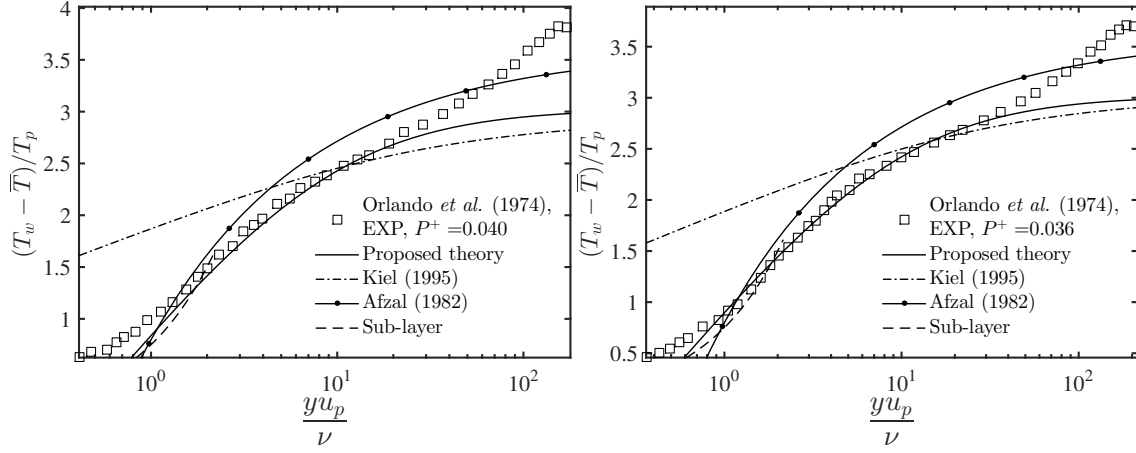


Figure 4.12: Comparisons between different theories and the data.

Mild APG boundary layer flows



Strong APG boundary layer flows



Backward facing step flow

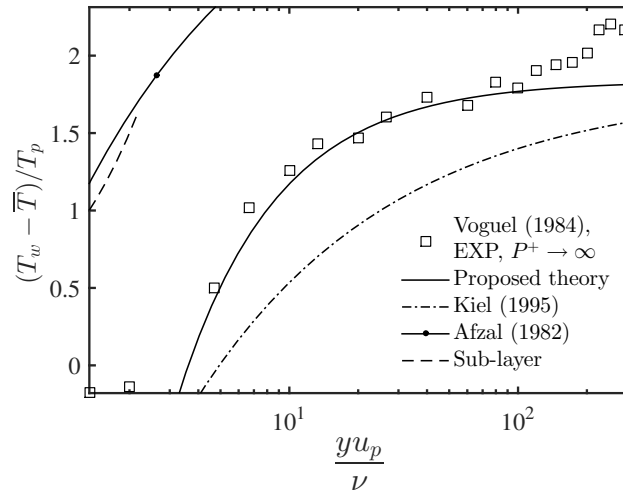


Figure 4.13: Comparisons between different theories and the data.

Zero pressure gradient boundary layer flows with wall injection

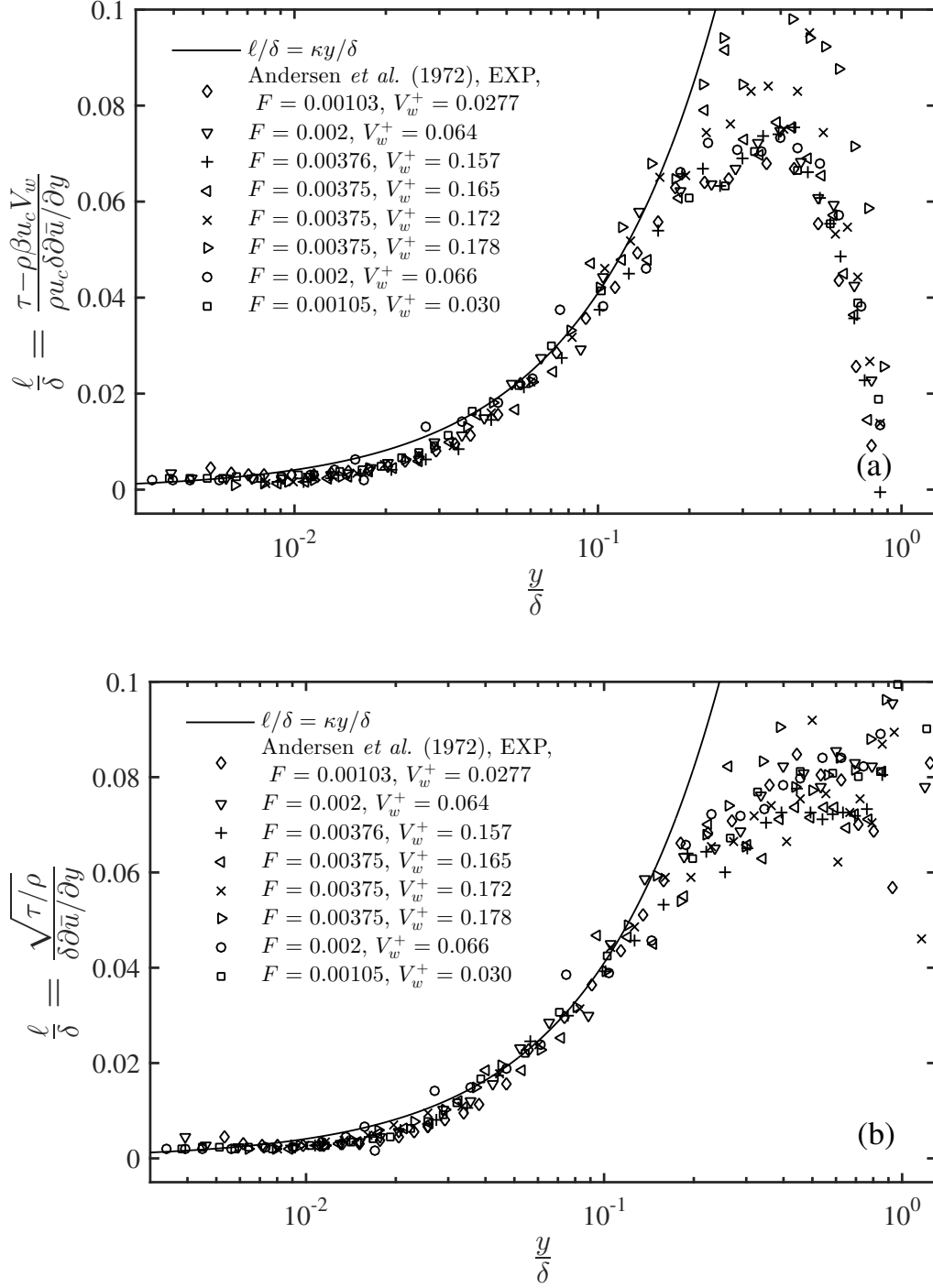


Figure 4.14: Experimental mixing length profiles according to; (a) the new theory; (b) the classic theory.

Strong and mild APG boundary layer flows with wall transpiration

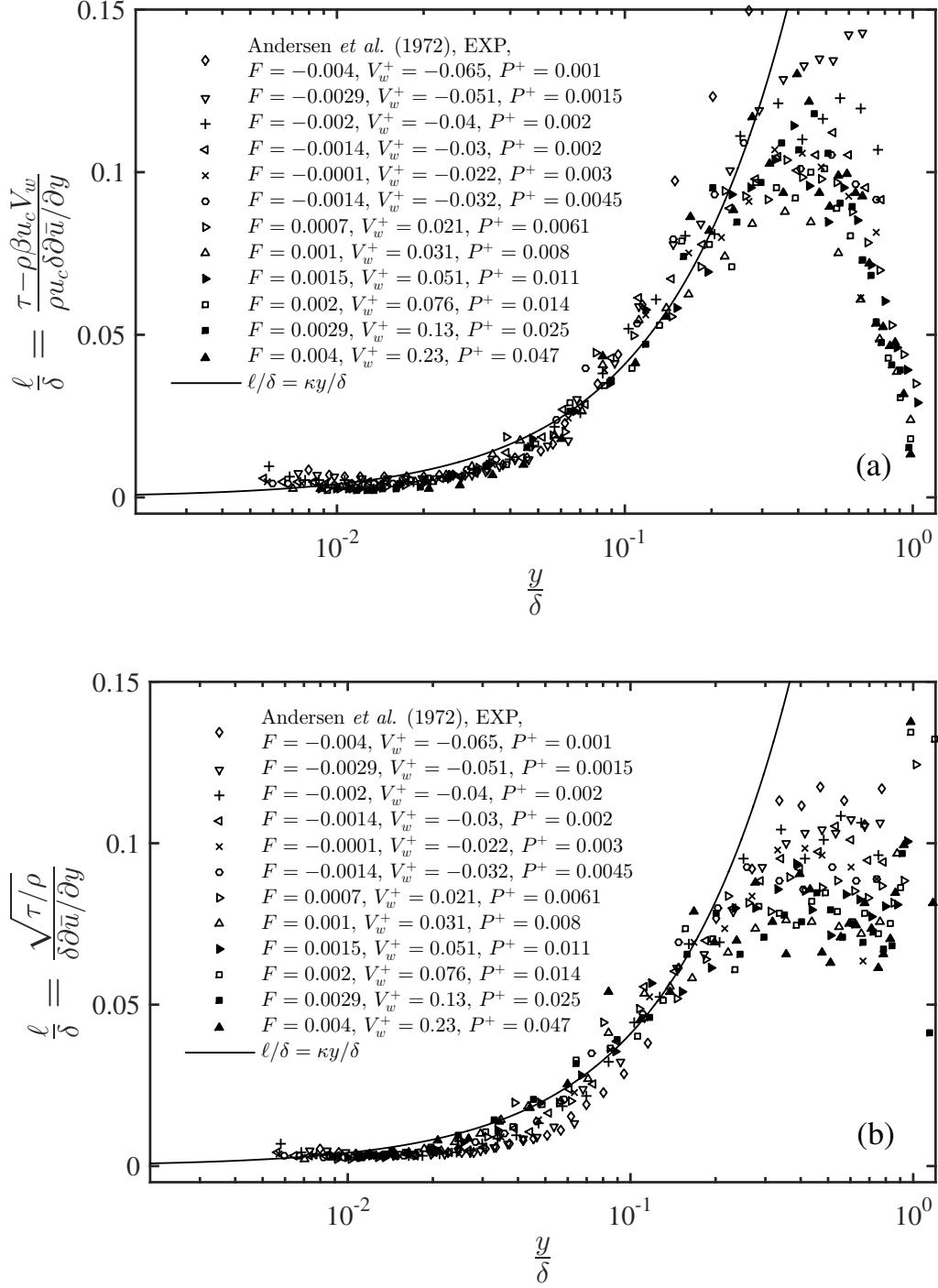


Figure 4.15: Experimental mixing length profiles according to; (a) the new theory; (b) the classic theory.

Strong APG boundary layer flows including profiles at the separation region

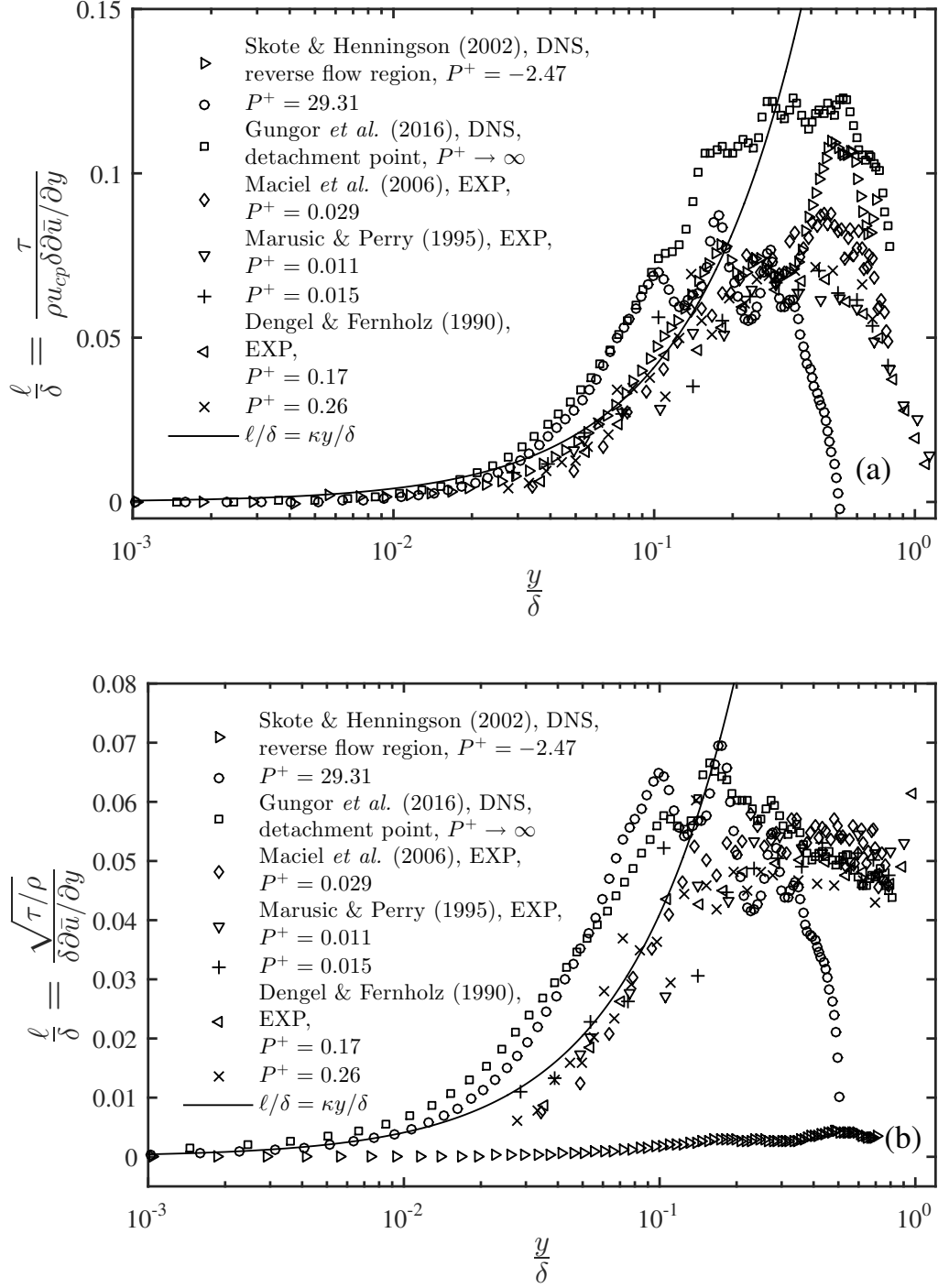


Figure 4.16: Experimental mixing length profiles according to; (a) the new theory; (b) the classic theory.

4.5 Thermal mixing length profiles

Figures 4.17 and 4.18 show experimental thermal mixing length profiles from several flow developments accordingly to the proposed theory and to the classic mixing length formulation with a logarithmic scale on the abscissa so the near wall region can be seen in detail. As it can be seen from those figures, these formulations give an equivalent fit to the data in the $y/\delta < 0.15$ inner region of the boundary layer—the new theory performs slightly better but the improvement is probably within the interval of experimental uncertainties. The advantage of the new theory in relation to the classical one is that the new theory allows an analytical solution for the mean temperature profile in the case of a flow with wall transpiration and non-zero pressure gradients.

Strong and mild APG boundary layer flows

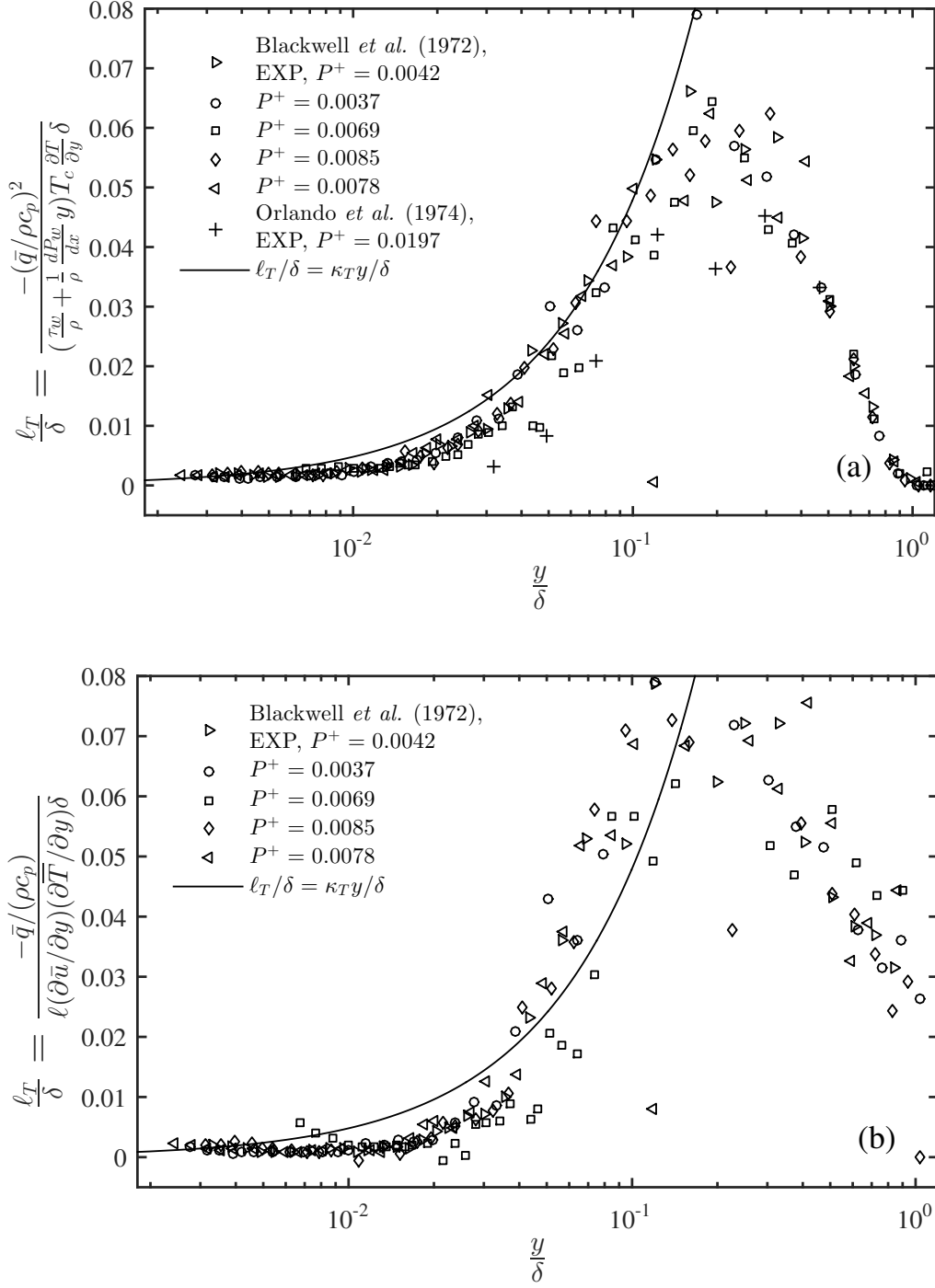


Figure 4.17: Experimental mixing length profiles accordingly to; (a) the new theory; (b) the classic theory.

Strong and mild APG boundary layer flows with wall transpiration

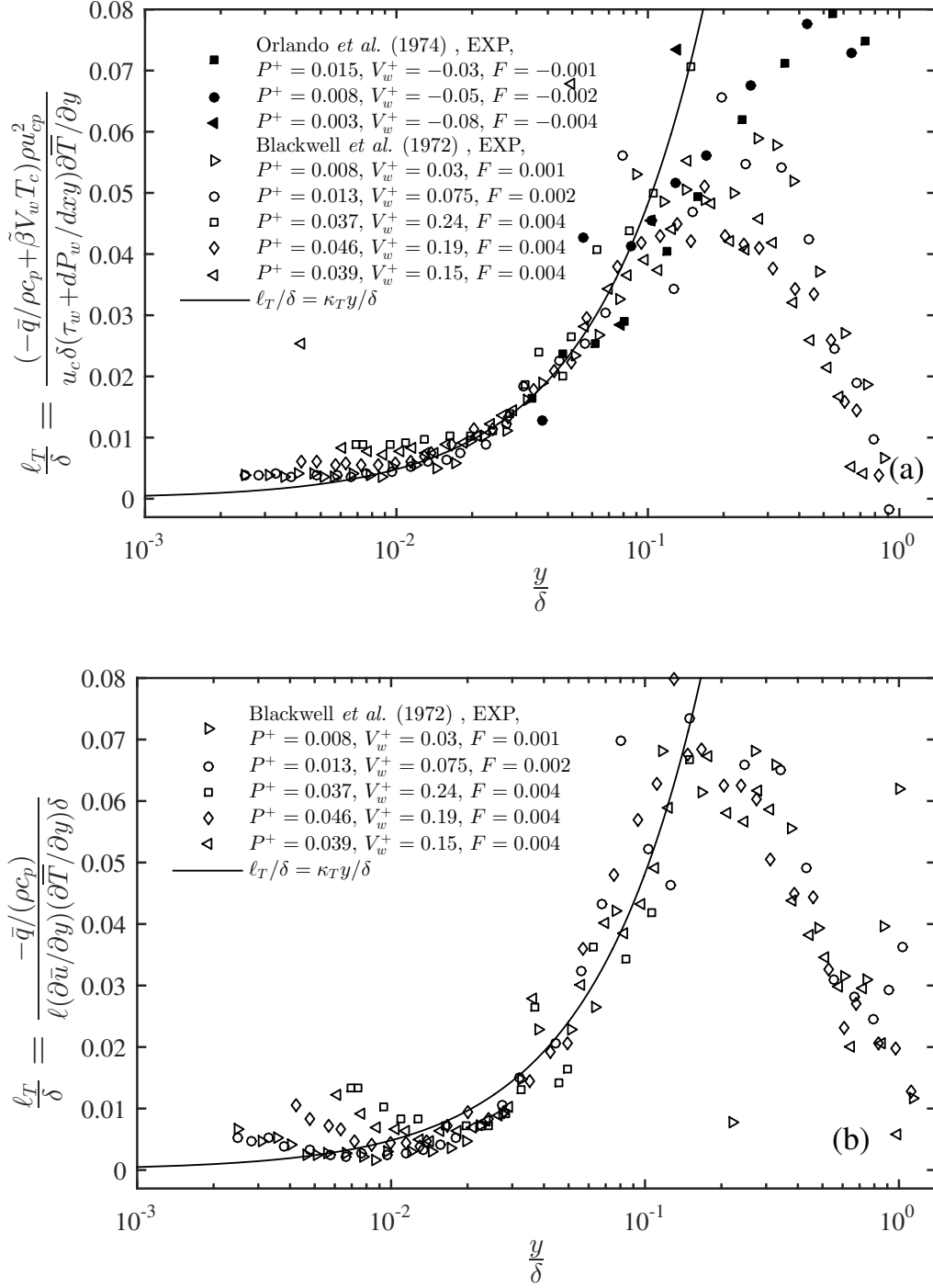


Figure 4.18: Experimental thermal mixing length profiles accordingly to; (a) the new theory; (b) the classic theory.

Chapter 5

Discussion and Conclusion

New scaling laws for transpired turbulent flows with non-zero pressure gradients and wall heat transfer were derived. To the present author knowledge, the new wall laws are the first presented in literature that consider flow transpiration and separation. It emerges from the proposed scaling that mean velocity and temperature profiles are self-similar with respect to the transpiration rate in the whole wall region of the flow— another key original result.

In the proposed formulation all free parameters are constants that do not vary with the transpiration rate or the pressure gradient parameter and no empirical corrections to the Von Karman constant and y -axis intercept were used. The domains of validity of the wall laws were extended, to include the outer region of the boundary layer, using the intermittent character of the flow in that region. The *intermittency factor* was found to be a universal function of the wall normal direction scaled by the boundary layer thickness.

The wall functions derived in this work can be used as boundary conditions in high Reynolds number turbulence models and the expressions for the mean velocity and temperature distributions in the outer region can provide the basis for integral methods of predicting such complex flows. The theoretical framework proposed here has a simple mathematical form so it can be extended to include the effects of surface roughness, flow compressibility, non Newtonian fluids and so on.

Finally, it is understood that the implicit rule in presenting any new theory that challenges well-established results is that the new theory should be more general, require fewer empirical inputs, and give a better or at least equivalent fit to the data. It is hoped that this study may meet those requirements.

Bibliography

- ABE, H., MIZOBUCHI, Y., MATSUO, Y., et al., 2012, “DNS and modeling of a turbulent boundary layer with separation and reattachment over a range of reynolds numbers”, *Annual Research Briefs*, v. 143.
- ABE, H., MIZOBUCHI, Y., MATSUO, Y., et al., 2013, “DIRECT NUMERICAL SIMULATION AND MODELING OF A TURBULENT BOUNDARY LAYER WITH SEPARATION AND REATTACHMENT”. In: *TSFP DIGITAL LIBRARY ONLINE*. Begel House Inc.
- AFZAL, N., 1975, “Effects of longitudinal curvature, vorticity and displacement for two-dimensional turbulent boundary layers with heat and mass transfer”, *Journal de Mecanique*, v. 14, pp. 823–841.
- AFZAL, N., 1982, “Thermal turbulent boundary layer under strong adverse pressure gradient near separation”, *ASME, Transactions, Journal of Heat Transfer*, v. 104, pp. 397–402.
- AFZAL, N., 1999, “Wake layer in a thermal turbulent boundary layer with pressure gradient”, *Heat and Mass Transfer*, v. 35, n. 4, pp. 281–288.
- AFZAL, N., 2001, “Power law and log law velocity profiles in turbulent boundary-layer flow: equivalent relations at large Reynolds numbers”, *Acta Mechanica*, v. 151, n. 3-4, pp. 195–216.
- AFZAL, N., 1983, “Analysis of a turbulent boundary layer subjected to a strong adverse pressure gradient”, *International Journal of Engineering Science*, v. 21, n. 6, pp. 563 – 576. ISSN: 0020-7225.
- AFZAL, N., 1976, “Millikan’s argument at moderately large Reynolds number”, *The Physics of Fluids*, v. 19, n. 4, pp. 600–602.
- AFZAL, N., 1996, “Wake layer in a turbulent boundary layer with pressure gradient- A new approach”. In: *IUTAM Symposium on Asymptotic Methods for Turbulent Shear Flows at High Reynolds Numbers, Bochum, Germany*, pp. 95–118.

- AFZAL, N., 2008, “Turbulent boundary layer with negligible wall stress”, *Journal of Fluids Engineering*, v. 130, n. 5, pp. 051205.
- AGRAWAL, A., DJENIDI, L., ANTONIA, R. A., 2010, “Near-field measurements and development of a new boundary layer over a flat plate with localized suction”, *Experiments in Fluids*, v. 48, n. 5, pp. 747–762. ISSN: 1432-1114. doi: 10.1007/s00348-009-0766-7. Available at: <<http://dx.doi.org/10.1007/s00348-009-0766-7>>.
- ALLAN, W. K., 1970, “Velocity Distribution in Turbulent Flow”, *Journal of Mechanical Engineering Science*, v. 12, n. 6, pp. 391–399.
- ALVING, A. E., FERNHOLZ, H., 1995, “Mean-velocity scaling in and around a mild, turbulent separation bubble”, *Physics of Fluids*, v. 7, n. 8, pp. 1956–1969.
- ANDERSEN, P. S., KAYS, W. M., MOFFAT, R. J., 1972, *The turbulent boundary layer on a porous plate: an experimental study of the fluid mechanics for adverse free stream pressure gradients*. In: Report HMT-15, Stanford University.
- ANTONIA, R. A., FULACHIER, L., KRISHNAMOORTHY, L. V., et al., 1988, “Influence of wall suction on the organized motion in a turbulent boundary layer”, *Journal of Fluid Mechanics*, v. 190 (005), pp. 217–240. doi: 10.1017/S0022112088001296.
- ANTONIA, R., FULACHIER, L., 1989, “Topology of a turbulent boundary layer with and without wall suction”, *Journal of Fluid Mechanics*, v. 198, pp. 429–451.
- ATKINSON, C., BUCHNER, A.-J., EISFELDER, M., et al., 2016, “Time-resolved PIV measurements of a self-similar adverse pressure gradient turbulent boundary layer”. In: *Proceedings of the 18th International Symposium on the Application of Laser and Imaging Techniques to Fluid Mechanics, Lisbon, Portugal*.
- AVSARKISOV, V., OBERLACK, M., HOYAS, S., 2014, “New scaling laws for turbulent Poiseuille flow with wall transpiration”, *Journal of Fluid Mechanics*, v. 746 (005), pp. 99–122. doi: 10.1017/jfm.2014.98.
- AVSARKISOV, V., OBERLACK, M., HOYAS, S., et al., 2013, “New mean velocity scaling laws for turbulent Poiseuille flow with wall transpiration”. In: *14th European Turbulence Conference (ETC-14)*.

- BAKER, R., LAUNDER, B., 1974a, “The turbulent boundary layer with foreign gas injection—II. Predictions and measurements in severe streamwise pressure gradients”, *International Journal of Heat and Mass Transfer*, v. 17, n. 2, pp. 293–306.
- BAKER, R., LAUNDER, B., 1974b, “The turbulent boundary layer with foreign gas injection—I. Measurements in zero pressure gradient”, *International Journal of Heat and Mass Transfer*, v. 17, n. 2, pp. 275–291.
- BARENBLATT, G., 1993, “Scaling laws for fully developed turbulent shear flows. Part 1. Basic hypotheses and analysis”, *Journal of Fluid Mechanics*, v. 248, pp. 513–520.
- BARENBLATT, G., MONIN, A., 1979, “Similarity laws for turbulent stratified shear flows”, *Archive for Rational Mechanics and Analysis*, v. 70, n. 4, pp. 307–317.
- BARENBLATT, G., CHORIN, A., PROSTOKISHIN, V., 1997, “Scaling laws for fully developed turbulent flow in pipes”, *Applied Mechanics Reviews*, v. 50, pp. 413–429.
- BARONTI, P., LIBBY, P., NAPOLITANO, L., 1964, “Study of the incompressible turbulent boundary layer with pressure gradient”, *AIAA Journal*, v. 2, n. 3, pp. 445–452.
- BAZIN, H., 1865, *Recherches hydrauliques*, v. 1. Impr. Impériale.
- BELLETTRE, J., 1998, *Transferts de masse et de chaleur dans la couche limite pariétale et à l’intérieur d’une paroi poreuse plane soumise à de l’effusion ou de la transpiration*. Ph.D Thesis. Available at: <<http://www.theses.fr/1998ISAL0094/document>>. Thèse de doctorat Thermique et énergétique Lyon, INSA 1998.
- BERNARD, A., FOUCAUT, J.-M., DUPONT, P., et al., 2003, “Decelerating boundary layer: a new scaling and mixing length model”, *AIAA Journal*, v. 41, n. 2, pp. 248–255.
- BERNARD, P. S., WALLACE, J. M., 2002, *Turbulent flow: analysis, measurement, and prediction*. John Wiley & Sons.
- BLACK, T., SARNECKI, A., 1958, *The Turbulent Boundary Layer with Suction Or Injection*. Report 3387, ARC.

- BLACKWELL, B. F., KAYS, W. M., MOFFAT, R. J., 1972, *The turbulent boundary layer on a porous plate: an experimental study of the heat transfer behavior with adverse pressure gradients*. Report, NASA Ngl 05-020-134, Stanford University.
- BOBKE, A., ÖRLÜ, R., SCHLATTER, P., 2016, “Simulations of turbulent asymptotic suction boundary layers”, *Journal of Turbulence*, v. 17, n. 2, pp. 157–180. doi: 10.1080/14685248.2015.1083574. Available at: <<http://dx.doi.org/10.1080/14685248.2015.1083574>>.
- BOUSSINESQ, J., 1870, “Essai théorique sur les lois trouvées expérimentalement par M. Bazin pour l’écoulement uniforme de l’eau dans les canaux découverts”, *CR Acad. Sci. Paris*, v. 71, pp. 389–393.
- BOUSSINESQ, J., 1877, “Essai sur la théorie des eaux courantes”, *Mem. pres. par div. savants a l’Acad. Sci.*, v. 23, pp. 1–680.
- BRADSHAW, P., 1967, “Mixing-length velocity profile in boundary layers with transpiration.” *AIAA Journal*, v. 5, n. 9 (Sep), pp. 1674–1675. ISSN: 0001-1452. doi: 10.2514/3.4267. Available at: <<http://dx.doi.org/10.2514/3.4267>>.
- BREUGEM, W., BOERSMA, B., UITTENBOGAARD, R., 2006, “The influence of wall permeability on turbulent channel flow”, *Journal of Fluid Mechanics*, v. 562, pp. 35–72.
- BROWN, K., JOUBERT, P., 1969, “The measurement of skin friction in turbulent boundary layers with adverse pressure gradients”, *Journal of Fluid Mechanics*, v. 35, n. 4, pp. 737–757.
- BULL, M. K., 1969, “Velocity Profiles of Turbulent Boundary Layers”, *The Aeronautical Journal (1968)*, v. 73, n. 698, pp. 143–147. doi: 10.1017/S000192400005329X.
- BUSCHMANN, M. H., GAD-EL HAK, M., 2003, “Generalized logarithmic law and its consequences”, *AIAA Journal*, v. 41, n. 1, pp. 40–48.
- BUSCHMANN, M. H., GAD-EL HAK, M., 2007, “Turbulent boundary layers: reality and myth”, *International Journal of Computing Science and Mathematics*, v. 1, n. 2-4, pp. 159–176.
- CASTILLO, L., GEORGE, W. K., 2001, “Similarity analysis for turbulent boundary layer with pressure gradient: outer flow”, *AIAA Journal*, v. 39, n. 1, pp. 41–47.

- CEBECI, T., 1970, “Behavior of turbulent flow near a porous wall with pressure gradient”, *AIAA Journal*, v. 8, n. 12 (Dec), pp. 2152–2156. ISSN: 0001-1452. doi: 10.2514/3.6079. Available at: <<http://dx.doi.org/10.2514/3.6079>>.
- CEBECI, T., 2004, *Analysis of Turbulent Flows with Computer Programs*. Elsevier Science. ISBN: 9780080527185. Available at: <<https://books.google.com.br/books?id=N8sRQE0kwG8C>>.
- CHAUHAN, K., NAGIB, H., MONKEWITZ, P., 2007, “On the composite logarithmic profile in zero pressure gradient turbulent boundary layers”. In: *45th AIAA Aerospace Sciences Meeting and Exhibit*, p. 532.
- CHAUHAN, K., PHILIP, J., MARUSIC, I., 2014, “Scaling of the turbulent/non-turbulent interface in boundary layers”, *Journal of Fluid Mechanics*, v. 751, pp. 298–328.
- CHOI, H., MOIN, P., KIM, J., 1994, “Active turbulence control for drag reduction in wall-bounded flows”, *Journal of Fluid Mechanics*, v. 262 (10), pp. 75–110.
- CHUNG, Y. M., SUNG, H. J., 2001, “Initial relaxation of spatially evolving turbulent channel flow with blowing and suction”, *AIAA Journal*, v. 39, n. 11, pp. 2091–2099.
- CLARKE, J. H., MENKES, H. R., LIBBY, P. A., 1955, “A Provisional Analysis of Turbulent Boundary Layers with Injection”, *Journal of the Aeronautical Sciences*, v. 22, n. 4 (Apr), pp. 255–260. doi: 10.2514/8.3322. Available at: <<http://dx.doi.org/10.2514/8.3322>>.
- CLAUSER, F. H., 1954, “Turbulent Boundary Layers in Adverse Pressure Gradients”, *Journal of the Aeronautical Sciences*, v. 21, n. 2 (Feb), pp. 91–108. doi: 10.2514/8.2938. Available at: <<http://dx.doi.org/10.2514/8.2938>>.
- CLAUSER, F. H., 1956, “The Turbulent Boundary Layer”. v. 4, *Advances in Applied Mechanics*, Elsevier, pp. 1 – 51.
- CLEMO, T., OTHERS, 2006, “Flow in perforated pipes: A comparison of models and experiments”, *SPE Production & Operations*, v. 21, n. 02, pp. 302–311.

- COLEMAN, G., GARBARUK, A., SPALART, P., 2015, “Direct numerical simulation, theories and modelling of wall turbulence with a range of pressure gradients”, *Flow, Turbulence and Combustion*, v. 95, n. 2-3, pp. 261–276.
- COLES, D., 1972, “A survey of data for turbulent boundary layers with mass transfer”, *AGARD Turbulent Shear Flows 15 p(SEE N 72-20273 11-12)*.
- COLES, D., 1956, “The law of the wake in the turbulent boundary layer”, *Journal of Fluid Mechanics*, v. 1, n. 02, pp. 191–226.
- COLES, D., 1968, *The young person’s guide to the data*. Report, DTIC Document.
- CORNISH, J. J. I., 1960, *A UNIVERSAL DESCRIPTION OF TURBULENT BOUNDARY LAYER PROFILES WITH OR WITHOUT TRANSPIRATION*. Report, Mississippi State University Aerophysics Dept.
- CORRSIN, S., KISTLER, A. L., 1955, *Free-stream boundaries of turbulent flows*. Report 1244, NACA.
- CRUZ, D. O., FREIRE, A. P. S., 1998, “On single limits and the asymptotic behaviour of separating turbulent boundary layers”, *International Journal of Heat and Mass Transfer*, v. 41, n. 14, pp. 2097 – 2111. ISSN: 0017-9310.
- CRUZ, D. O., FREIRE, A. P. S., 2002, “Note on a thermal law of the wall for separating and recirculating flows”, *International Journal of heat and Mass transfer*, v. 45, n. 7, pp. 1459–1465.
- CUVIER, C., SRINATH, S., STANISLAS, M., et al., 2017, “Extensive characterization of a high Reynolds number decelerating boundary layer using advanced optical metrology”, *arXiv preprint arXiv:1702.02834*.
- DA SILVA, C. B., TAVEIRA, R. R., 2010, “The thickness of the turbulent/nonturbulent interface is equal to the radius of the large vorticity structures near the edge of the shear layer”, *Physics of Fluids*, v. 22, n. 12, pp. 121702.
- DA SILVA, C. B., HUNT, J. C., EAMES, I., et al., 2014, “Interfacial layers between regions of different turbulence intensity”, *Annual Review of Fluid Mechanics*, v. 46, pp. 567–590.
- DA SILVA, C. B., DOS REIS, R. J. N., 2011, “The role of coherent vortices near the turbulent/non-turbulent interface in a planar jet”, *Philosophical Transactions of the Royal Society of London A: Mathematical, Physical and Engineering Sciences*, v. 369, n. 1937, pp. 738–753.

- DAHLM, T. J., KENDALL, R. M., 1968, "Comment on "Inner Region of Transpired Turbulent Boundary Layers"", *AIAA Journal*, v. 6, n. 9 (Sep), pp. 1822–1824. ISSN: 0001-1452. doi: 10.2514/3.55422. Available at: <<http://dx.doi.org/10.2514/3.55422>>.
- DARCY, H., 1858, *Recherches Experimentales Relatives aux Mouvements de l'eau Dans les Tuyaux*. Mémoires de l'Académie des Sciences de l'Institut Impérial de France, Paris.
- DAS, D. K., WHITE, F. M., 1986, "Integral Skin Friction Prediction for Turbulent Separated Flows", *Journal of Fluids Engineering*, v. 108, n. 4 (Dec), pp. 476–482. ISSN: 0098-2202. doi: 10.1115/1.3242606. Available at: <<http://dx.doi.org/10.1115/1.3242606>>.
- DAS, D., 1987, "A numerical study of turbulent separated flows". In: *Forum on Turbulent Flows - 1987*, pp. 85–90.
- DE SILVA, C. M., PHILIP, J., HUTCHINS, N., et al., 2017, "Interfaces of uniform momentum zones in turbulent boundary layers", *Journal of Fluid Mechanics*, v. 820, pp. 451–478.
- DEAN, R. B., 1976, "A single formula for the complete velocity profile in a turbulent boundary layer", *Journal of Fluids Engineering*, v. 3, n. 4, pp. 723.
- DENGEL, P., FERNHOLZ, H., 1990, "An experimental investigation of an incompressible turbulent boundary layer in the vicinity of separation", *Journal of Fluid Mechanics*, v. 212, pp. 615–636.
- DEVENPORT, W., SUTTON, E., 1991, "Near-wall behavior of separated and reattaching flows", *AIAA Journal*, v. 29, n. 1, pp. 25–31.
- DIANAT, M., CASTRO, I., 1989, "Measurements in separating boundary layers", *AIAA Journal*, v. 27, n. 6, pp. 719–724.
- DIXIT, S. A., RAMESH, O., 2009, "Determination of skin friction in strong pressure-gradient equilibrium and near-equilibrium turbulent boundary layers", *Experiments in Fluids*, v. 47, n. 6, pp. 1045.
- DORRANCE, W. H., 1956, "Readers Forum", *Journal of the Aeronautical Sciences*, v. 23, n. 3 (Mar), pp. 272–288. doi: 10.2514/8.3546. Available at: <<http://dx.doi.org/10.2514/8.3546>>.
- DORRANCE, W. H., DORE, F. J., 1954, "The Effect of Mass Transfer on the Compressible Turbulent Boundary-Layer Skin Friction and Heat Transfer",

- Journal of the Aeronautical Sciences*, v. 21, n. 6 (Jun), pp. 404–410. doi: 10.2514/8.3050. Available at: <<http://dx.doi.org/10.2514/8.3050>>.
- DRIVER, D., 1991, “Reynolds shear stress measurements in a separated boundary layer flow”. In: *22nd Fluid Dynamics, Plasma Dynamics and Lasers Conference*, p. 1787.
- DRIVER, D. M., SEEGMILLER, H. L., 1985, “Features of a reattaching turbulent shear layer in divergent channel flow”, *AIAA Journal*, v. 23, n. 2, pp. 163–171.
- DURBIN, P., BELCHER, S., 1992, “Scaling of adverse-pressure-gradient turbulent boundary layers”, *Journal of Fluid Mechanics*, v. 238, pp. 699–722.
- DURBIN, P. A., REIF, B. P., 2011, *Statistical Theory and Modeling for Turbulent Flows*. John Wiley & Sons.
- DUTTON, R. A., 1960, *The effects of distributed suction on the development of turbulent boundary layer*. R. & M. 3155, Aeronautical Research Council.
- ELENA, M., 1977, *Study of the dynamic and thermal fields in a turbulent pipe flow with wall suction*. Report, France. CEA-R-4843.
- ERSHIN, S. A., ZHAPBASBAEV, U. K., KOZHAKHMETOV, T. B., et al., 1991, “Turbulent incompressible fluid flow in a channel with unilateral mass transfer”, *Journal of Applied Mechanics and Technical Physics*, v. 32, n. 1, pp. 57–63. ISSN: 1573-8620. doi: 10.1007/BF00852264. Available at: <<http://dx.doi.org/10.1007/BF00852264>>.
- FARACO-MEDEIROS, M. A., SILVA-FREIRE, A. P., 1992, “The transfer of heat in turbulent boundary layers with injection or suction: universal laws and Stanton number equations”, *International Journal of Heat and Mass Transfer*, v. 35, n. 4, pp. 991–995.
- FAVRE, A., DUMAS, R., VEROLLET, E., et al., 1966, “Couche limite turbulente sur paroi poreuse avec transpiration”, *Journal de Mécanique*, v. 5, n. 1, pp. 3–28.
- FERRO, M., FALLENIIUS, B. E. G., FRANSSON, J. H. M., 2017, “On the scaling of turbulent asymptotic suction boundary layers”. In: *10th International Symposium on Turbulence and Shear Flow Phenomena (TSFP10)*, Chicago, USA.
- FERRO, M., 2017, *Experimental study on turbulent boundary-layer flows with wall transpiration*. Ph.D Thesis, KTH Royal Institute of Technology.

- FINLEY, P. J., PHOE, K. C., POH, J., 1966, “Velocity measurements in a thin turbulent water layer”, *La Houille Blanche*, , n. 6, pp. 713–721. doi: 10.1051/lhb/1966045. Available at: <<https://doi.org/10.1051/lhb/1966045>>.
- FINNIGAN, J., 2000, “Turbulence in plant canopies”, *Annual review of fluid mechanics*, v. 32, n. 1, pp. 519–571.
- FREWER, M., KHUJADZE, G., FOYSI, H., 2014, “Is the log-law a first principle result from Lie-group invariance analysis?” *arXiv preprint arXiv:1412.3069*.
- FRISCH, U., 1995, *Turbulence: the legacy of AN Kolmogorov*. Cambridge University Press.
- FULACHIER, L., VEROLLET, E., DEKEYSER, I., 1977, “Resultats experimentaux concernant une couche limite turbulente avec aspiration et chauffage a la paroi”, *International Journal of Heat and Mass Transfer*, v. 20, n. 7, pp. 731 – 739. ISSN: 0017-9310.
- FULACHIER, L., BENABID, T., ANSELMET, F., et al., 1987, “Behaviour of Coherent Structures in a Turbulent Boundary Layer with Wall Suction”. In: Comte-Bellot, G., Mathieu, J. (Eds.), *Advances in Turbulence: Proceedings of the First European Turbulence Conference Lyon, France, 1–4 July 1986*, pp. 399–407, Berlin, Heidelberg, Springer Berlin Heidelberg. ISBN: 978-3-642-83045-7.
- FULACHIER, L., 1972, *Contribution à l’étude des analogies des champs dynamique et thermique dans une couche limite turbulente: effet de l’aspiration*. Ph.D Thesis, Université de Provence.
- GAD-EL HAK, M., 2000, *Flow Control; Passive, Active and Reactive Flow Management*. Cambridge University Press.
- GEORGE, W. K., 2007, “Is there a universal log law for turbulent wall-bounded flows?” *Philosophical Transactions of the Royal Society of London A: Mathematical, Physical and Engineering Sciences*, v. 365, n. 1852, pp. 789–806.
- GEORGE, W. K., CASTILLO, L., KNECHT, P., 1997, “Zero-pressure-gradient turbulent boundary layer”, *Applied Mechanics Reviews*, v. 50, pp. 689–730.

- GERSTEN, K., 1998, “Turbulent Boundary Layers I”. In: Kluwick, A. (Ed.), *Recent Advances in Boundary Layer Theory*, pp. 107–144, Vienna, Springer Vienna.
- GERSTEN, K., KLAUER, J., VIETH, D., 1993, “Asymptotic Analysis of Two—Dimensional Turbulent Separating Flows”. In: *Physics of Separated Flows—Numerical, Experimental, and Theoretical Aspects*, Springer, pp. 125–132.
- GOLDSTEIN, R. J., 1971, “Film cooling”, *Advances in heat transfer*, v. 7, pp. 321–379.
- GÓMEZ, F., BLACKBURN, H. M., RUDMAN, M., et al., 2016, “Streamwise-varying steady transpiration control in turbulent pipe flow”, *Journal of Fluid Mechanics*, v. 796 (006), pp. 588–616. doi: 10.1017/jfm.2016.279.
- GRANVILLE, P. S., 1987, “Three indirect methods for the drag characterization of arbitrarily rough surfaces on flat plates”. In: *Proceedings of the Twenty-first American Towing Tank Conference*, p. 117. National Academies.
- GRANVILLE, P. S., 1976, “A modified law of the wake for turbulent shear layers”, *Journal of Fluids Engineering*, v. 98, n. 3, pp. 578–580.
- GRANVILLE, P., 1989, “A modified van Driest formula for the mixing length of turbulent boundary layers in pressure gradients”, *ASME, Transactions, Journal of Fluids Engineering*, v. 111, pp. 94–97.
- GUNGOR, A., MACIEL, Y., SIMENS, M., et al., 2016, “Scaling and statistics of large-defect adverse pressure gradient turbulent boundary layers”, *International Journal of Heat and Fluid Flow*, v. 59, pp. 109–124.
- GUO, J., JULIEN, P. Y., 2001, “Turbulent velocity profiles in sediment-laden flows”, *Journal of Hydraulic Research*, v. 39, n. 1, pp. 11–23.
- GUO, J., JULIEN, P. Y., 2003, “Modified log-wake law for turbulent flow in smooth pipes”, *Journal of Hydraulic Research*, v. 41, n. 5, pp. 493–501.
- HINZE, J., 1959, *Turbulence*. McGraw-Hill.
- HUDIMOTO, B., 1935, *On the turbulent boundary layer with pressure rise and fall*. Ph.D Thesis, kyoto Imperial University.
- ISAKSON, A., 1937, “On the Formula for the Velocity Distribution Near Walls”, *Zh. Eksp. Teor. Fiz*, v. 7.

- JARŻA, A., 1988, “Struktura turbulencji i bilans jej energii w warstwie przyściennej na powierzchni przepuszczalnej”, *Journal of Theoretical and Applied Mechanics*, v. 26, n. 2, pp. 329–345.
- JIMÉNEZ, J., UHLMANN, M., PINELLI, A., et al., 2001, “Turbulent shear flow over active and passive porous surfaces”, *Journal of Fluid Mechanics*, v. 442 (09), pp. 89–117. doi: 10.1017/S0022112001004888.
- JOHNSON, D. A., KING, L., 1984, “A new turbulence closure model for boundary layer flows with strong adverse pressure gradients and separation”. In: *AIAA, Aerospace Sciences Meeting*.
- JONSSON, V., SCOTT, C., 1965, *Uniform air injection into a turbulent boundary layer flow over an axial circular cylinder*. Report, MINNESOTA UNIV MINNEAPOLIS HEAT TRANSFER LAB.
- JOVIC, S., DRIVER, D. M., 1994, *Backward-facing step measurements at low Reynolds number, $Re (sub h) = 5000$* . Report 108807, NASA.
- KADER, B. A., YAGLOM, A. M., 1978, “Similarity treatment of moving-equilibrium turbulent boundary layers in adverse pressure gradients”, *Journal of Fluid Mechanics*, v. 89, n. 2, pp. 305–342. doi: 10.1017/S0022112078002621.
- KADER, B., 1981, “Temperature and concentration profiles in fully turbulent boundary layers”, *International Journal of Heat and Mass Transfer*, v. 24, n. 9, pp. 1541–1544.
- KADER, B., 1991, “Heat and mass transfer in pressure-gradient boundary layers”, *International Journal of Heat and Mass Transfer*, v. 34, n. 11, pp. 2837–2857.
- KAMETANI, Y., FUKAGATA, K., 2011, “Direct numerical simulation of spatially developing turbulent boundary layers with uniform blowing or suction”, *Journal of Fluid Mechanics*, v. 681, pp. 154–172.
- KAY, J. M., 1948, *Boundary Layer Flow with Uniform Suction*. In: Report ARC R and M 2628.
- KAYS, W. M., 1994, “Turbulent Prandtl number—where are we?” *Journal of Heat Transfer*, v. 116, n. 2, pp. 284–295.
- KENDALL, R. M., RUBESIN, M. W., DAHM, T. J., et al., 1964, *Mass, momentum, and heat transfer within a turbulent boundary layer with foreign gas mass transfer at the surface. Part 1*.

- KEULEGAN, G. H., 1938, *Laws of turbulent flow in open channels*, v. 21. National Bureau of Standards US.
- KHAPKO, T., SCHLATTER, P., DUGUET, Y., et al., 2016, “Turbulence collapse in a suction boundary layer”, *Journal of Fluid Mechanics*, v. 795, pp. 356–379.
- KIEL, R., 1995, *Experimentelle Untersuchung einer Strömung mit beheiztem lokalen Ablösewirbel an einer geraden Wand*. VDI-Verlag.
- KITSIOS, V., ATKINSON, C., SILLERO, J. A., et al., 2016, “Direct numerical simulation of a self-similar adverse pressure gradient turbulent boundary layer”, *International Journal of Heat and Fluid Flow*, v. 61, pp. 129–136.
- KLEBANOFF, P., 1955, “Characteristics of turbulence in boundary layer with zero pressure gradient”, .
- KLINE, S. J., CANTWELL, B. J., LILLEY, G. M., 1980, *The 1980-81 AFOSR-HTTM-Stanford Conference on Complex Turbulent Flows: Comparison of Computation & Experiment- Volume I*. Report AFOSR-TR-83-1001, Stanford University.
- KNOPP, T., BUCHMANN, N., SCHANZ, D., et al., 2015, “Investigation of scaling laws in a turbulent boundary layer flow with adverse pressure gradient using PIV”, *Journal of Turbulence*, v. 16, n. 3, pp. 250–272.
- KORNILOV, V. I., BOIKO, A. V., 2014, “Formation of the turbulent boundary layer at air blowing through a wall with an abrupt change in boundary conditions”, *Thermophysics and Aeromechanics*, v. 21, n. 4, pp. 421–439. ISSN: 1531-8699.
- KORNILOV, V., 2015, “Current state and prospects of researches on the control of turbulent boundary layer by air blowing”, *Progress in Aerospace Sciences*, v. 76, pp. 1 – 23. ISSN: 0376-0421.
- KORNILOV, V., BOIKO, A., 2016, “Experimental modeling of air blowing into a turbulent boundary layer using an external pressure flow”, *Technical Physics*, v. 61, n. 10, pp. 1480–1488.
- KRAHEBERGER, S., HOYAS, S., OBERLACK, M., 2018, “DNS of a turbulent Couette flow at constant wall transpiration up to $Re_\tau = 1000$ ”, *Journal of Fluid Mechanics*, v. 835, pp. 421–443.

- KRAHEBERGER, S., HOYAS, S., OBERLACK, M., 2017, “DNS of Couette Flows With Wall Transpiration up to $Re_\tau = 1000$ ”. In: *Progress in Turbulence VII*, Springer, pp. 45–50.
- KRUG, D., PHILIP, J., MARUSIC, I., 2017, “Revisiting the law of the wake in wall turbulence”, *Journal of Fluid Mechanics*, v. 811, pp. 421–435.
- LAUFER, J., 1954, *The structure of turbulence in fully developed pipe flow*. Report, NACA.
- LAUNDER, B., SPALDING, D., 1974, “The numerical computation of turbulent flows”, *Computer Methods in Applied Mechanics and Engineering*, v. 3, n. 2, pp. 269 – 289. ISSN: 0045-7825.
- LE, H., MOIN, P., KIM, J., 1997, “Direct numerical simulation of turbulent flow over a backward-facing step”, *Journal of Fluid Mechanics*, v. 330, pp. 349–374.
- LEE, J.-H., SUNG, H. J., 2008, “Effects of an adverse pressure gradient on a turbulent boundary layer”, *International Journal of Heat and Fluid Flow*, v. 29, n. 3, pp. 568–578.
- LEE, J.-H., SUNG, H. J., 2009, “Structures in turbulent boundary layers subjected to adverse pressure gradients”, *Journal of Fluid Mechanics*, v. 639, pp. 101–131.
- LEWKOWICZ, A., 1982, “An improved universal wake function for turbulent boundary layers and some of its consequences”, *Zeitschrift fuer Flugwissenschaften und Weltraumforschung*, v. 6, pp. 261–266.
- LIN, P., KARUNARATHNA, S., 2006, “Turbulent boundary layer flows above a porous surface subject to flow injection”, *Journal of engineering mechanics*, v. 132, n. 10, pp. 1133–1140.
- LONG, R. R., CHEN, T.-C., 1981, “Experimental evidence for the existence of the ‘mesolayer’ in turbulent systems”, *Journal of Fluid Mechanics*, v. 105, pp. 19–59. doi: 10.1017/S0022112081003108.
- LOUREIRO, J., PINHO, F., FREIRE, A. S., 2007, “Near wall characterization of the flow over a two-dimensional steep smooth hill”, *Experiments in Fluids*, v. 42, n. 3, pp. 441–457.
- LU, Y., CHIEW, Y.-M., CHENG, N.-S., 2008, “Review of seepage effects on turbulent open-channel flow and sediment entrainment”, *Journal of Hydraulic*

- Research*, v. 46, n. 4, pp. 476–488. doi: 10.3826/jhr.2008.2942. Available at: <<http://dx.doi.org/10.3826/jhr.2008.2942>>.
- MACIEL, Y., ROSSIGNOL, K.-S., LEMAY, J., 2006, “A study of a turbulent boundary layer in stalled-airfoil-type flow conditions”, *Experiments in Fluids*, v. 41, n. 4, pp. 573–590.
- MALKUS, W. V., 1979, “Turbulent velocity profiles from stability criteria”, *Journal of Fluid Mechanics*, v. 90, n. 3, pp. 401–414.
- MANES, C., RIDOLFI, L., KATUL, G., 2012, “A phenomenological model to describe turbulent friction in permeable-wall flows”, *Geophysical Research Letters*, v. 39, n. 14, pp. n/a–n/a. ISSN: 1944-8007. doi: 10.1029/2012GL052369. Available at: <<http://dx.doi.org/10.1029/2012GL052369>>. L14403.
- MANES, C., POGGI, D., RIDOLFI, L., 2011, “Turbulent boundary layers over permeable walls: scaling and near-wall structure”, *Journal of Fluid Mechanics*, v. 687, pp. 141–170.
- MANHART, M., FRIEDRICH, R., 2002, “DNS of a turbulent boundary layer with separation”, *International Journal of Heat and Fluid Flow*, v. 23, n. 5, pp. 572–581.
- MARIANI, P., SPALART, P., KOLLMANN, W., 1993, “Direct simulation of a turbulent boundary layer with suction”. In: So, R. M., Speziale, C. G., Launder, B. E. (Eds.), *Proceedings of the International Conference on Near-Wall Turbulent Flows, Tempe, Arizona, U.S.A.* ELSEVIER.
- MARUŠIĆ, I., PERRY, A., 1995, “A wall-wake model for the turbulence structure of boundary layers. Part 2. Further experimental support”, *Journal of Fluid Mechanics*, v. 298, pp. 389–407.
- MARXMAN, G., GILBERT, M., 1963, “Turbulent boundary layer combustion in the hybrid rocket”. In: *Symposium (International) on Combustion*, v. 9, pp. 371–383. Elsevier.
- MCDONALD, H., 1969, “The effect of pressure gradient on the law of the wall in turbulent flow”, *Journal of Fluid Mechanics*, v. 35, n. 02, pp. 311–336.
- MCQUAID, J., 1968, *The Calculation of Turbulent Boundary Layers with Injection*. In: Report 3542, AERONAUTICAL RESEARCH COUNCIL REPORTS AND MEMORANDA, London.

- MELLOR, G. L., 1972, “The large reynolds number, asymptotic theory of turbulent boundary layers”, *International Journal of Engineering Science*, v. 10, n. 10, pp. 851 – 873. ISSN: 0020-7225. doi: [http://dx.doi.org/10.1016/0020-7225\(72\)90055-9](http://dx.doi.org/10.1016/0020-7225(72)90055-9).
- MELLOR, G. L., 1966, “The effects of pressure gradients on turbulent flow near a smooth wall”, *Journal of Fluid Mechanics*, v. 24, n. 2, pp. 255–274. doi: 10.1017/S0022112066000624.
- MELLOR, G., GIBSON, D., 1966, “Equilibrium turbulent boundary layers”, *Journal of Fluid Mechanics*, v. 24, n. 02, pp. 225–253.
- MENDOZA, C., ZHOU, D., 1992, “Effects of porous bed on turbulent stream flow above bed”, *Journal of Hydraulic Engineering*, v. 118, n. 9, pp. 1222–1240.
- MEYER, R., 1967, “On the approximation of double limits by single limits and the Kaplun extension theorem”, *IMA Journal of Applied Mathematics*, v. 3, n. 3, pp. 245–249.
- MICKLEY, H. S., DAVIS, R. S., 1957, *Momentum transfer for flow over a flat plate with blowing*. In: Report TN 4017, National Advisory Committee for Aeronautics.
- MICKLEY, H., SMITH, K., 1963, “Velocity defect law for a transpired turbulent boundary layer”, *AIAA Journal*, v. 1, n. 7, pp. 1685–1685.
- MILLIKAN, C. B., 1938, “A critical discussion of turbulent flows in channels and circular tubes”. In: *Proc. 5th Int. Congr. Appl. Mech*, v. 386.
- MIN, T., KANG, S. M., SPEYER, J. L., et al., 2006, “Sustained sub-laminar drag in a fully developed channel flow”, *Journal of Fluid Mechanics*, v. 558 (07), pp. 309–318. doi: 10.1017/S0022112006000206.
- MIRONOV, B., LUGOVSKOI, P., 1972, “Study concerning the laminar sublayer region of a turbulent boundary layer with injection”, *Journal of Engineering Physics and Thermophysics*, v. 22, n. 3, pp. 322–326.
- MOFFAT, R., KAYS, W., 1984, “A Review of Turbulent-Boundary-Layer Heat Transfer Research at Stanford, 1958-1983”. v. 16, *Advances in Heat Transfer*, Elsevier, pp. 241 – 365. doi: [http://dx.doi.org/10.1016/S0065-2717\(08\)70206-5](http://dx.doi.org/10.1016/S0065-2717(08)70206-5).
- MORRISON, J. F., 2007, “The interaction between inner and outer regions of turbulent wall-bounded flow”, *Philosophical Transactions of the Royal*

- Society of London A: Mathematical, Physical and Engineering Sciences*, v. 365, n. 1852, pp. 683–698.
- MOSES, H. L., 1964, *The behavior of turbulent boundary layers in adverse pressure gradients*. Report, DTIC Document.
- MUGALEV, V., 1959, “Experimental investigation of a subsonic turbulent boundary layer on a plate with blowing”, *Izv. Vyssh. Uchebn. Zaved., Aviats. Tekh.*, n. 3, pp. 72–79.
- NA, Y., MOIN, P., 1998, “Direct numerical simulation of a separated turbulent boundary layer”, *Journal of Fluid Mechanics*, v. 374, pp. 379–405.
- NAGIB, H., CHRISTOPHOROU, C., MONKEWITZ, P., 2006, “High Reynolds number turbulent boundary layers subjected to various pressure-gradient conditions”. In: *IUTAM symposium on one hundred Years of boundary layer research*, pp. 383–394. Springer.
- NAGIB, H. M., CHAUHAN, K. A., 2008, “Variations of von Kármán coefficient in canonical flows”, *Physics of Fluids*, v. 20, n. 10, pp. 101518.
- NAKAGAWA, H., NEZU, I., 1979, “TURBULENT STRUCTURE IN PERMEABLE OPEN-CHANNEL FLOWS WITH TRANSPIRATION”. In: *Proceedings of the Japan Society of Civil Engineers*, v. 1979, pp. 45–56. Japan Society of Civil Engineers.
- NAKAYAMA, A., KOYAMAT, H., 1984, “A wall law for turbulent boundary layers in adverse pressure gradients”, *AIAA Journal*, v. 22, n. 10, pp. 1386–1389.
- NAYAK, U. S. L., BARDEN, R. G., 1972, “Velocity and Shear Stress Distributions in a Transpired Turbulent Boundary Layer”, *Journal of Basic Engineering*, v. 94, n. 1 (Mar), pp. 193–199. ISSN: 0098-2202.
- NELSON, D., 1964, *A TURBULENT BOUNDARY-LAYER CALCULATION METHOD BASED ON THE LAW OF THE WALL AND THE LAW OF THE WAKE*. Report, NAVAL ORDNANCE TEST STATION CHINA LAKE CALIF.
- NEWMAN, B. G., 1951, *Some contributions to the study of the turbulent boundary-layer near separation*. In: Report ACA-53, Department of Supply, Aeronautical Research Consultative Committee.
- NEZU, I., 1977, “Turbulent structure in open-channel flows”, *English translation of the Japanese dissertation of Iehisa Nezu*.

- NICKELS, T., 2004, “Inner scaling for wall-bounded flows subject to large pressure gradients”, *Journal of Fluid Mechanics*, v. 521, pp. 217–239.
- NIKITIN, N. V., PAVELEV, A. A., 1998, “Turbulent flow in a channel with permeable walls. Direct numerical simulation and results of three-parameter model”, *Fluid Dynamics*, v. 33, n. 6, pp. 826–832. ISSN: 1573-8507. doi: 10.1007/BF02698650. Available at: <<http://dx.doi.org/10.1007/BF02698650>>.
- NIKURADSE, J., 1933, “Strömungsgesetze in rauhen Rohren”, *VDI-Fortschungsheft*, v. 361.
- OBERLACK, M., 2001, “A unified approach for symmetries in plane parallel turbulent shear flows”, *Journal of Fluid Mechanics*, v. 427, pp. 299–328. doi: 10.1017/S0022112000002408.
- OLSON, R. M., ECKERT, E. R. G., 1966, “Experimental Studies of Turbulent Flow in a Porous Circular Tube With Uniform Fluid Injection Through the Tube Wall”, *Journal of Applied Mechanics*, v. 33, n. 1 (Mar), pp. 7–17. ISSN: 0021-8936. doi: 10.1115/1.3625030. Available at: <<http://dx.doi.org/10.1115/1.3625030>>.
- ORLANDO, A. F., R. J. MOFFAT, R., KAYS, W. M., 1974, *Turbulent transport of heat and momentum in a boundary layer subject to deceleration, suction and variable wall temperature*. Report, NASA HMT-17, Stanford University.
- PAK, J., 1999, *A study of the thermal law of the wall for separated flow caused by a backward facing step*. Ph.D Thesis, Texas Tech University.
- PANTON, R. L., 2005, “Review of wall turbulence as described by composite expansions”, *Applied Mechanics Reviews*, v. 58, n. 1, pp. 1–36.
- PATEL, V. C., 1965, *Contributions to the study of turbulent boundary layers*. Ph.D Thesis, University of Cambridge.
- PATEL, V. C., 1973, “A Unified View of the Law of the Wall Using Mixing-Length Theory”, *Aeronautical Quarterly*, v. 24, n. 1, pp. 55–70. doi: 10.1017/S0001925900006429.
- PERRY, A. E., 1966, “Turbulent boundary layers in decreasing adverse pressure gradients”, *Journal of Fluid Mechanics*, v. 26, n. 3, pp. 481–506. doi: 10.1017/S0022112066001344.

- PERRY, A. E., SCHOFIELD, W. H., 1973, “Mean velocity and shear stress distributions in turbulent boundary layers”, *The Physics of Fluids*, v. 16, n. 12, pp. 2068–2074. doi: 10.1063/1.1694267. Available at: <http://aip.scitation.org/doi/abs/10.1063/1.1694267>.
- PERRY, A., BELL, J., JOUBERT, P., 1966, “Velocity and temperature profiles in adverse pressure gradient turbulent boundary layers”, *Journal of Fluid Mechanics*, v. 25, n. 2, pp. 299–320.
- POPE, S. B., 2000, *Turbulent flows*. Cambridge University Press.
- POSTL, D., FASEL, H. F., 2006, “Direct numerical simulation of turbulent flow separation from a wall-mounted hump”, *AIAA Journal*, v. 44, n. 2, pp. 263.
- PRANDTL, L., 1925, “Bericht über Untersuchungen zur ausgebildeten Turbulenz”, *Zeitschrift für angew. Math. u. Mechanik*, v. 5, n. 2, pp. 136–139.
- PRANDTL, L., 1932, “Zur turbulenten Strömung in Röhren und längs Platten”, *Ergeb. Aerodyn. Versuch., Series*, v. 4, pp. 18–29.
- QINGYANG, S., 2009, “Velocity distribution and wake-law in gradually decelerating flows”, *Journal of Hydraulic Research*, v. 47, n. 2, pp. 177–184. doi: 10.3826/jhr.2009.3254. Available at: <http://iahr.tandfonline.com/doi/abs/10.3826/jhr.2009.3254>.
- QUADRIO, M., FLORYAN, J. M., LUCHINI, P., 2007, “Effect of streamwise-periodic wall transpiration on turbulent friction drag”, *Journal of Fluid Mechanics*, v. 576 (004), pp. 425–444. doi: 10.1017/S0022112007004727.
- RANNIE, W. D., 1956, “Heat Transfer in Turbulent Shear Flow”, *Journal of the Aeronautical Sciences*, v. 23, n. 5 (May), pp. 485–489.
- REYNOLDS, O., 1894, “On the dynamical theory of incompressible viscous fluids and the determination of the criterion.” *Proceedings of the Royal Society of London*, v. 56, n. 336-339, pp. 40–45.
- ROSS, D., ROBERTSON, J., 1951, “A superposition analysis of the turbulent boundary layer in an adverse pressure gradient”, *JOURNAL OF APPLIED MECHANICS-TRANSACTIONS OF THE ASME*, v. 18, n. 1, pp. 95–100.
- ROSTI, M. E., CORTELEZZI, L., QUADRIO, M., 2015, “Direct numerical simulation of turbulent channel flow over porous walls”, *Journal of Fluid Mechanics*, v. 784, pp. 396–442.

- ROTTA, J., 1950, “Über die Theorie der turbulenten Grenzschichten, Mitt”, *Max-Planck-Inst., Göttingen*, , n. 1.
- ROTTA, J., 1953, “On the theory of the turbulent boundary layer”, *NACA TM No. 1344*.
- ROTTA, J., 1962, “Turbulent boundary layers in incompressible flow”, *Progress in Aerospace Sciences*, v. 2, n. 1, pp. 1 – 95. ISSN: 0376-0421. doi: [http://dx.doi.org/10.1016/0376-0421\(62\)90014-3](http://dx.doi.org/10.1016/0376-0421(62)90014-3).
- ROTTA, J. C., 1970, *Control of turbulent boundary layers by uniform injection and suction of fluid*. Report, DTIC Document.
- RUBESIN, M. W., 1954, *An analytical estimation of the effect of transpiration cooling on the heat-transfer and skin-friction characteristics of a compressible turbulent boundary layer*. In: Report NACA3341.
- RUMSEY, C., GATSKI, T., SELLERS, W., et al., 2004, cap. Summary of the 2004 CFD Validation Workshop on Synthetic Jets and Turbulent Separation Control, American Institute of Aeronautics and Astronautics, Jun. doi: 10.2514/6.2004-2217. Available at: <<https://doi.org/10.2514/6.2004-2217>>. 0.
- SAMUEL, A., JOUBERT, P., 1974, “A boundary layer developing in an increasingly adverse pressure gradient”, *Journal of Fluid Mechanics*, v. 66, n. 3, pp. 481–505.
- SANO, M., 1992, “Numerical analysis of turbulent boundary layers with injection and suction through a slit”, *JSME international journal. Ser. 2, Fluids engineering, heat transfer, power, combustion, thermophysical properties*, v. 35, n. 4, pp. 479–485.
- SANO, M., HIRAYAMA, N., 1984, “Study on the turbulence structure and turbulence model of turbulent boundary layer with a suction”, *Bulletin of JSME*, v. 27, n. 232, pp. 2134–2141.
- SANO, M., SUZUKI, I., SAKURABA, K., 2009, “Control of turbulent channel flow over a backward-facing step by suction”, *Journal of Fluid Science and Technology*, v. 4, n. 1, pp. 188–199.
- SARMA, K. V., LAKSHMINARAYANA, P., RAO, N. L., 1983, “Velocity distribution in smooth rectangular open channels”, *Journal of Hydraulic Engineering*, v. 109, n. 2, pp. 270–289.

- SARNECKI, A., 1959, *The turbulent boundary layer on a permeable surface*. Ph.D Thesis, Cambridge University.
- SCHILDKNECHT, M., MILLER, J. A., MEIER, G. E. A., 1979, “The influence of suction on the structure of turbulence in fully developed pipe flow”, *Journal of Fluid Mechanics*, v. 90, n. 1 (001), pp. 67–107. doi: 10.1017/S0022112079002081.
- SCHLATTER, P., ÖRLÜ, R., 2011, “Turbulent asymptotic suction boundary layers studied by simulation”. In: *Journal of Physics: Conference Series*, v. 318, p. 022020. IOP Publishing.
- SCHLICHTING, H., 1942, “The Boundary Layer of the Flat Plate under Conditions of Suction and Air Injection”, *Luftfahrtforschung*, v. 19, pp. 178.
- SCHLICHTING, H., 1968, *Boundary-layer theory*, v. 6. New York, N.Y., McGraw-Hill Book Co., Inc.
- SCHLICHTING, H., GERSTEN, K., 2017, *Boundary-layer theory*, v. 9. Springer.
- SCHMITT, F. G., 2007, “About Boussinesq’s turbulent viscosity hypothesis: historical remarks and a direct evaluation of its validity”, *Comptes Rendus Mécanique*, v. 335, n. 9-10, pp. 617–627.
- SCHWEIKERT, S., VON WOLFERSDORF, J., SELZER, M., et al., 2013, “Experimental investigation on velocity and temperature distributions of turbulent cross flows over transpiration cooled C/C wall segments”. In: *5th European Conference for Aeronautics and Space Sciences (EUCASS)*, München, Germany.
- SENDA, M., KAWAGUCHI, Y., SUZUKI, K., et al., 1981, “Study on a Turbulent Boundary Layer with Injection: Turbulent Scales”, *Bulletin of JSME*, v. 24, n. 196, pp. 1748–1755.
- SHIH, T.-H., POVINELLI, L., LIU, N.-S., et al., 1999, “Turbulent surface flow and wall function”. In: *35th Joint Propulsion Conference and Exhibit*, p. 2392.
- SHIH, T.-H., POVINELLI, L. A., LIU, N.-S., 2003, “Application of generalized wall function for complex turbulent flows*”, *Journal of Turbulence*, v. 4, n. 1, pp. 1–16.
- SHULTZ-GRUNOW, F., 1940, “Neues Widerstand für glatte Platten”, *Luftfahrtforschung*, v. 17, pp. 239–246.

- SILVA, T. S., DA SILVA, C. B., 2017, “The behaviour of the scalar gradient across the turbulent/non-turbulent interface in jets”, *Physics of Fluids*, v. 29, n. 8, pp. 085106.
- SILVA-FREIRE, A. P., 1988, “An asymptotic solution for transpired incompressible turbulent boundary layers”, *International Journal of Heat and Mass Transfer*, v. 31, n. 5, pp. 1011 – 1021. ISSN: 0017-9310. doi: [http://dx.doi.org/10.1016/0017-9310\(88\)90090-7](http://dx.doi.org/10.1016/0017-9310(88)90090-7).
- SIMPSON, R. L., 1967, *The turbulent boundary layer on a porous plate: an experimental study of the fluid dynamics with injection and suction*. Ph.D Thesis, Stanford University.
- SIMPSON, R. L., 1985, “Two-Dimensional Turbulent Separated Flows”, *AGARD No 287, vol.1*.
- SIMPSON, R., 1981, “Review-a review of some phenomena in turbulent flow separation”, *ASME Journal of Fluids Engineering*, v. 103, pp. 520–533.
- SIMPSON, R. L., 1983, “A model for the backflow mean velocity profile”, *AIAA Journal*, v. 21, n. 1, pp. 142–143.
- SIMPSON, R. L., 1989, “Turbulent boundary-layer separation”, *Annual Review of Fluid Mechanics*, v. 21, n. 1, pp. 205–232.
- SIMPSON, R. L., 1970, “Characteristics of turbulent boundary layers at low Reynolds numbers with and without transpiration”, *Journal of Fluid Mechanics*, v. 42, n. 4, pp. 769–802. doi: 10.1017/S002211207000160X.
- SIMPSON, R. L., STRICKLAND, J., BARR, P., 1977, “Features of a separating turbulent boundary layer in the vicinity of separation”, *Journal of Fluid Mechanics*, v. 79, n. 3, pp. 553–594.
- SIMPSON, R. L., CHEW, Y.-T., SHIVAPRASAD, B., 1981, “The structure of a separating turbulent boundary layer. Part 1. Mean flow and Reynolds stresses”, *Journal of Fluid Mechanics*, v. 113, pp. 23–51.
- SKOTE, M., 2001, *Studies of turbulent boundary layer flow through direct numerical simulation*. Ph.D Thesis, KTH, Stockholm, Sweden.
- SKOTE, M., HENNINGSON, D. S., 2002, “Direct numerical simulation of a separated turbulent boundary layer”, *Journal of Fluid Mechanics*, v. 471 (11), pp. 107–136. doi: 10.1017/S0022112002002173.

- SKOTE, M., HENNINGSON, D. S., HENKES, R. A., 1998, “Direct numerical simulation of self-similar turbulent boundary layers in adverse pressure gradients”, *Flow, Turbulence and Combustion*, v. 60, n. 1, pp. 47–85.
- SKÅRE, P. E., KROGSTAD, P.-G., 1994, “A turbulent equilibrium boundary layer near separation”, *Journal of Fluid Mechanics*, v. 272, pp. 319–348. doi: 10.1017/S0022112094004489.
- SPALART, P. R., 2011, “The law of the wall. Indications from DNS, and opinion”. In: *Progress in Wall Turbulence: Understanding and Modeling*, Springer, pp. 9–20.
- SPALART, P. R., COLEMAN, G. N., 1997, “Numerical study of a separation bubble with heat transfer”, *European journal of mechanics. B, Fluids*, v. 16, n. 2, pp. 169–189.
- SPALART, P. R., LEONARD, A., 1987, “Direct numerical simulation of equilibrium turbulent boundary layers”. In: *Turbulent Shear Flows 5*, Springer, pp. 234–252.
- SPALART, P. R., WATMUFF, J. H., 1993, “Experimental and numerical study of a turbulent boundary layer with pressure gradients”, *Journal of Fluid Mechanics*, v. 249, pp. 337–371.
- SPALDING, D., 1961, “A single formula for the “law of the wall””, *Journal of Applied Mechanics*, v. 28, n. 3, pp. 455–458.
- SPALDING, D., 1967, “Heat transfer from turbulent separated flows”, *Journal of Fluid Mechanics*, v. 27, n. 1, pp. 97–109.
- SPALDING, D. B., 1965, *A unified theory of friction, heat transfer and mass transfer in the turbulent boundary layer and wall jet*. Report.
- SQUIRE, L. C., 1980, *Turbulent boundary layers with suction or blowing*. In: Report Conference on Data and Computation for Complex Turbulent Flow, Cambridge University Engineering Department.
- STEVENSON, T. N., 1963a, *A law of the wall for turbulent boundary layers with injection and suction*. Report 166, Cranfield College of Aero Rep Aero, a.
- STEVENSON, T., 1963b, *A modified velocity defect law for turbulent boundary layers with injection*. Report, College of Aeronautics Cranfield, b.
- STEVENSON, T., 1964a, *Experiments on injection into an incompressible turbulent boundary layer*. Report 177, College of Aeronautics Cranfield, a.

- STEVENSON, T., 1964b, “Turbulent boundary layers with transpiration”, *AIAA Journal*, v. 2, n. 8, pp. 1500–1502.
- STRATFORD, B., 1959, “An experimental flow with zero skin friction throughout its region of pressure rise”, *Journal of Fluid Mechanics*, v. 5, n. 01, pp. 17–35.
- SUCEC, J., OLJACA, M., 1995, “Calculation of turbulent boundary layers with transpiration and pressure gradient effects”, *International Journal of Heat and Mass Transfer*, v. 38, n. 15, pp. 2855–2862.
- SUGA, K., MATSUMURA, Y., ASHITAKA, Y., et al., 2010, “Effects of wall permeability on turbulence”, *International Journal of Heat and Fluid Flow*, v. 31, n. 6, pp. 974–984.
- SUMITANI, Y., KASAGI, N., 1995, “Direct numerical simulation of turbulent transport with uniform wall injection and suction”, *AIAA Journal*, v. 33, n. 7 (Jul), pp. 1220–1228. ISSN: 0001-1452. doi: 10.2514/3.12363. Available at: <<http://dx.doi.org/10.2514/3.12363>>.
- SYCHEV, V., SYCHEV, V. V., 1987, “On turbulent boundary layer structure”, *Journal of Applied Mathematics and Mechanics*, v. 51, n. 4, pp. 462–467.
- SZABLEWSKI, W., 1972, “Inkompressible turbulente temperatur-grenzschichten mit konstanter wandtemperatur”, *International Journal of Heat and Mass Transfer*, v. 15, n. 4, pp. 673 – 706. ISSN: 0017-9310. doi: [http://dx.doi.org/10.1016/0017-9310\(72\)90113-5](http://dx.doi.org/10.1016/0017-9310(72)90113-5).
- TAYLOR, G. I., 1915, “Eddy motion in the atmosphere”, *Philosophical Transactions of the Royal Society of London. Series A, Containing Papers of a Mathematical or Physical Character*, v. 215, pp. 1–26.
- TELBANY, M. M. M. E., REYNOLDS, A. J., 1980, “Velocity distributions in plane turbulent channel flows”, *Journal of Fluid Mechanics*, v. 100, n. 1, pp. 1–29. doi: 10.1017/S0022112080000973.
- TENNEKES, H., 1964, *Similarity Laws for Turbulent Boundary Layers with Suction Or Injection*. Report VTH-119.
- TENNEKES, H., 1965a, “Similarity laws for turbulent boundary layers with suction or injection”, *Journal of Fluid Mechanics*, v. 21, n. 4 (004), pp. 689–703. doi: 10.1017/S0022112065000423.
- TENNEKES, H., 1965b, “Velocity-defect laws for transpired turbulent boundary layers.” *AIAA Journal*, v. 3, pp. 1950–1951.

- TENNEKES, H., LUMLEY, J. L., 1972, *A First Course in Turbulence*. MIT press.
- THOMPSON, B. G. J., 1969a, *A Three-Parameter Family of Mean Velocity Profiles for Incompressible Turbulent Boundary Layers with Distributed Suction and Small Pressure Gradient*. In: Report ARC-3622, AERONAUTICAL RESEARCH COUNCIL REPORTS AND MEMORANDA, London, a.
- THOMPSON, B. G. J., 1969b, *An Experimental Investigation Into the Behaviour of the Turbulent Boundary Layer with Distributed Suction in Regions of Adverse Pressure Gradient*. In: Report ARC-3621, AERONAUTICAL RESEARCH COUNCIL REPORTS AND MEMORANDA, London, b.
- THOMPSON, B. G. J., 1967, *A new two-parameter family of mean velocity profiles for incompressible turbulent boundary layers on smooth walls*. Report, Ministry of Technology, AERONAUTICAL RESEARCH COUNCIL REPORTS AND MEMORANDA.
- THOMPSON, R. L., MOMPEAN, G., THAIS, L., 2010, “A methodology to quantify the nonlinearity of the Reynolds stress tensor”, *Journal of Turbulence*, , n. 11, pp. N33.
- TORII, K., NISHIWAKI, N., HIRATA, M., 1966, “Heat transfer and skin friction in turbulent boundary layer with mass injection”. In: *Proceedings of the Third International Heat Transfer Conference*, v. 3, pp. 34–48. Am. Inst. Chem. Engrs New York.
- TOWNSEND, A. A., 1961, “Equilibrium layers and wall turbulence”, *Journal of Fluid Mechanics*, v. 11, n. 1 (008), pp. 97–120. doi: 10.1017/S0022112061000883.
- TOWNSEND, A., 1956, “The properties of equilibrium boundary layers”, *Journal of Fluid Mechanics*, v. 1, n. 06, pp. 561–573.
- TOWNSEND, A., 1976, “The structure of turbulent shear flows”, *Cambridge University Press, Cambridge, UK*.
- TRIP, R., FRANSSON, J. H. M., 2014, “Boundary layer modification by means of wall suction and the effect on the wake behind a rectangular forebody”, *Physics of Fluids*, v. 26, n. 12, pp. 125105.
- TURCOTTE, D. L., 1960, “A Sublayer Theory for Fluid Injection Into the Incompressible Turbulent Boundary Layer”, *Journal of the Aerospace Sciences*, v. 27, n. 9 (Sep), pp. 675–678. doi: 10.2514/8.8708. Available at: <<http://dx.doi.org/10.2514/8.8708>>.

- URUBA, V., JONÁŠ, P., MAZUR, O., 2007, “Control of a channel-flow behind a backward-facing step by suction/blowing”, *International Journal of Heat and Fluid Flow*, v. 28, n. 4, pp. 665–672.
- VAN-DRIEST, E. R., 1957, *On Mass Transfer near the Stagnation Point*. In: Report TN 57-458, Air Force Office of Scientific Research.
- VAN DRIEST, E. R., 1956, “On turbulent flow near a wall”, *J. Aeronaut. Sci.*, v. 23, n. 11, pp. 1007–1011.
- VAN DYKE, M., 1975, *Perturbation methods in fluid mechanics*. The Parabolic Press.
- VEROLLET, E., 1977, *Study of turbulent boundary layer with suction and heating at the wall*. Report, France. CEA-R-4872.
- VÉROLLET, E., 1972, *Etude d’une couche limite turbulente avec aspiration et chauffage à la paroi*. Ph.D Thesis, Université de Provence.
- VIETH, D., 1997, *Berechnung der Impuls-und Wärmeübertragung in ebenen turbulenten Strömungen mit Ablösung bei hohen Reynolds-Zahlen*. VDI-Verlag.
- VIGDOROVICH, I., 2016, “A law of the wall for turbulent boundary layers with suction: Stevenson’s formula revisited”, *Physics of Fluids*, v. 28, n. 8, pp. 085102. doi: 10.1063/1.4960182. Available at: <<http://dx.doi.org/10.1063/1.4960182>>.
- VIGDOROVICH, I., 2004, “Velocity, temperature, and Reynolds-stress scaling in the wall region of turbulent boundary layer on a permeable surface”, *Journal of Experimental and Theoretical Physics*, v. 99, n. 5, pp. 1028–1038.
- VOGEL, J. C., 1984, *Heat transfer and fluid mechanics measurements in the turbulent reattaching flow behind a backward-facing step*. Ph.D Thesis, Stanford University.
- VON KARMAN, T., 1930, “Mechanische Ähnlichkeit und turbulenz”, *Nachrichten von der Gesellschaft der Wissenschaften zu Göttingen, Mathematisch-Physikalische Klasse*, v. 1930, pp. 58–76.
- WANG, X., CASTILLO, L., ARAYA, G., 2008, “Temperature scalings and profiles in forced convection turbulent boundary layers”, *Journal of Heat Transfer*, v. 130, n. 2, pp. 021701.

- WATTS, K. C., 1972, *The Development of Asymptotic Turbulent, Transitional, and Laminar Boundary Layers Induced by Suction*. Ph.D Thesis, University of Waterloo.
- WHITE, F., 1974, *Viscous Fluid Flow*. New York: McGraw-Hill, Inc.
- WHITTEN, D. G., 1967, *The turbulent boundary layer on a porous plate- Experimental heat transfer with variable suction, blowing and surface temperature (Turbulent boundary layer on porous plate, and heat transfer with variable suction, blowing and surface temperature)*. Report, Stanford University.
- WILCOX, D., TRACI, R., 1976, “A complete model of turbulence”. In: *9th Fluid and Plasma Dynamics Conference*, p. 351.
- WILCOX, D. C., 1989, “Wall matching, a rational alternative to wall functions”. In: *27th AIAA Aerospace Sciences Meeting*.
- WILCOX, D. C., OTHERS, 1998, *Turbulence modeling for CFD*, v. 2. DCW industries La Canada, CA.
- WILLERT, C. E., 2015, “High-speed particle image velocimetry for the efficient measurement of turbulence statistics”, *Experiments in Fluids*, v. 56, n. 1, pp. 17.
- WOOLDRIDGE, C., MUZZY, R., 1965, “Measurements in a turbulent boundary layer with porous wall injection and combustion”. In: *Symposium (International) on Combustion*, v. 10, pp. 1351–1362. Elsevier.
- WOOLDRIDGE, C., MUZZY, R., 1966, “Boundary layer turbulence measurements with mass addition and combustion”, *AIAA J*, v. 4, n. 11, pp. 2009–2016.
- YAGLOM, A. M., 1979, “Similarity Laws for Constant-Pressure and Pressure-Gradient Turbulent Wall Flows”, *Annual Review of Fluid Mechanics*, v. 11, n. 1, pp. 505–540.
- YAJNIK, K. S., 1970, “Asymptotic theory of turbulent shear flows”, *Journal of Fluid Mechanics*, v. 42, n. 2, pp. 411–427. doi: 10.1017/S0022112070001350.
- YANG, J.-T., TSAI, B.-B., TSAI, G.-L., 1994, “Separated-Reattaching Flow Over a Backstep With Uniform Normal Mass Bleed (Data Bank Contribution)”, *Journal of Fluids Engineering*, v. 116, n. 1, pp. 29–35.

- YOSHIOKA, S., ALFREDSSON, P. H., 2006, “CONTROL OF TURBULENT BOUNDARY LAYERS BY UNIFORM WALL SUCTION AND BLOWING”. In: Govindarajan, R. (Ed.), *IUTAM Symposium on Laminar-Turbulent Transition*, pp. 437–442, Dordrecht, Springer Netherlands. ISBN: 978-1-4020-4159-4.
- ZAGAROLA, M. V., SMITS, A. J., 1998, “Mean-flow scaling of turbulent pipe flow”, *Journal of Fluid Mechanics*, v. 373, pp. 33–79. doi: 10.1017/S0022112098002419.
- ZAGUSTIN, A., ZAGUSTIN, K., 1969, “Analytical solution for turbulent flow in pipes”, *La Houille Blanche*, , n. 2, pp. 113–118.
- ZHAPBASBAEV, U. K., ISAKHANOVA, G. Z., 1998, “Developed turbulent flow in a plane channel with simultaneous injection through one porous wall and suction through the other”, *Journal of Applied Mechanics and Technical Physics*, v. 39, n. 1, pp. 53–59. ISSN: 1573-8620. doi: 10.1007/BF02467997. Available at: <<http://dx.doi.org/10.1007/BF02467997>>.
- ZHAPBASBAYEV, U., YERSHIN, S., 2003, “Developed turbulent flow in a channel with mass exchange through porous walls”. In: *Proceedings of the Fourth International Symposium on Turbulence, Heat and Mass Transfer*. (ed. Hanjalic K. et. al.) Begell House, Inc, pp. 173–180.

Appendix A

Some demonstrations

In this section it will be shown that in the fully turbulent region of the flow the closure expression given by,

$$-\overline{u'v'} = u_c \ell \partial \bar{u} / \partial y + \beta u_c V_w, \quad (\text{A.1})$$

is consistent with the assumption that the turbulent fluctuations are of the order of the characteristic velocity scale,

$$O(\overline{u'v'}) = O(u_c^2). \quad (\text{A.2})$$

If the assumptions made in section 3.1 are repeated here, one might obtain from an order of magnitude analysis of equation A.1 that,

$$O(\overline{u'v'}) = O(u_c^2) + O(u_c V_w). \quad (\text{A.3})$$

Doing the same analysis for the approximated equation of motion, equation 3.1, leads to,

$$O(V_w u_c) = O(u_\tau^2) + O(u_c^2). \quad (\text{A.4})$$

Equation A.4 will be scrutinized in the light of seven different possibilities regarding the relative order of magnitude of its terms. It will be considered first the only two cases where equation A.1 is not consistent with A.2 and it will be explained why this is not a problem.

$$\text{Case A: } O(V_w u_c) = O(u_\tau^2) \gg O(u_c^2). \quad (\text{A.5})$$

In that case $O(V_w u_c) \gg O(u_c^2)$ so, from equation A.3, $O(\overline{u'v'}) = O(u_c V_w) \neq O(u_c^2)$, but in that situation the turbulent shear stress is negligibly small when compared to the viscous and inertia terms so one can not speak of a fully turbulent layer.

$$\text{Case B: } O(V_w u_c) \gg O(u_\tau^2) = O(u_c^2). \quad (\text{A.6})$$

Here the scenario is similar and $O(V_w u_c) \gg O(u_c^2)$ so, from equation A.3, $O(\overline{u'v'}) = O(u_c V_w) \neq O(u_c^2)$, but in that case the turbulent shear stress, although being of the same order of the viscous stress, is much smaller than the inertia term so again there is no fully turbulent layer.

$$\text{Case C: } O(V_w u_c) = O(u_c^2) \ll O(u_\tau^2). \quad (\text{A.7})$$

$$\text{Case D: } O(V_w u_c) = O(u_c^2) \gg O(u_\tau^2). \quad (\text{A.8})$$

$$\text{Case E: } O(V_w u_c) = O(u_c^2) = O(u_\tau^2). \quad (\text{A.9})$$

In these three cases $O(\overline{u'v'}) = O(u_c^2) + O(u_c V_w) = O(u_c^2)$ because $O(V_w u_c) = O(u_c^2)$.

$$\text{Case F: } O(V_w u_c) \ll O(u_\tau^2) = O(u_c^2). \quad (\text{A.10})$$

$$\text{Case G: } O(V_w u_c) = O(u_\tau^2) \ll O(u_c^2). \quad (\text{A.11})$$

In these two cases $O(\overline{u'v'}) = O(u_c^2) + O(u_c V_w) = O(u_c^2)$ because $O(u_c^2) \gg O(V_w u_c)$.

The analysis above also shows that the characteristic velocity scale can be of the order of three different velocity scales, depending on the relative strength of the transpiration rate,

$$O(u_c) = \begin{cases} O(u_\tau^2/V_w), & O(|V_w|/u_\tau) \gg 1 \vee O(V_w/u_\tau) = 1, & (\text{A.12.a}) \\ O(V_w), & O(V_w/u_\tau) \gg 1 \vee O(V_w/u_\tau) = 1, & (\text{A.12.b}) \\ O(u_\tau), & O(V_w/u_\tau) \ll 1 \vee O(V_w/u_\tau) = 1. & (\text{A.12.c}) \end{cases} \quad (\text{A.12})$$

In section 3.1.1, it was shown that the proposed expression for the characteristic velocity scale,

$$u_c = \frac{\alpha V_w + \sqrt[2]{\alpha^2 V_w^2 + 4u_\tau^2}}{2}, \quad (\text{A.13})$$

contain these three different expressions given in equation A.12 as particular cases.

Appendix B

Comparisons with other theories and databases

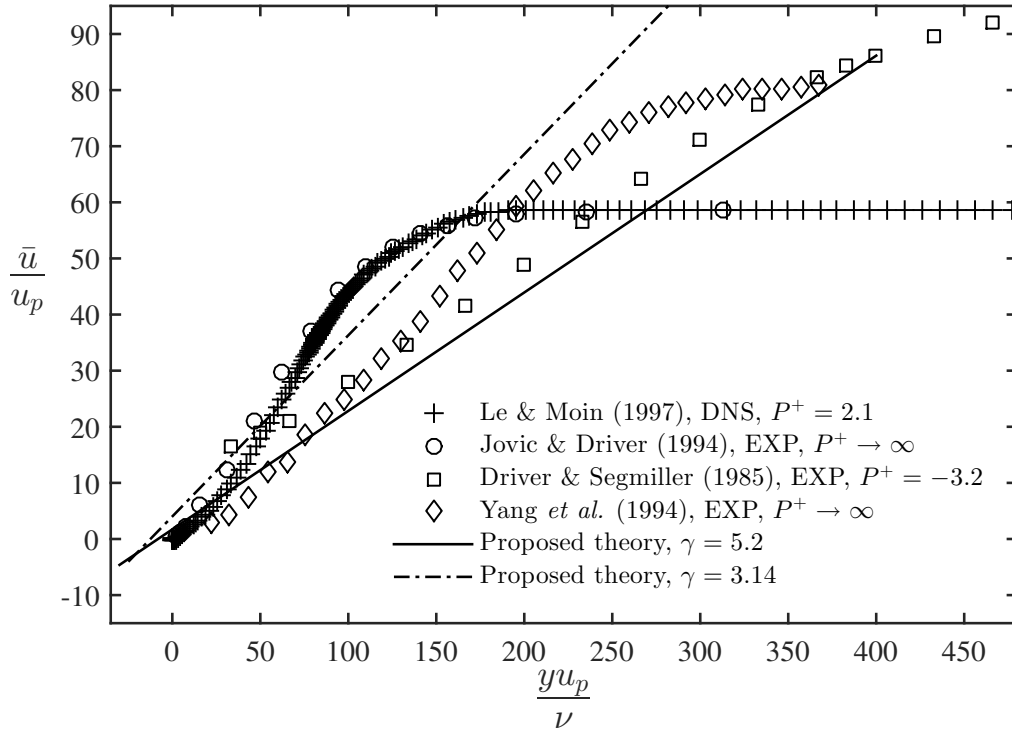


Figure B.1: EXP and DNS mean velocity profiles in the reattachment point of backward facing step flows.

This chapter shows an extensive number of comparisons between different theories and data sets. Any theory that has been cited in this work but is not shown in the figures presented in this chapter did not perform well when compared to the data.

B.1 Zero pressure gradient and confined flows with wall transpiration

Figures B.2 to B.65 show comparisons between different formulations and the data. It needs to be mentioned that, although the results from the selected models are shown in every comparison, some of these models were not calibrated to predict the behavior of some flows included in the database. AVSARKISOV's *et al.* (2014) formulation was developed for channel flows with $0 \leq V_w^+ \leq 0.1$. BRADSHAW's (1967) version of the *bi-logarithmic law* was calibrated with data from boundary layer flows with wall suction only while KORNILOV's (2015) version was calibrated with data from boundary layer flows with $0 \leq V_w^+ \leq 0.067$. TENNEKES's (1964) first version of the *semi-logarithmic law* was developed for the asymptotic suction boundary layer only while his other version (labeled as version 1 in the figures) was considered provisional, as reliable data for transpired flows were scarce when Tennekes performed the calibrations. SILVA FREIRE's (1988) model was calibrated with data from boundary layer flows with wall injection and VIGDOROVICH (2016) formula contain a parameter obtained from a Taylor series expansion for small V_w^+ .

Another point that deserves some attention is the poor fit that most of the models give for two mean velocity profiles obtained from AVSARKISOV *et al.* (2014) DNSs; the profiles with $V_w^+ = 1.902$ and $V_w^+ = 2.612$. For these two flow conditions, the injection rates are very high and the assumption made in most of the models that $\tau = \tau_w + V_w \bar{u}$ was found to be very inaccurate, which explains the poor performance of those models. Two exceptions are CEBECI's (1970) and CLARKE's *et al.* (1955) formulations which, very impressively, can predict even those profiles well.

Asymptotic suction boundary layer

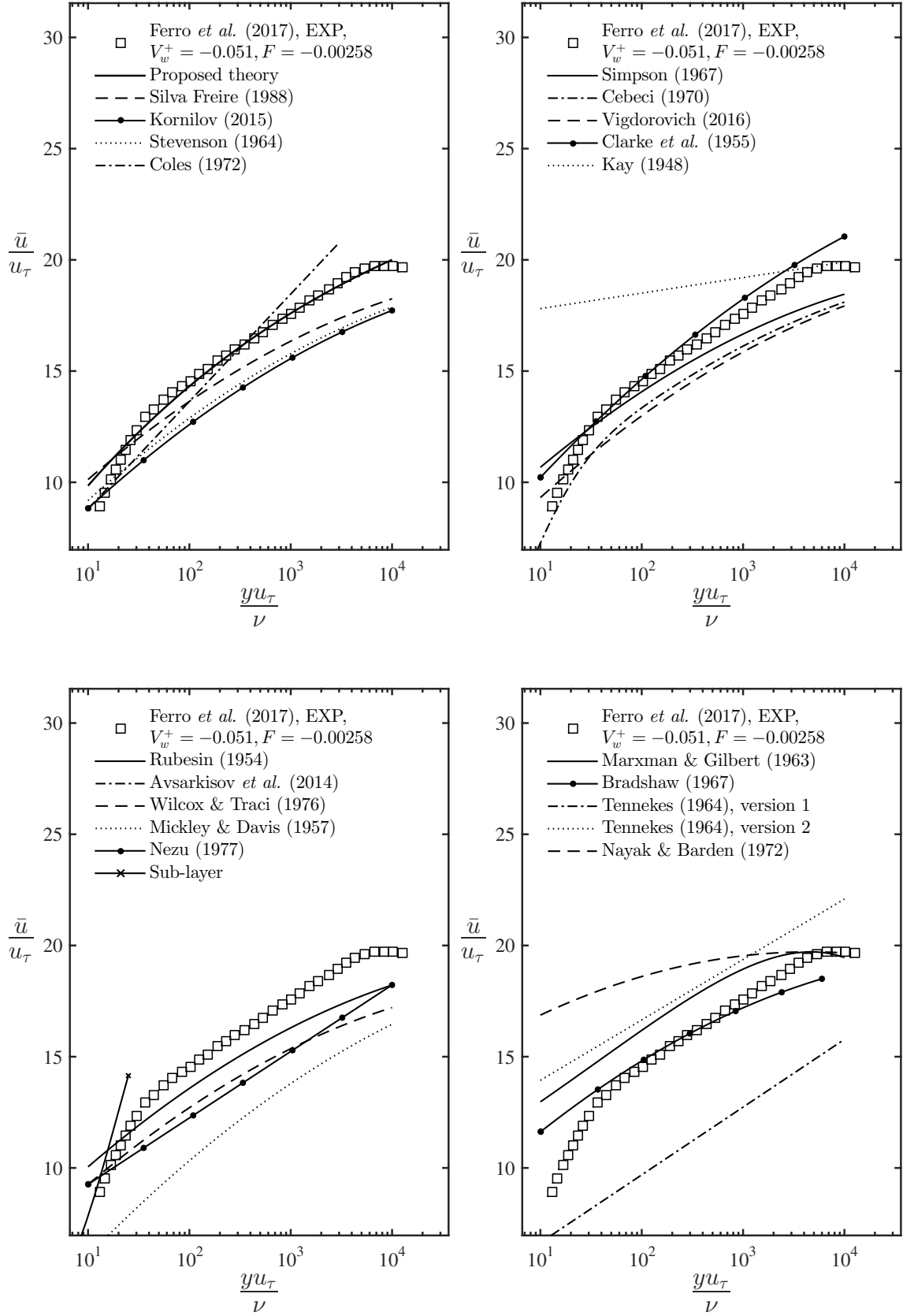


Figure B.2: Mean velocity profiles data compared to different formulations.

Asymptotic suction boundary layer

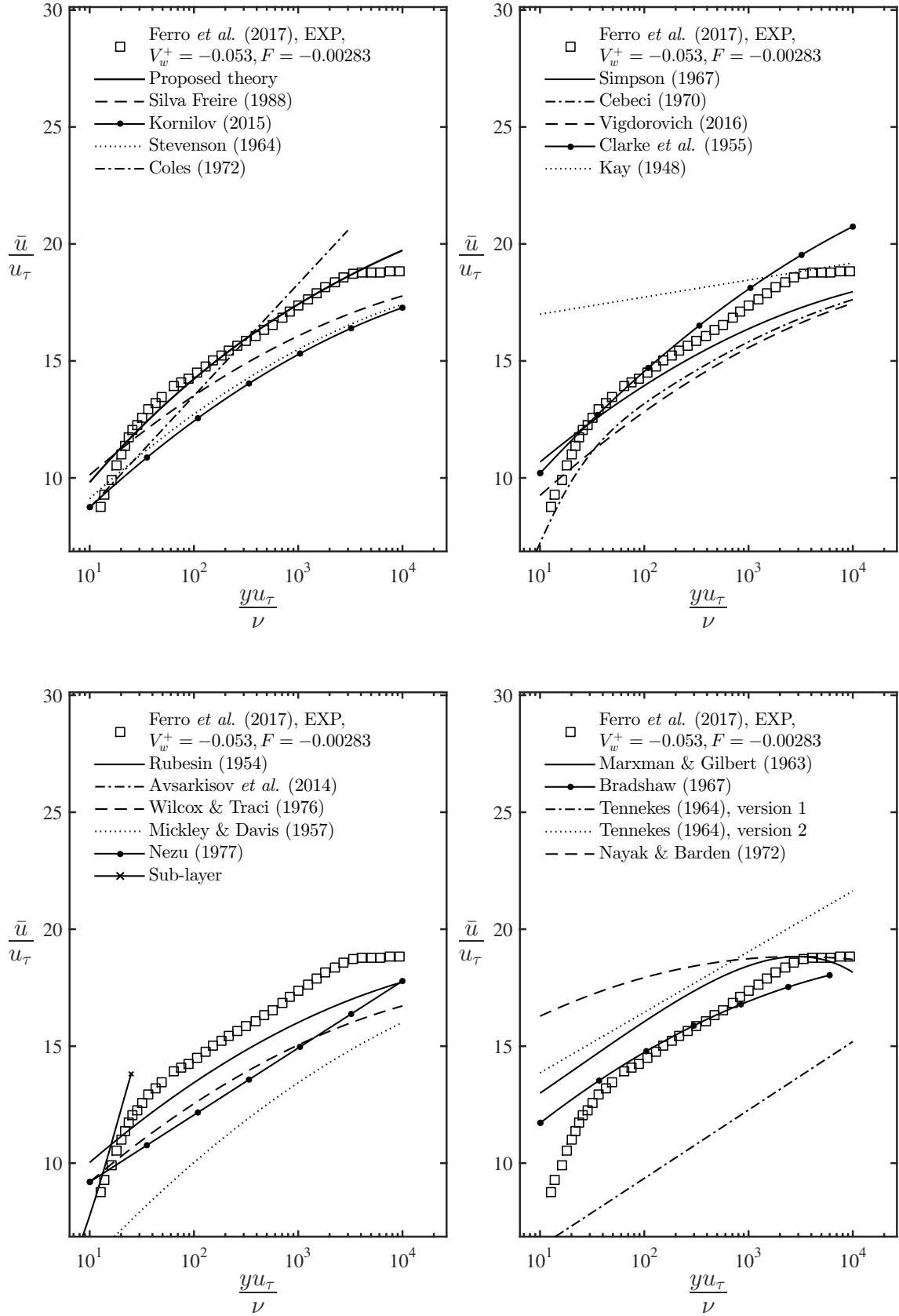


Figure B.3: Mean velocity profiles data compared to different formulations.

Asymptotic suction boundary layer

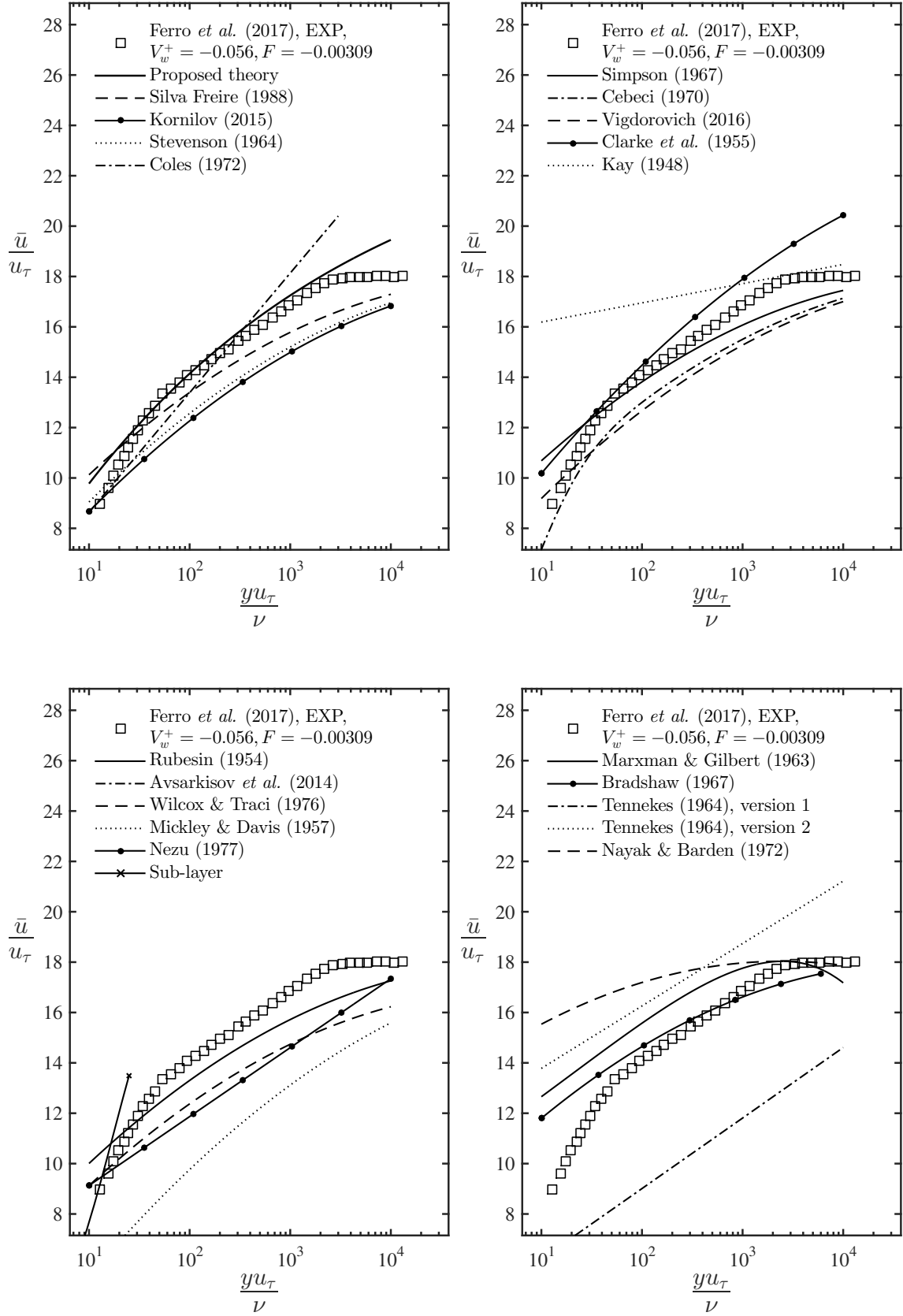


Figure B.4: Mean velocity profiles data compared to different formulations.

Asymptotic suction boundary layer

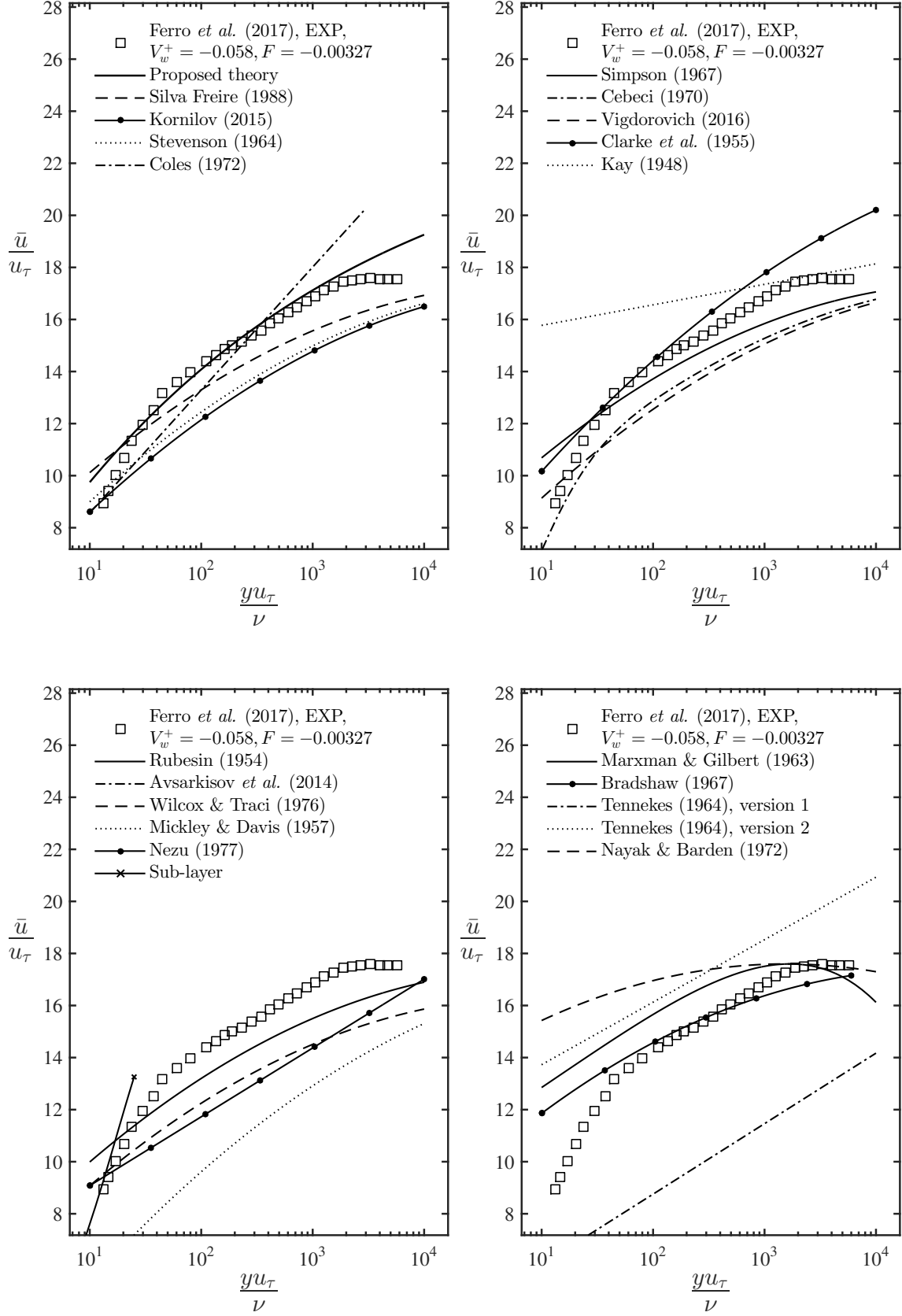


Figure B.5: Mean velocity profiles data compared to different formulations.

Boundary layer flow with blowing

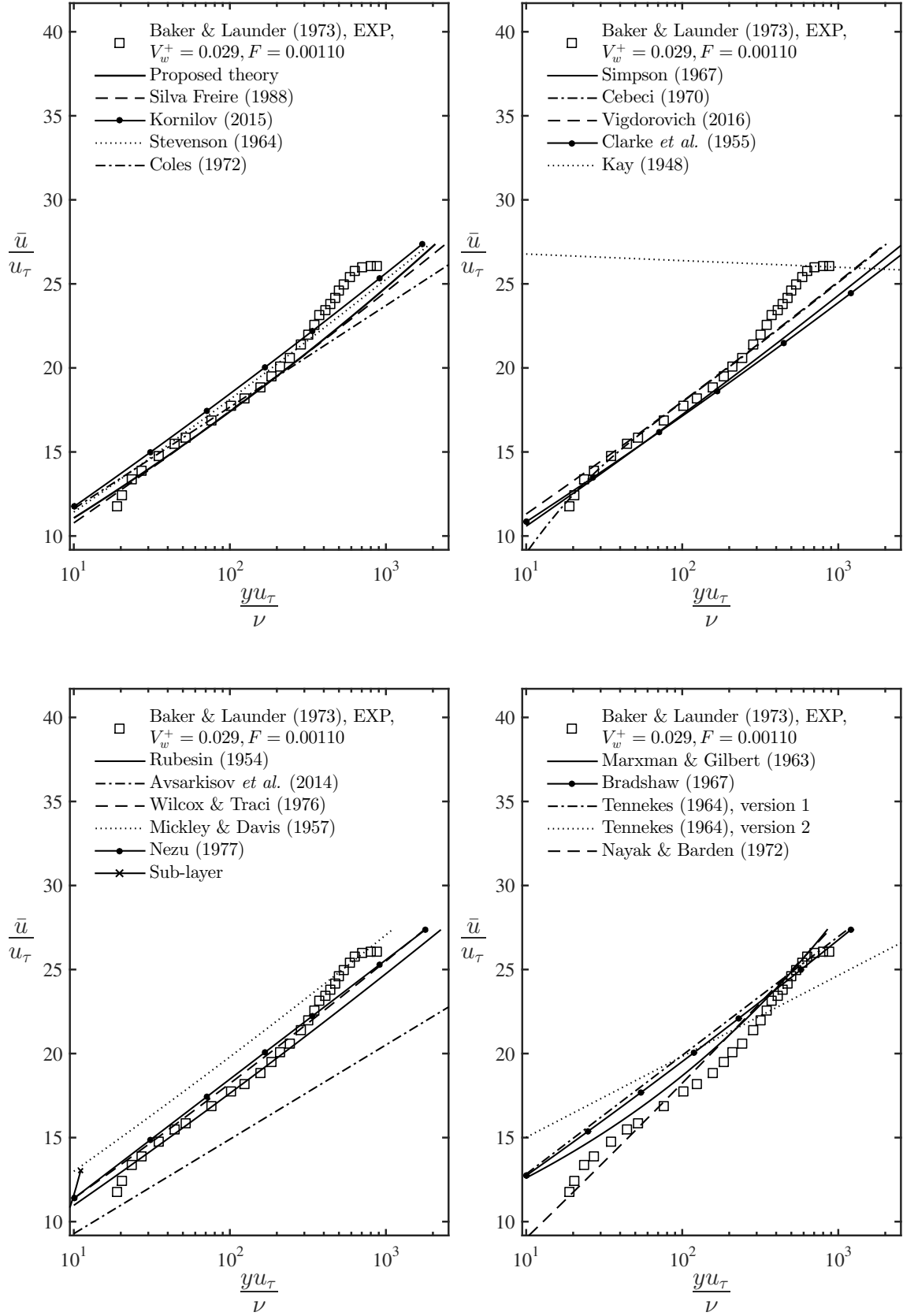


Figure B.6: Mean velocity profiles data compared to different formulations.

Boundary layer flow with blowing

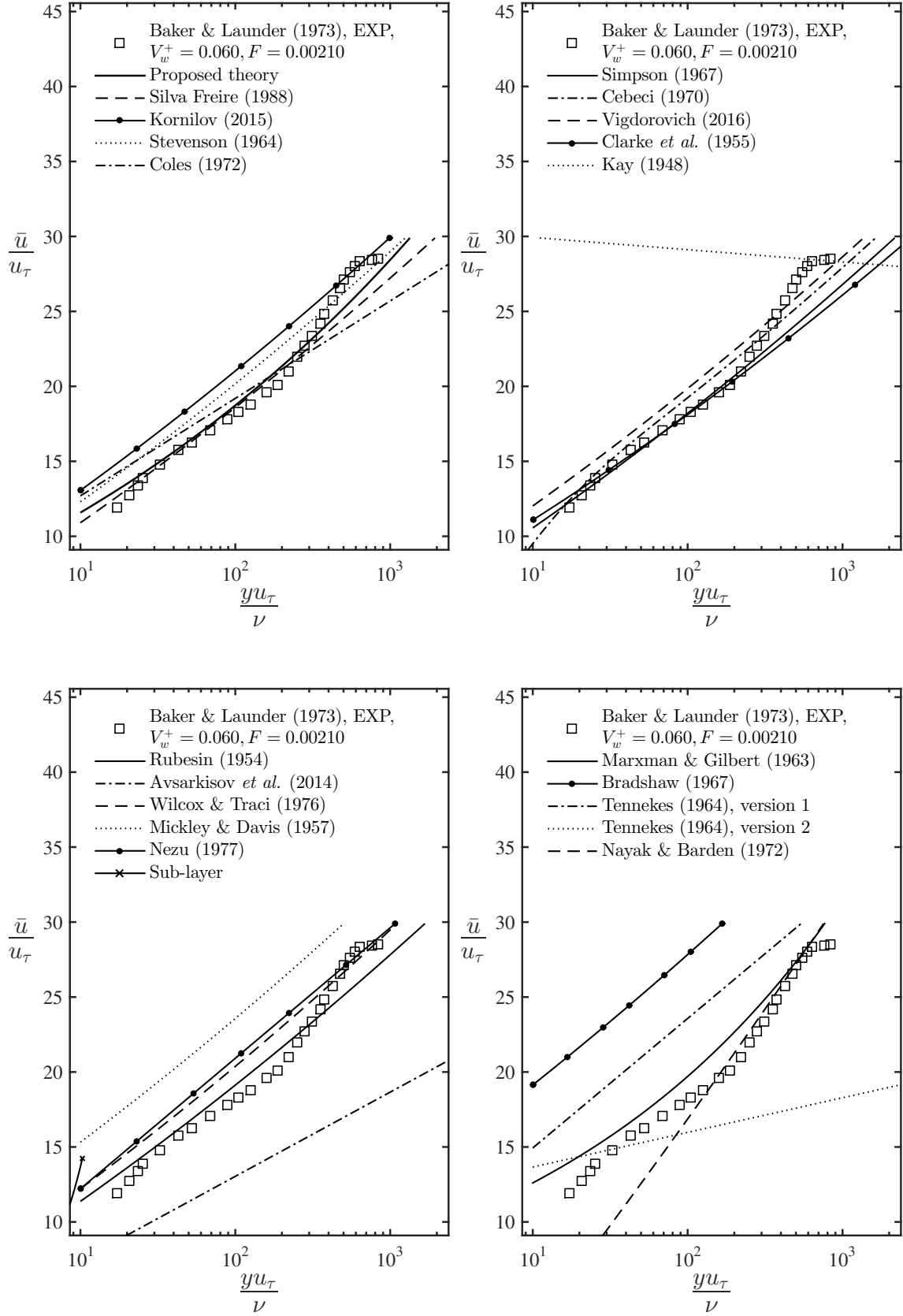


Figure B.7: Mean velocity profiles data compared to different formulations.

Boundary layer flow with blowing

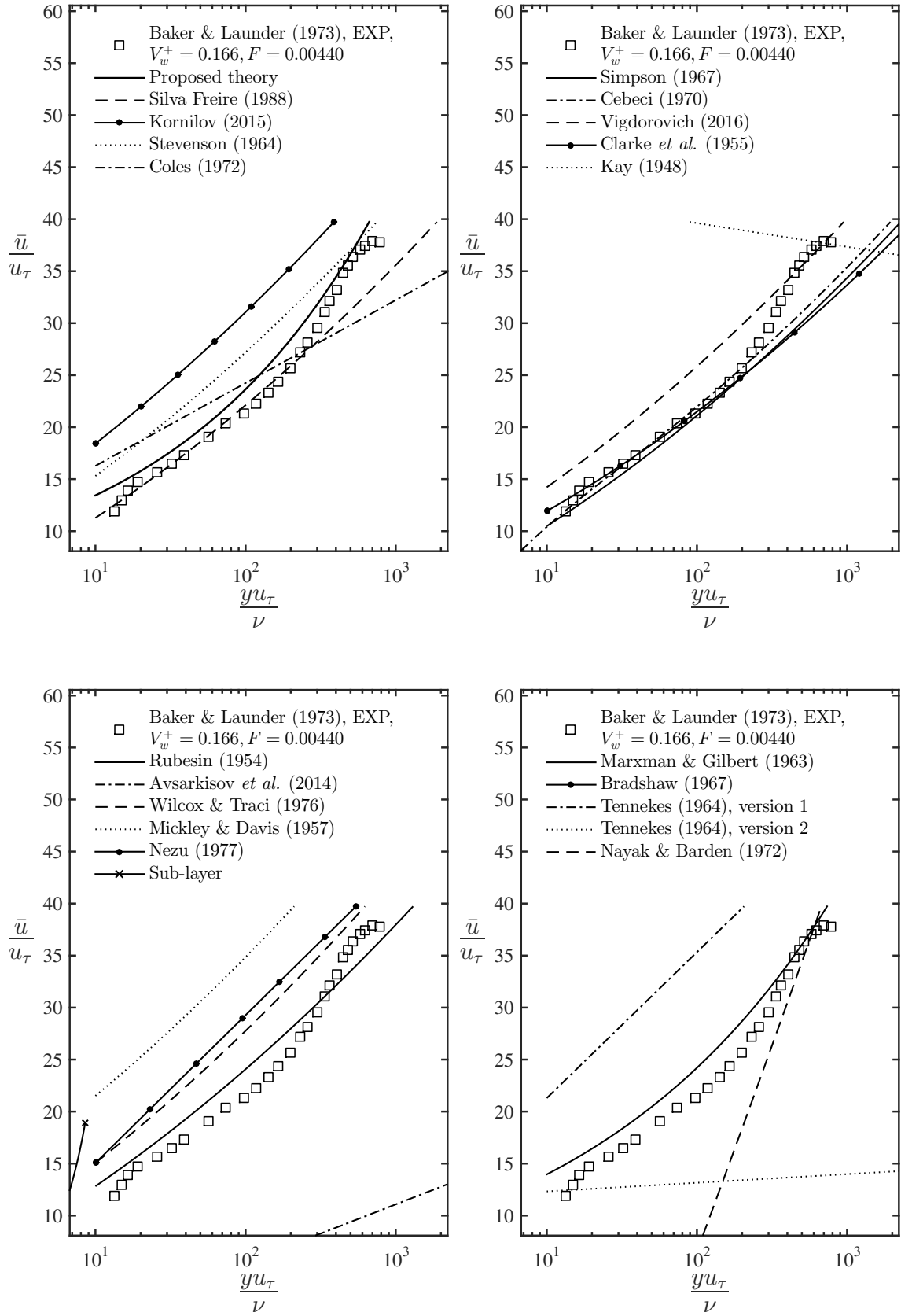


Figure B.8: Mean velocity profiles data compared to different formulations.

Boundary layer flow with blowing

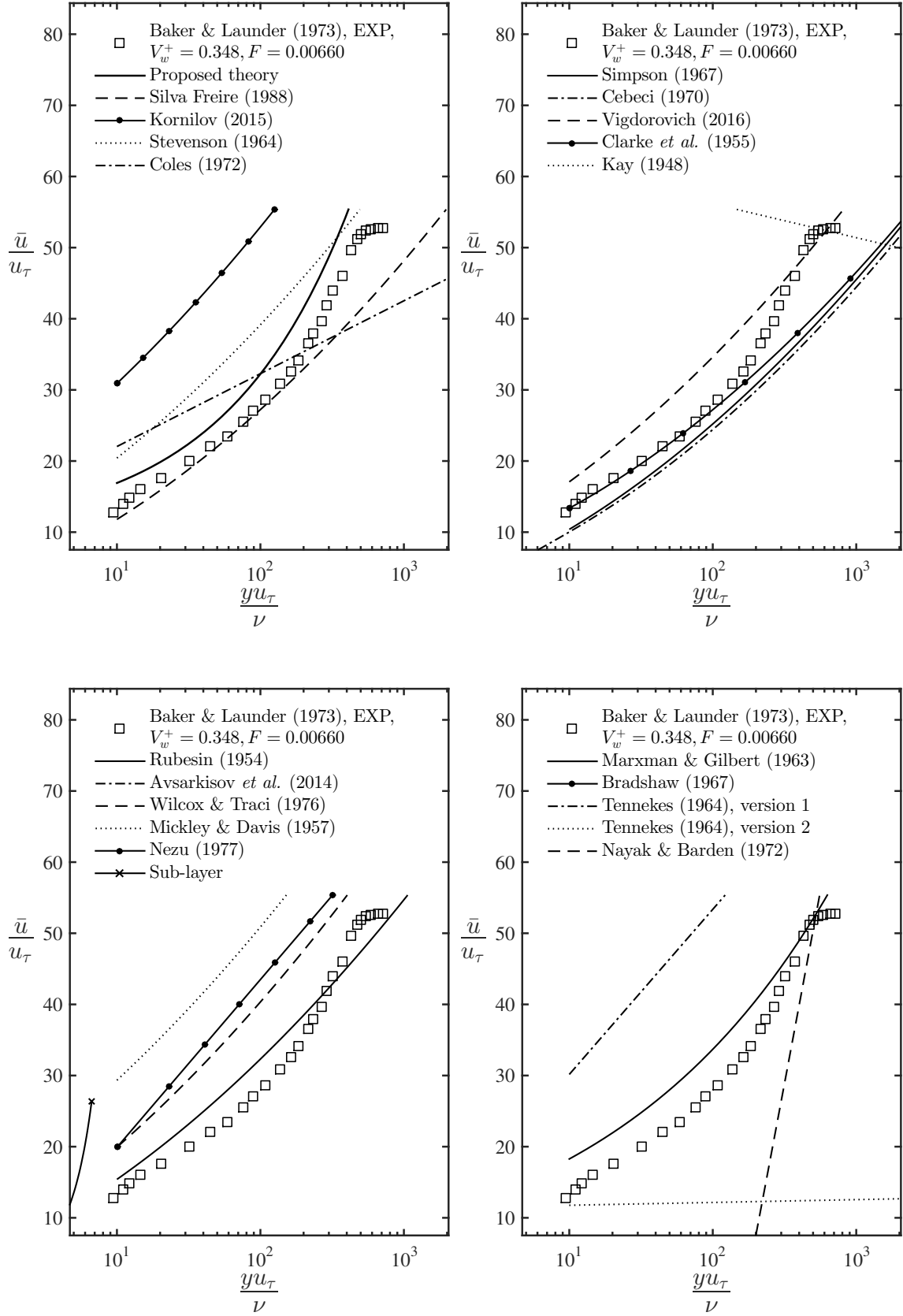


Figure B.9: Mean velocity profiles data compared to different formulations.

Boundary layer flow with blowing

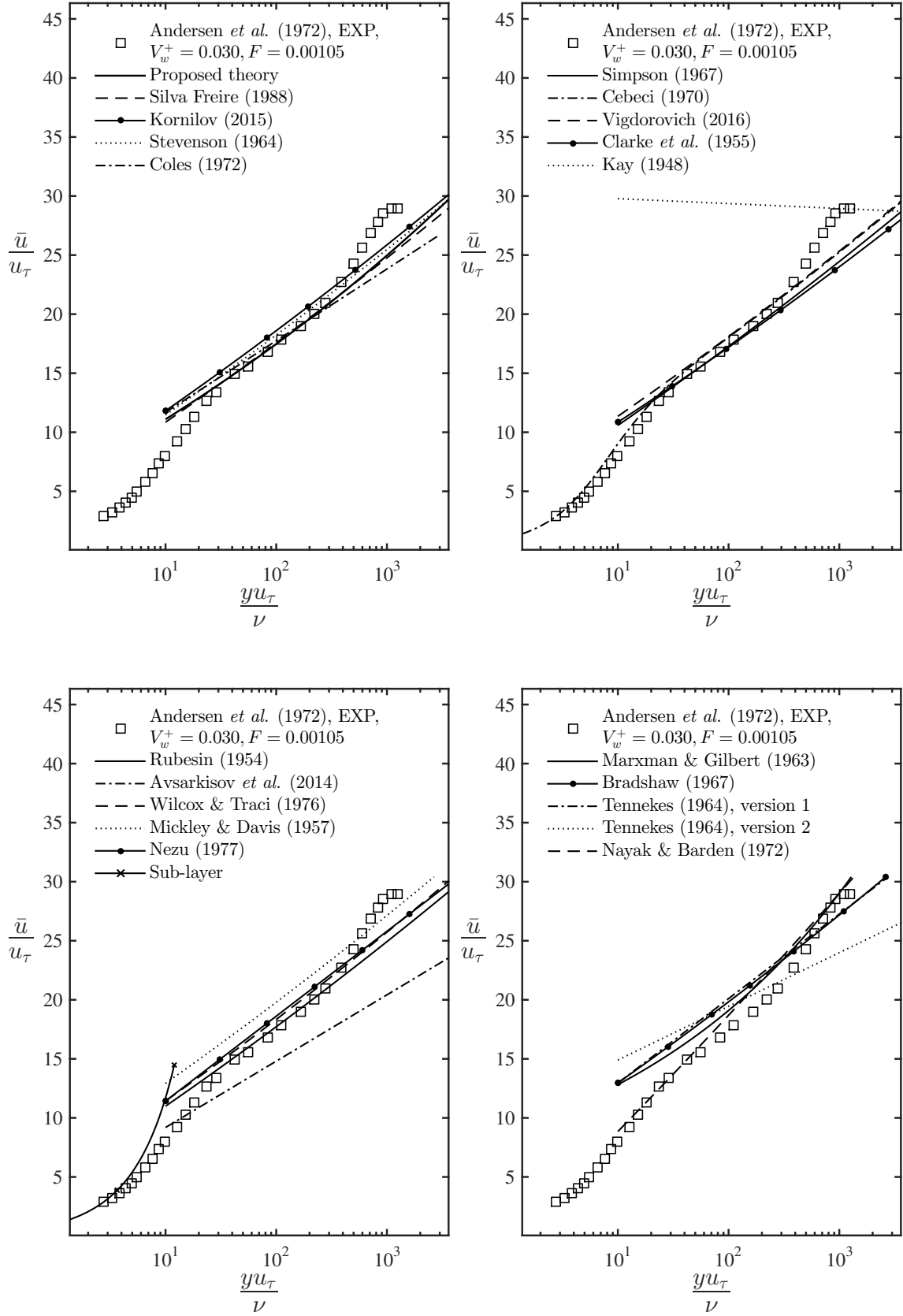


Figure B.10: Mean velocity profiles data compared to different formulations.

Boundary layer flow with blowing

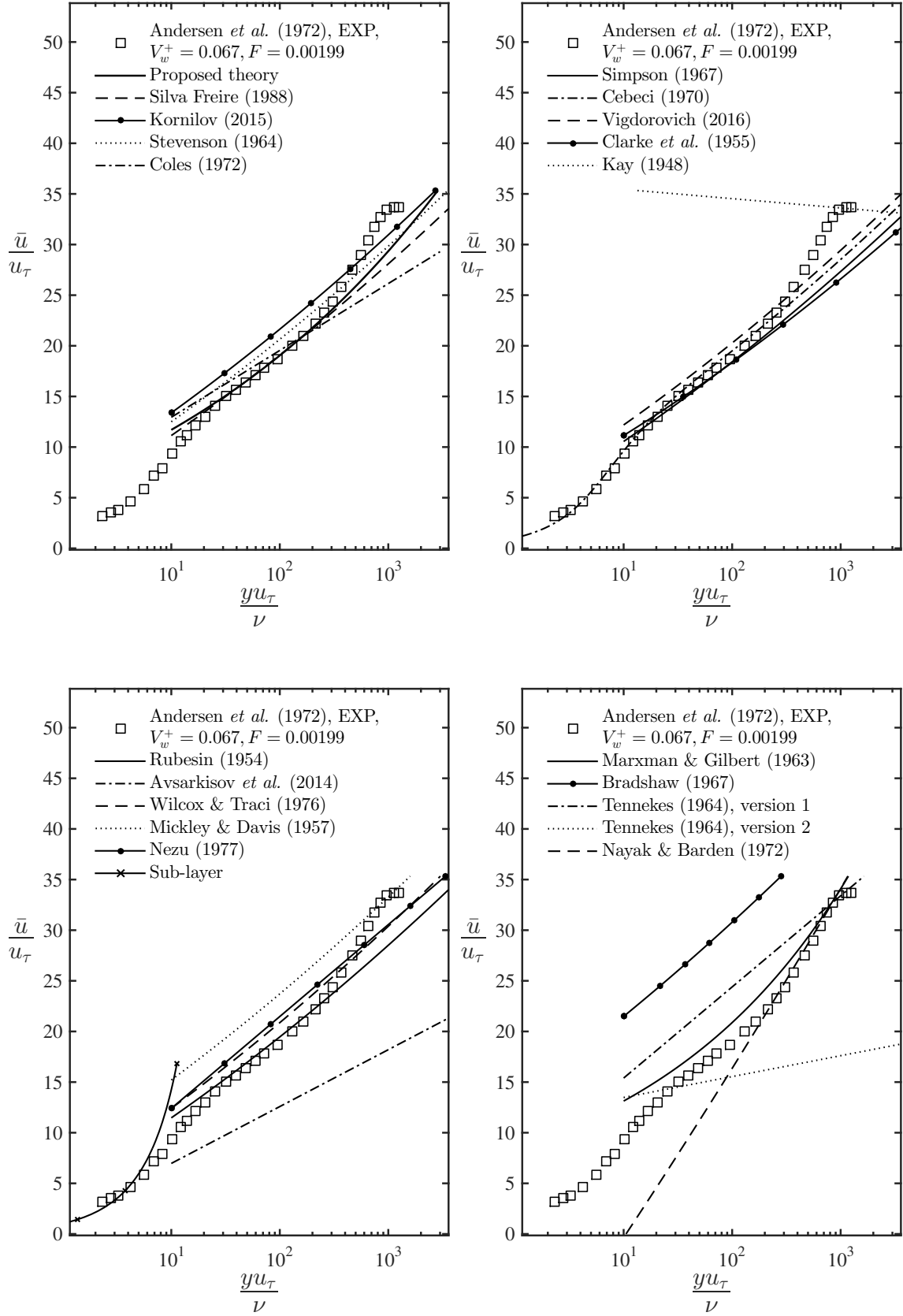


Figure B.11: Mean velocity profiles data compared to different formulations.

Boundary layer flow with blowing

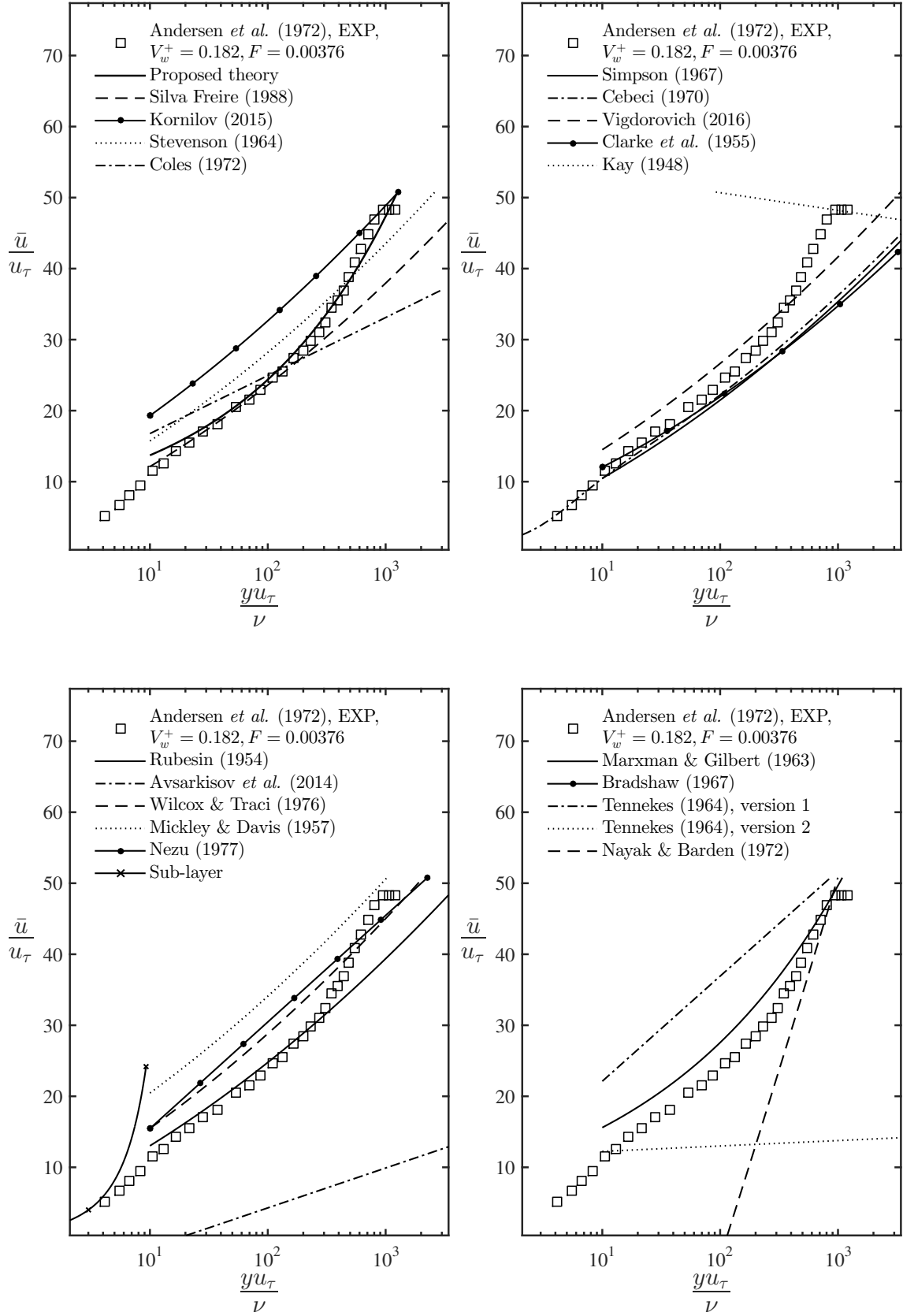


Figure B.12: Mean velocity profiles data compared to different formulations.

Boundary layer flow with blowing

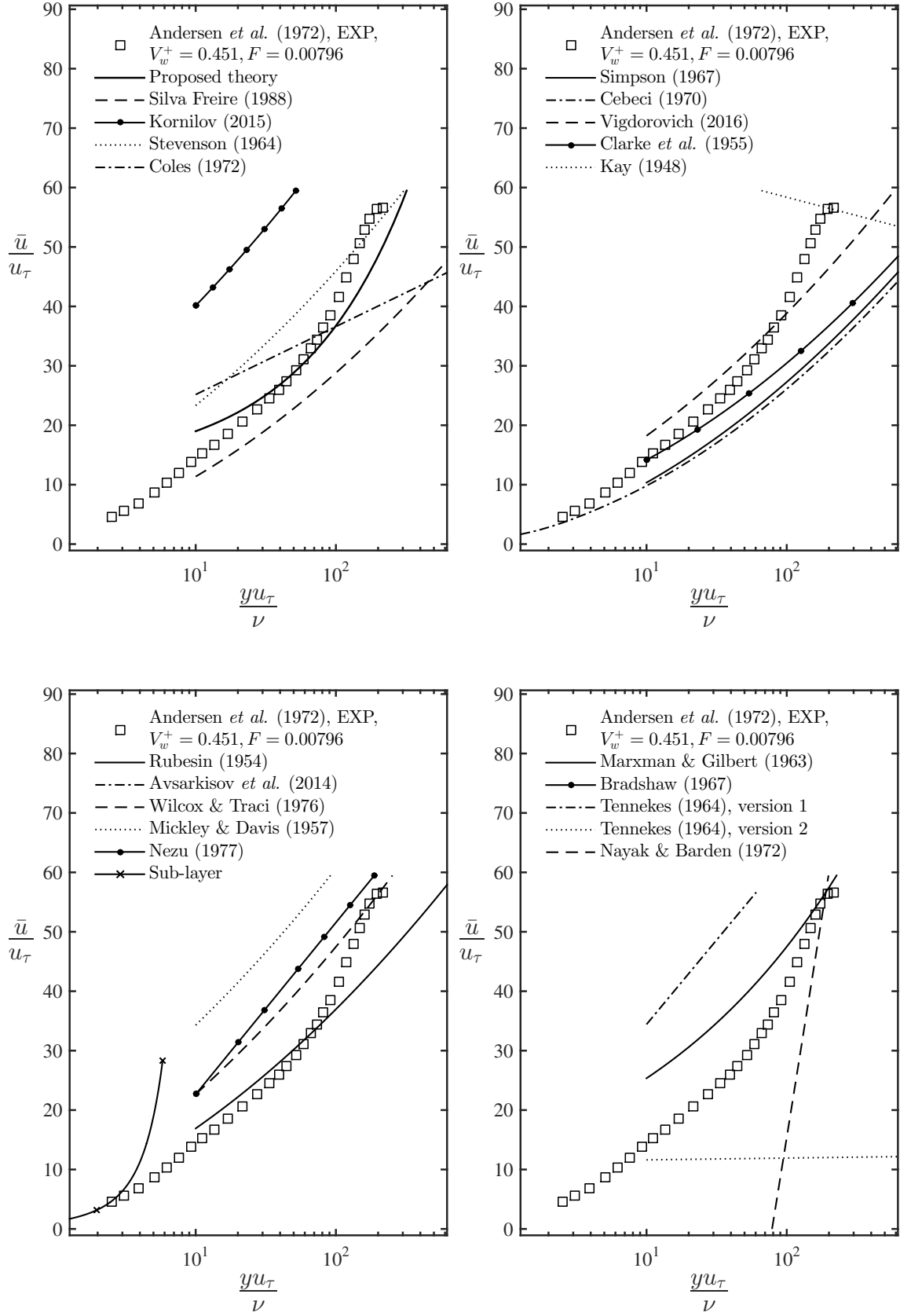


Figure B.13: Mean velocity profiles data compared to different formulations.

Boundary layer flow with blowing

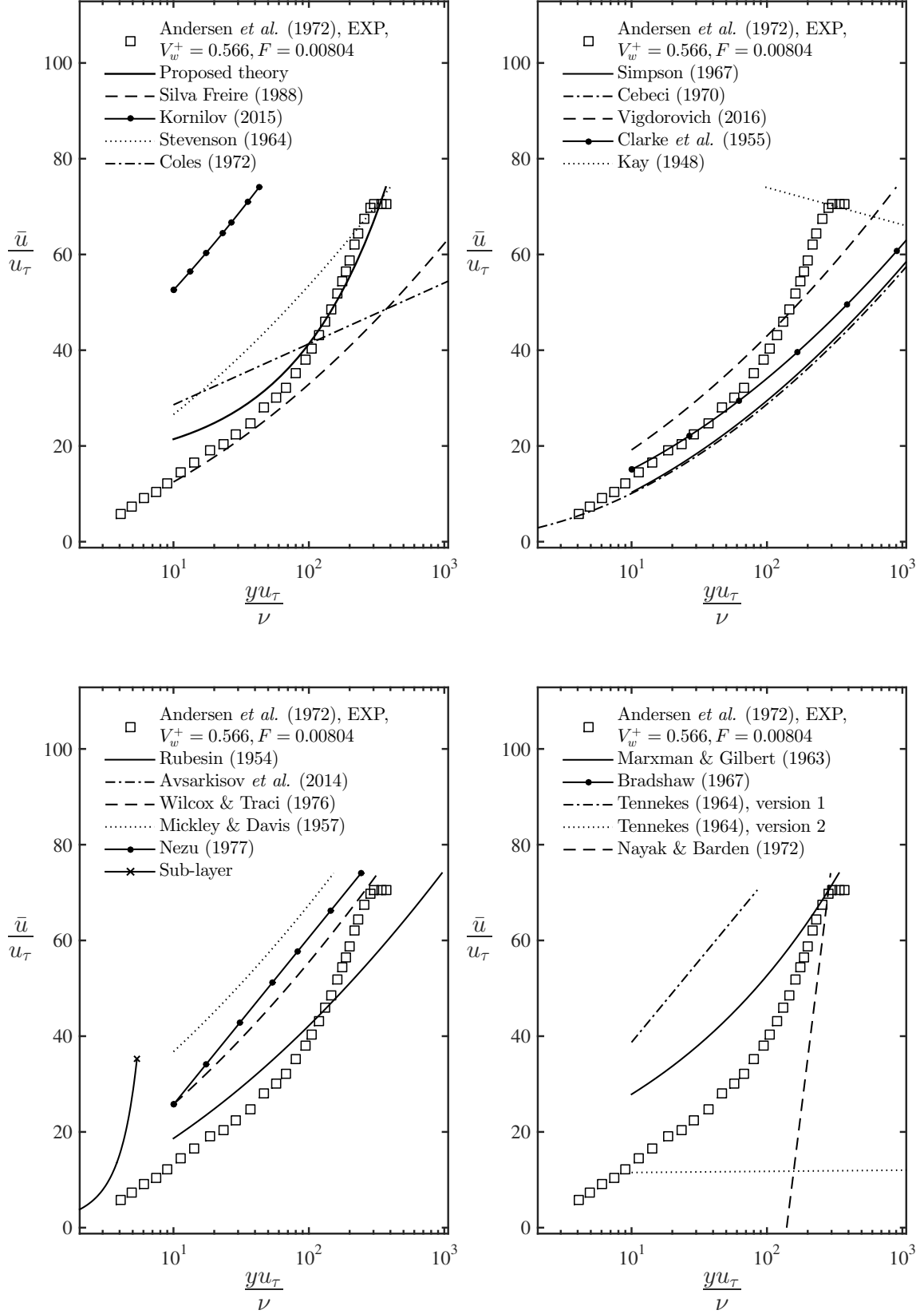


Figure B.14: Mean velocity profiles data compared to different formulations.

Boundary layer flow with blowing

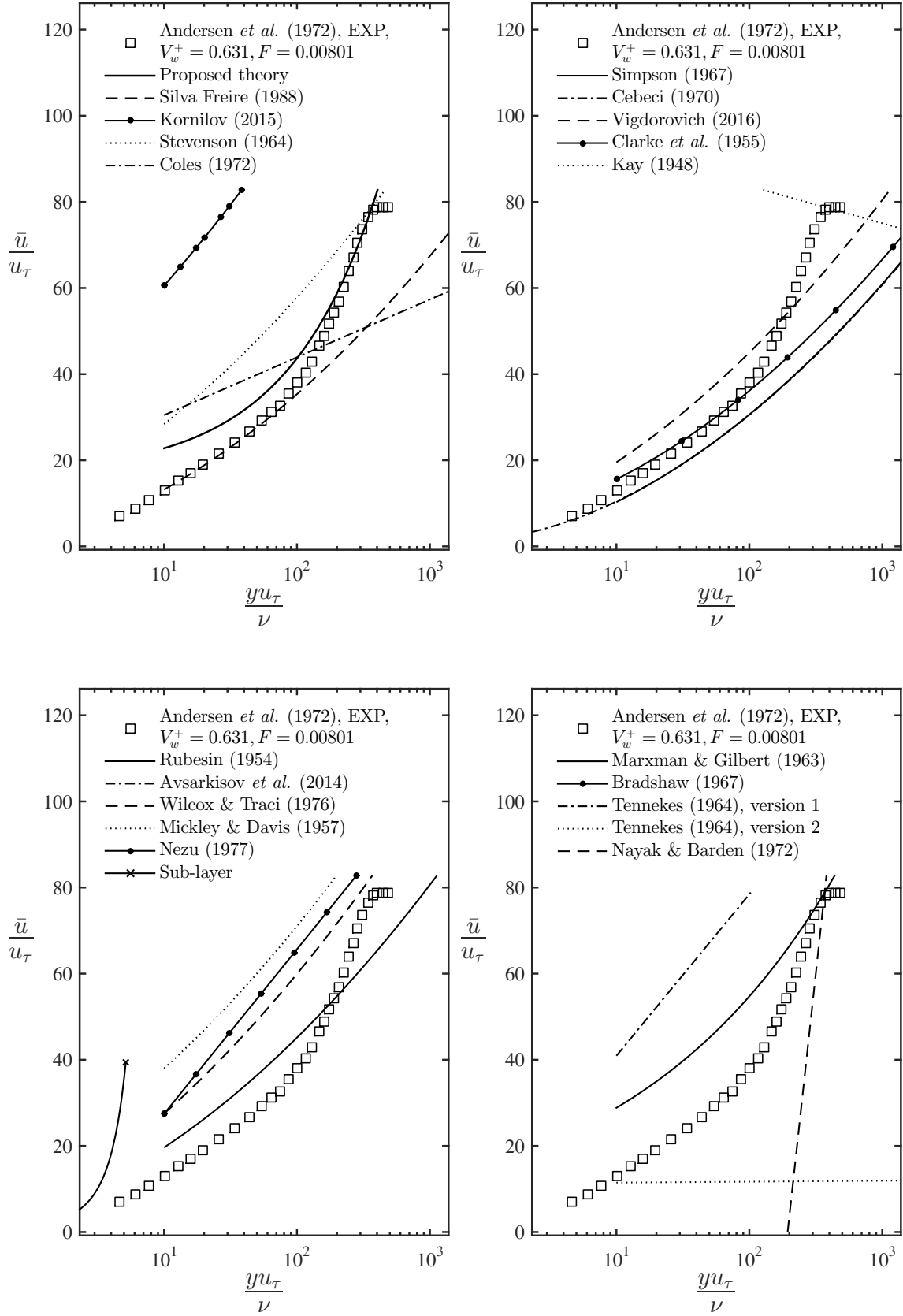


Figure B.15: Mean velocity profiles data compared to different formulations.

Boundary layer flow with blowing

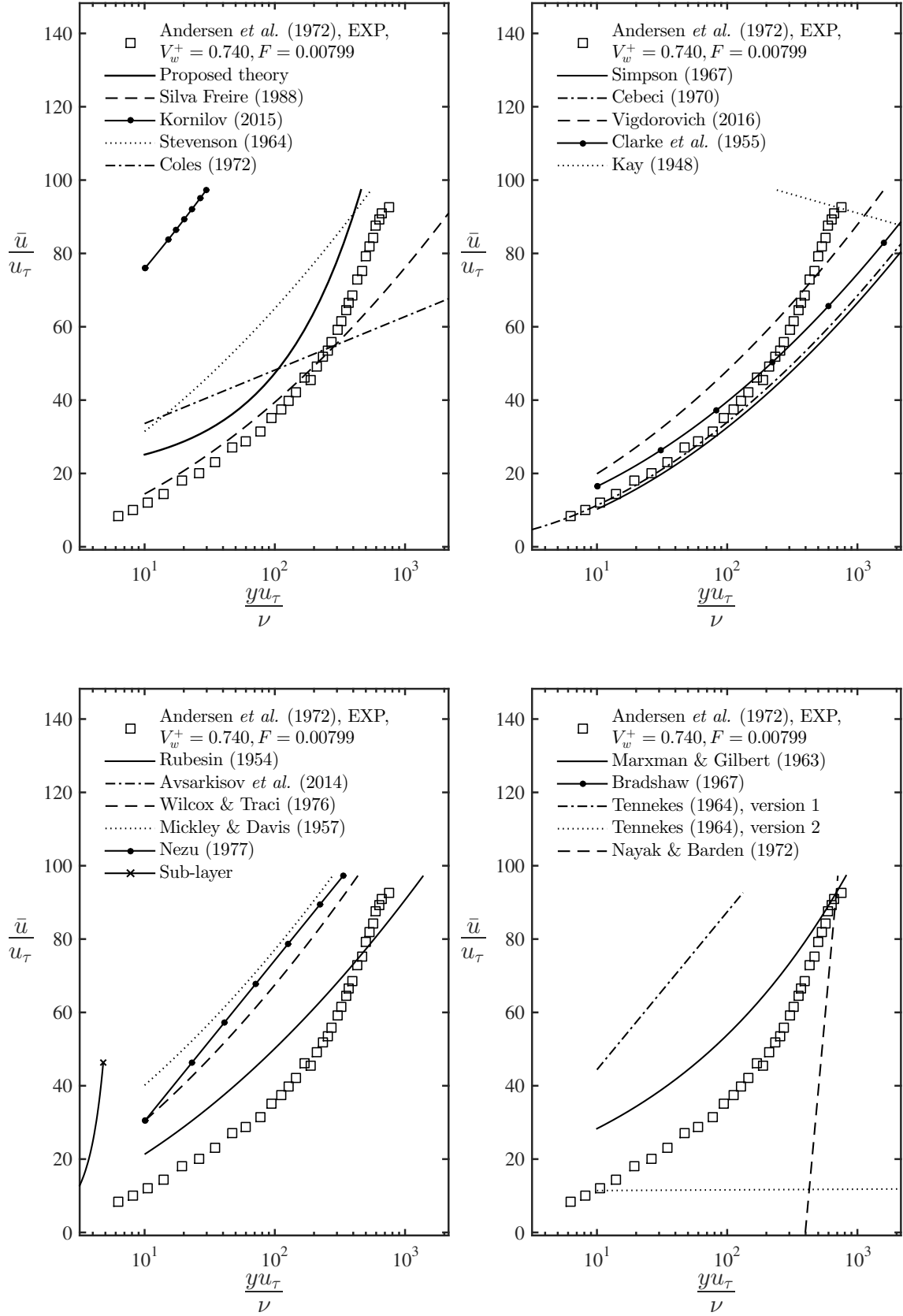


Figure B.16: Mean velocity profiles data compared to different formulations.

Asymptotic suction boundary layer

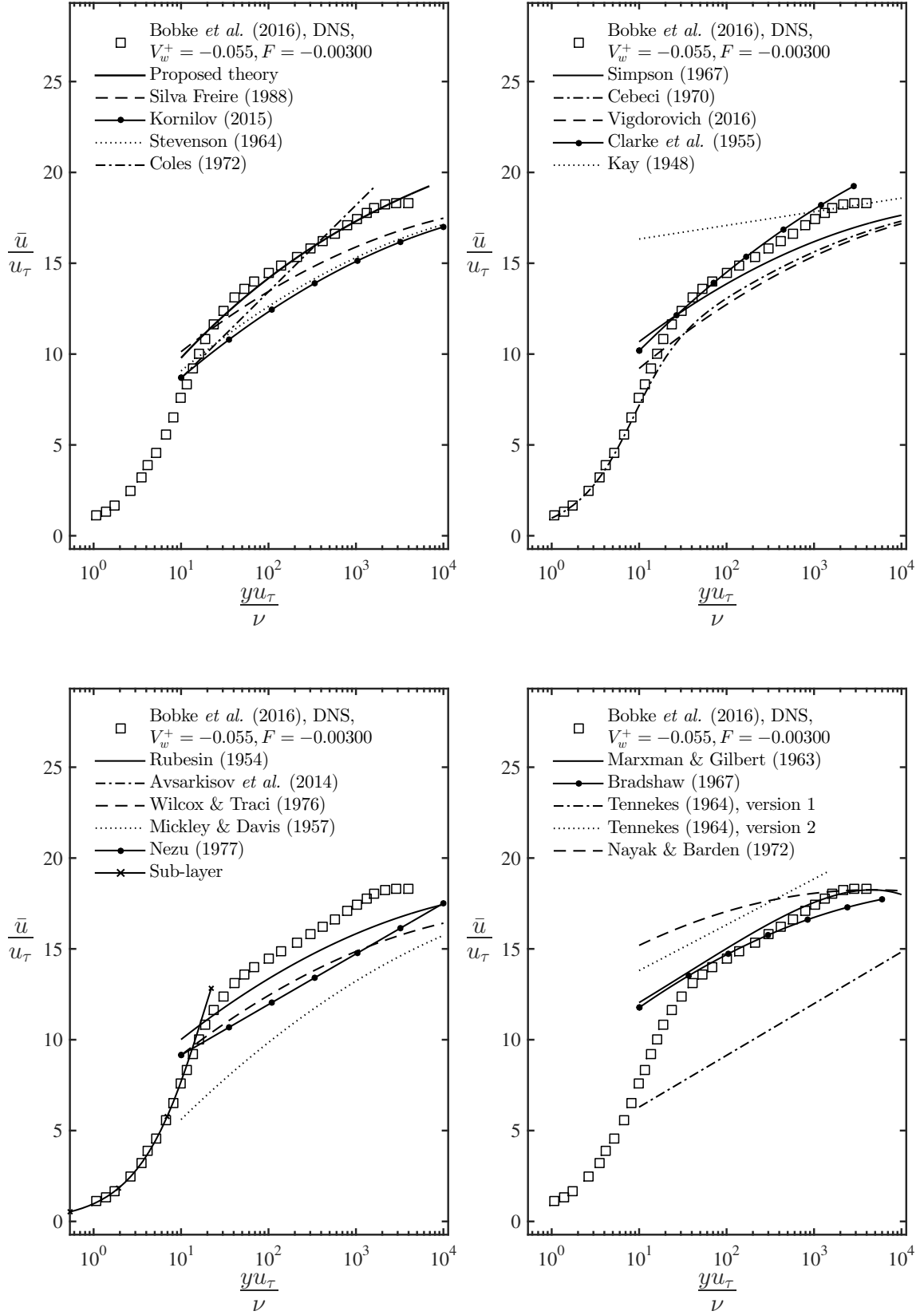


Figure B.17: Mean velocity profiles data compared to different formulations.

Asymptotic suction boundary layer

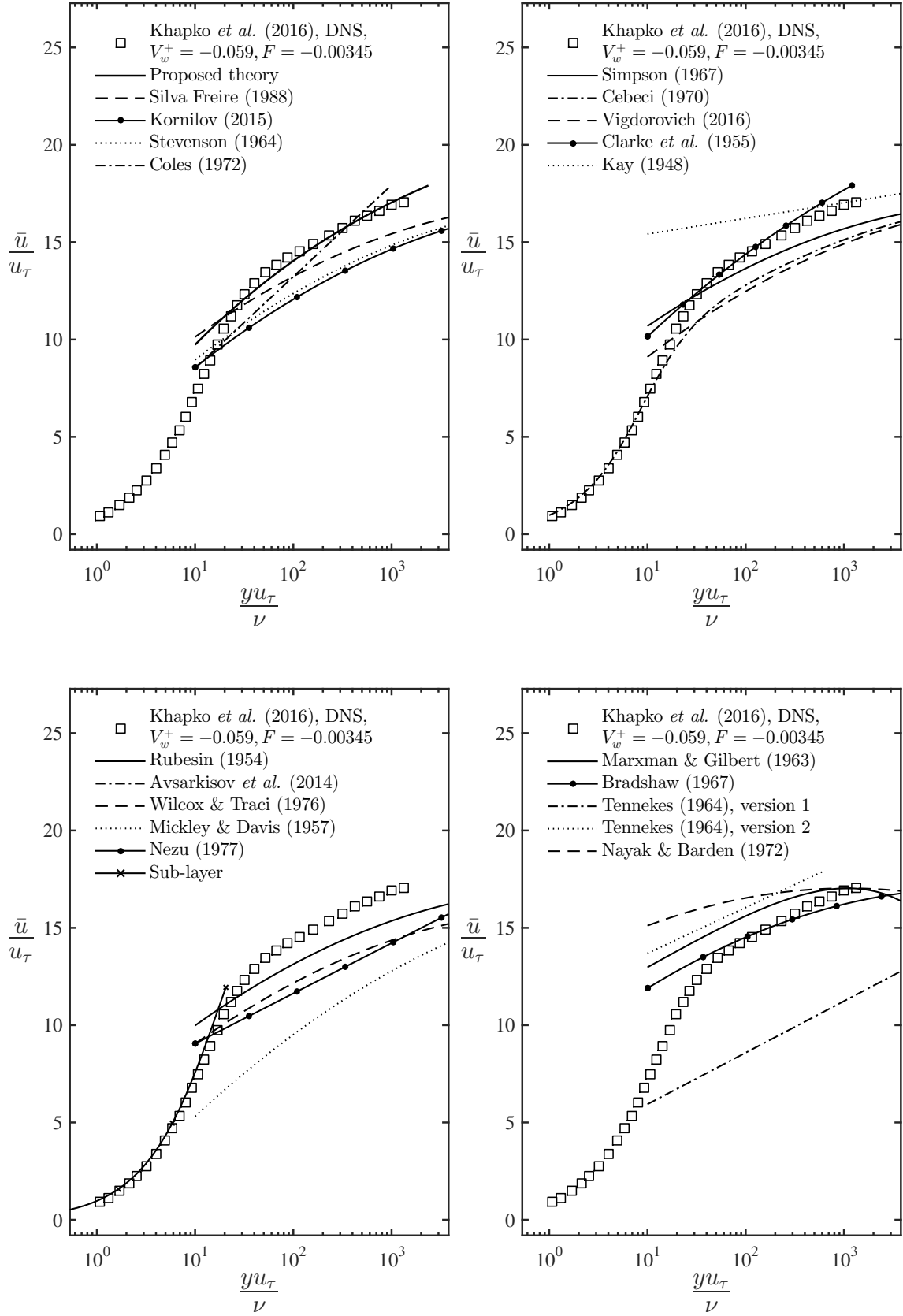


Figure B.18: Mean velocity profiles data compared to different formulations.

Asymptotic suction boundary layer

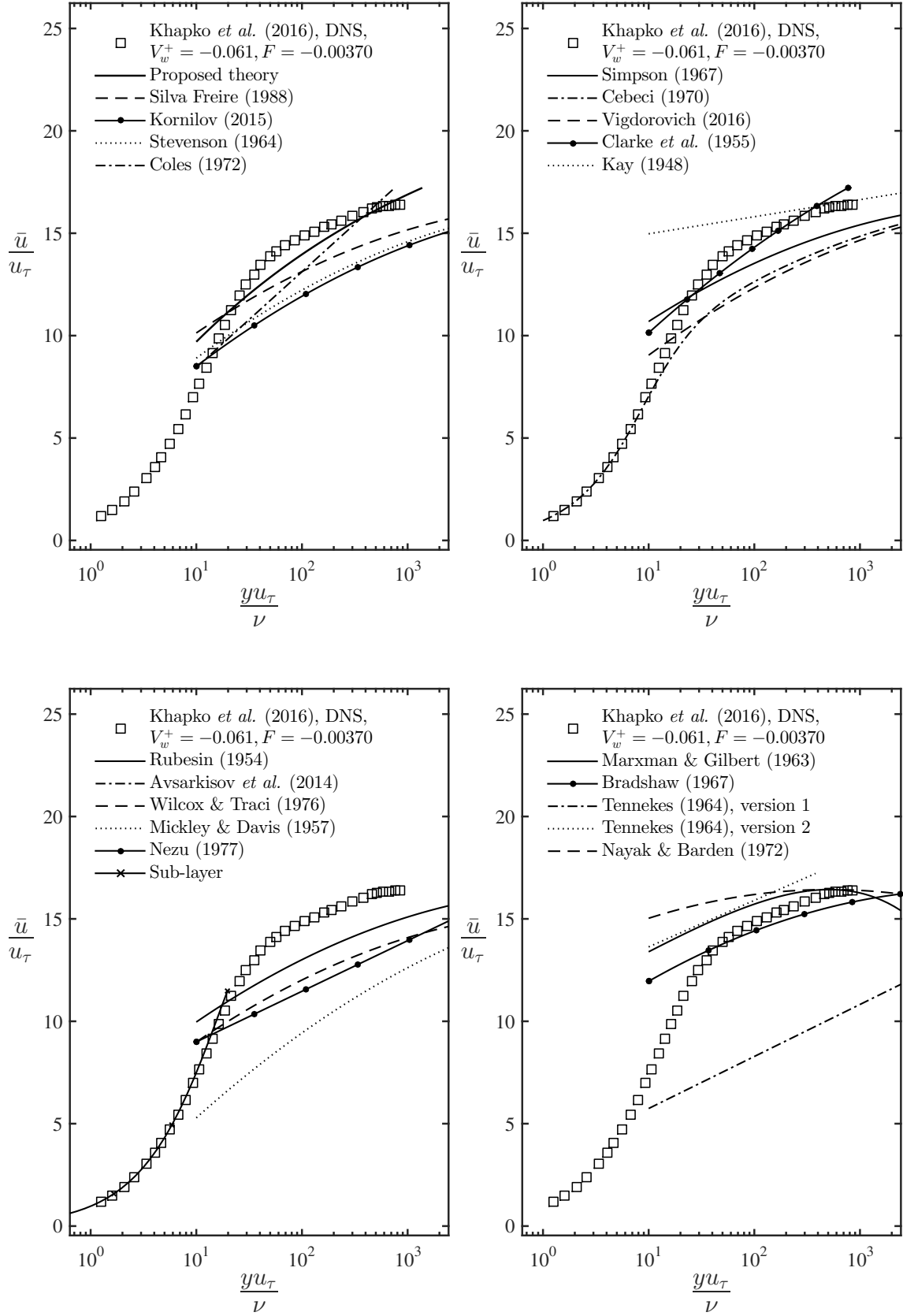


Figure B.19: Mean velocity profiles data compared to different formulations.

Asymptotic suction boundary layer

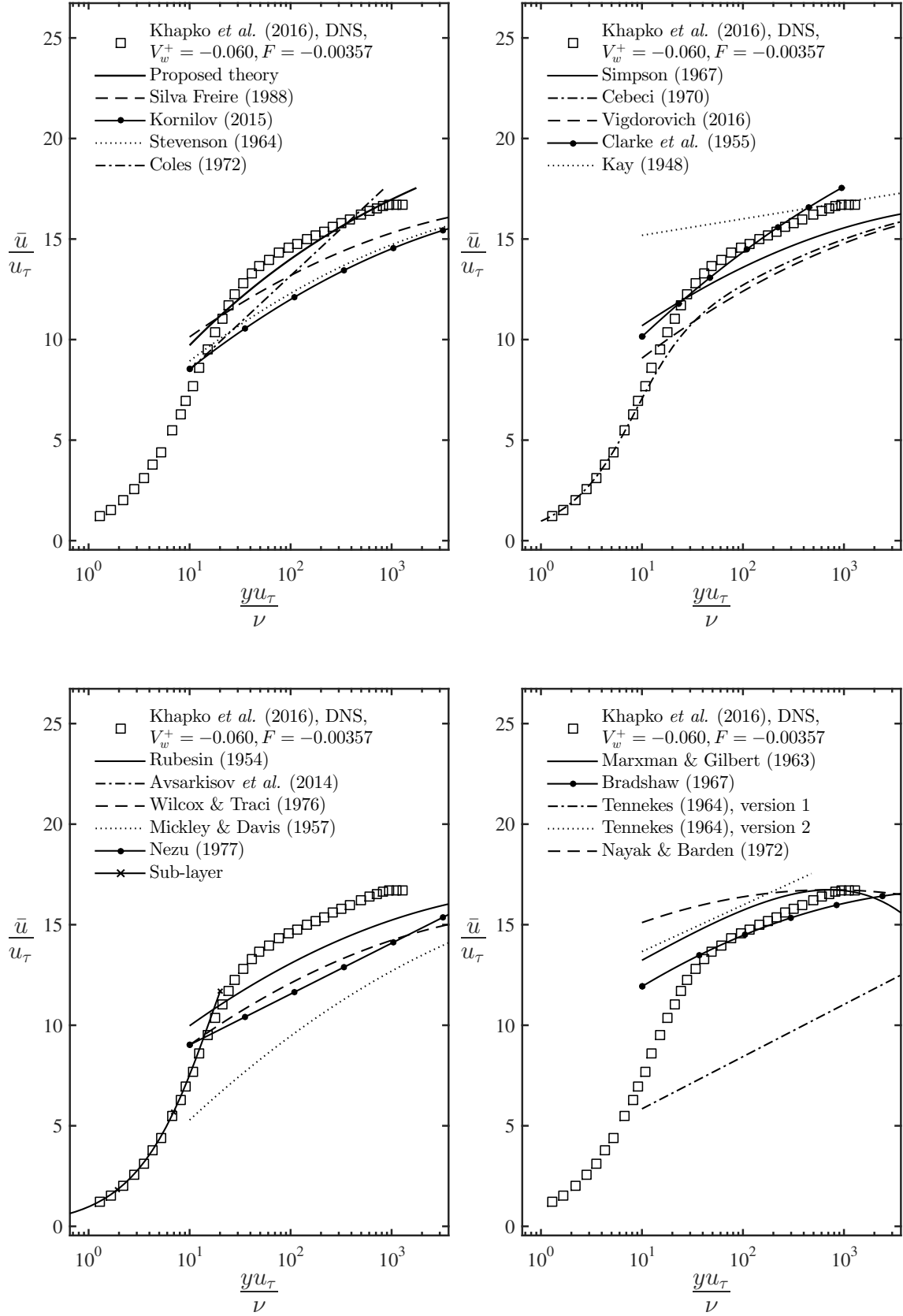


Figure B.20: Mean velocity profiles data compared to different formulations.

Pipe flow with suction

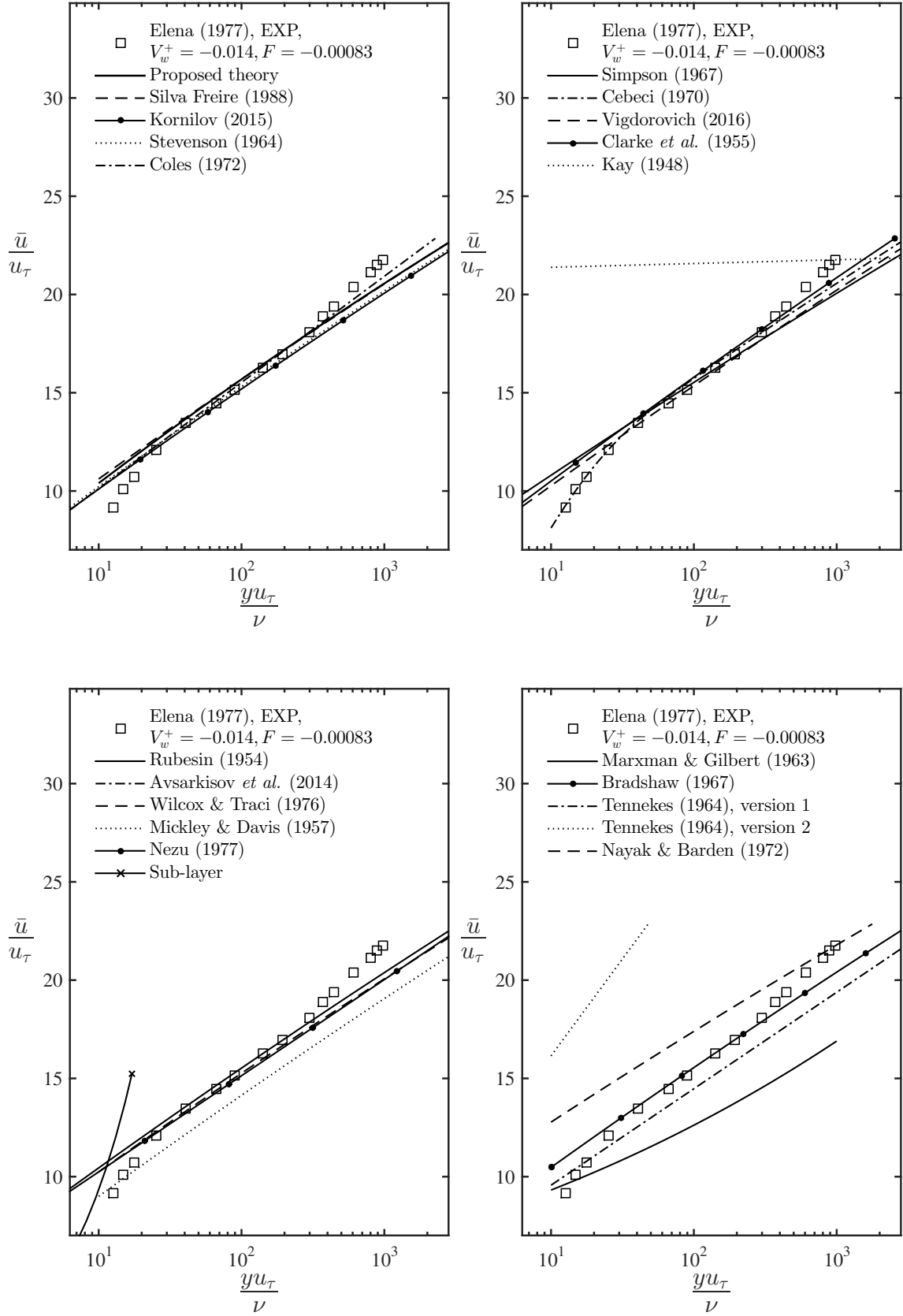


Figure B.21: Mean velocity profiles data compared to different formulations.

Pipe flow with suction

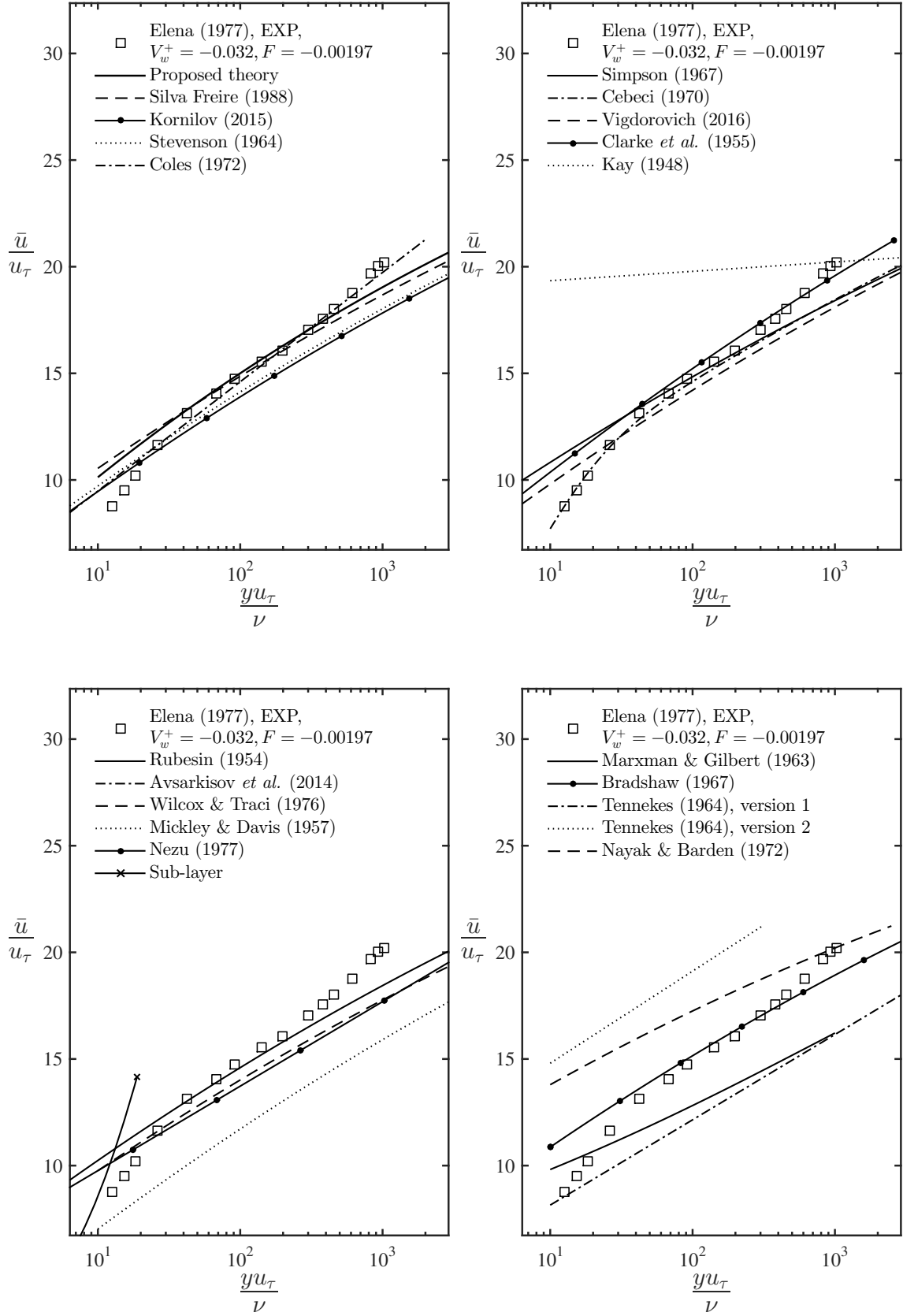


Figure B.22: Mean velocity profiles data compared to different formulations.

Pipe flow with suction

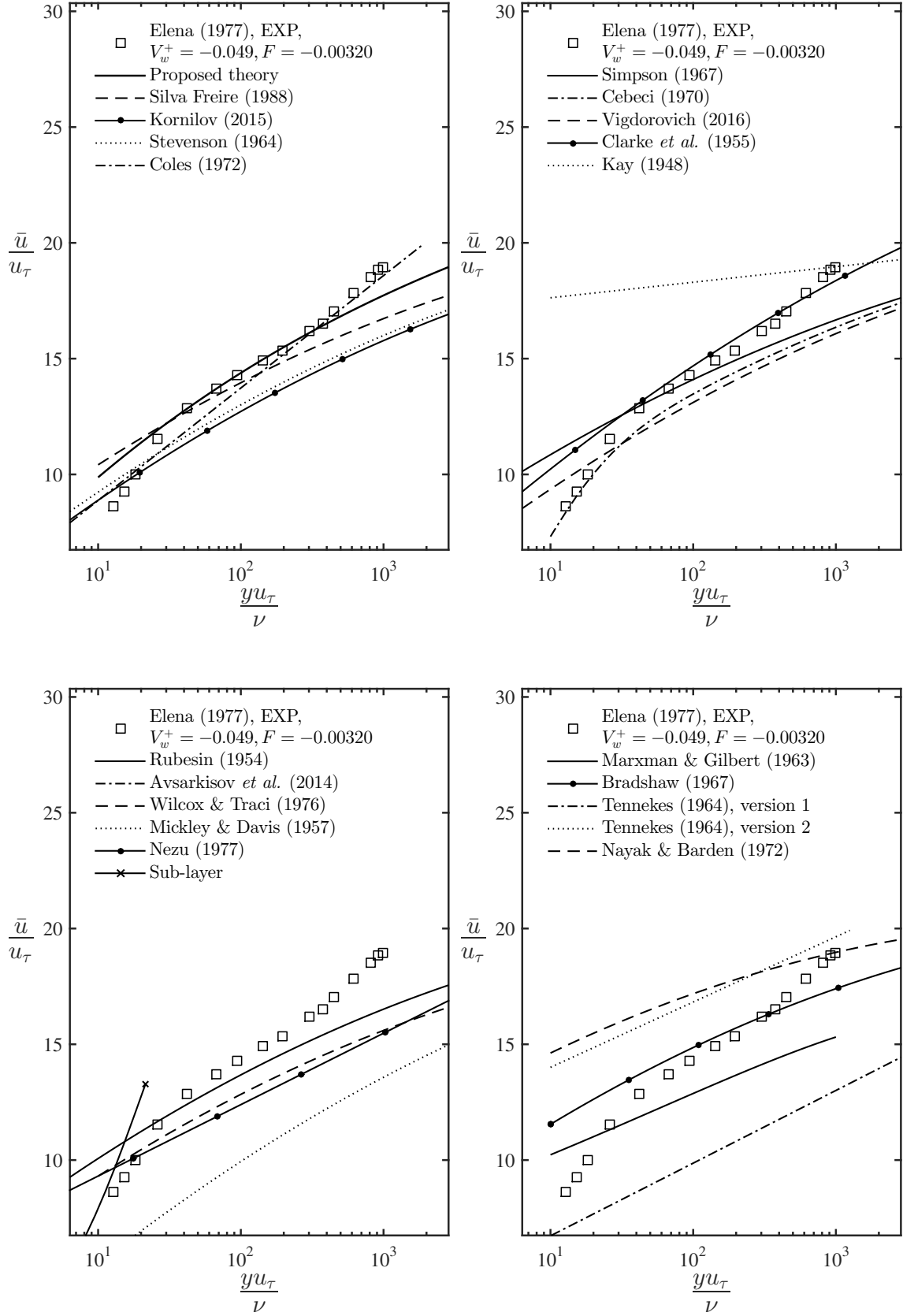


Figure B.23: Mean velocity profiles data compared to different formulations.

Boundary layer flow

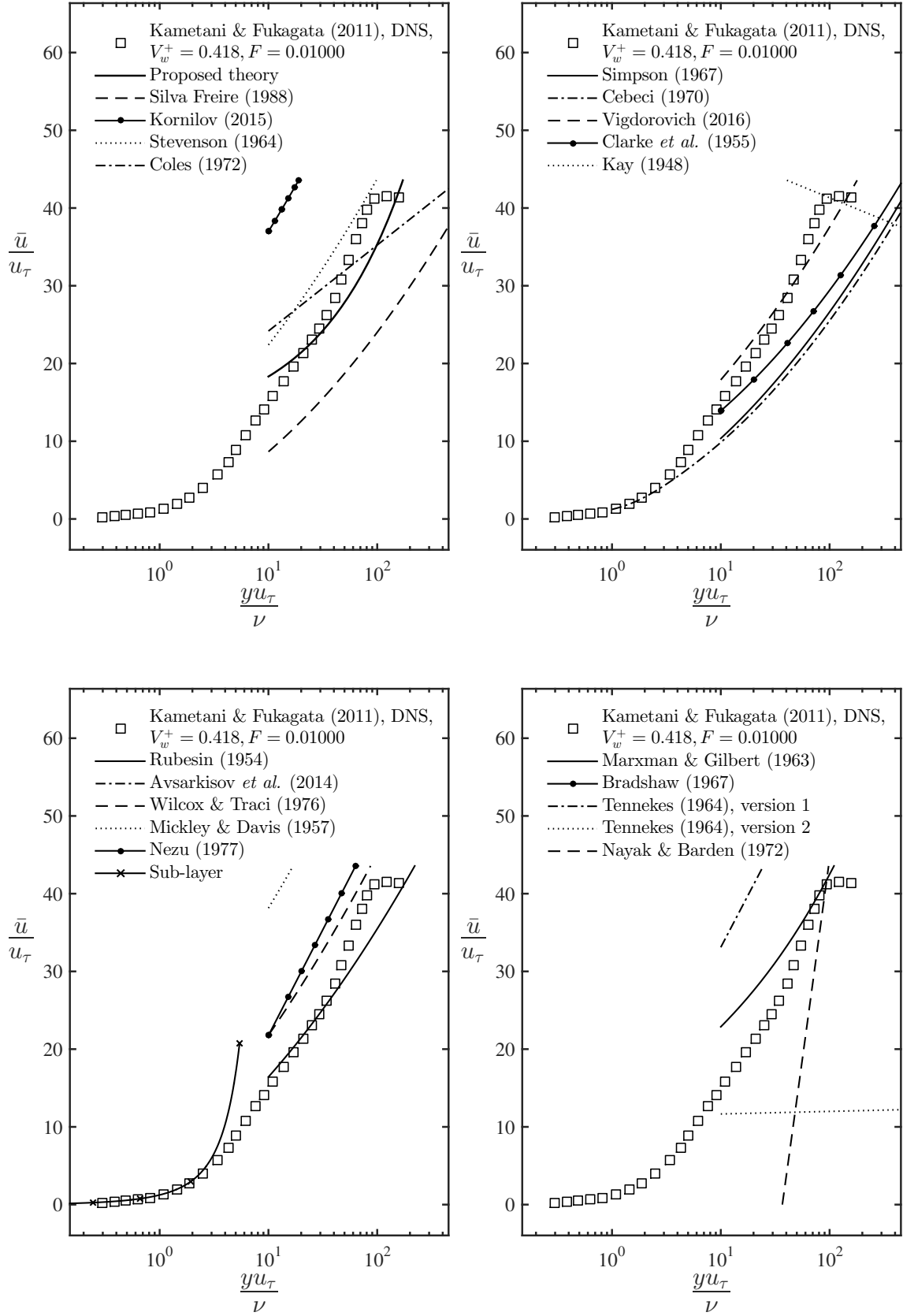


Figure B.24: Mean velocity profiles data compared to different formulations.

Boundary layer flow

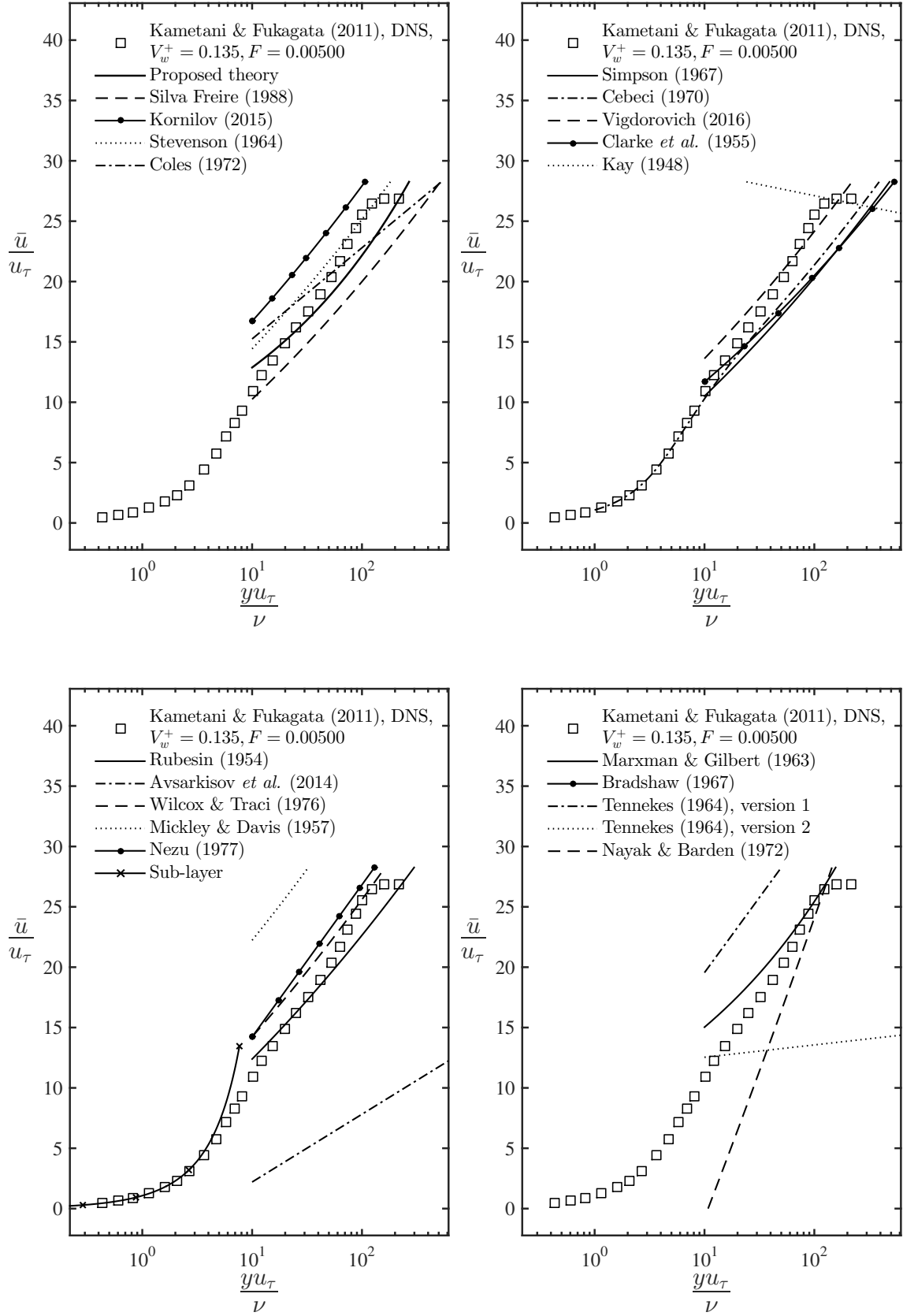


Figure B.25: Mean velocity profiles data compared to different formulations.

Boundary layer flow

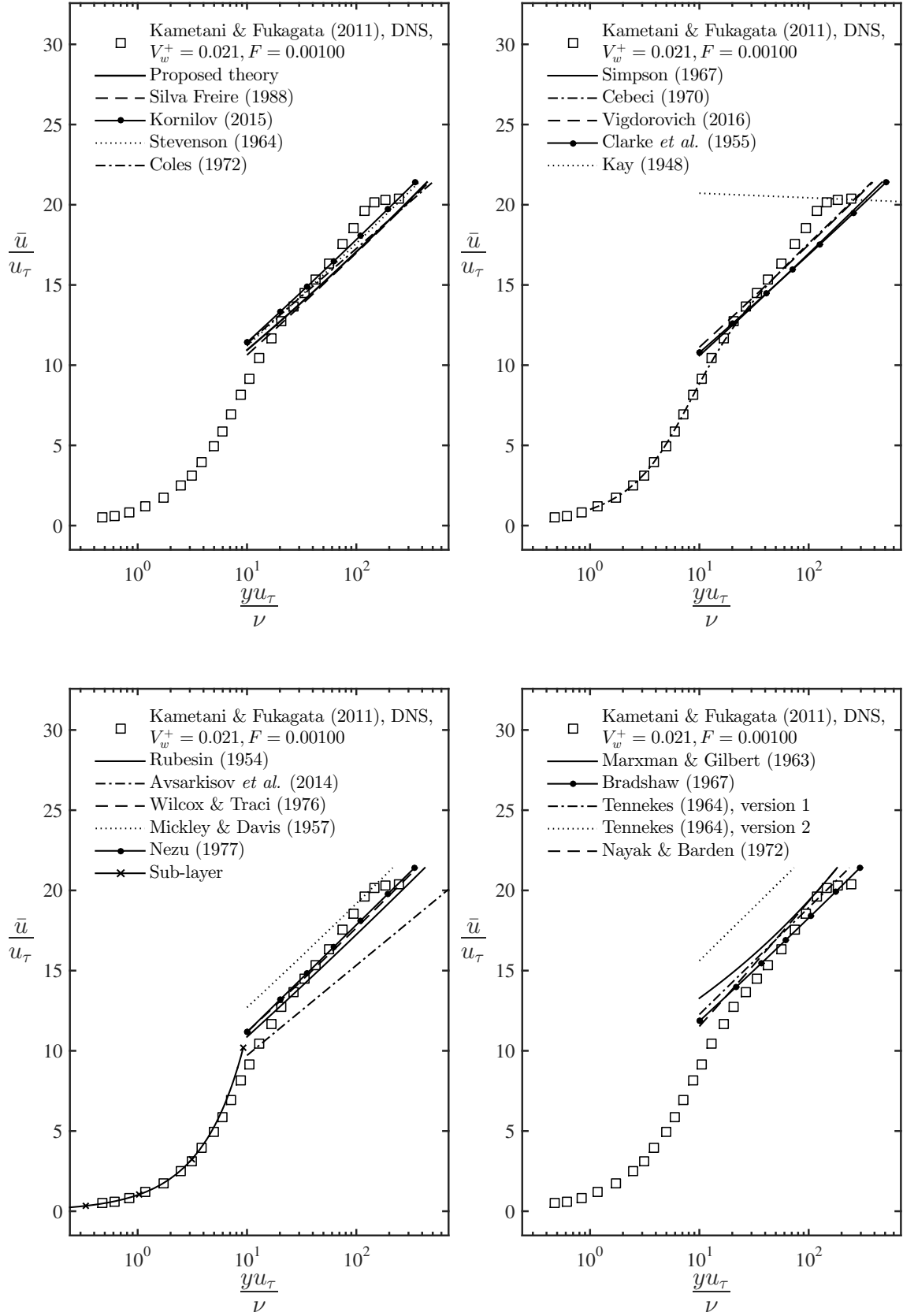


Figure B.26: Mean velocity profiles data compared to different formulations.

Boundary layer flow

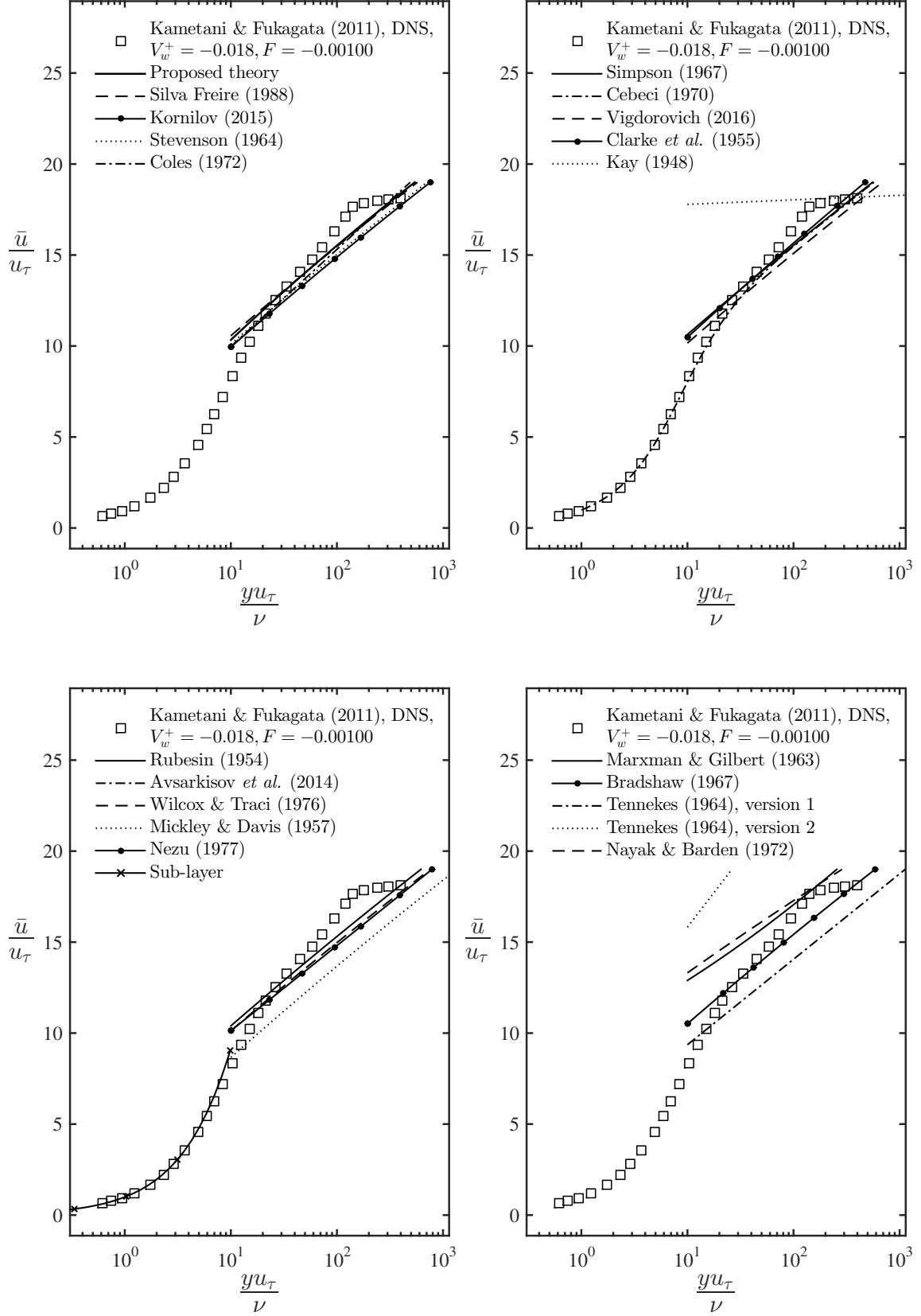


Figure B.27: Mean velocity profiles data compared to different formulations.

Boundary layer flow with blowing

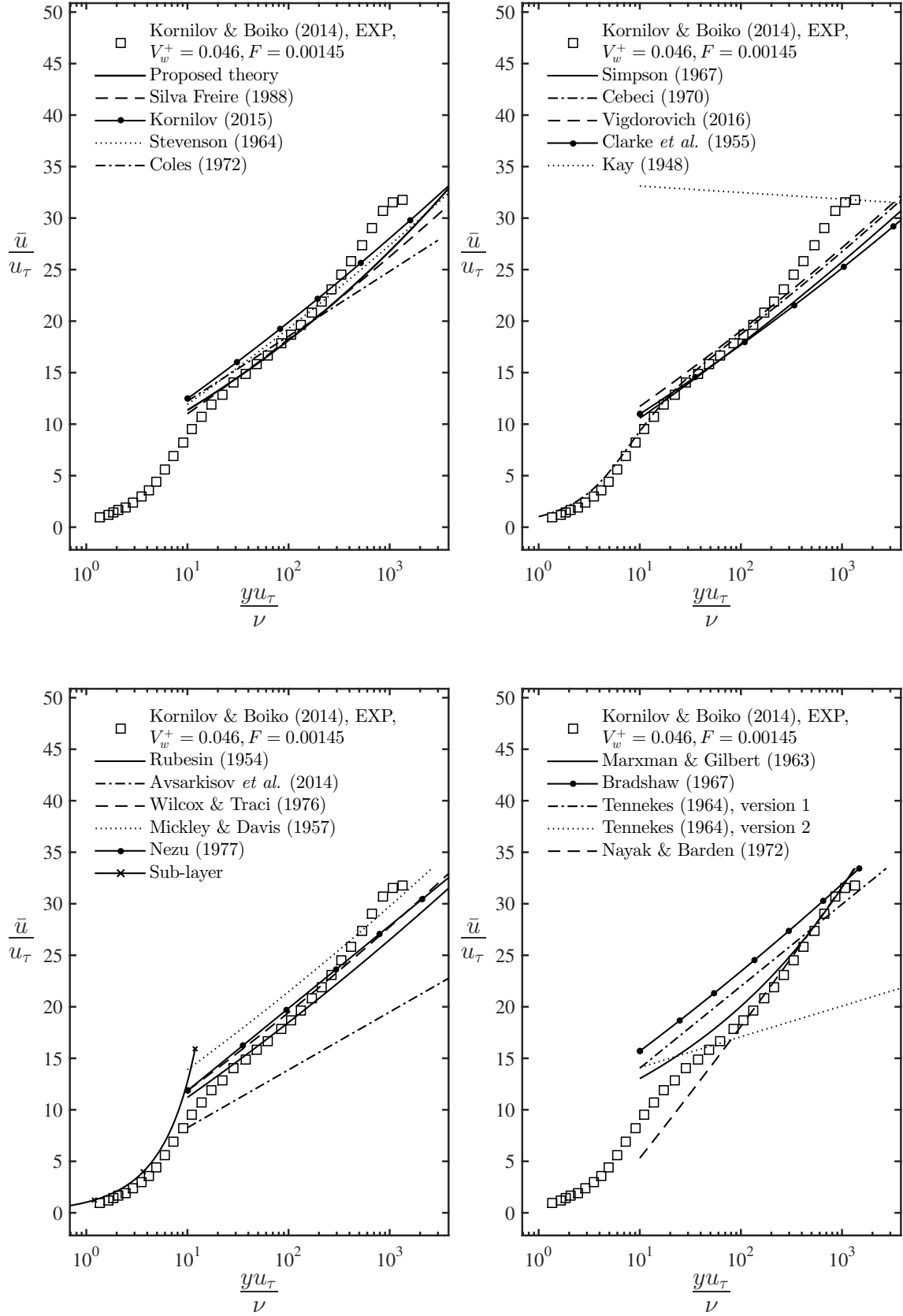


Figure B.28: Mean velocity profiles data compared to different formulations.

Boundary layer flow with blowing

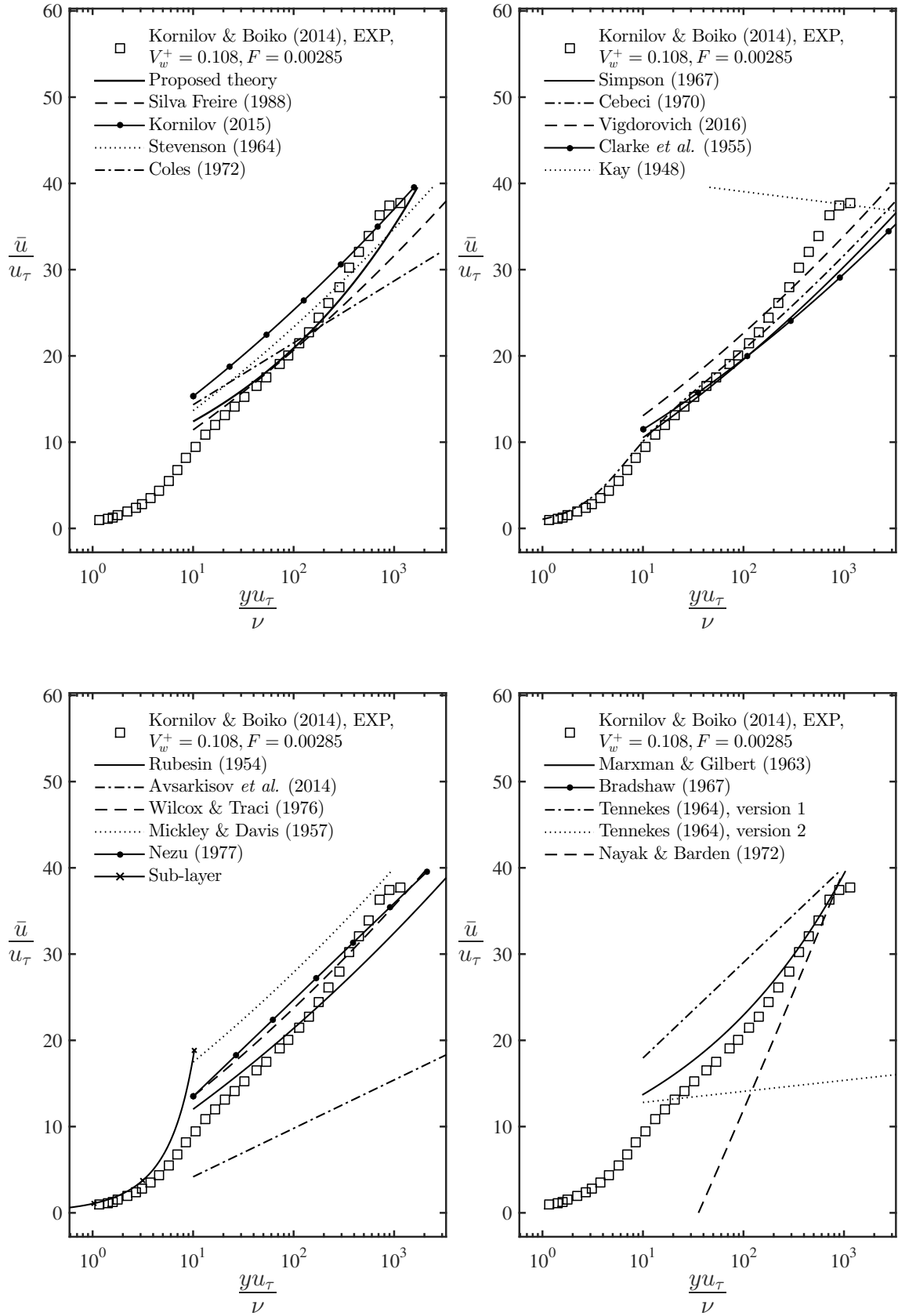


Figure B.29: Mean velocity profiles data compared to different formulations.

Boundary layer flow with blowing

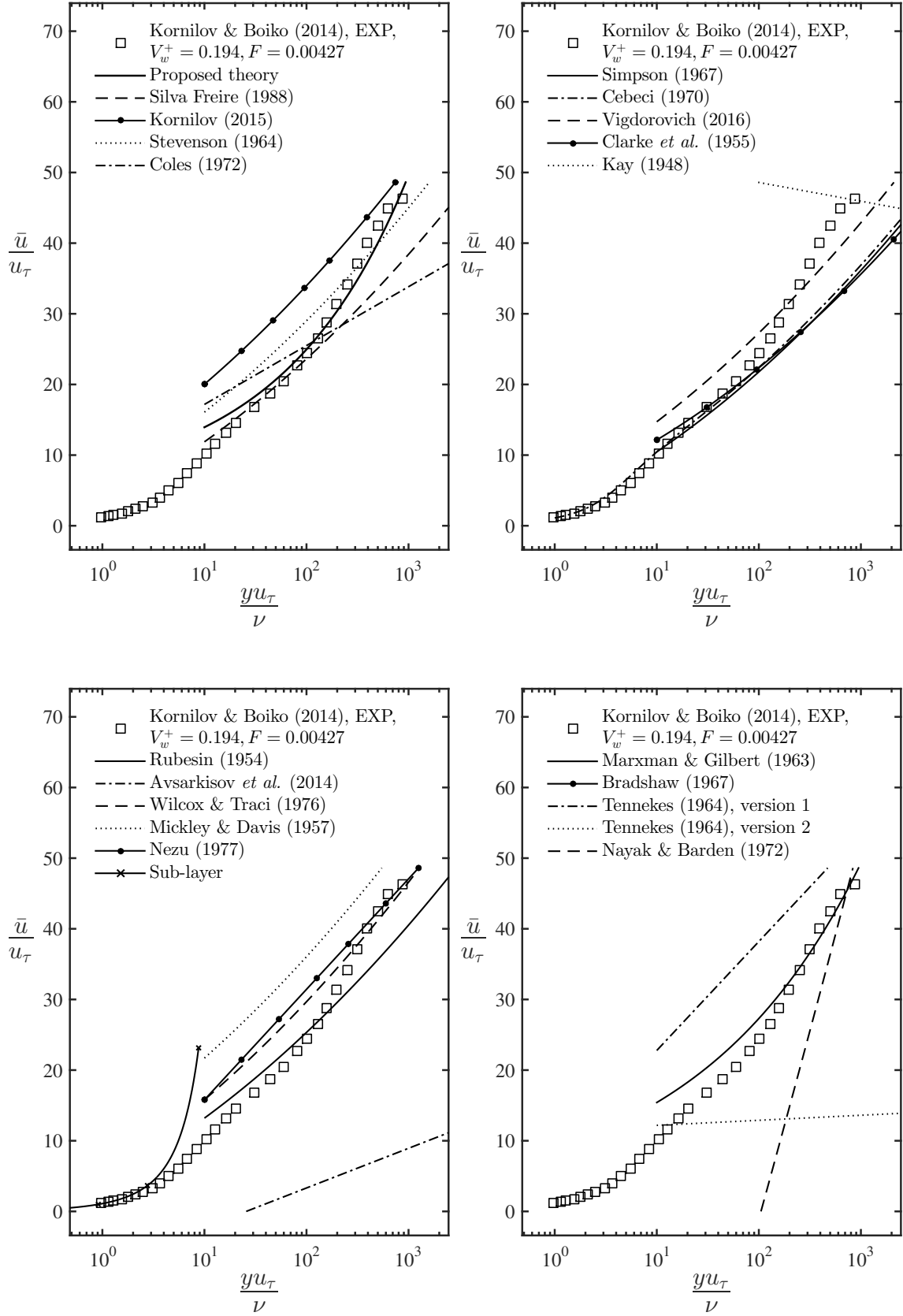


Figure B.30: Mean velocity profiles data compared to different formulations.

Boundary layer flow with blowing

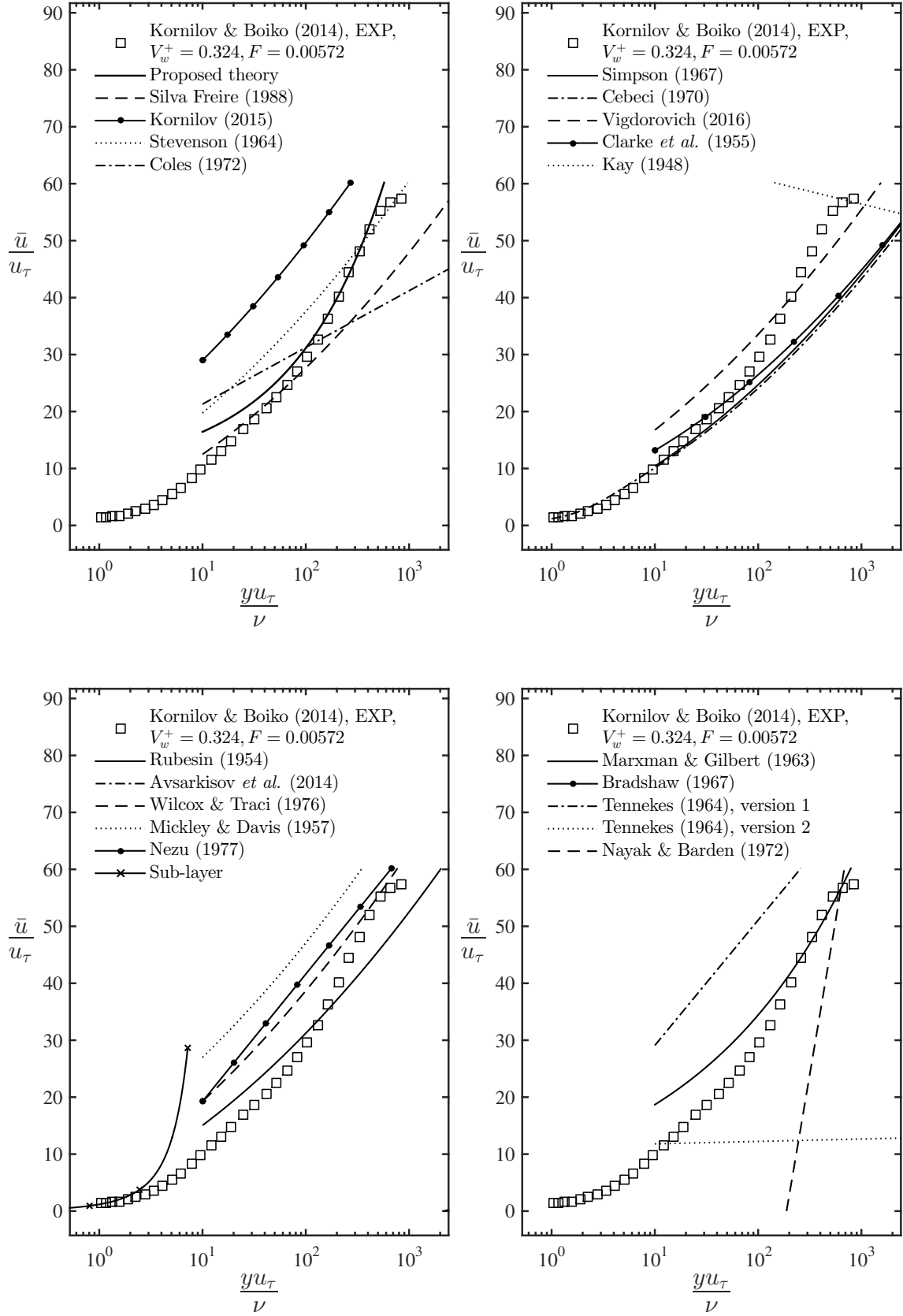


Figure B.31: Mean velocity profiles data compared to different formulations.

Boundary layer flow with blowing

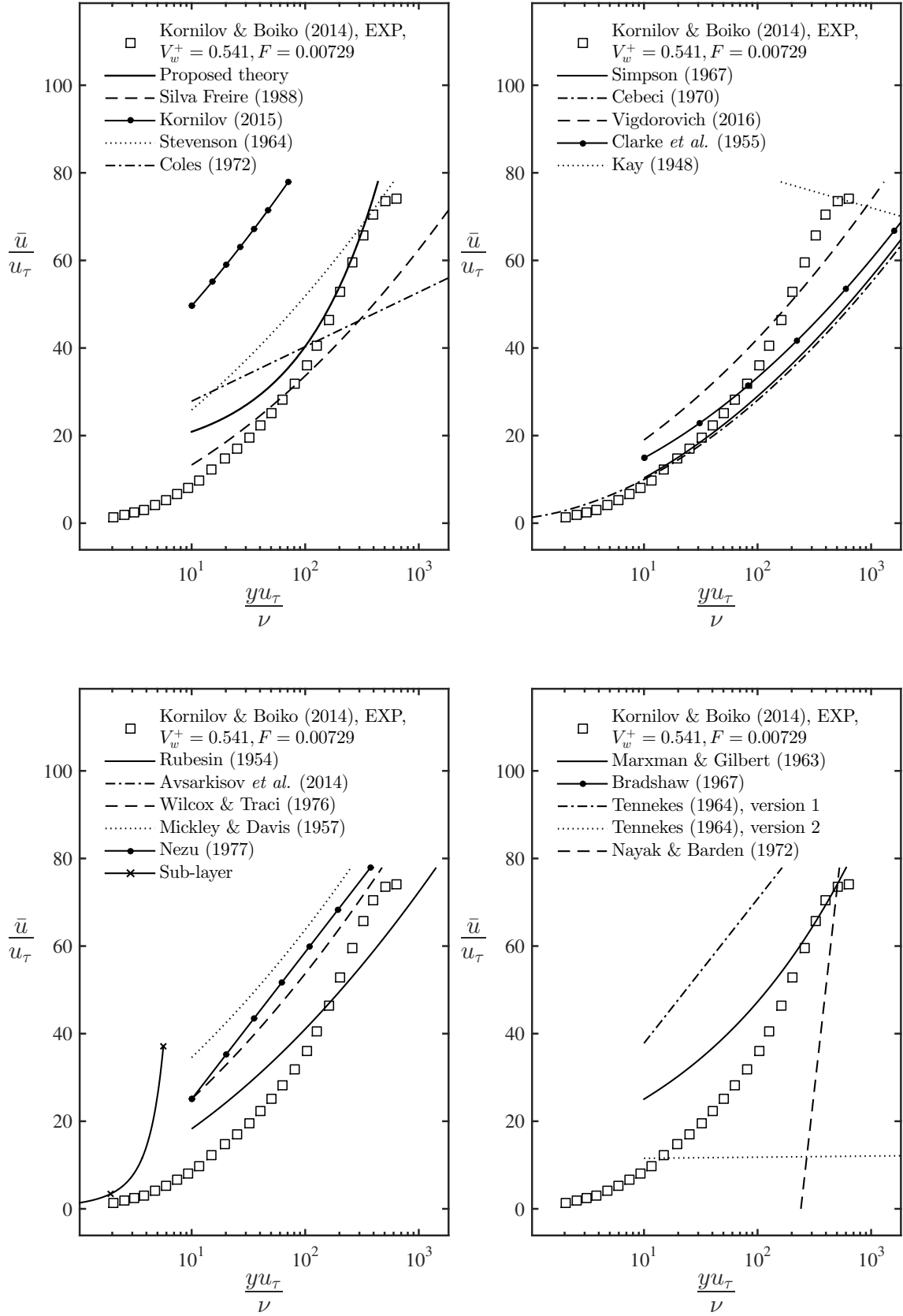


Figure B.32: Mean velocity profiles data compared to different formulations.

Boundary layer flow with blowing

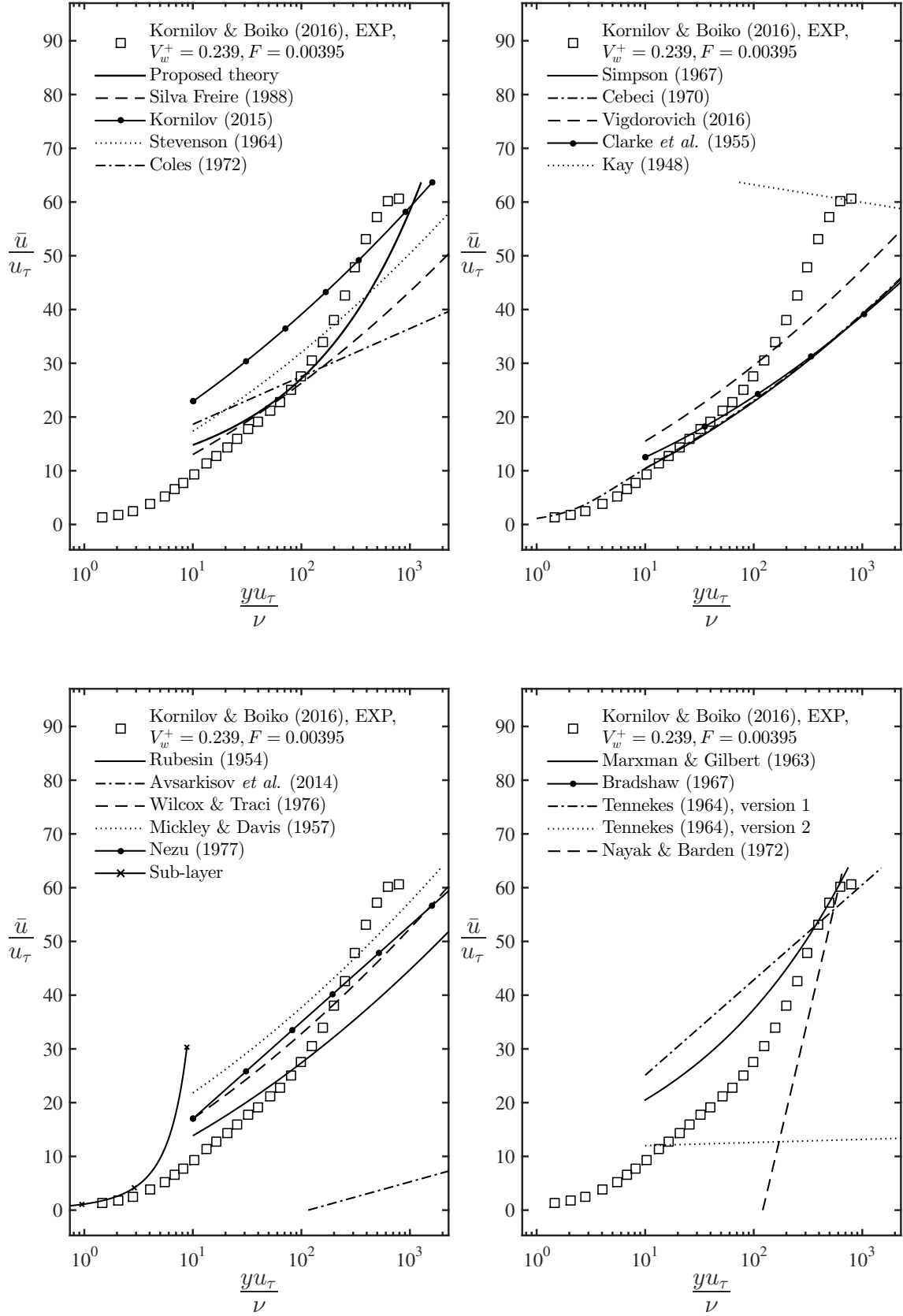


Figure B.33: Mean velocity profiles data compared to different formulations.

Open channel flow

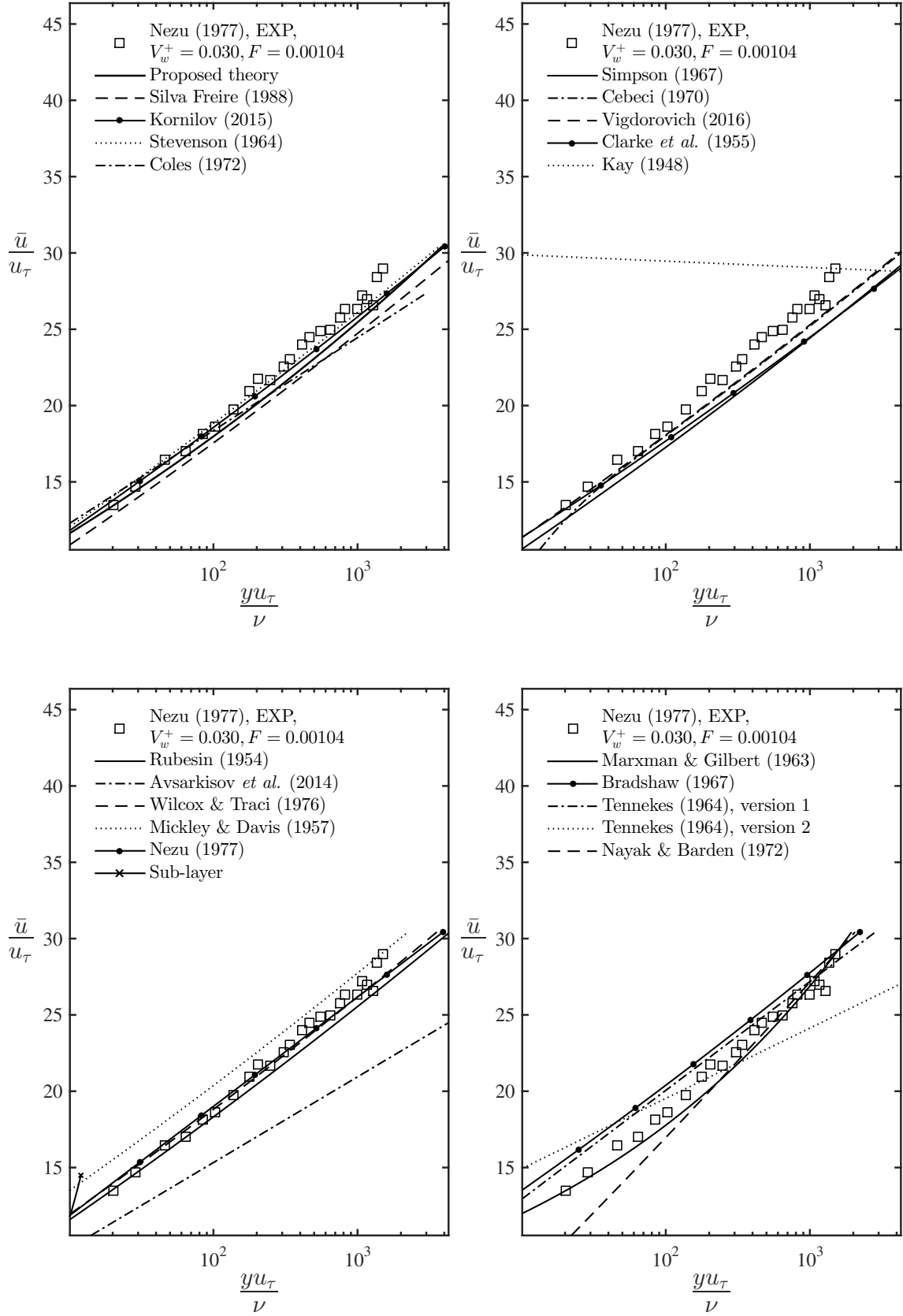


Figure B.34: Mean velocity profiles data compared to different formulations.

Open channel flow

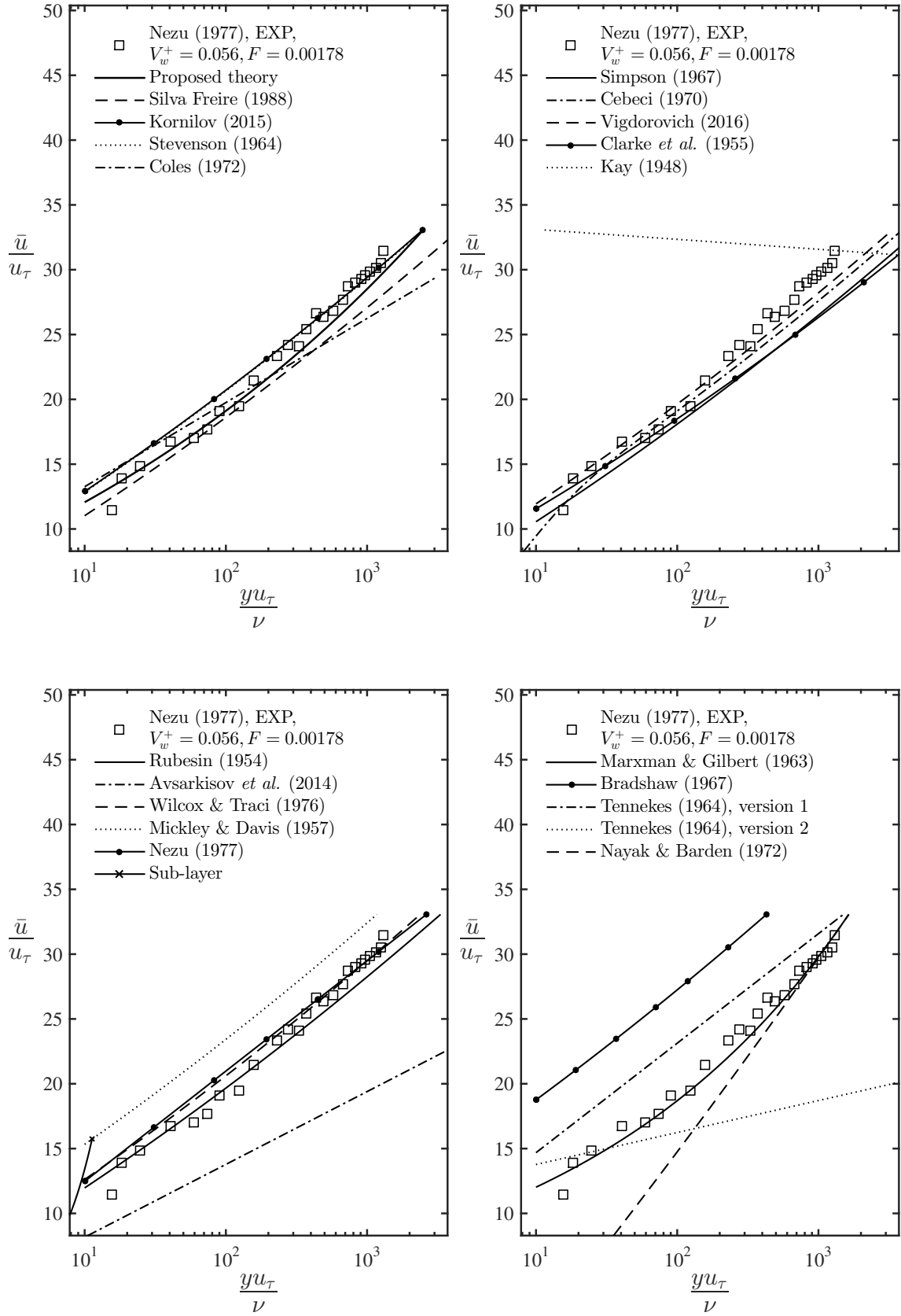


Figure B.35: Mean velocity profiles data compared to different formulations.

Open channel flow

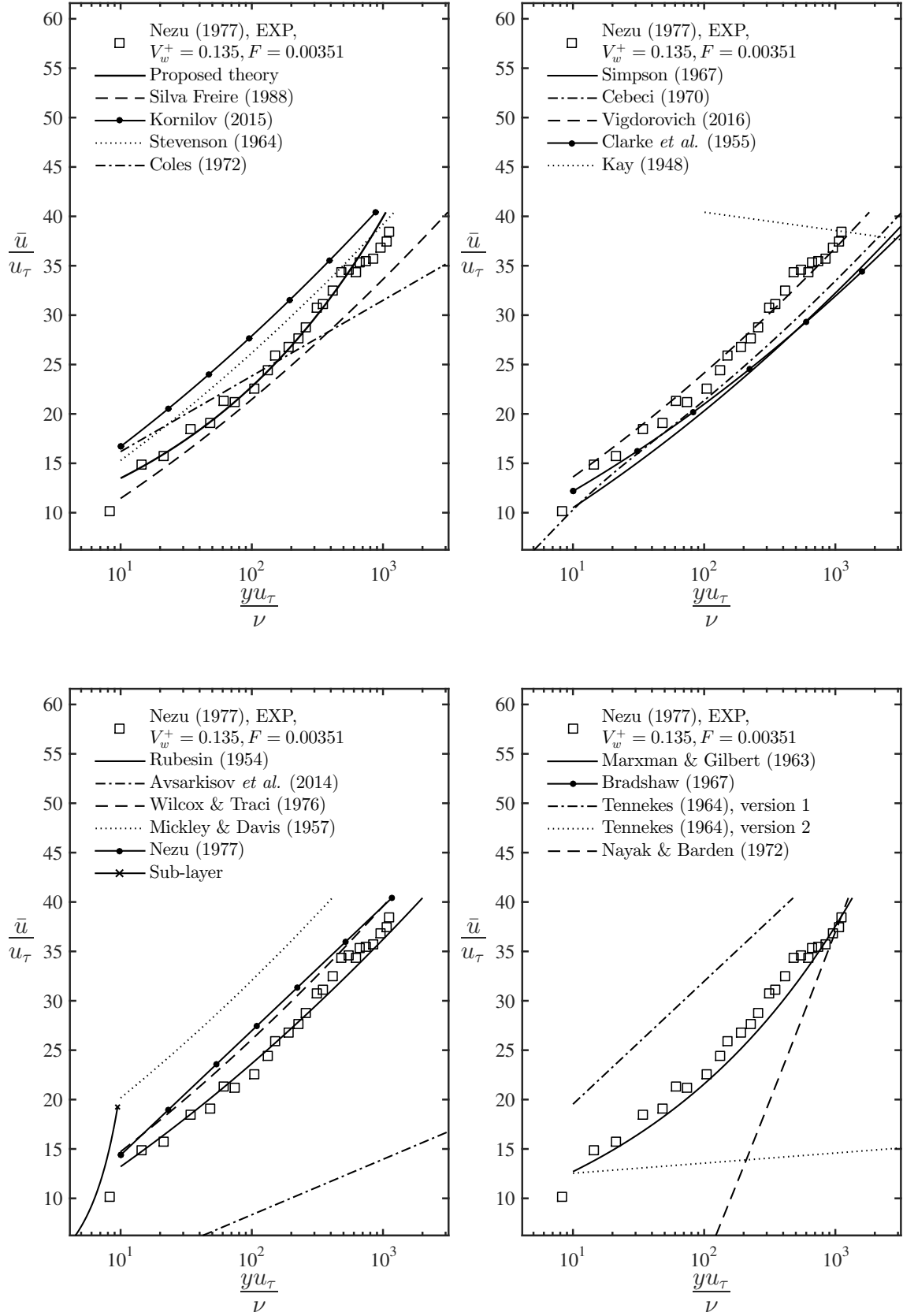


Figure B.36: Mean velocity profiles data compared to different formulations.

Open channel flow

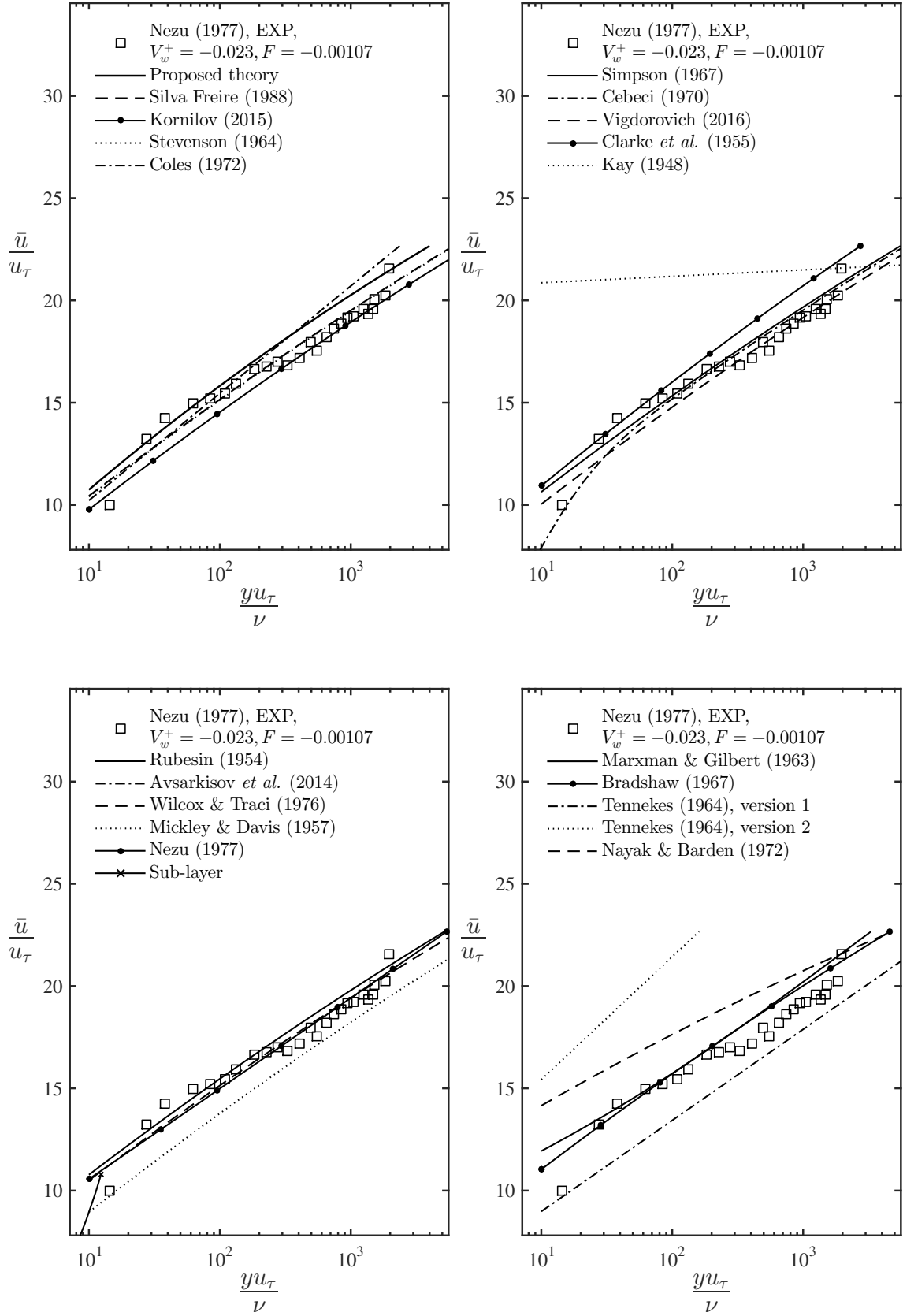


Figure B.37: Mean velocity profiles data compared to different formulations.

Open channel flow

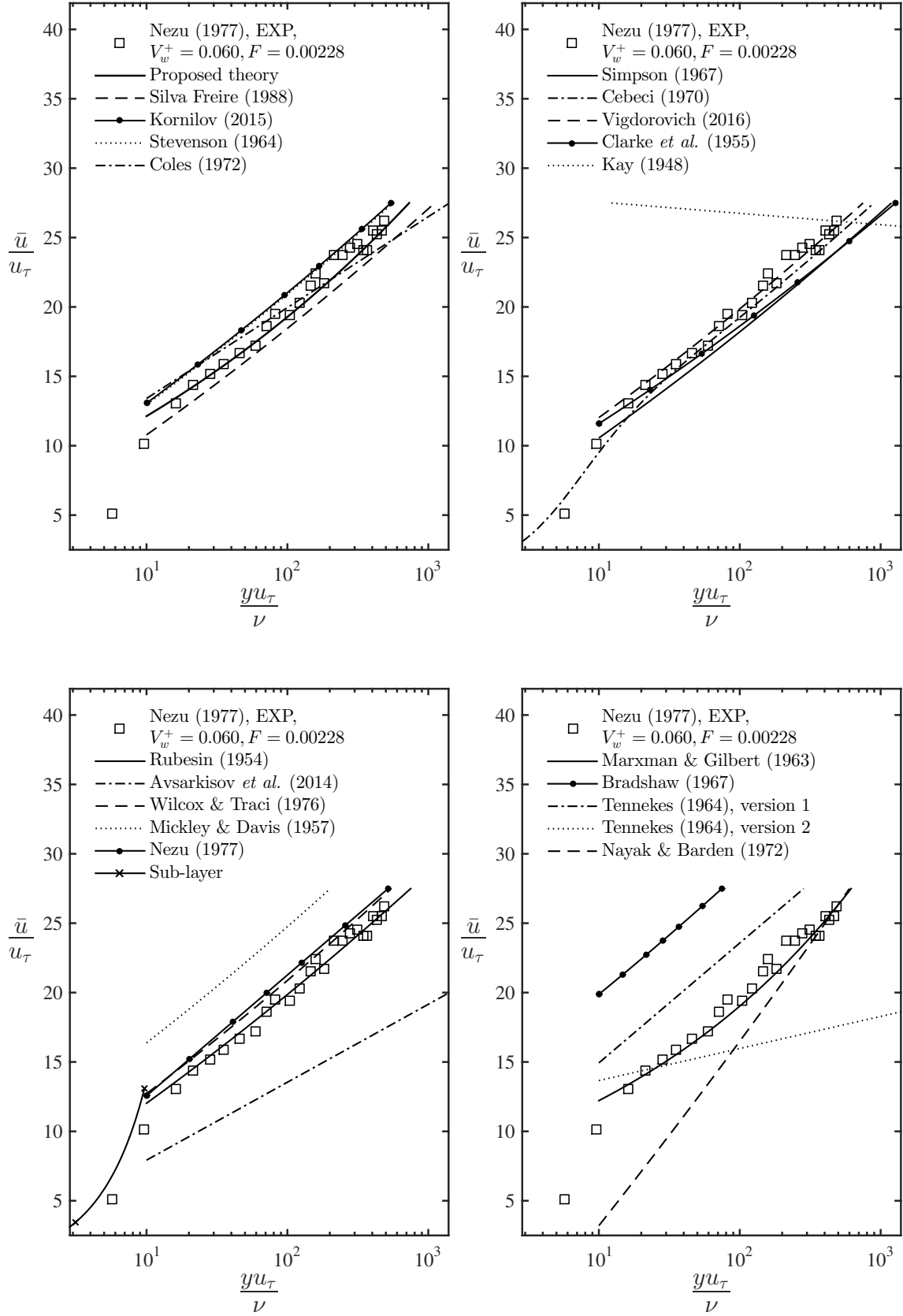


Figure B.38: Mean velocity profiles data compared to different formulations.

Open channel flow

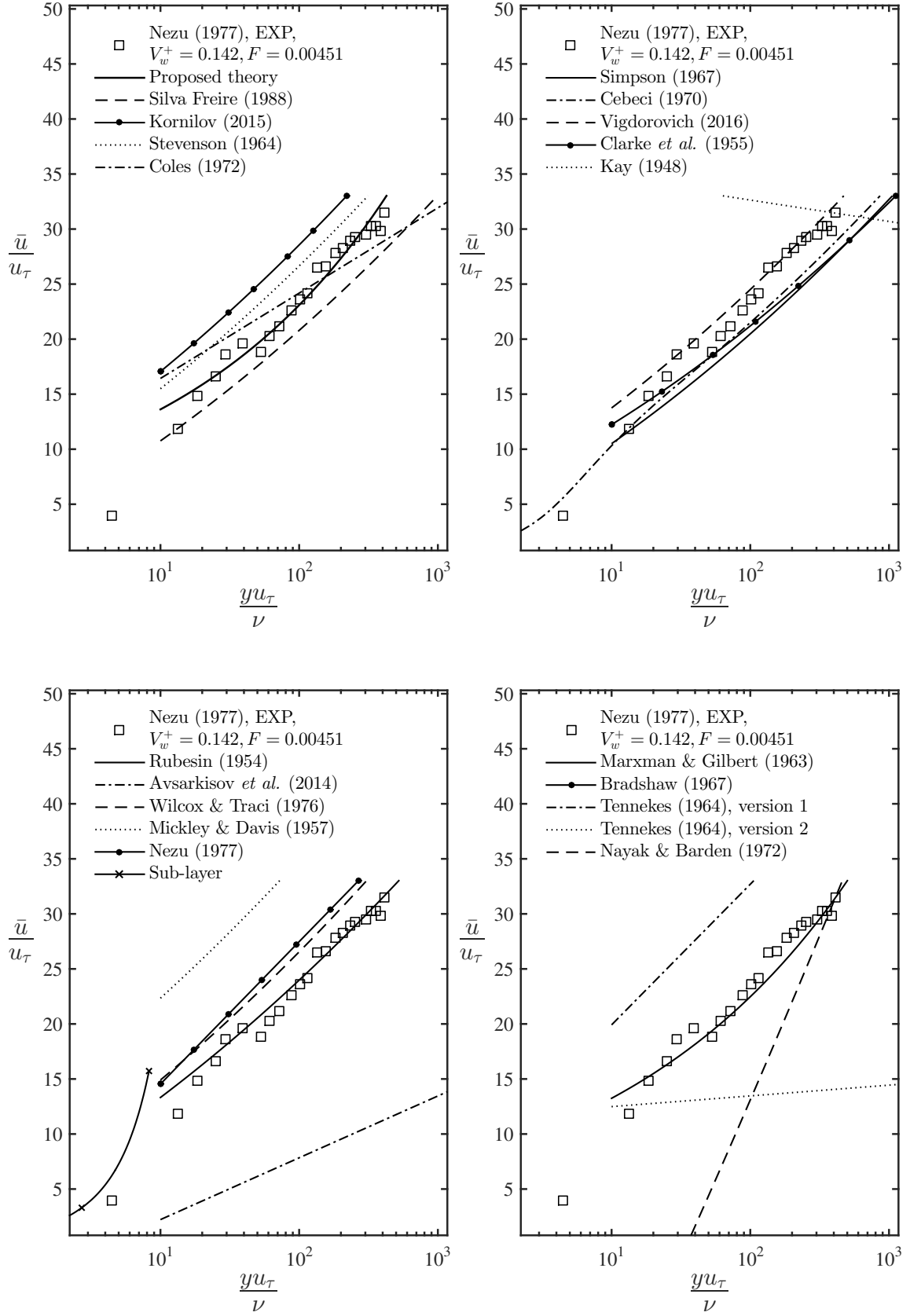


Figure B.39: Mean velocity profiles data compared to different formulations.

Channel flow at the wall with blowing

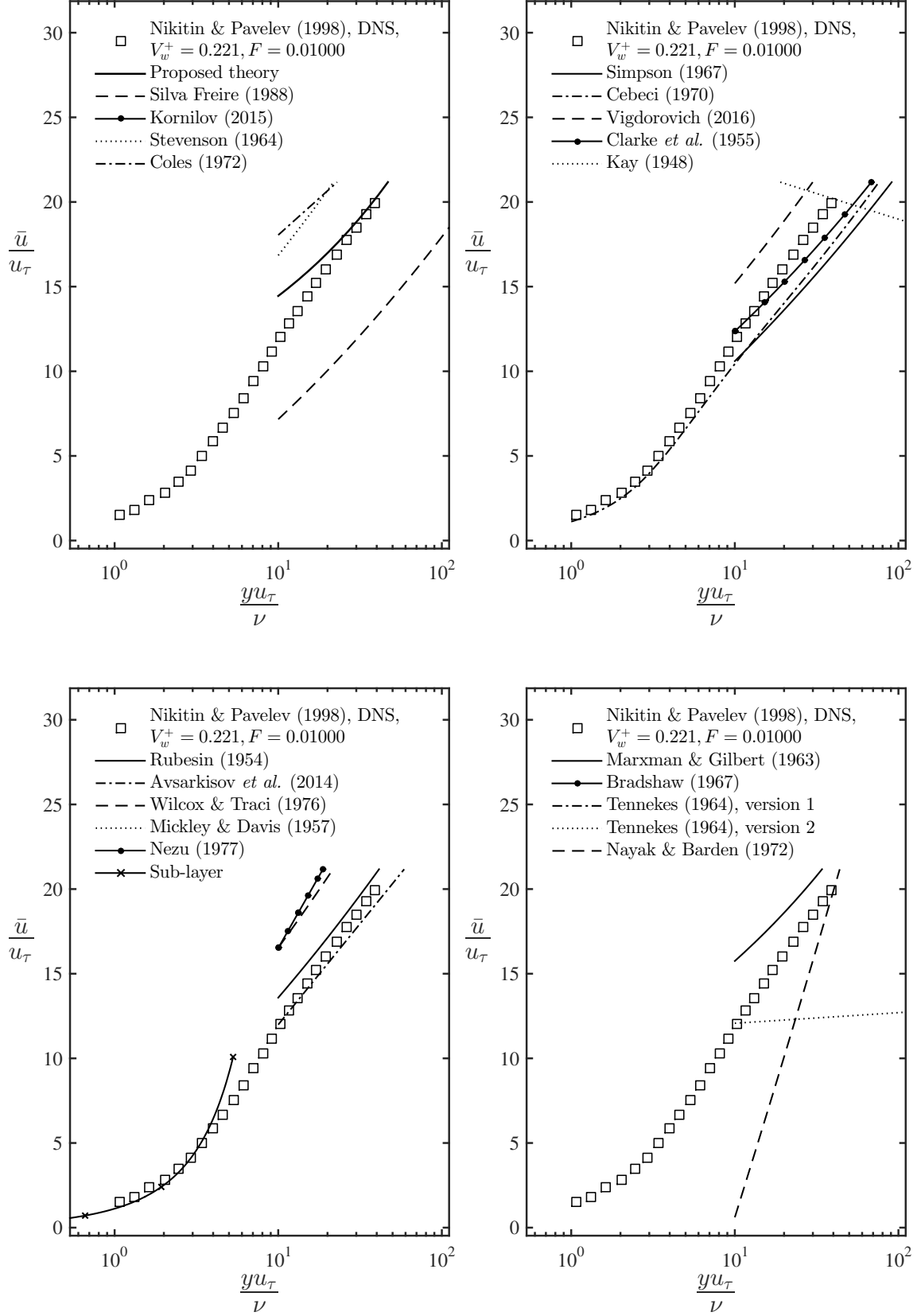


Figure B.40: Mean velocity profiles data compared to different formulations.

Channel flow at the wall with blowing

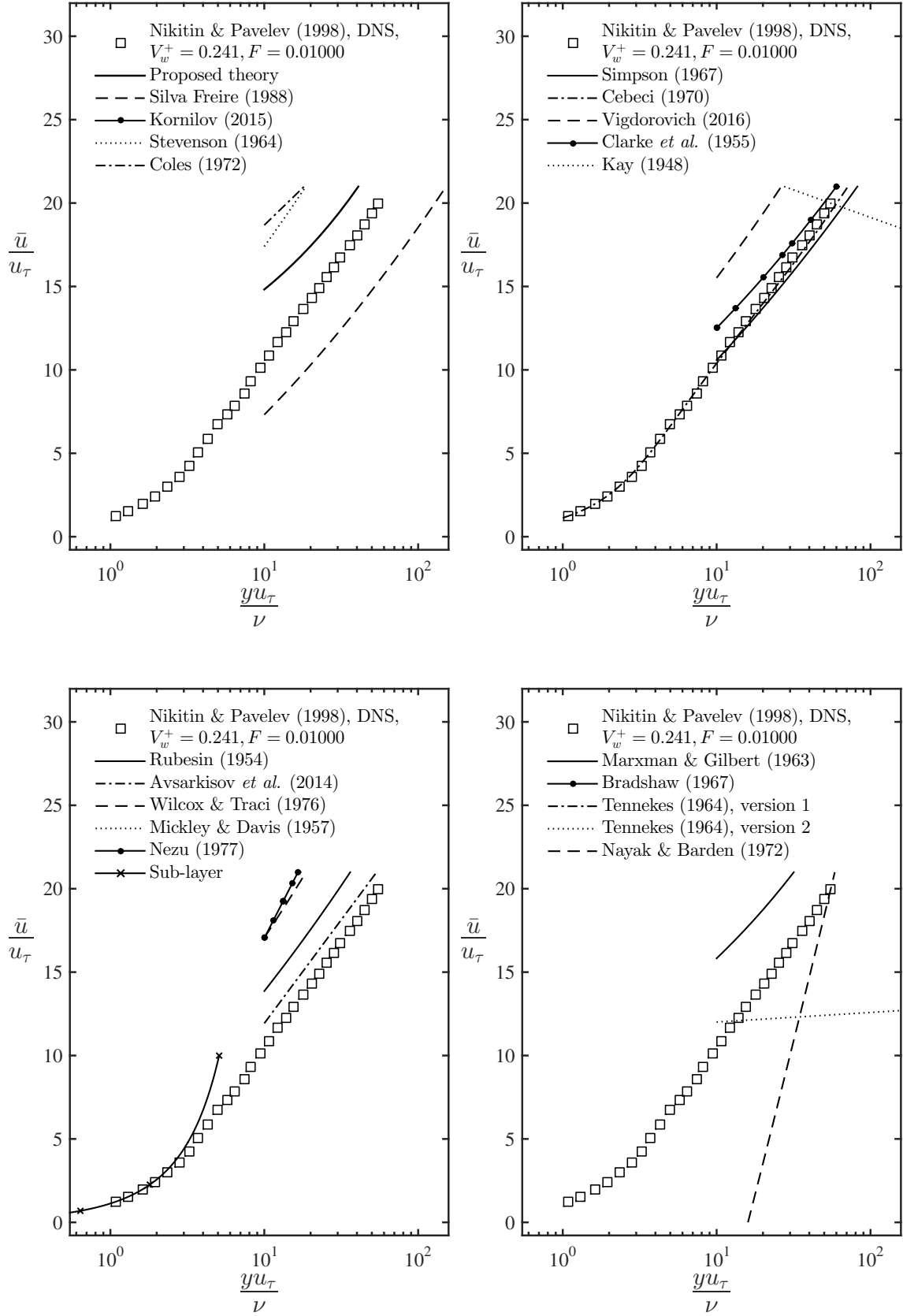


Figure B.41: Mean velocity profiles data compared to different formulations.

Channel flow at the wall with blowing

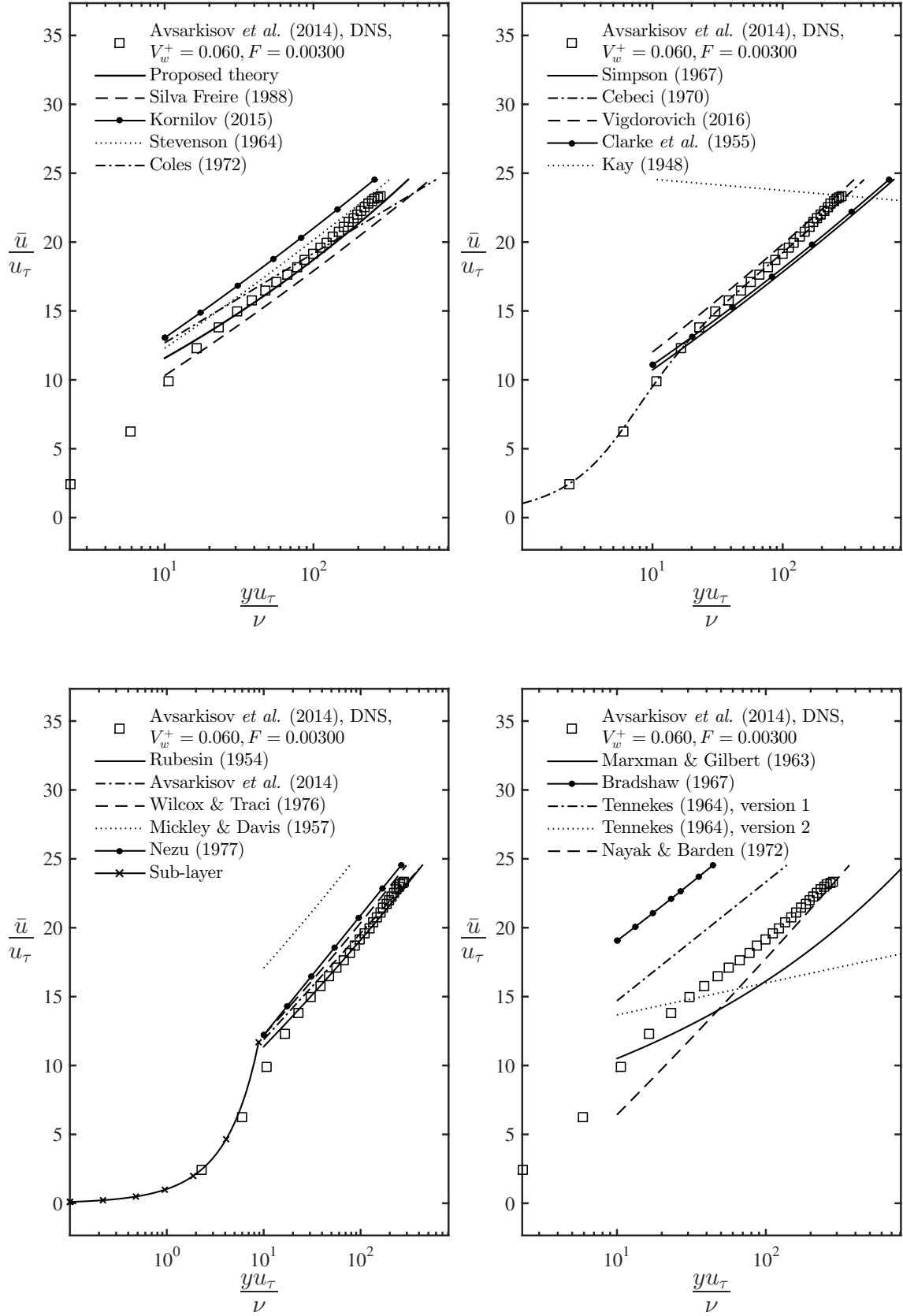


Figure B.42: Mean velocity profiles data compared to different formulations.

Channel flow at the wall with blowing

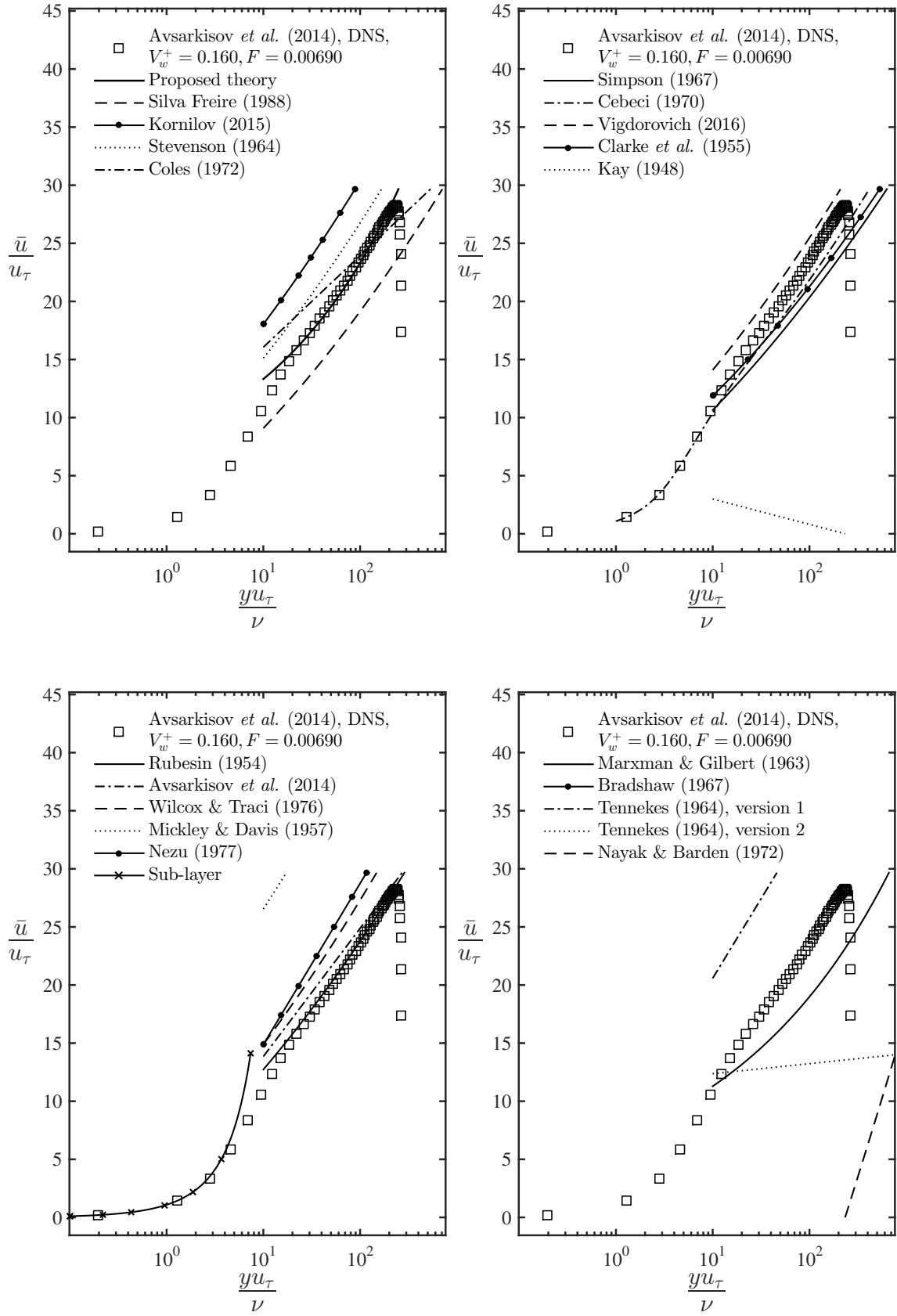


Figure B.43: Mean velocity profiles data compared to different formulations.

Channel flow at the wall with blowing

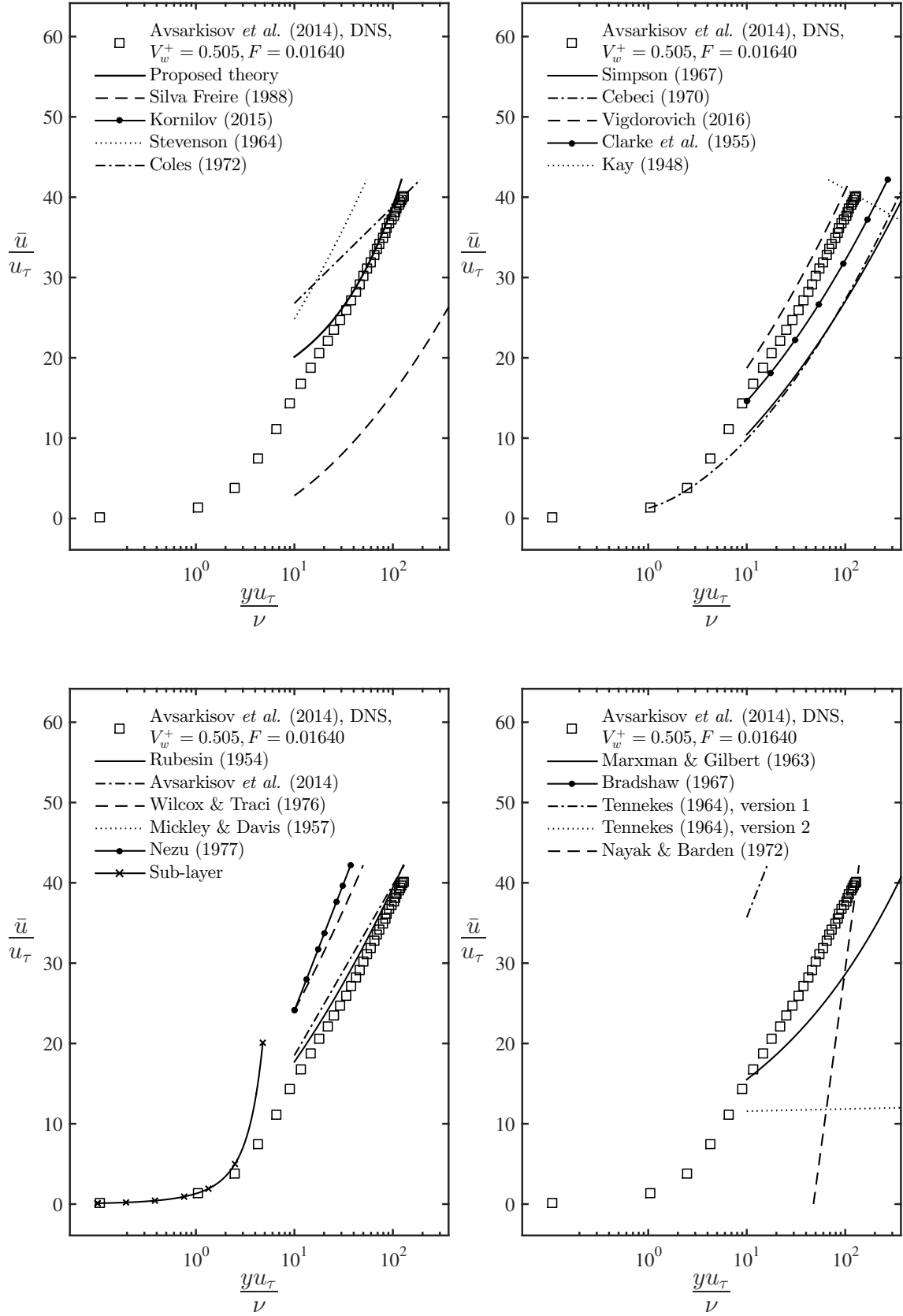


Figure B.44: Mean velocity profiles data compared to different formulations.

Channel flow at the wall with blowing

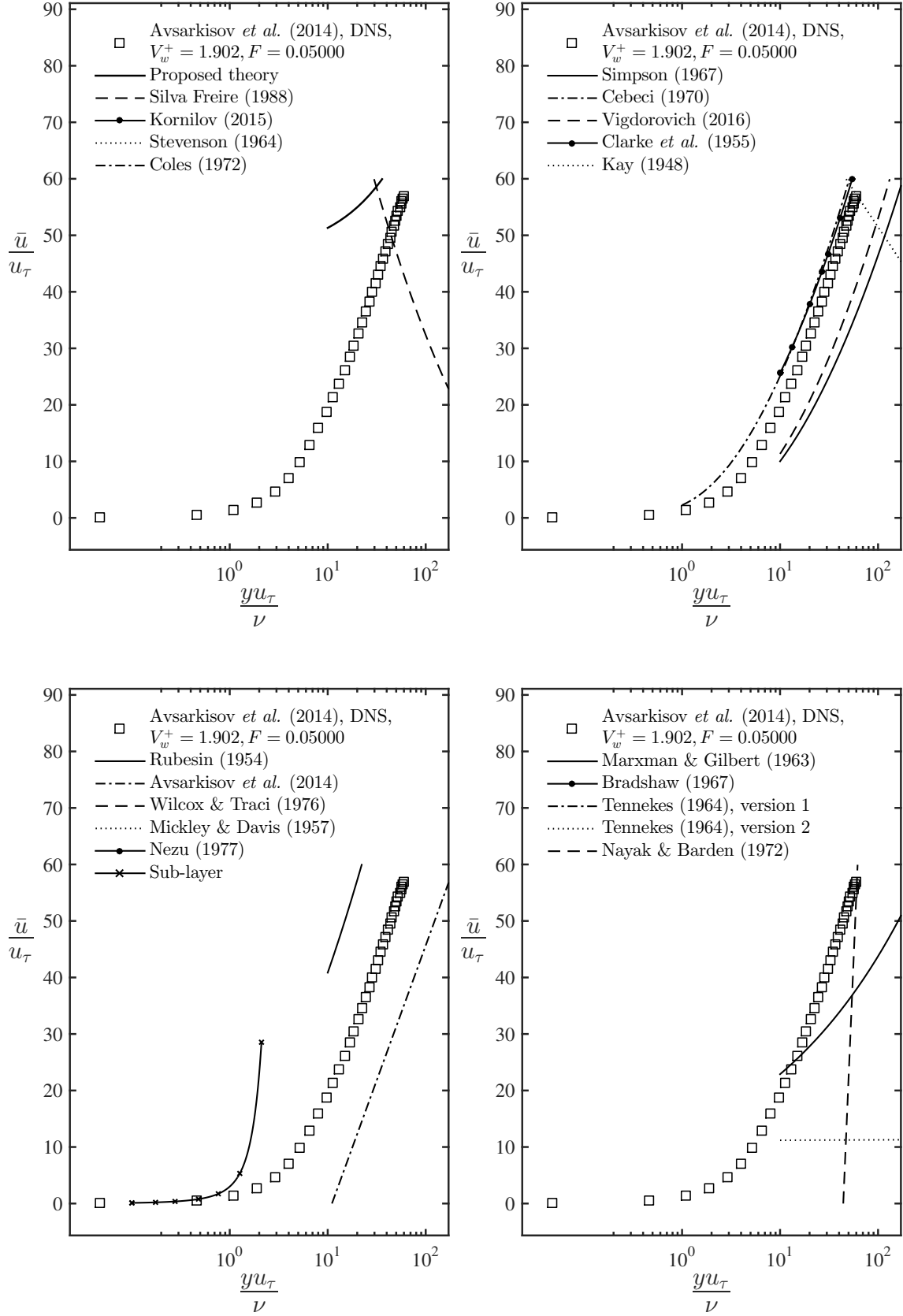


Figure B.45: Mean velocity profiles data compared to different formulations.

Channel flow at the wall with blowing

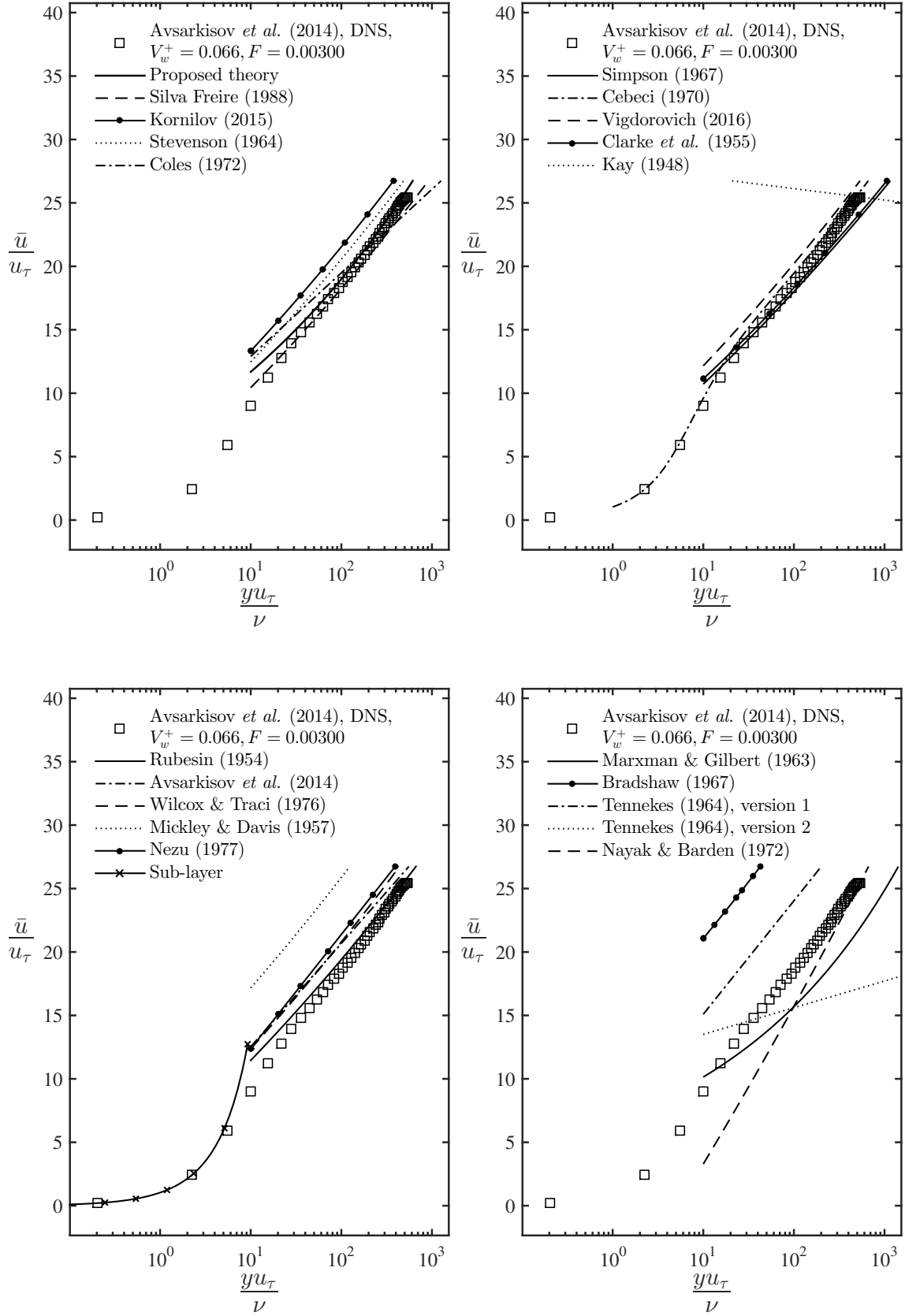


Figure B.46: Mean velocity profiles data compared to different formulations.

Channel flow at the wall with blowing

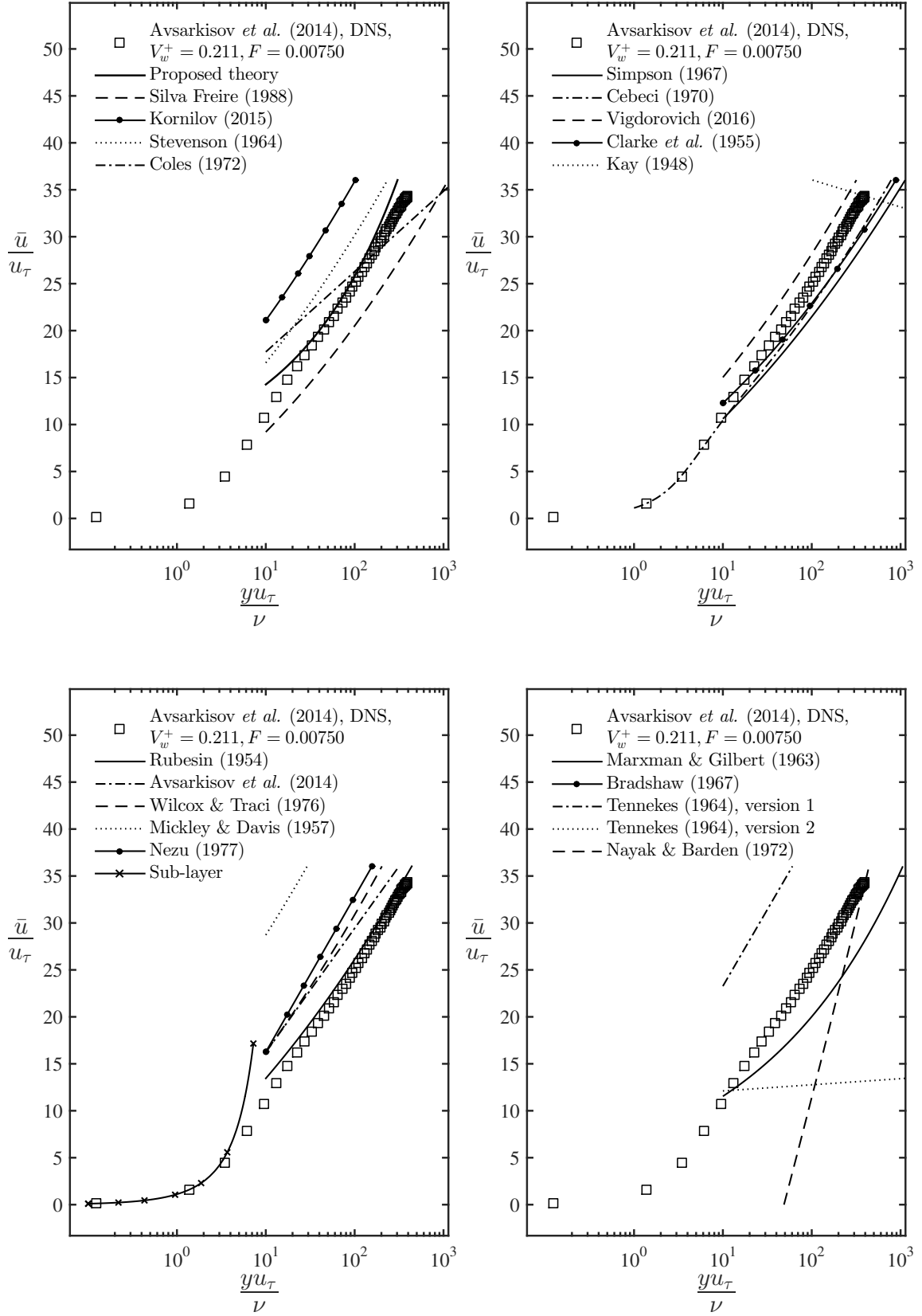


Figure B.47: Mean velocity profiles data compared to different formulations.

Channel flow at the wall with blowing

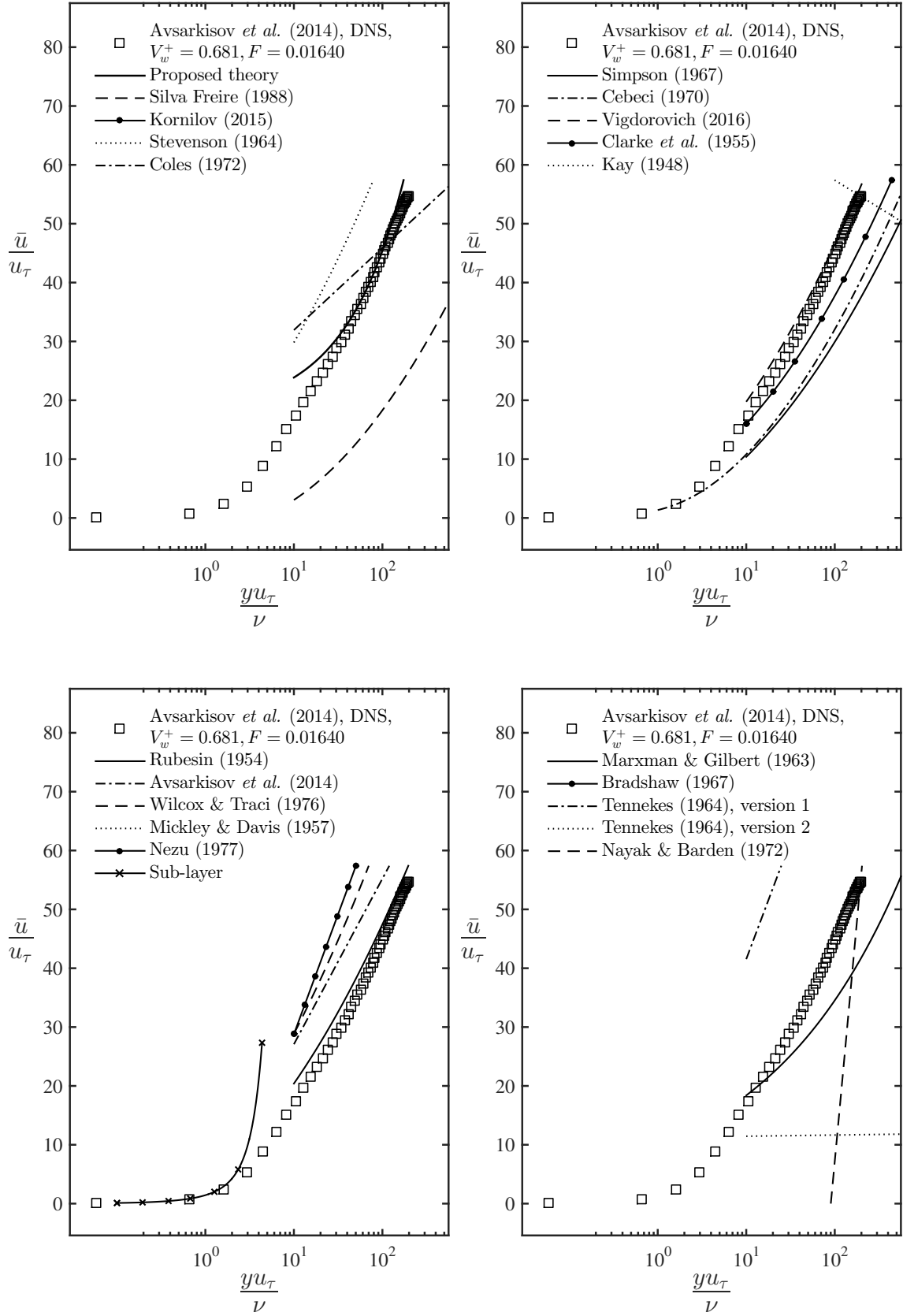


Figure B.48: Mean velocity profiles data compared to different formulations.

Channel flow at the wall with blowing

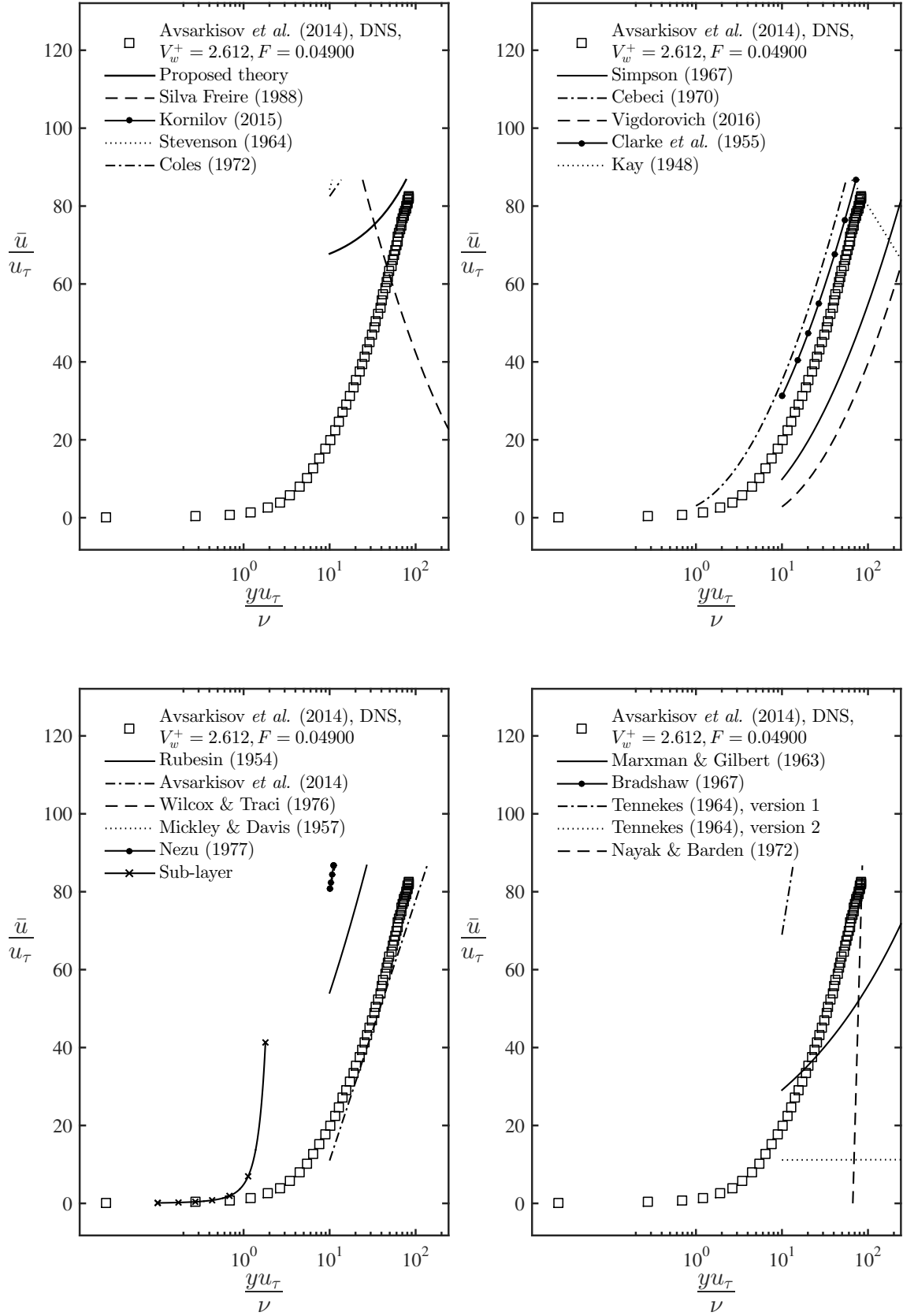


Figure B.49: Mean velocity profiles data compared to different formulations.

Channel flow at the wall with blowing

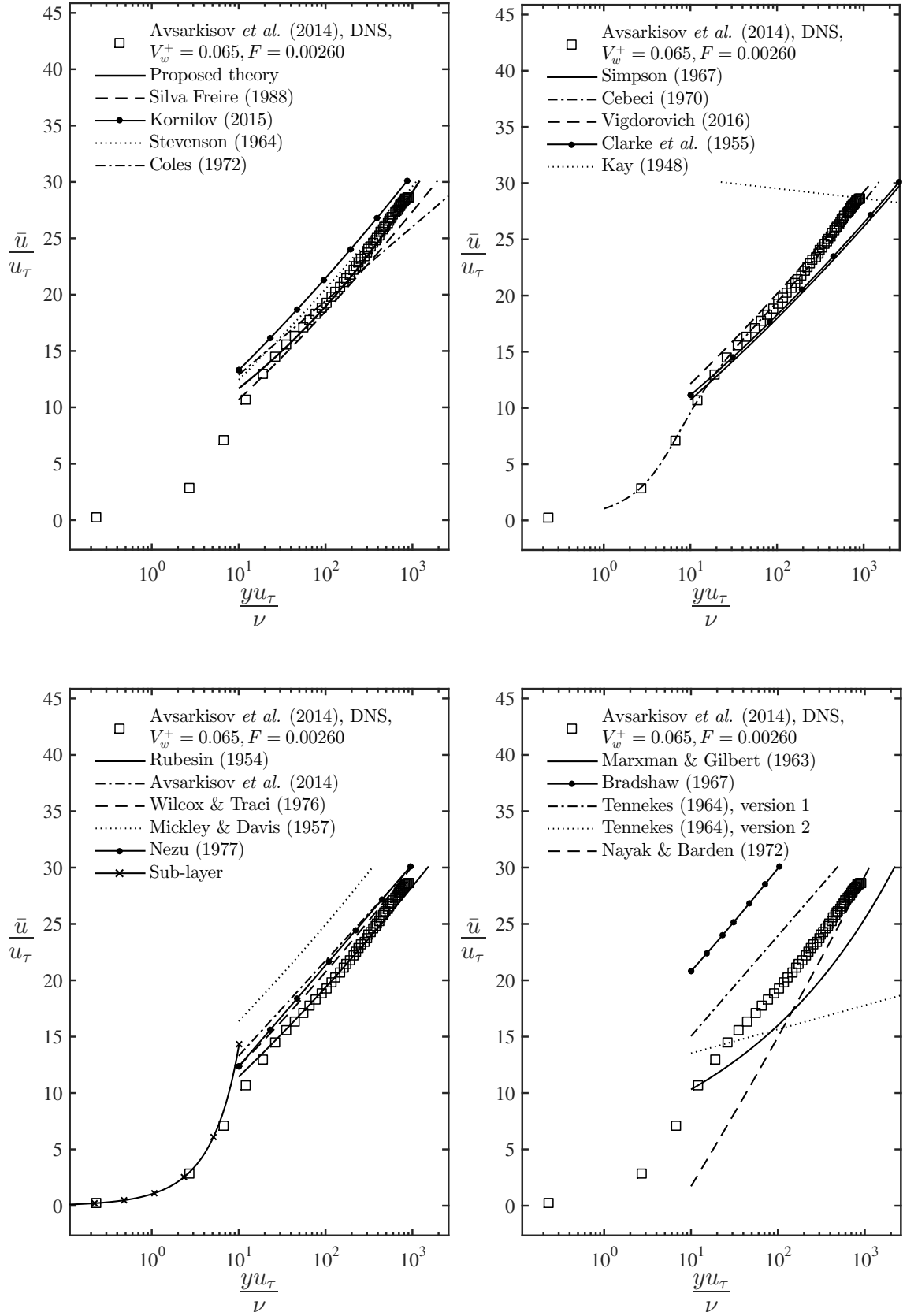


Figure B.50: Mean velocity profiles data compared to different formulations.

Channel flow at the wall with blowing

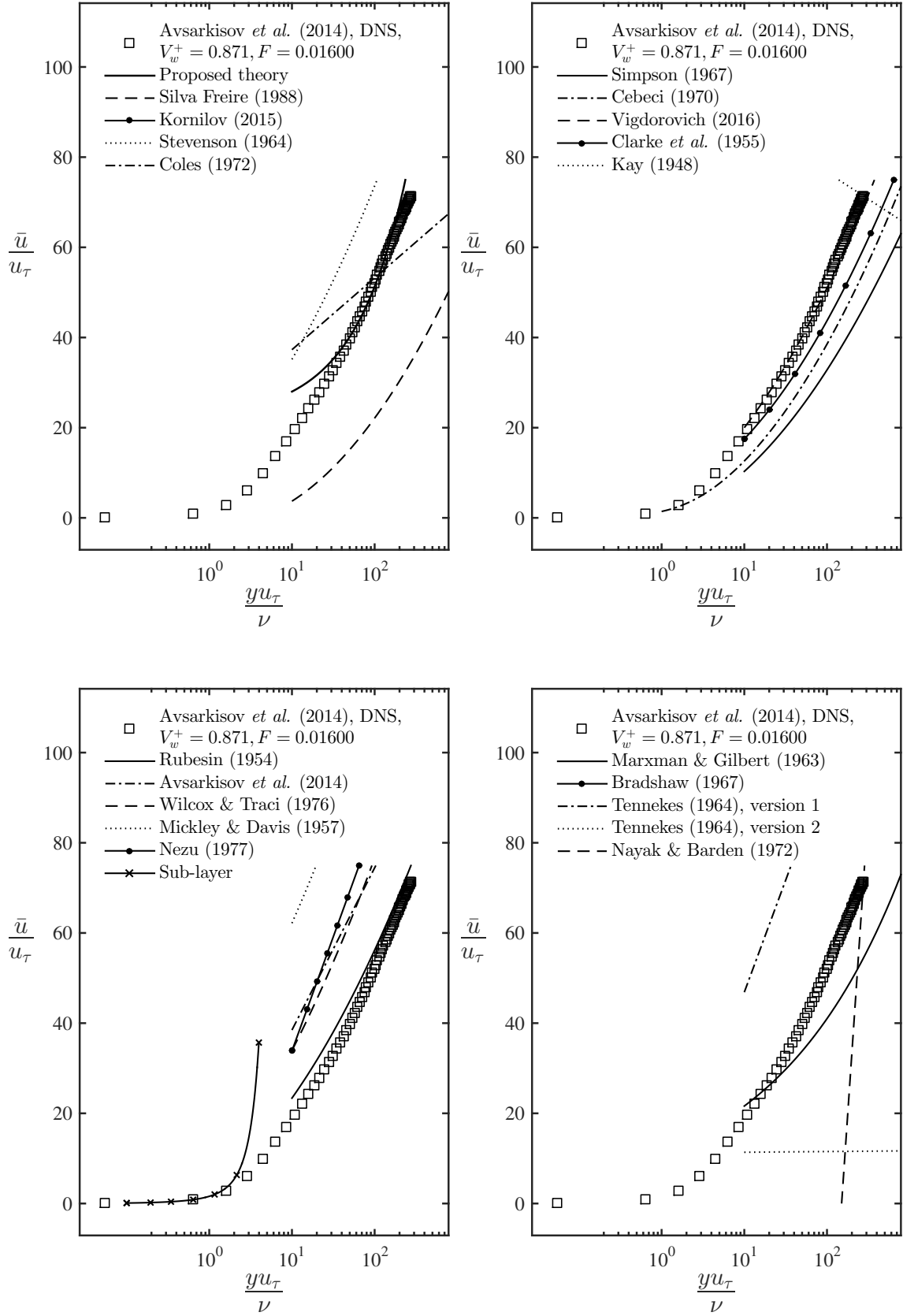


Figure B.51: Mean velocity profiles data compared to different formulations.

Boundary layer flow with blowing

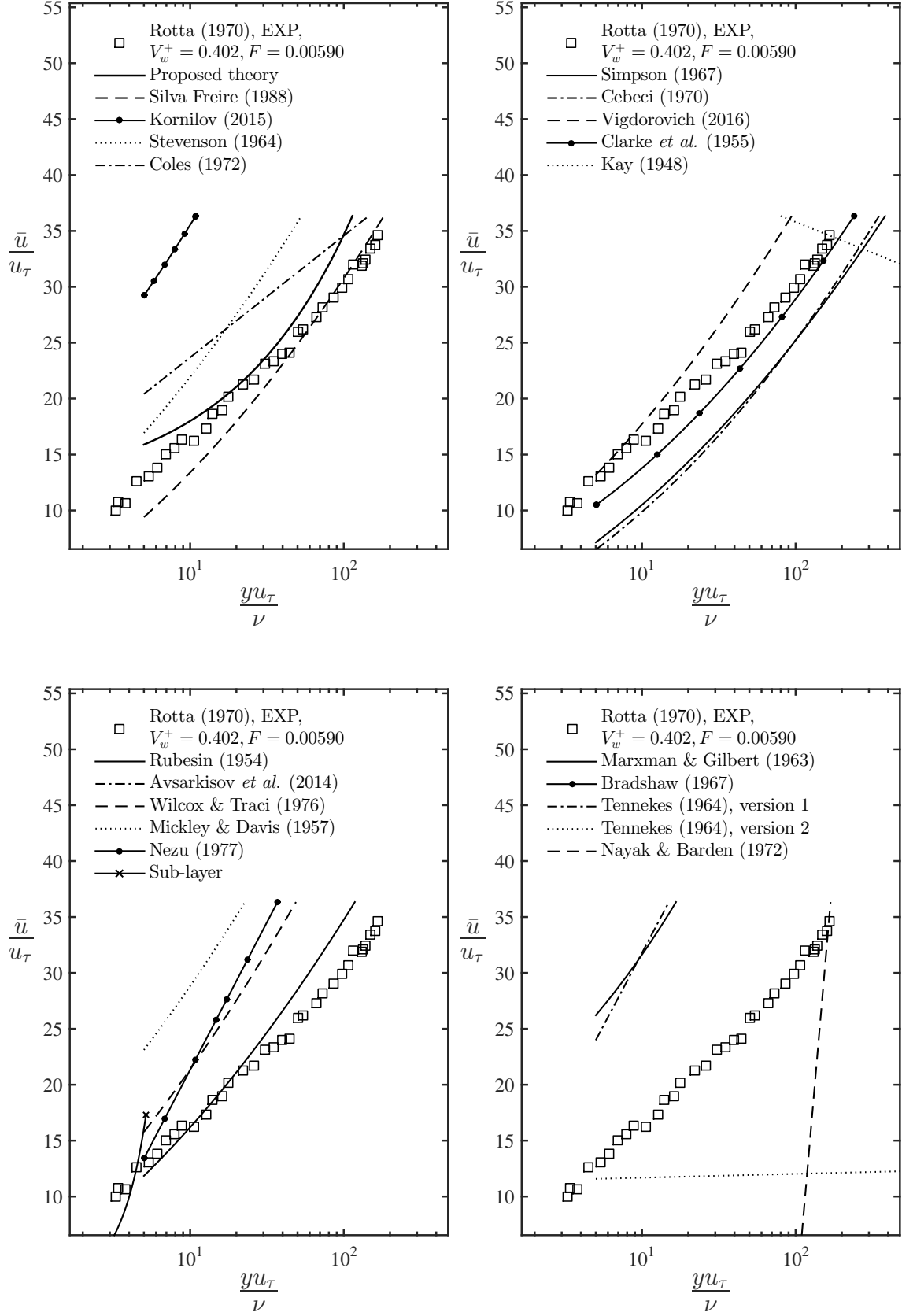


Figure B.52: Mean velocity profiles data compared to different formulations.

Boundary layer flow with blowing

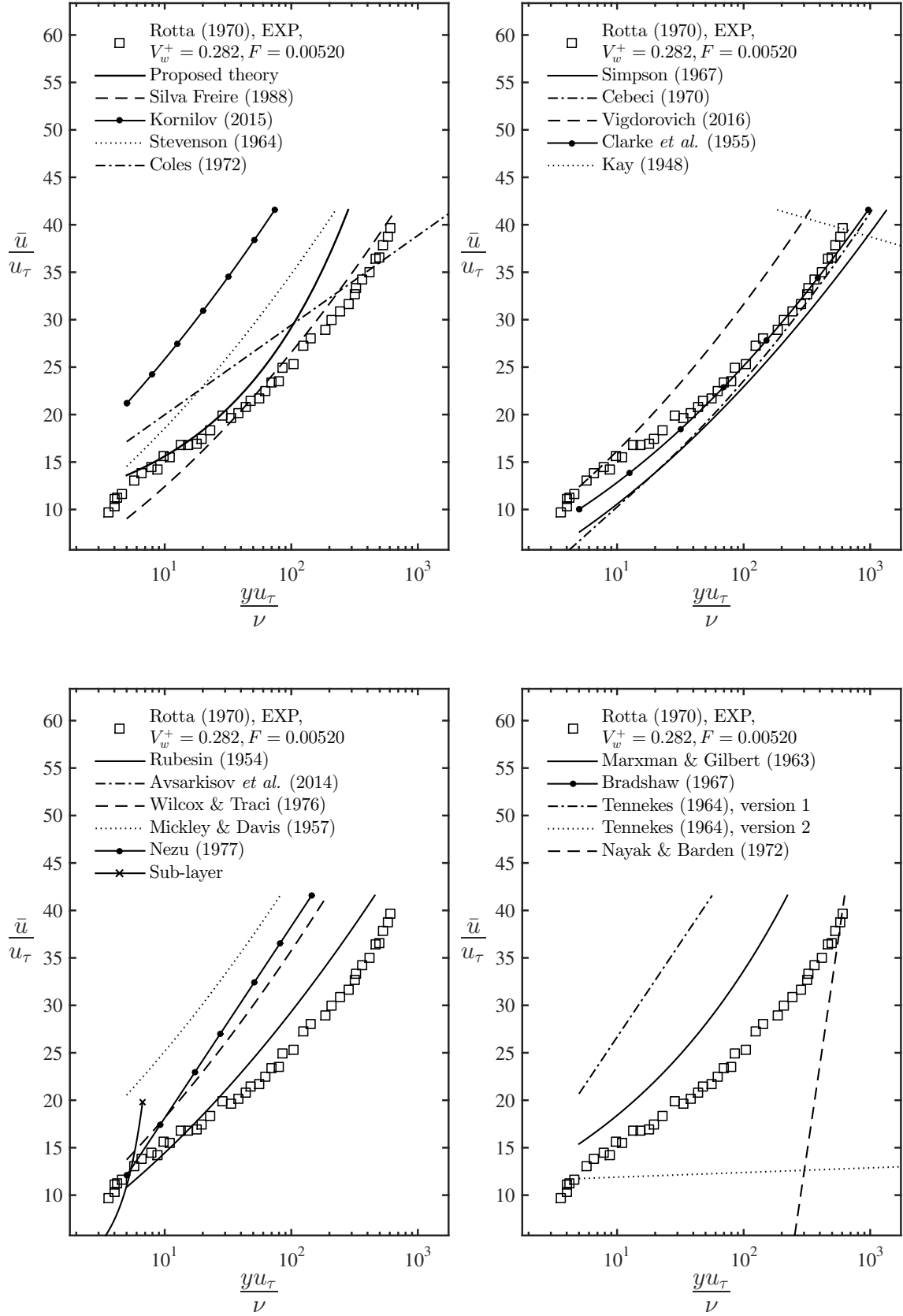


Figure B.53: Mean velocity profiles data compared to different formulations.

Boundary layer flow with blowing

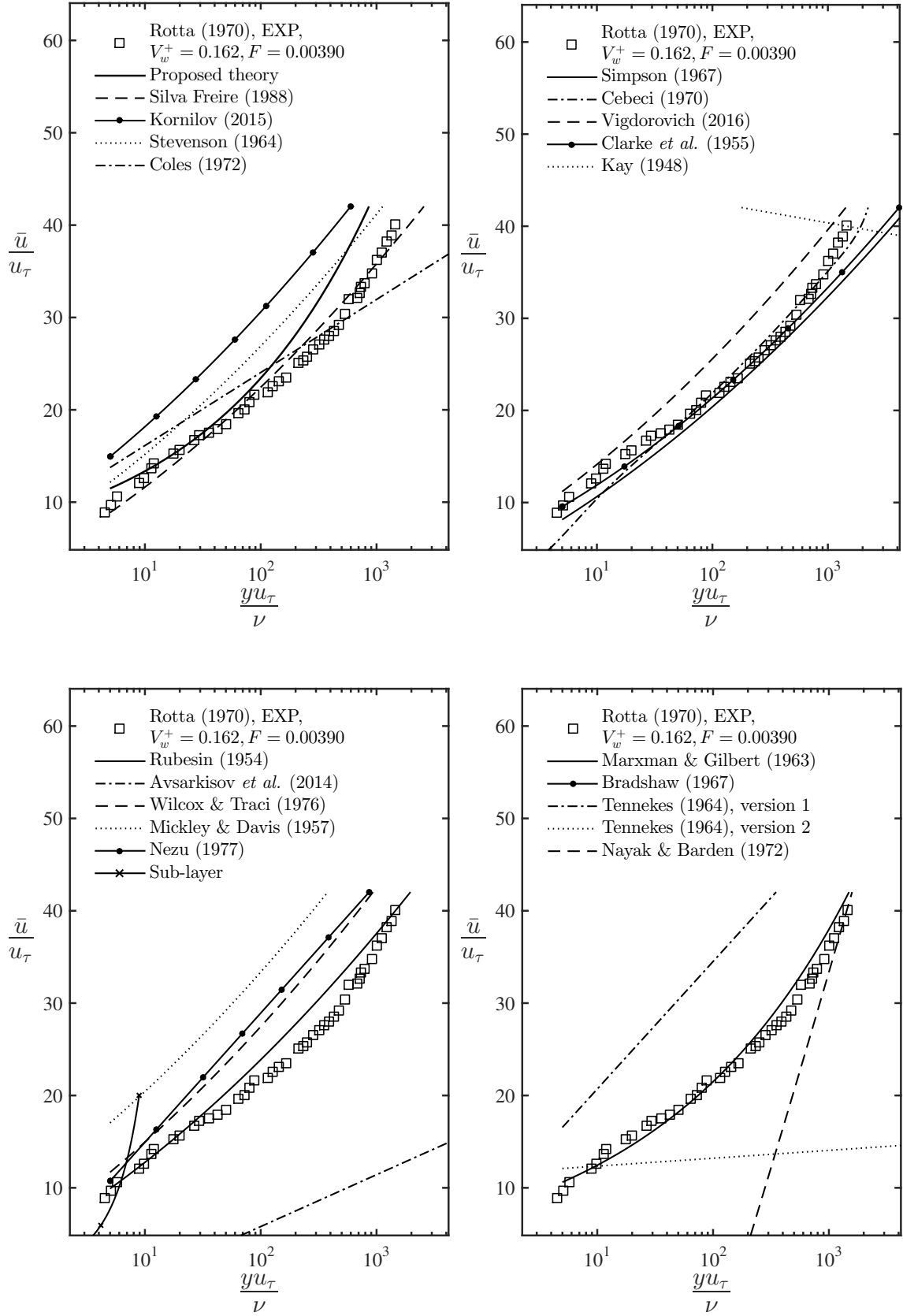


Figure B.54: Mean velocity profiles data compared to different formulations.

Boundary layer flow with blowing

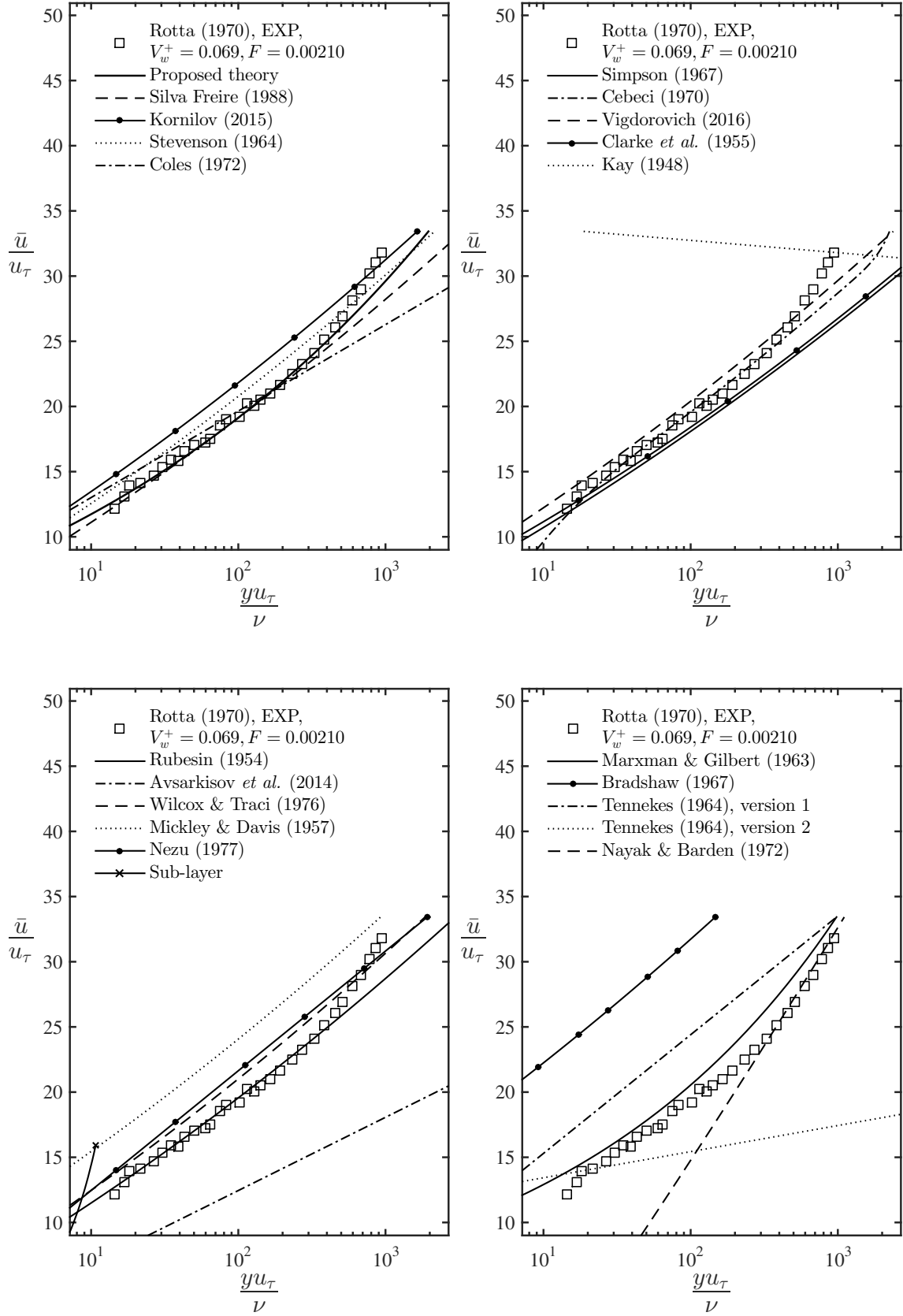


Figure B.55: Mean velocity profiles data compared to different formulations.

Boundary layer flow with suction

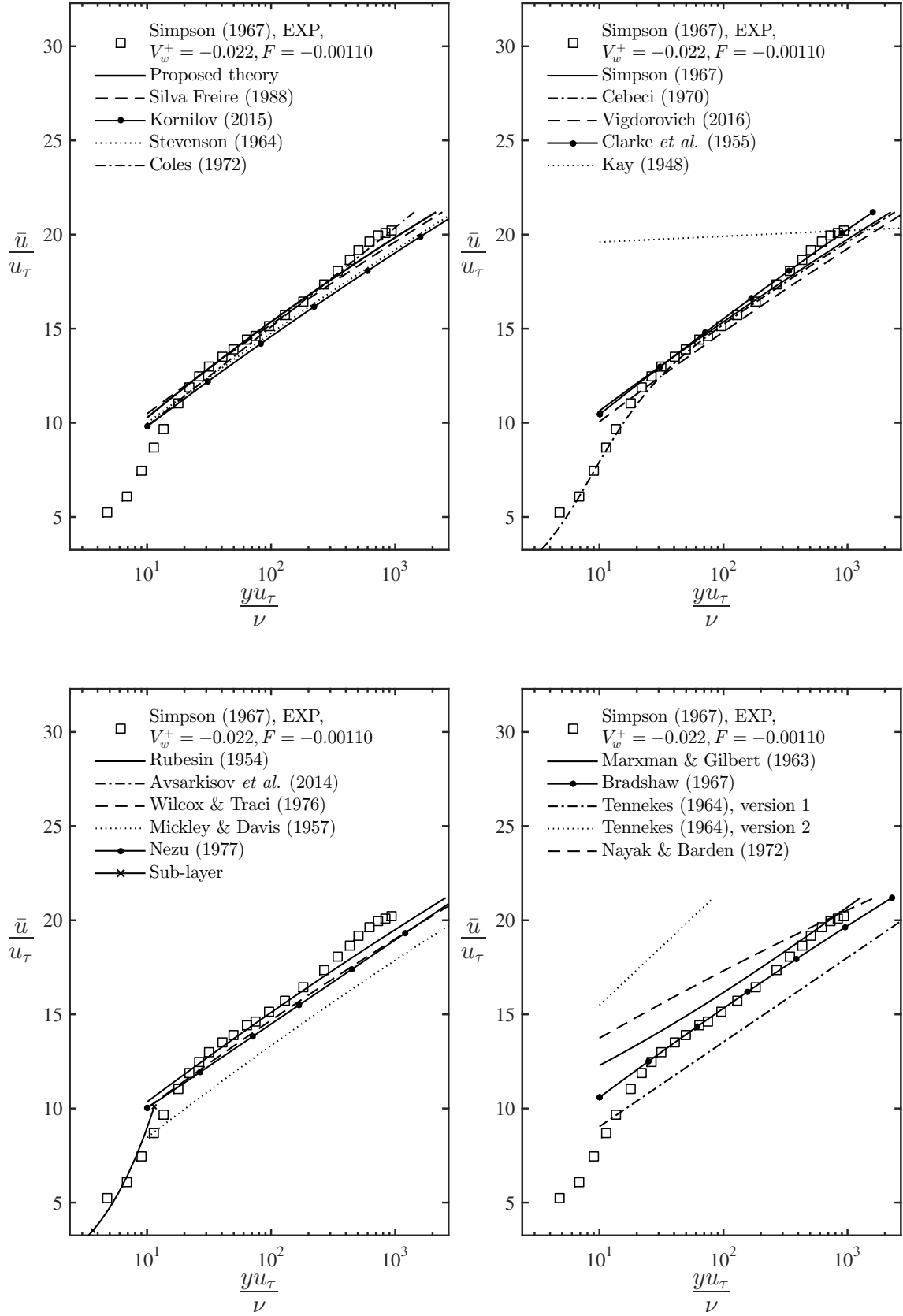


Figure B.56: Mean velocity profiles data compared to different formulations.

Boundary layer flow with suction

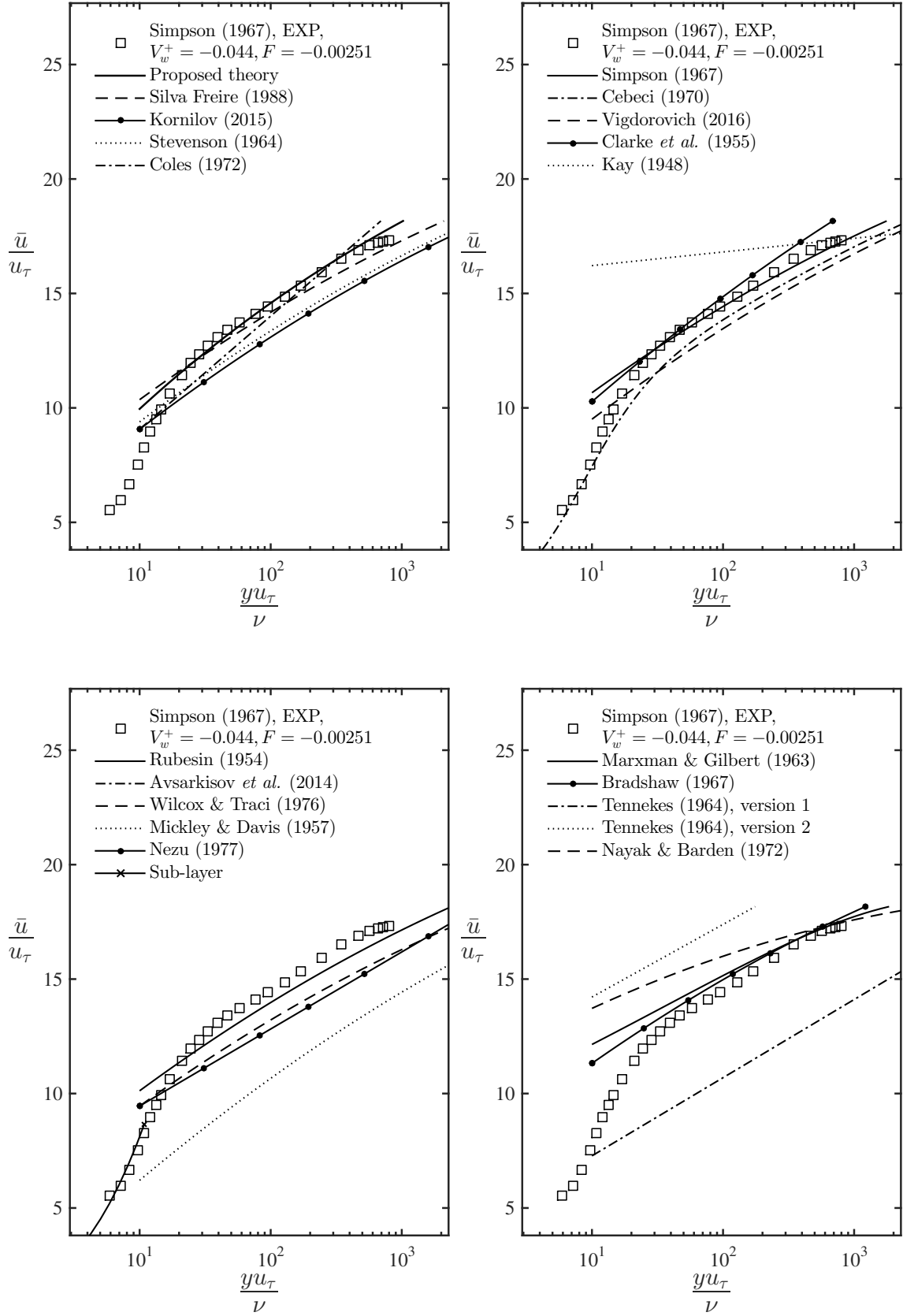


Figure B.57: Mean velocity profiles data compared to different formulations.

Boundary layer flow with suction

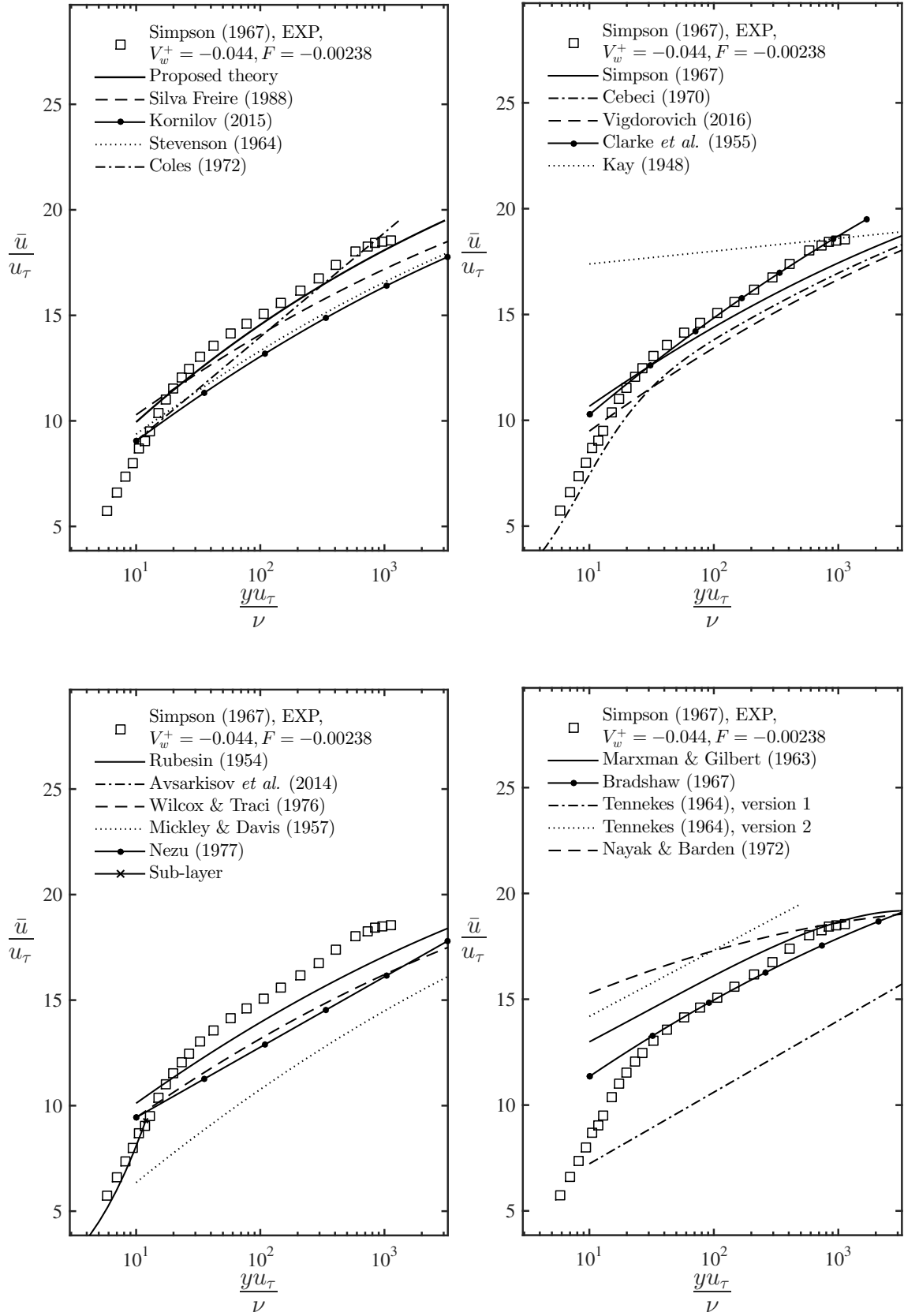


Figure B.58: Mean velocity profiles data compared to different formulations.

Channel flow at the wall with blowing

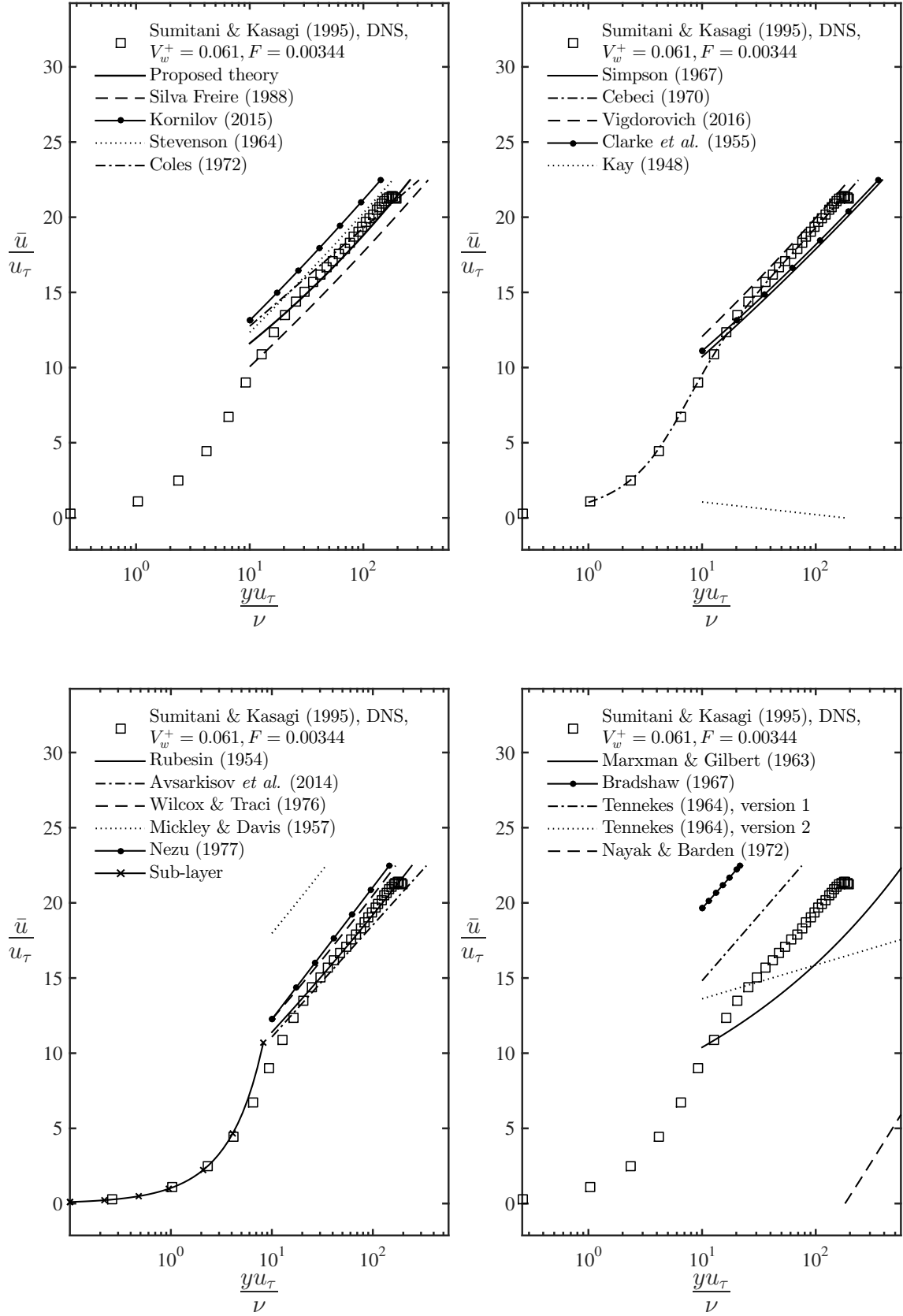


Figure B.59: Mean velocity profiles data compared to different formulations.

Boundary layer flow with suction

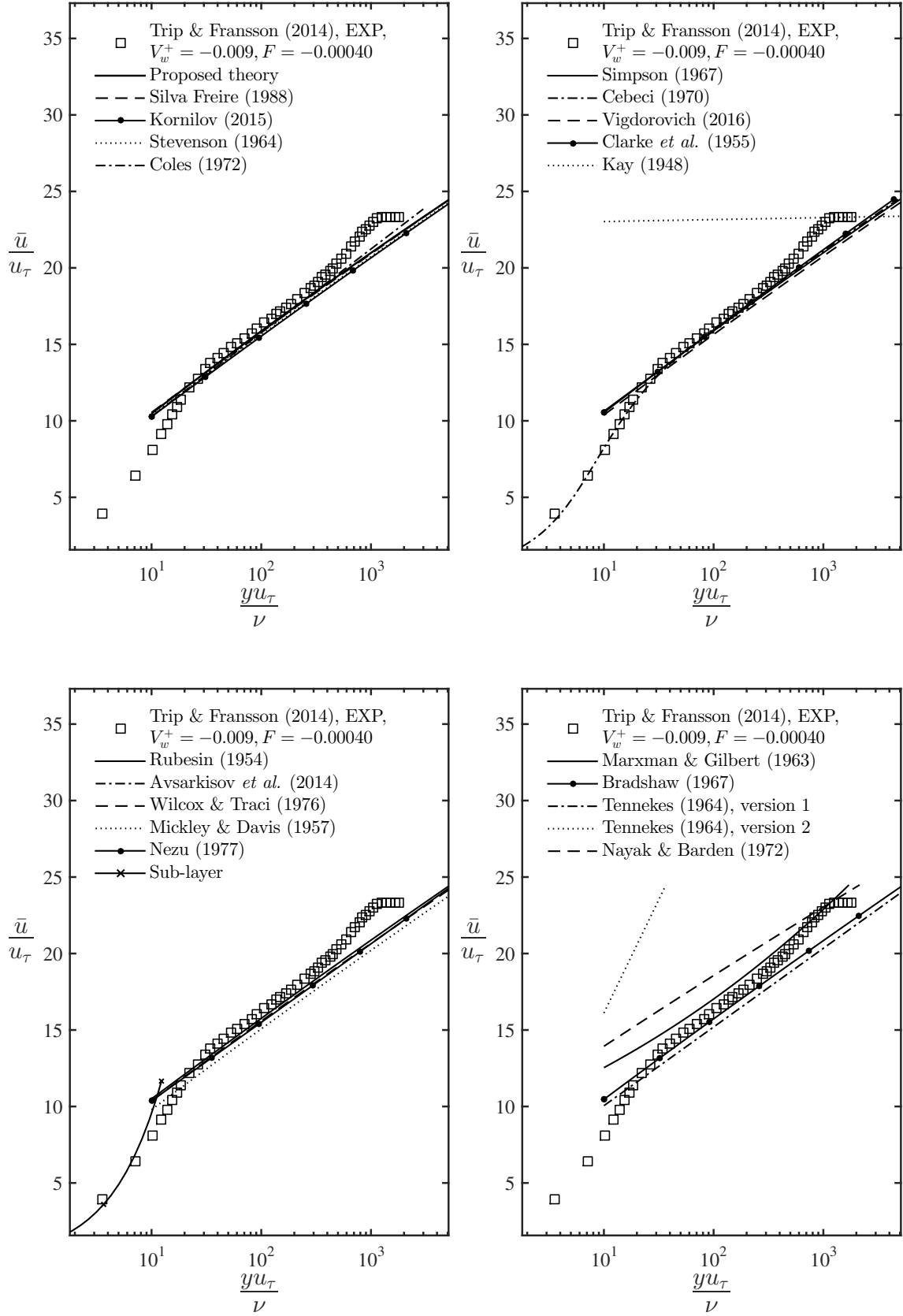


Figure B.60: Mean velocity profiles data compared to different formulations.

Boundary layer flow with suction

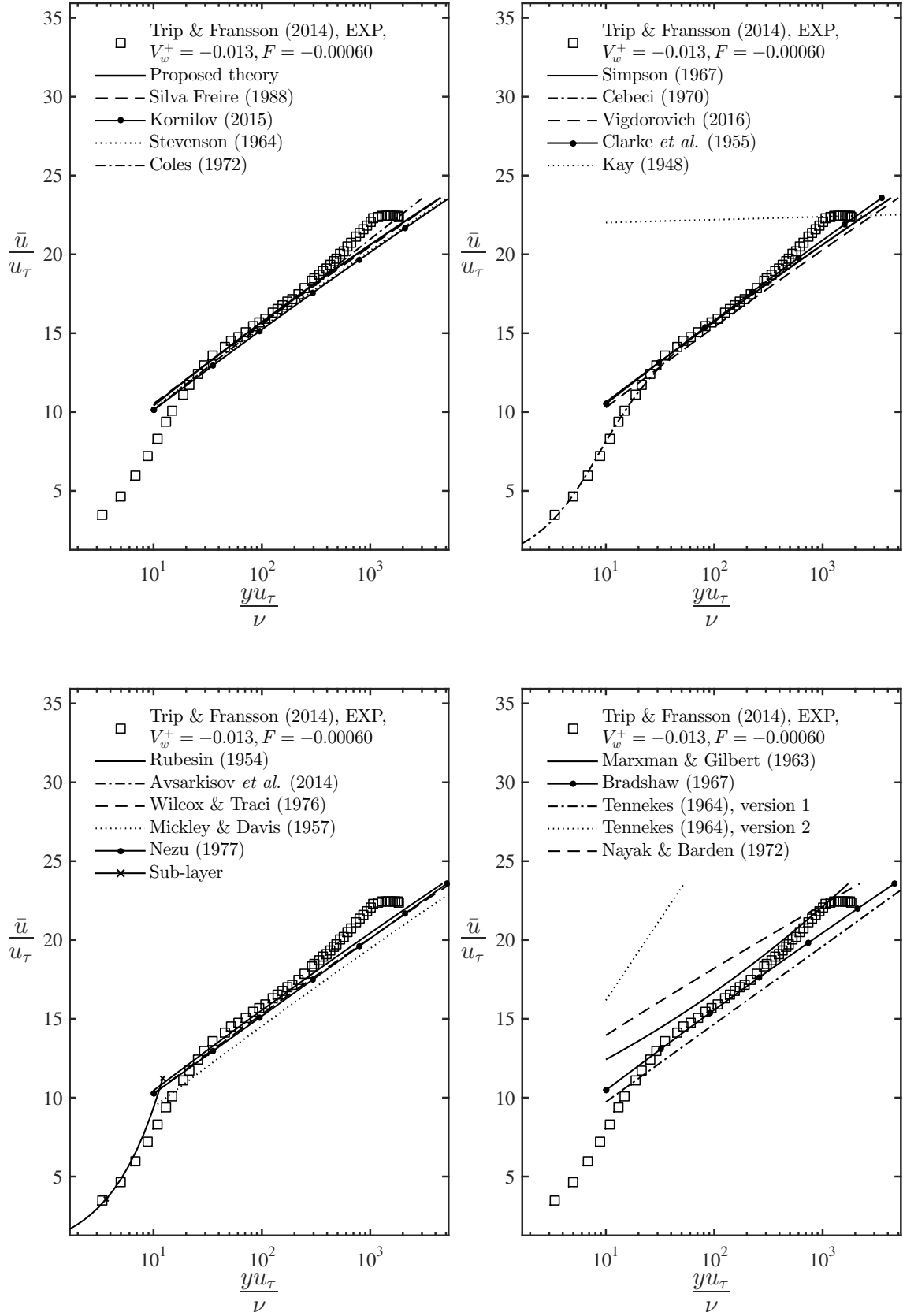


Figure B.61: Mean velocity profiles data compared to different formulations.

Boundary layer flow with suction

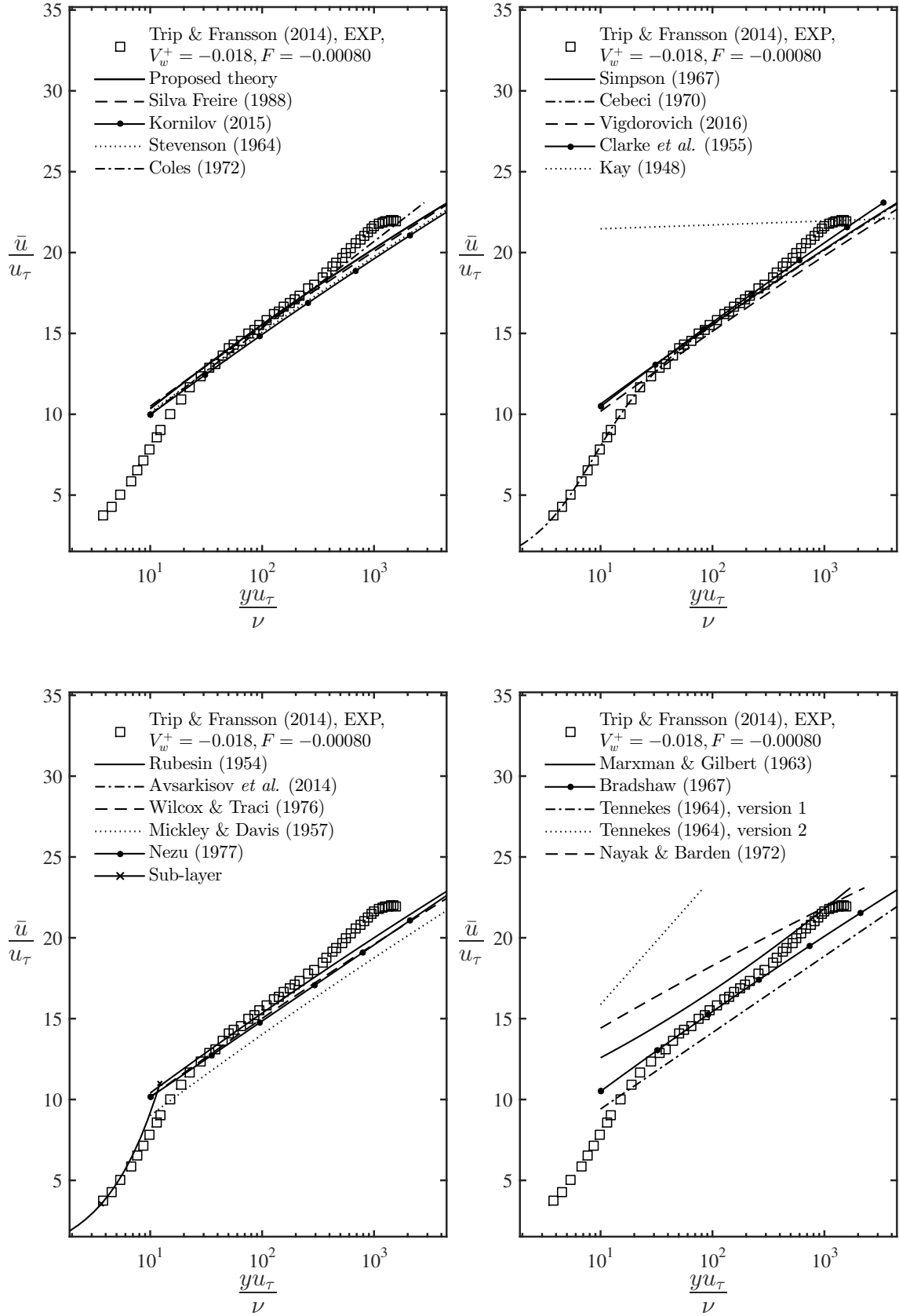


Figure B.62: Mean velocity profiles data compared to different formulations.

Boundary layer flow with suction

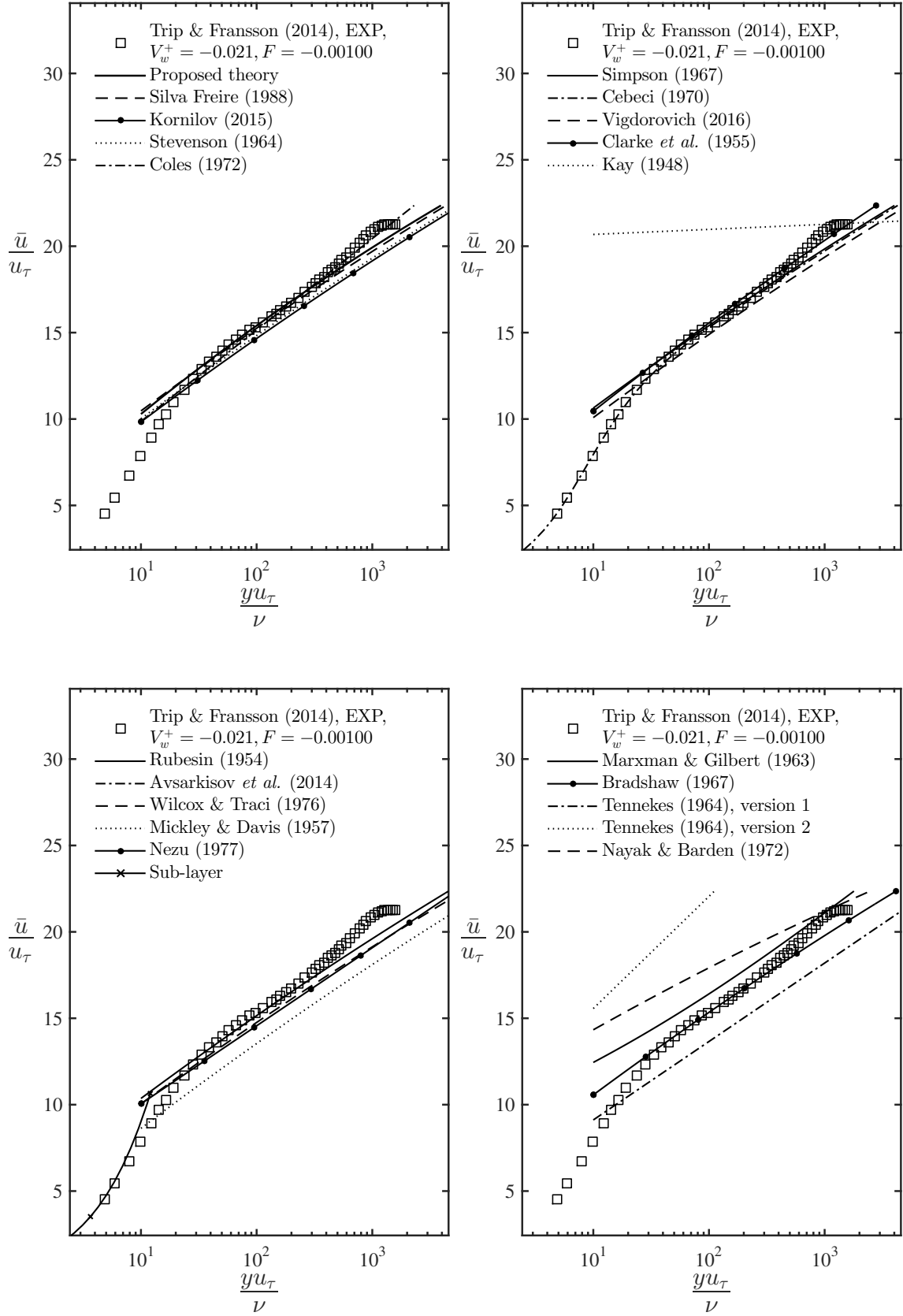


Figure B.63: Mean velocity profiles data compared to different formulations.

Boundary layer flow with suction

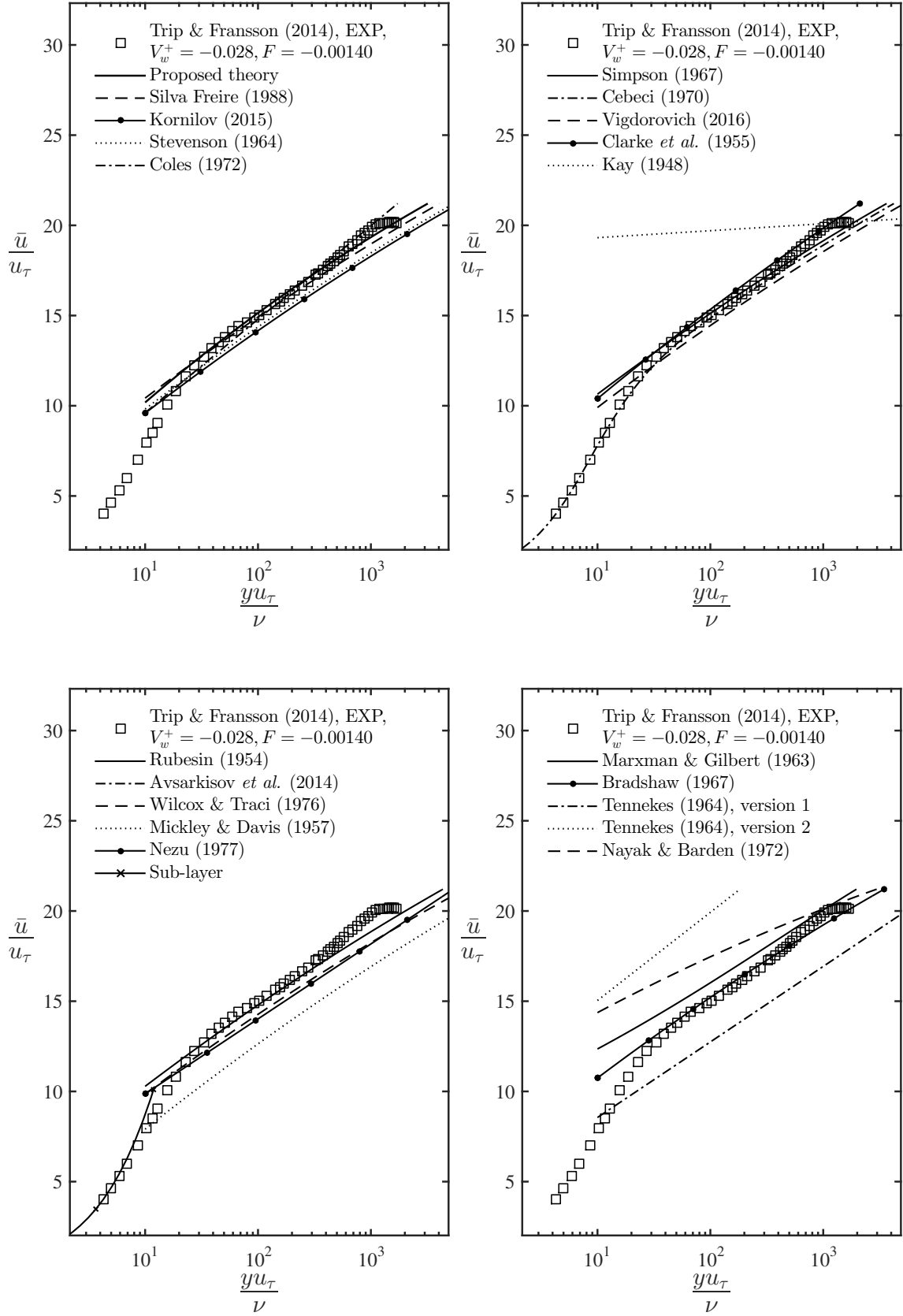


Figure B.64: Mean velocity profiles data compared to different formulations.

Boundary layer flow with suction

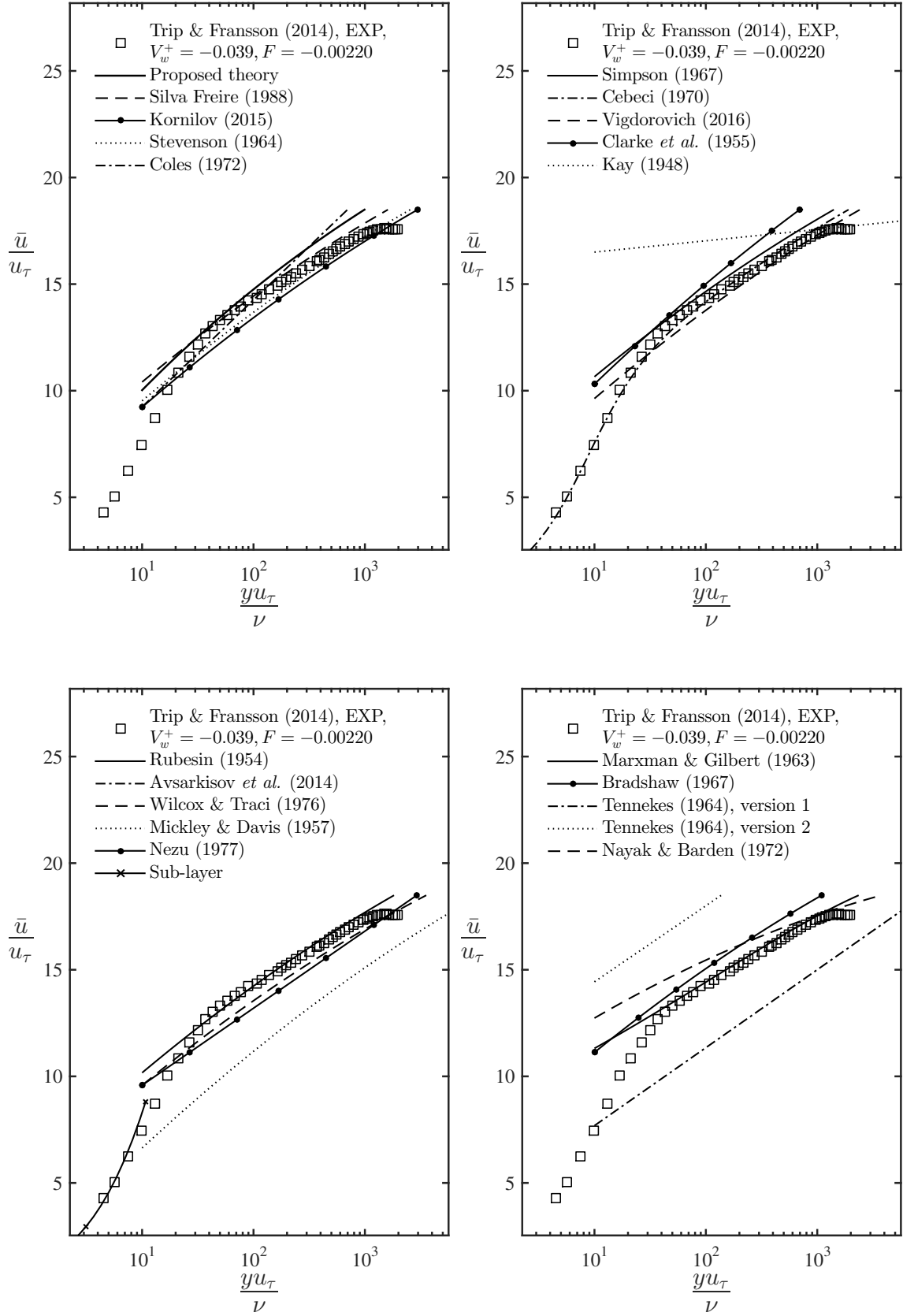


Figure B.65: Mean velocity profiles data compared to different formulations.

B.2 Non-zero pressure gradient flows

Bondary layer flow with separation

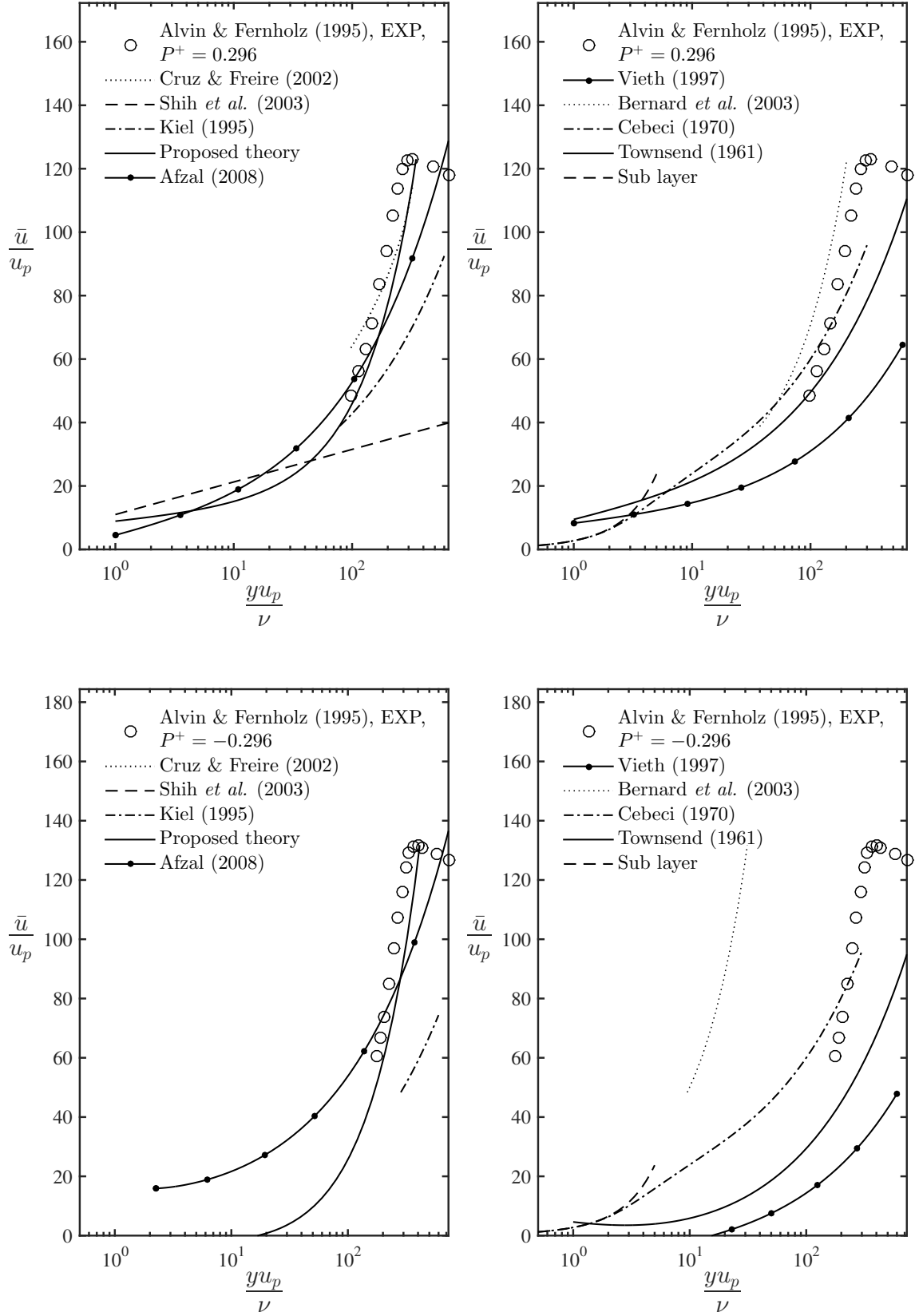


Figure B.66: Mean velocity profiles data compared to different formulations.

Bondary layer flow with separation

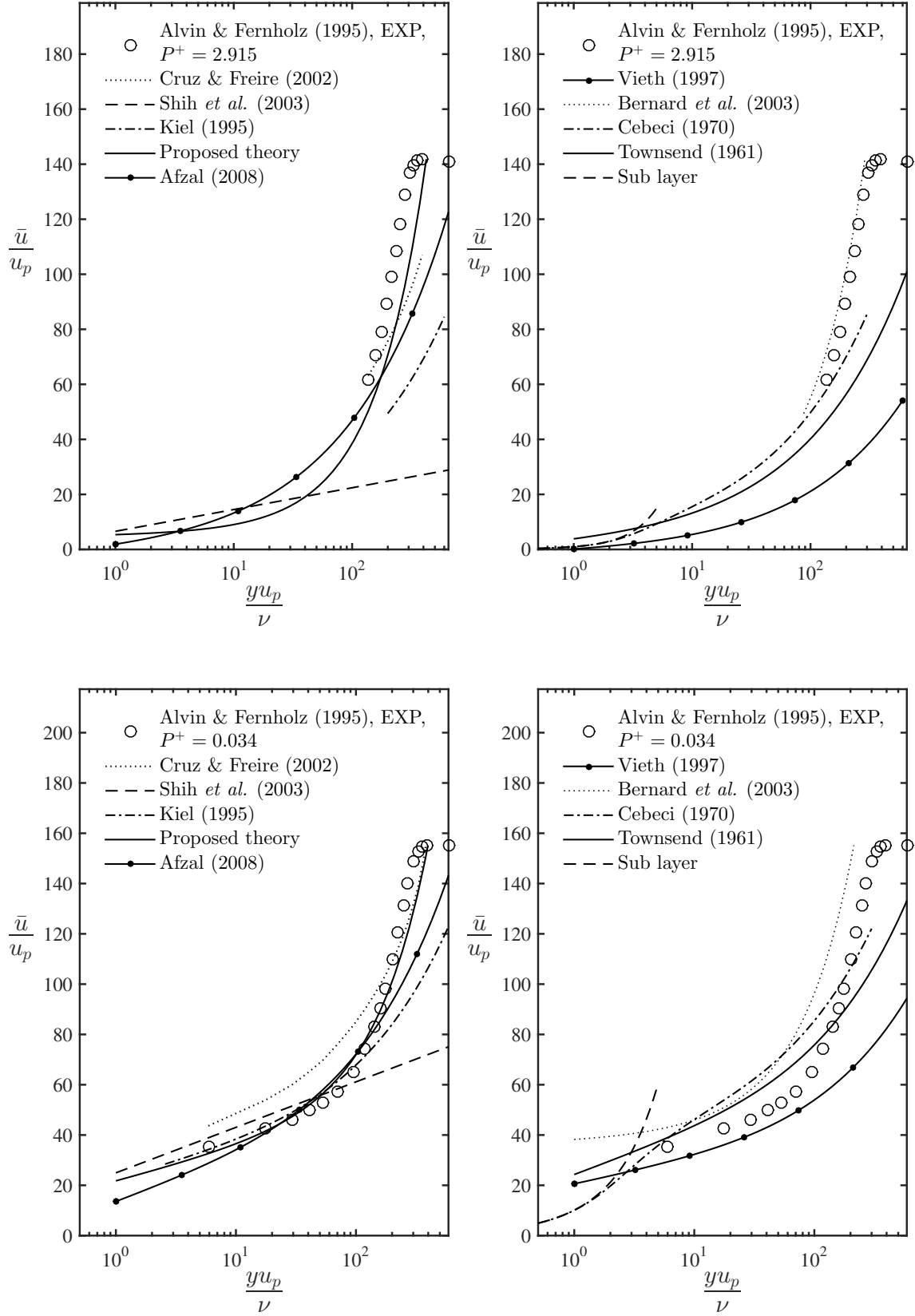


Figure B.67: Mean velocity profiles data compared to different formulations.

Bondary layer flow with separation

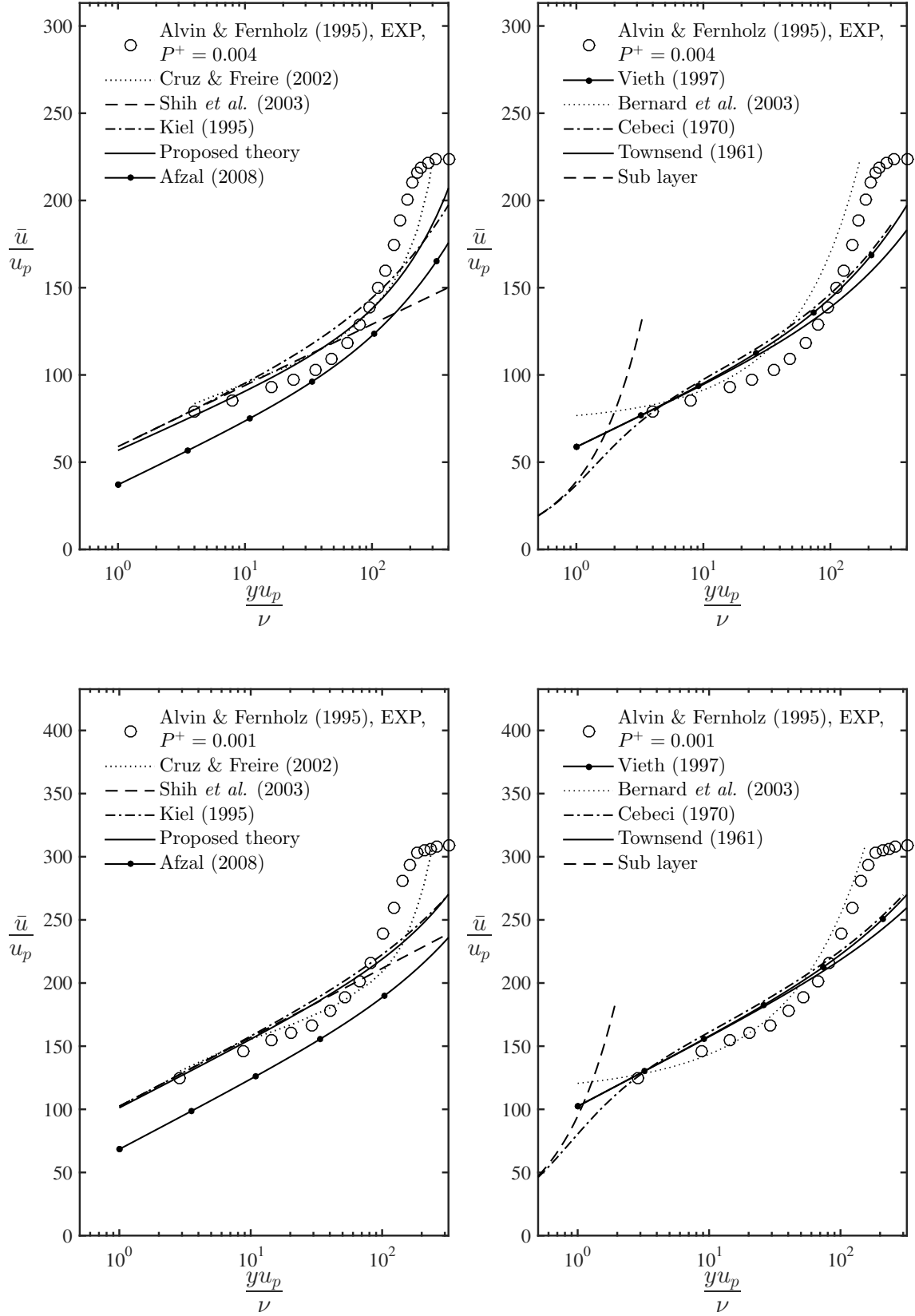


Figure B.68: Mean velocity profiles data compared to different formulations.

Bondary layer flow with separation

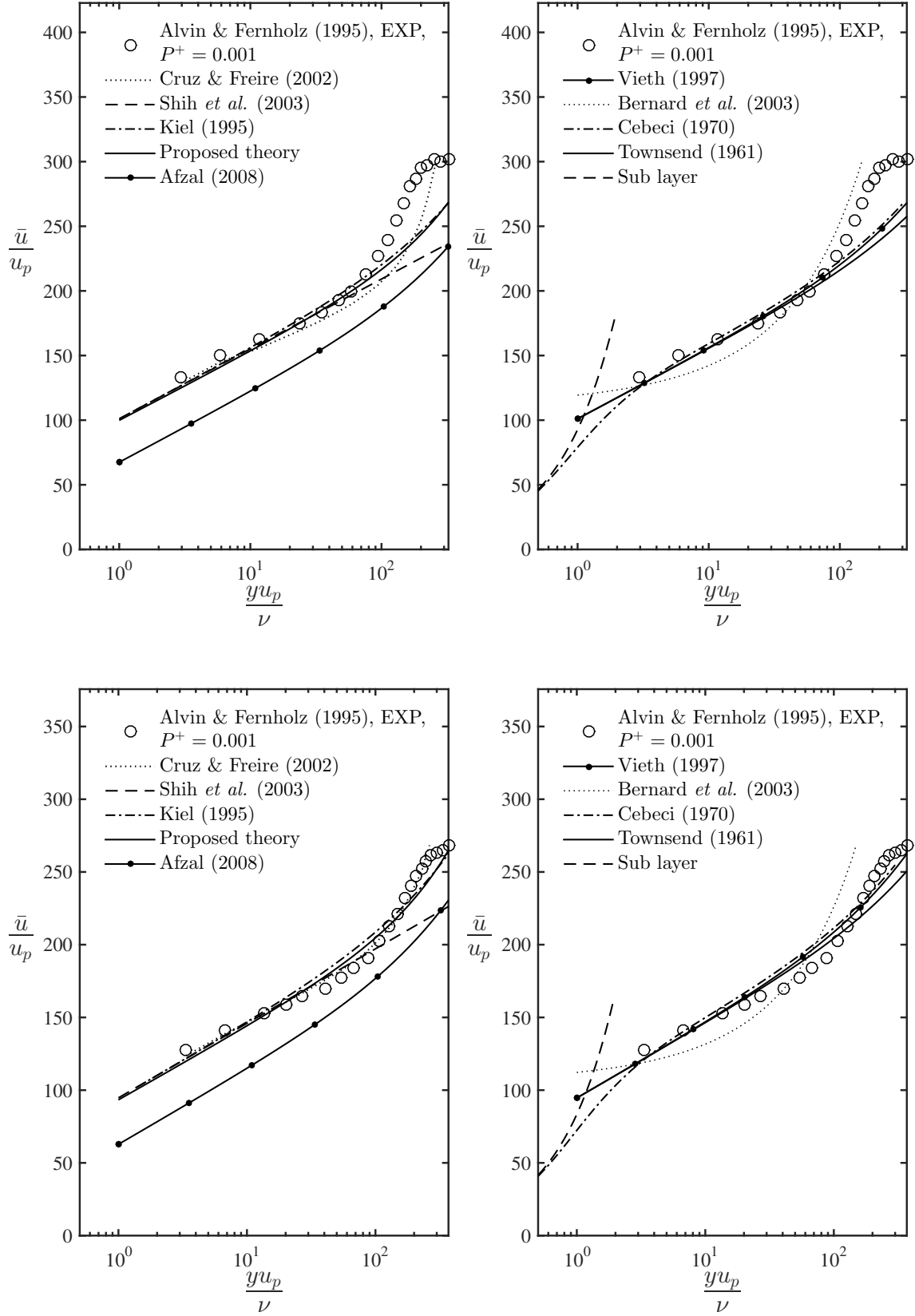


Figure B.69: Mean velocity profiles data compared to different formulations.

Bondary layer flow with separation

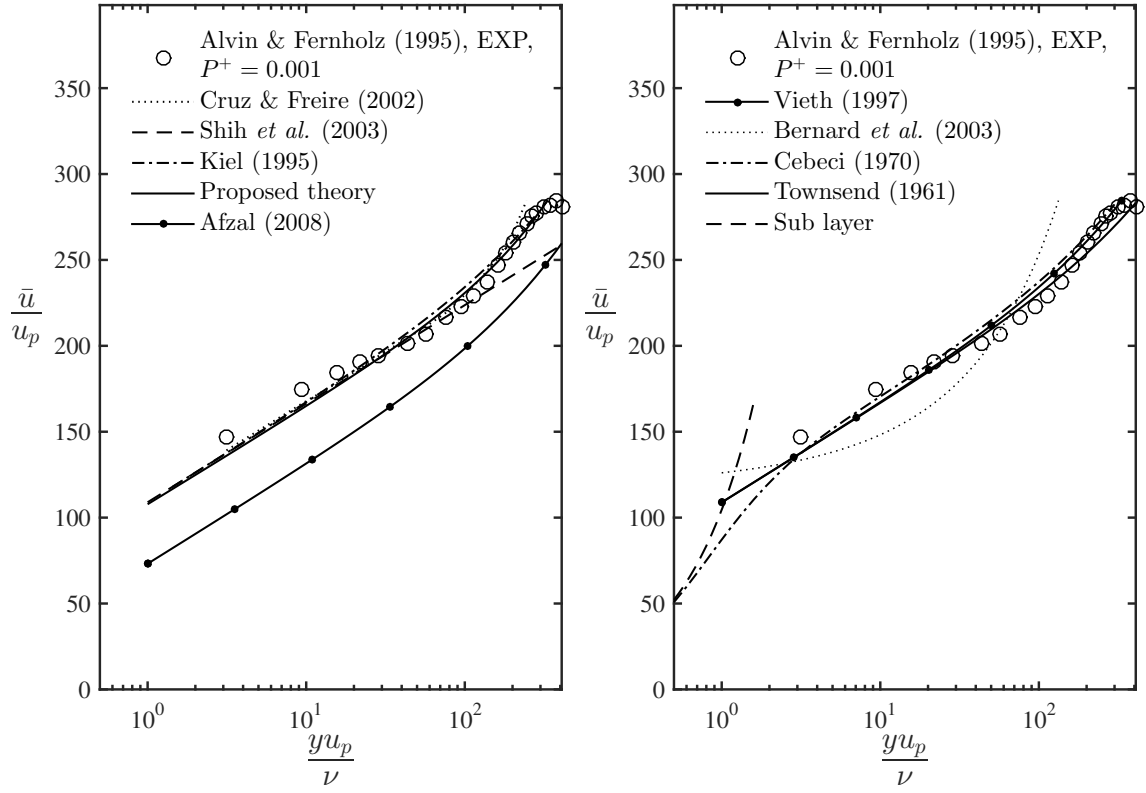


Figure B.70: Mean velocity profiles data compared to different formulations.

High APG boundary layer flow

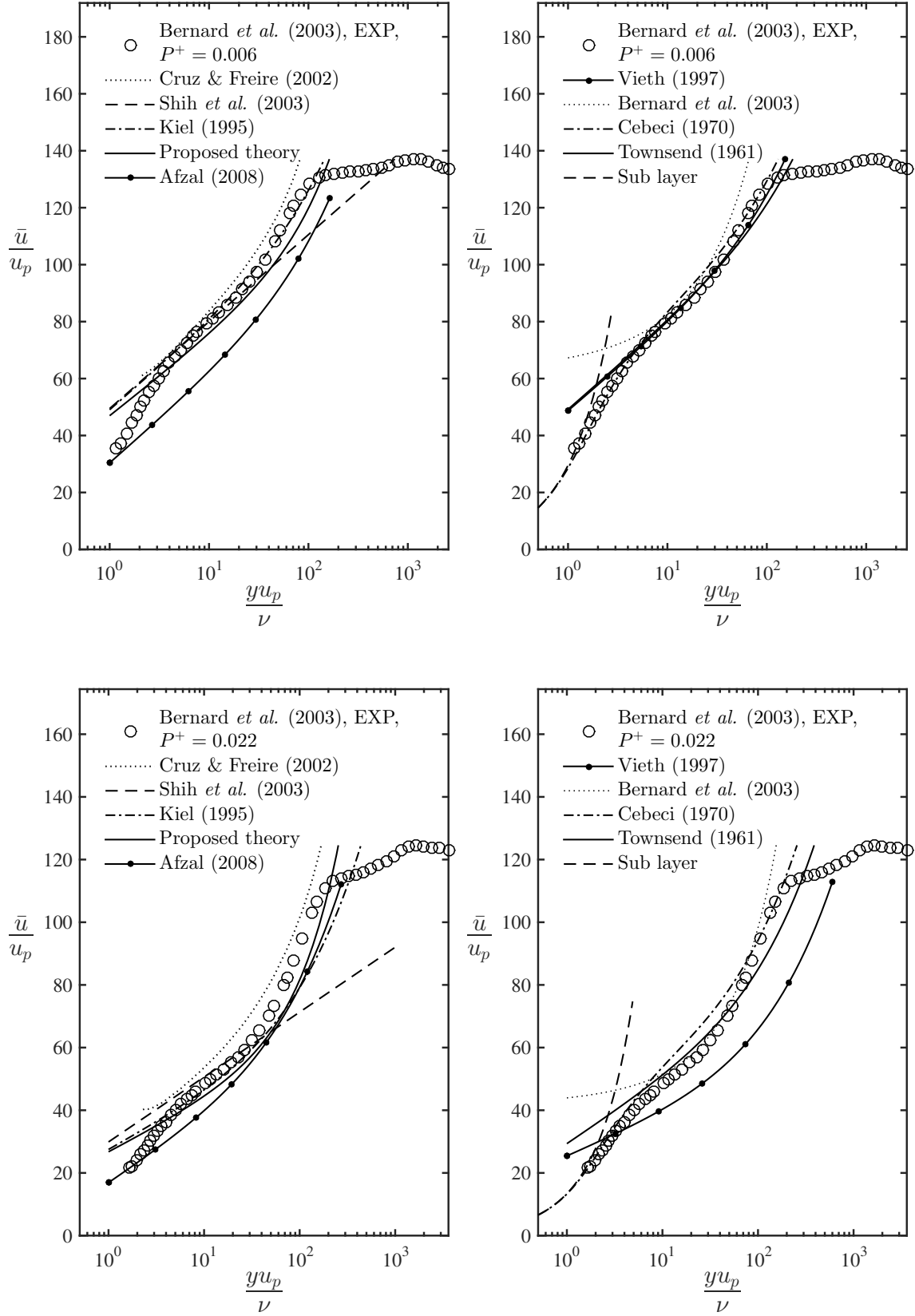


Figure B.71: Mean velocity profiles data compared to different formulations.

High APG boundary layer flow

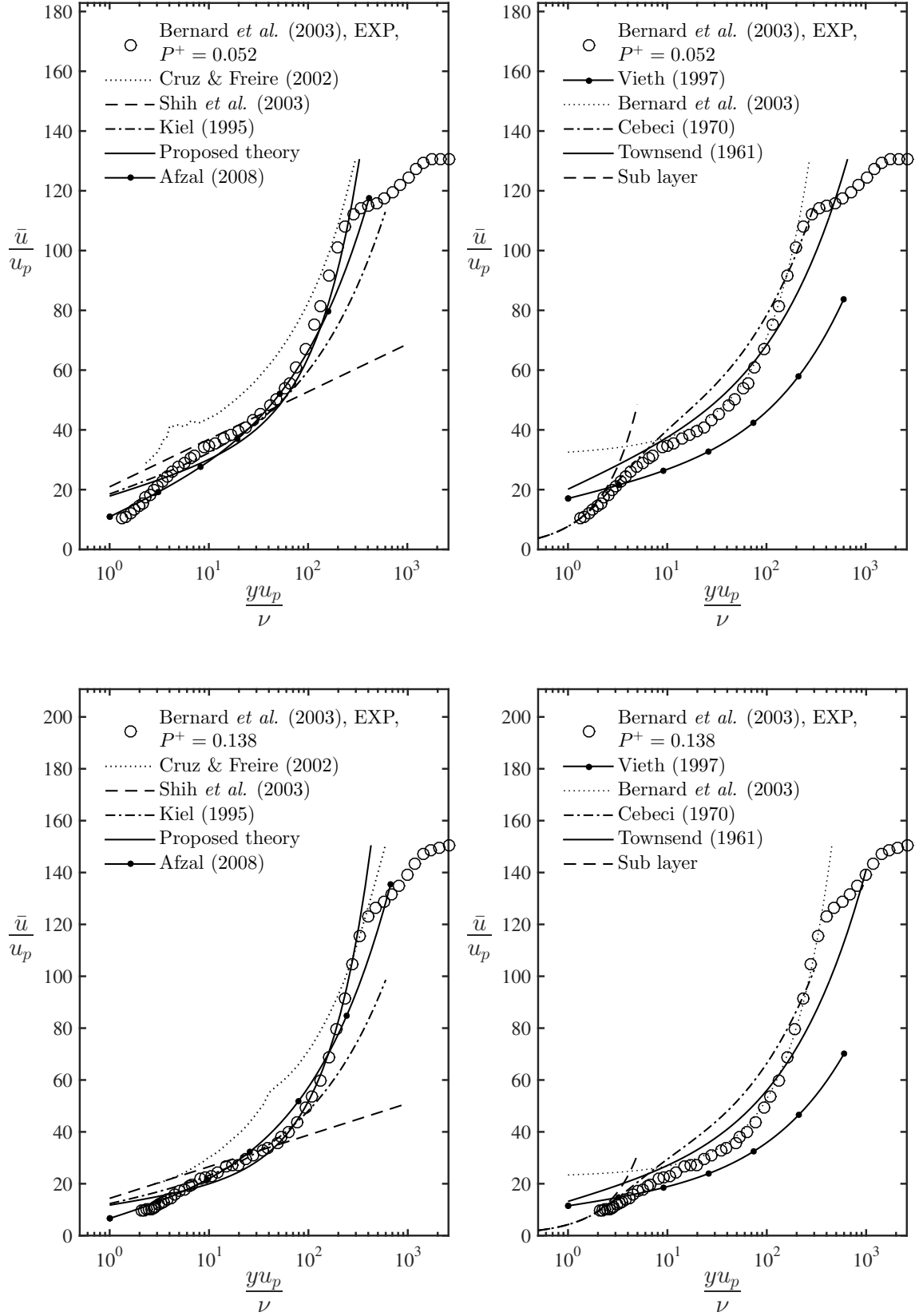


Figure B.72: Mean velocity profiles data compared to different formulations.

High APG boundary layer flow

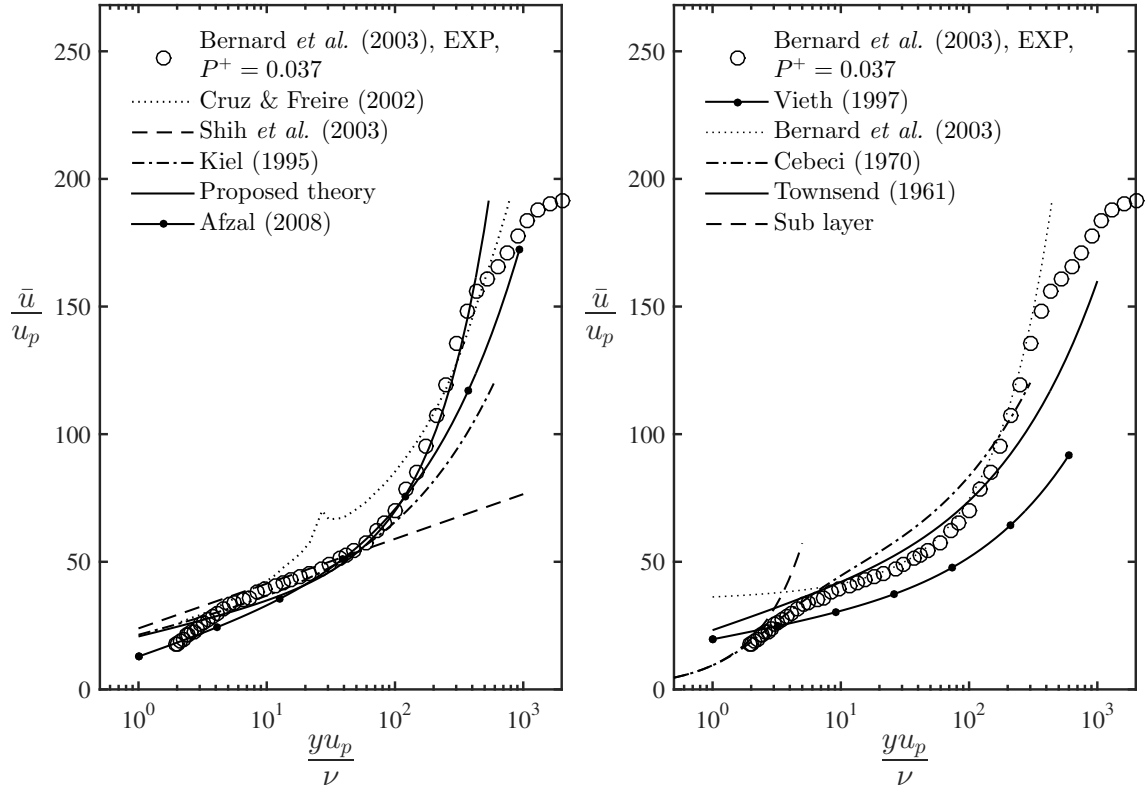


Figure B.73: Mean velocity profiles data compared to different formulations.

Bondary layer flow with separation

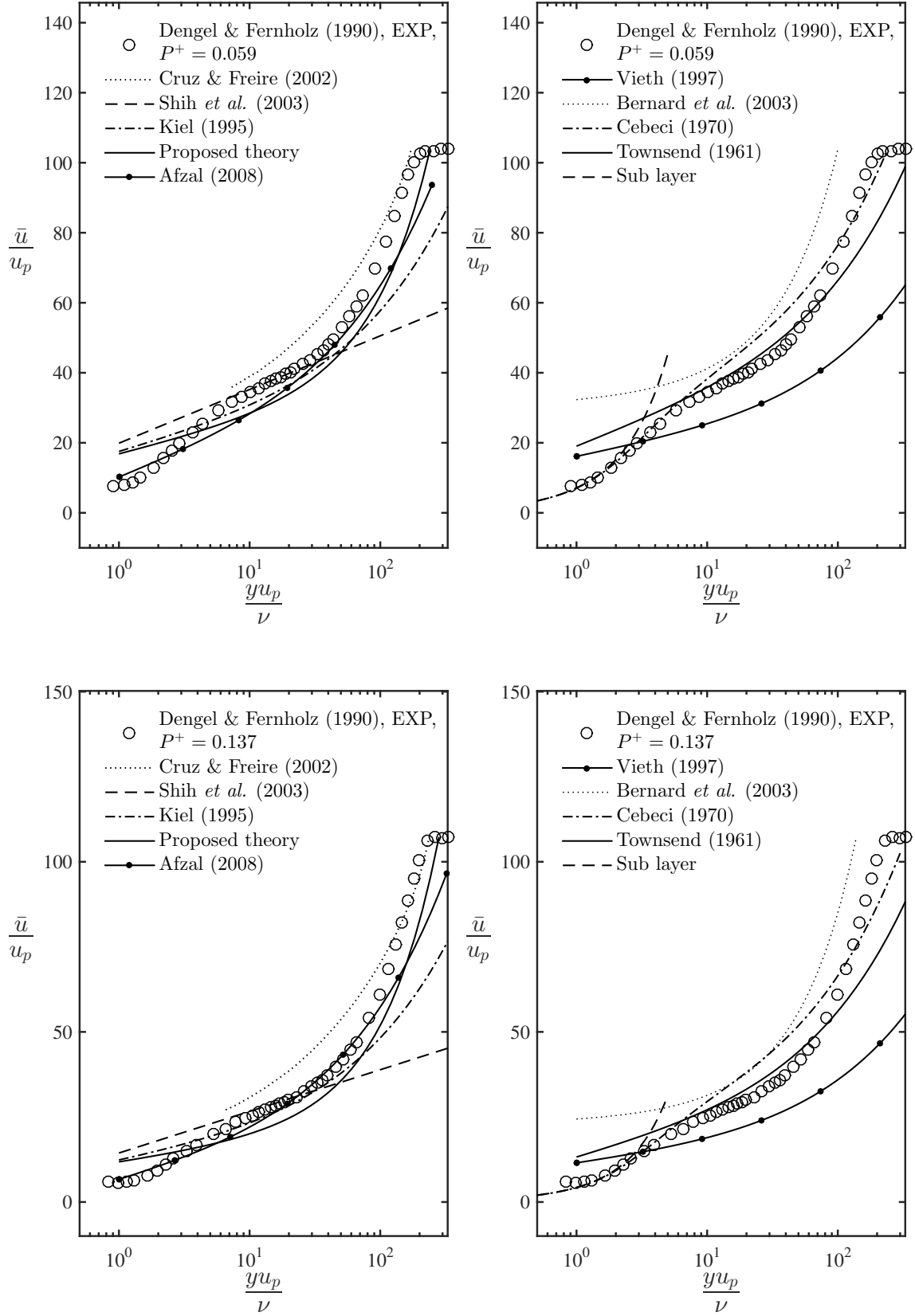


Figure B.74: Mean velocity profiles data compared to different formulations.

Bondary layer flow with separation

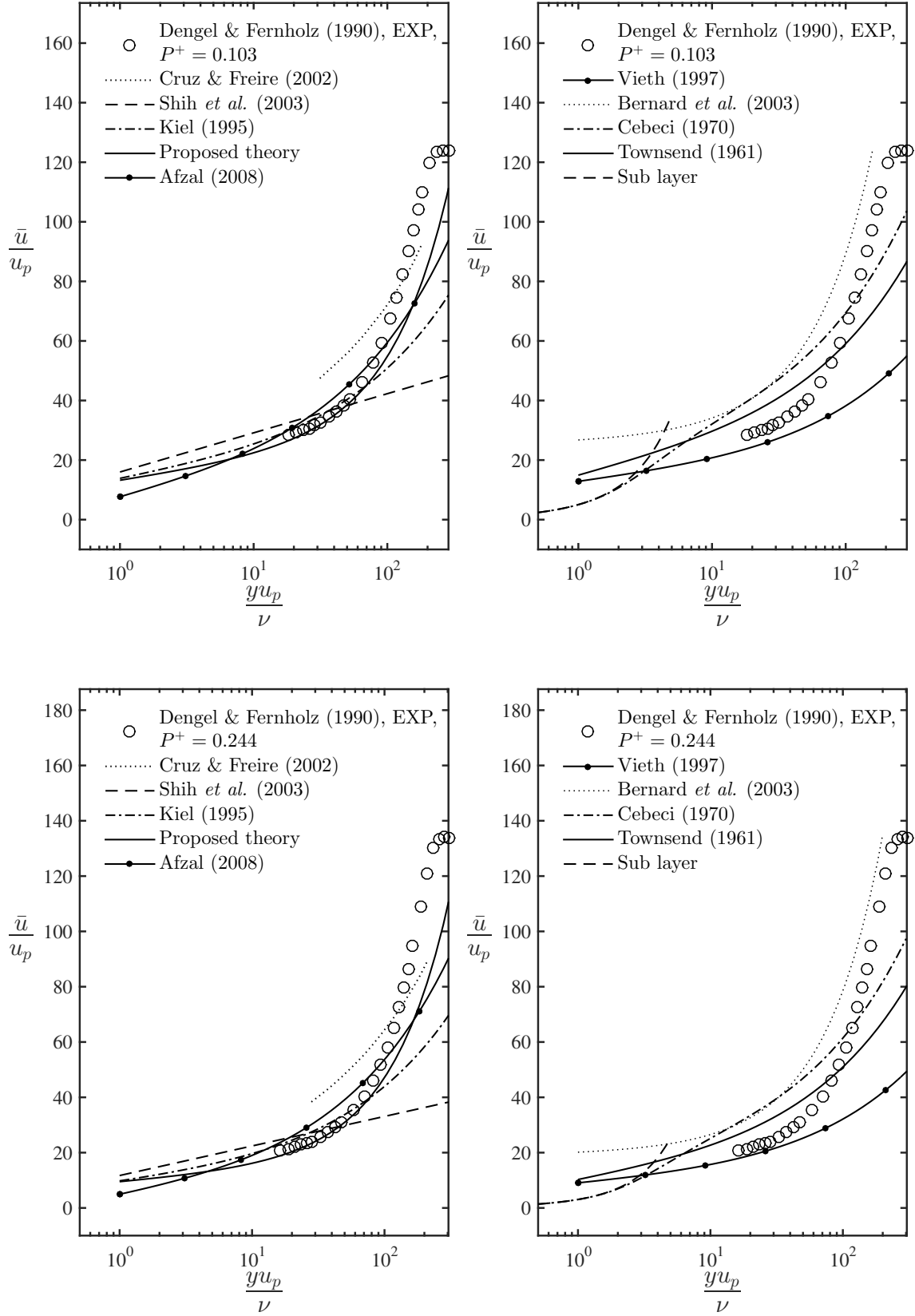


Figure B.75: Mean velocity profiles data compared to different formulations.

Bondary layer flow with separation

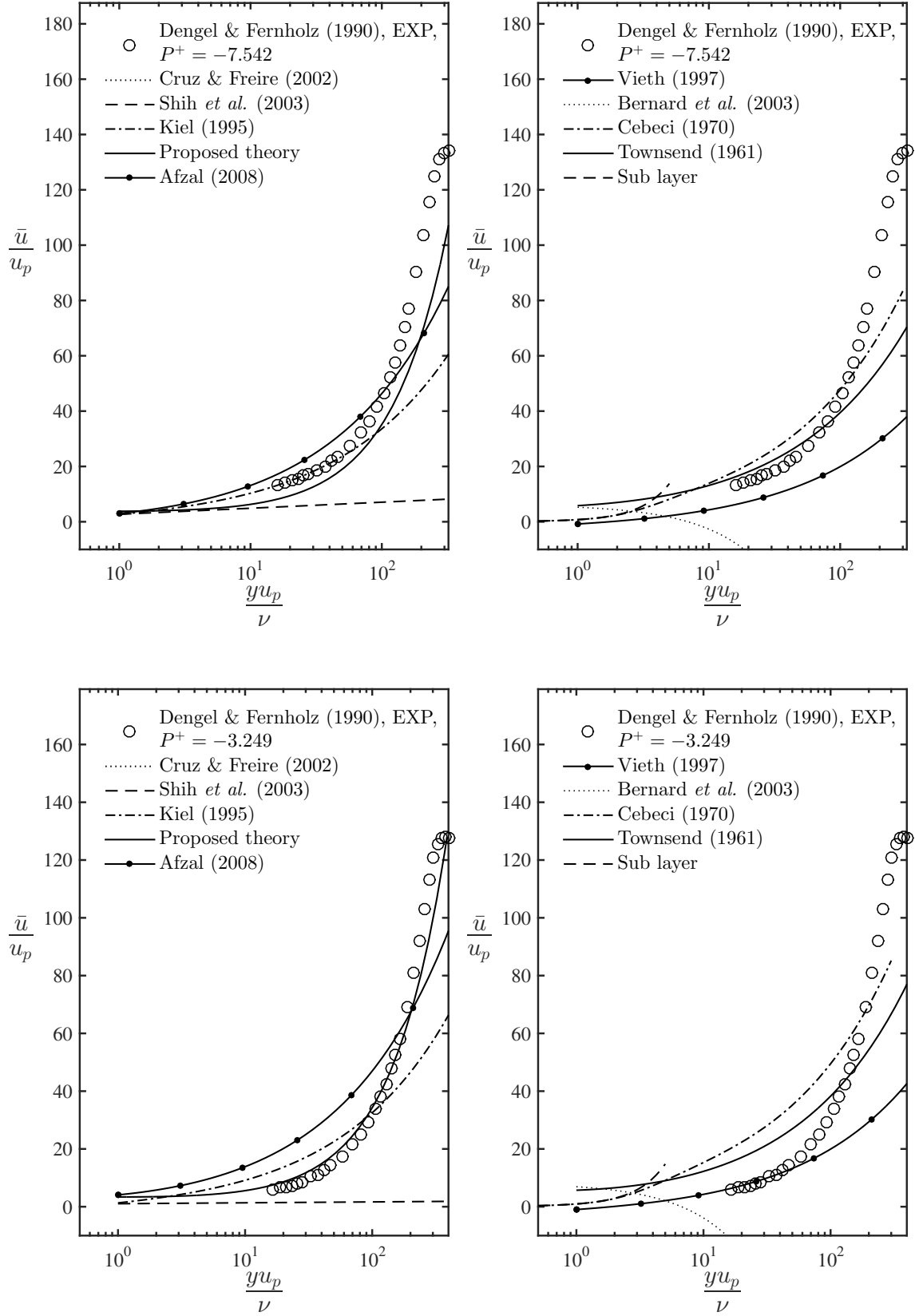


Figure B.76: Mean velocity profiles data compared to different formulations.

Bondary layer flow with separation

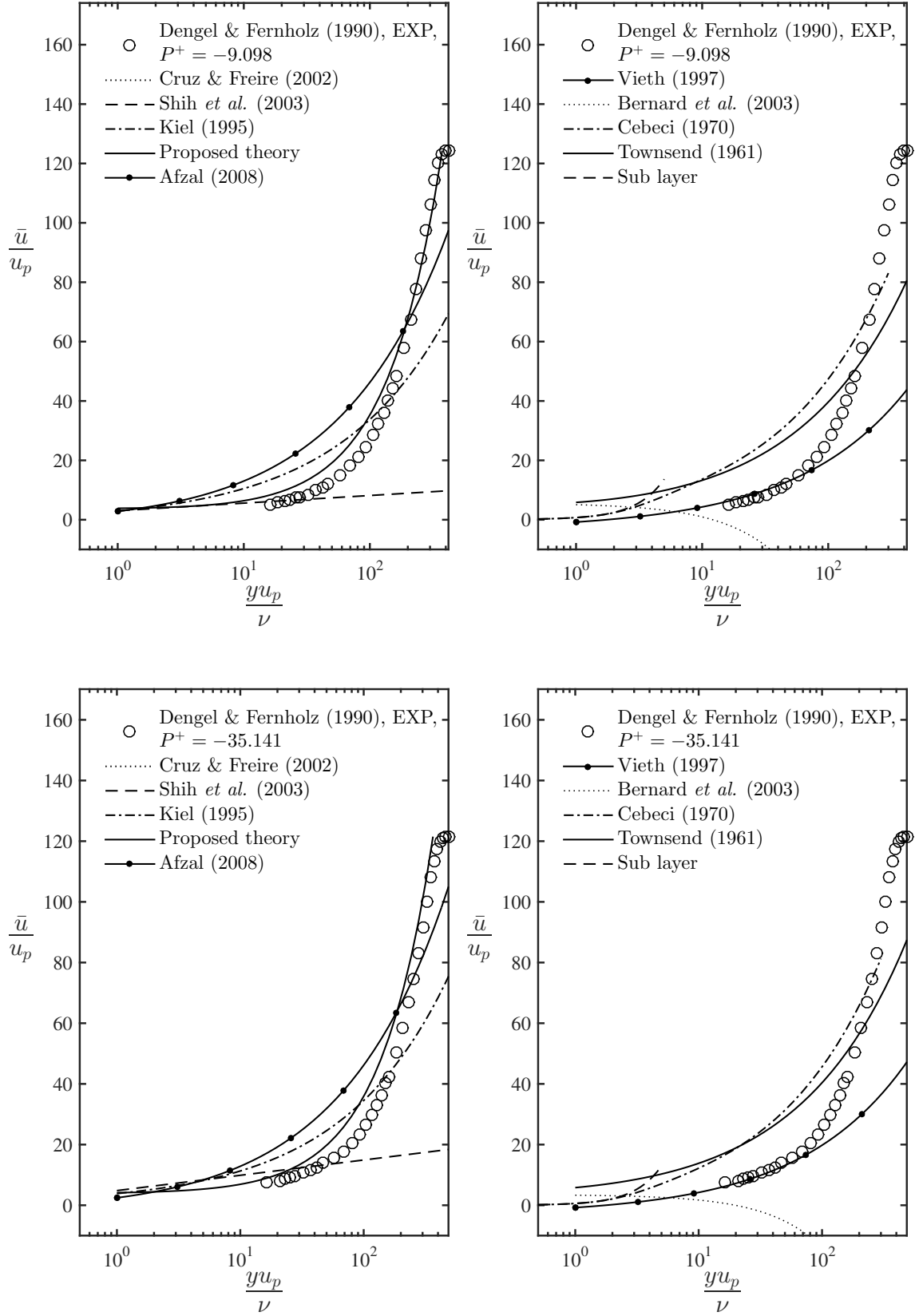


Figure B.77: Mean velocity profiles data compared to different formulations.

Bondary layer flow with separation

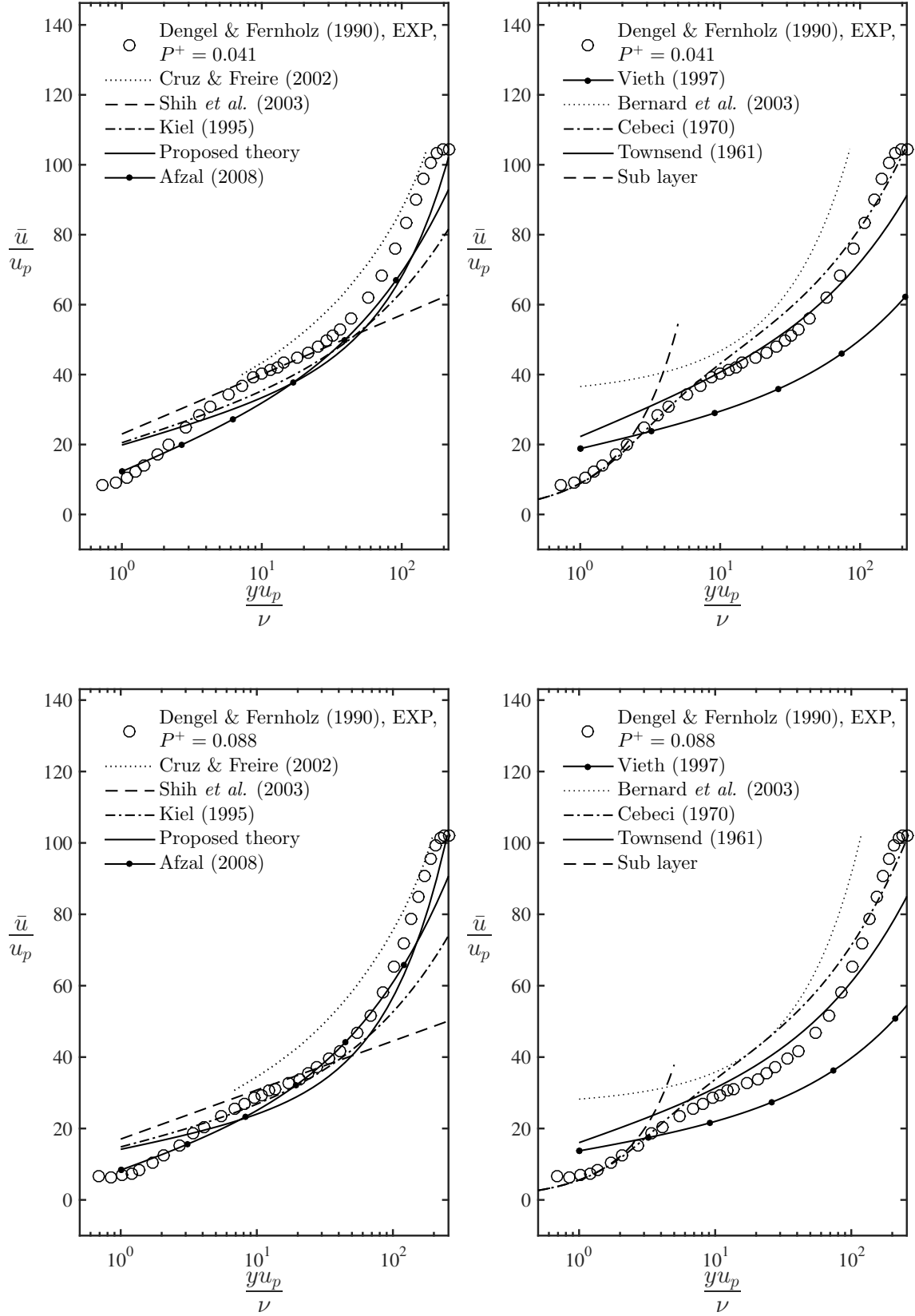


Figure B.78: Mean velocity profiles data compared to different formulations.

Bondary layer flow with separation

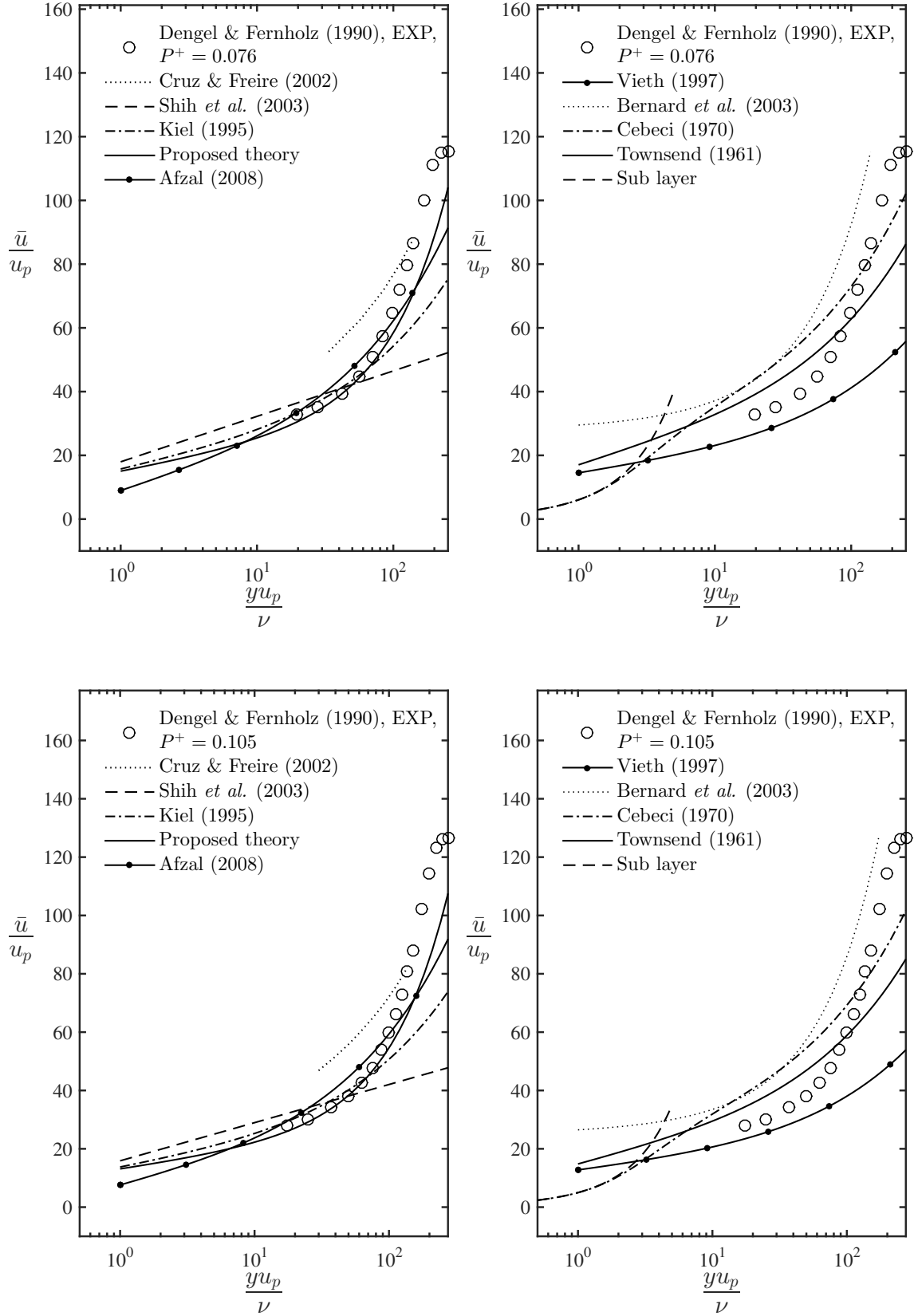


Figure B.79: Mean velocity profiles data compared to different formulations.

Bondary layer flow with separation

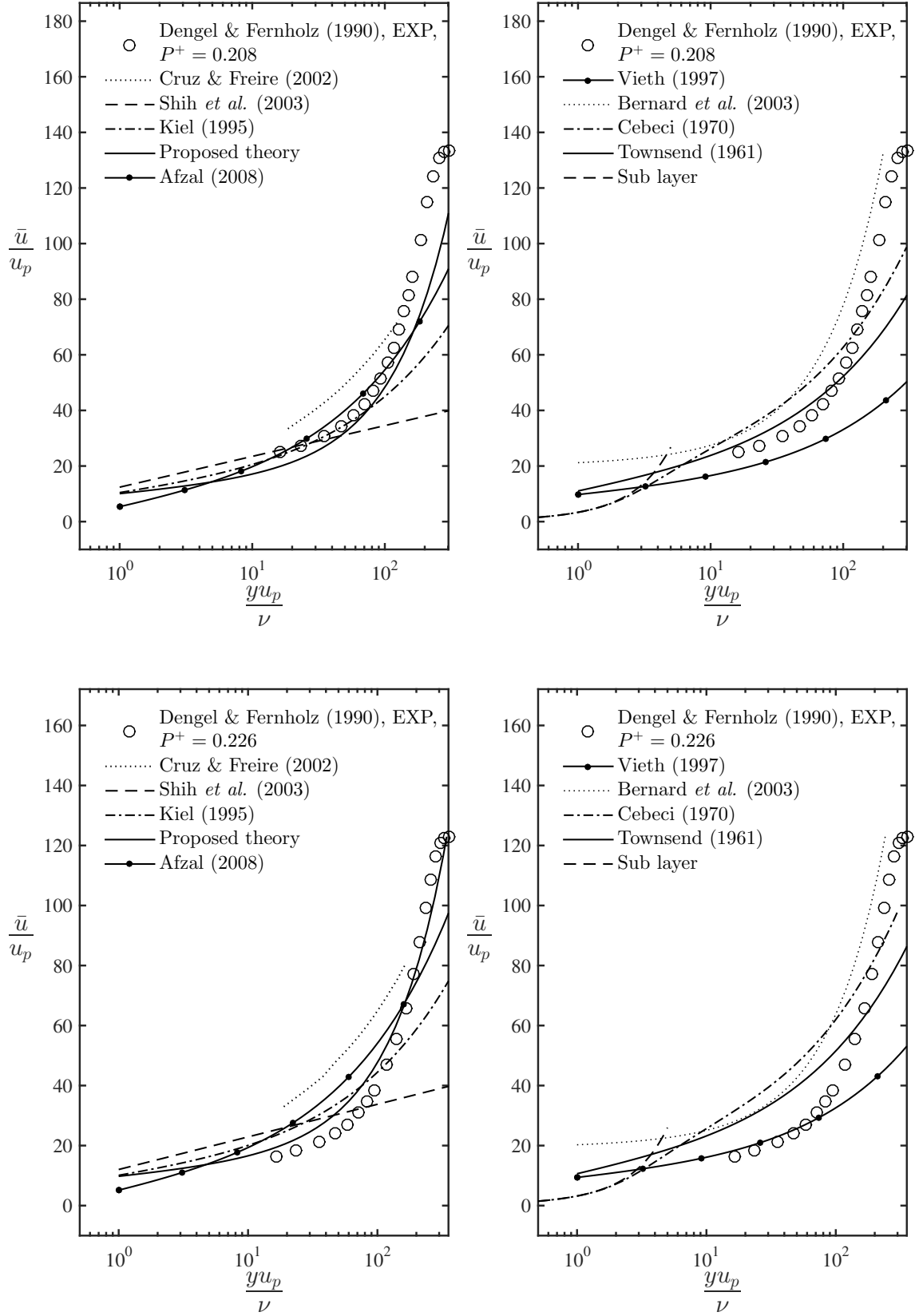


Figure B.80: Mean velocity profiles data compared to different formulations.

Bondary layer flow with separation

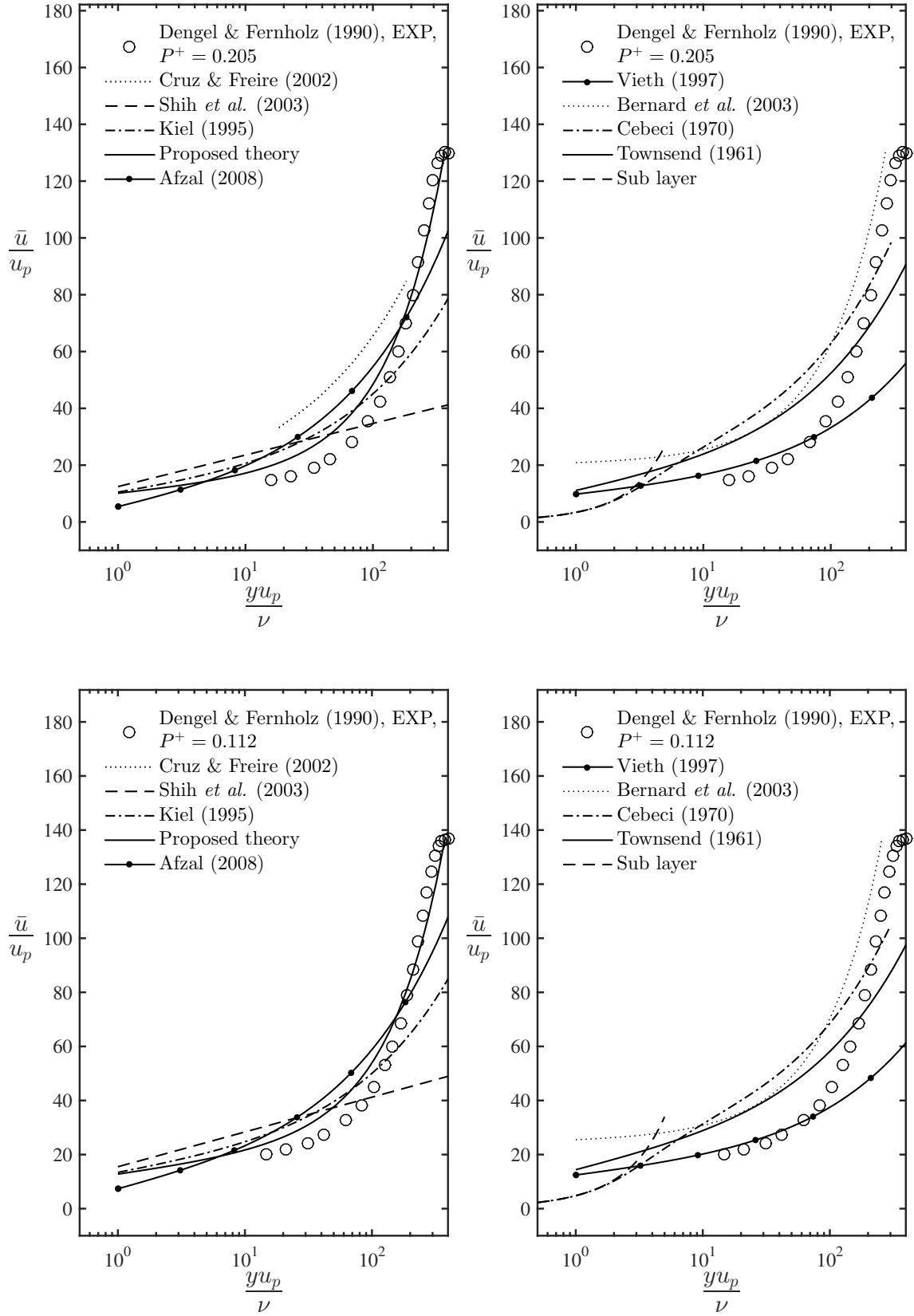


Figure B.81: Mean velocity profiles data compared to different formulations.

Bondary layer flow with separation

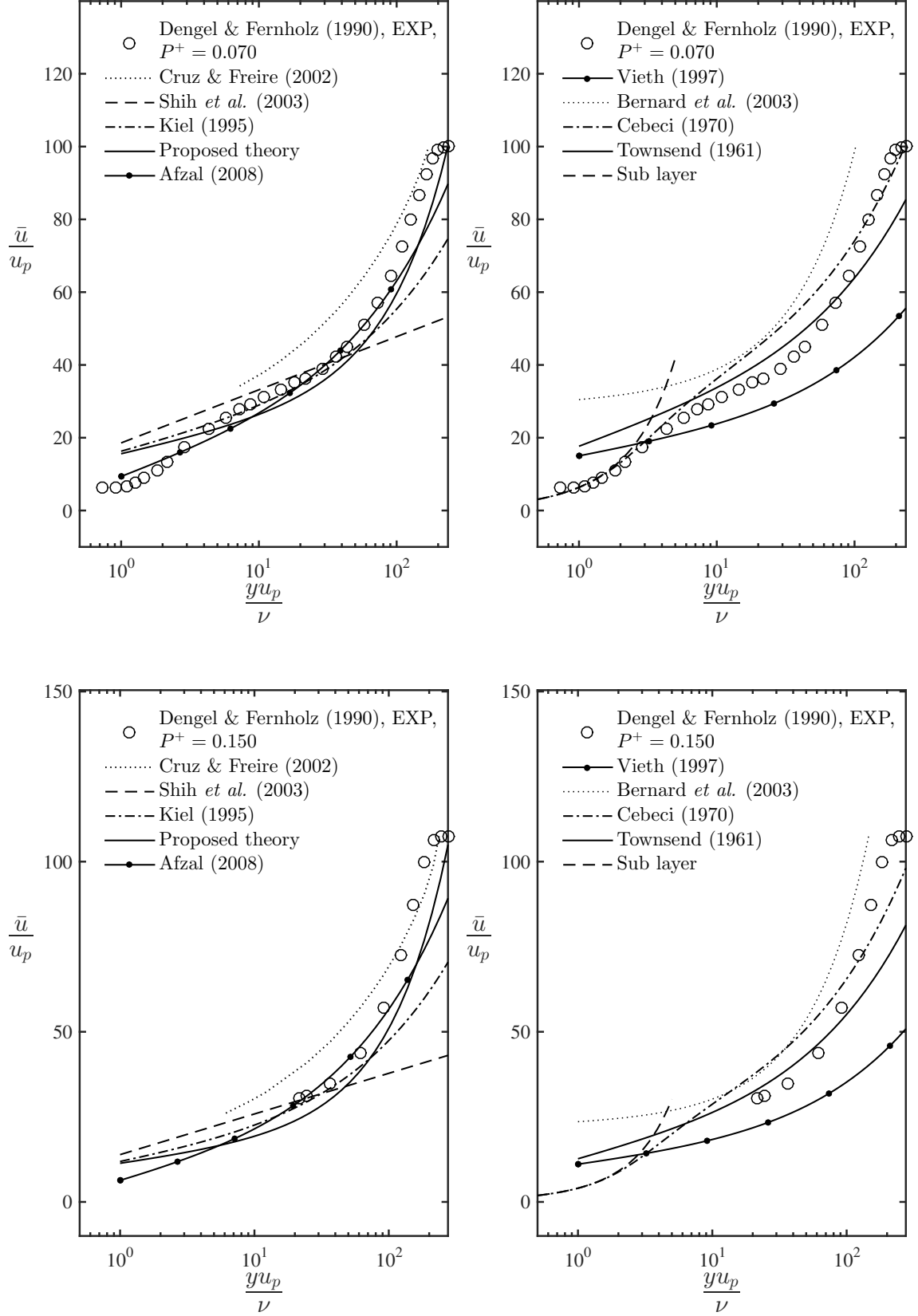


Figure B.82: Mean velocity profiles data compared to different formulations.

Bondary layer flow with separation

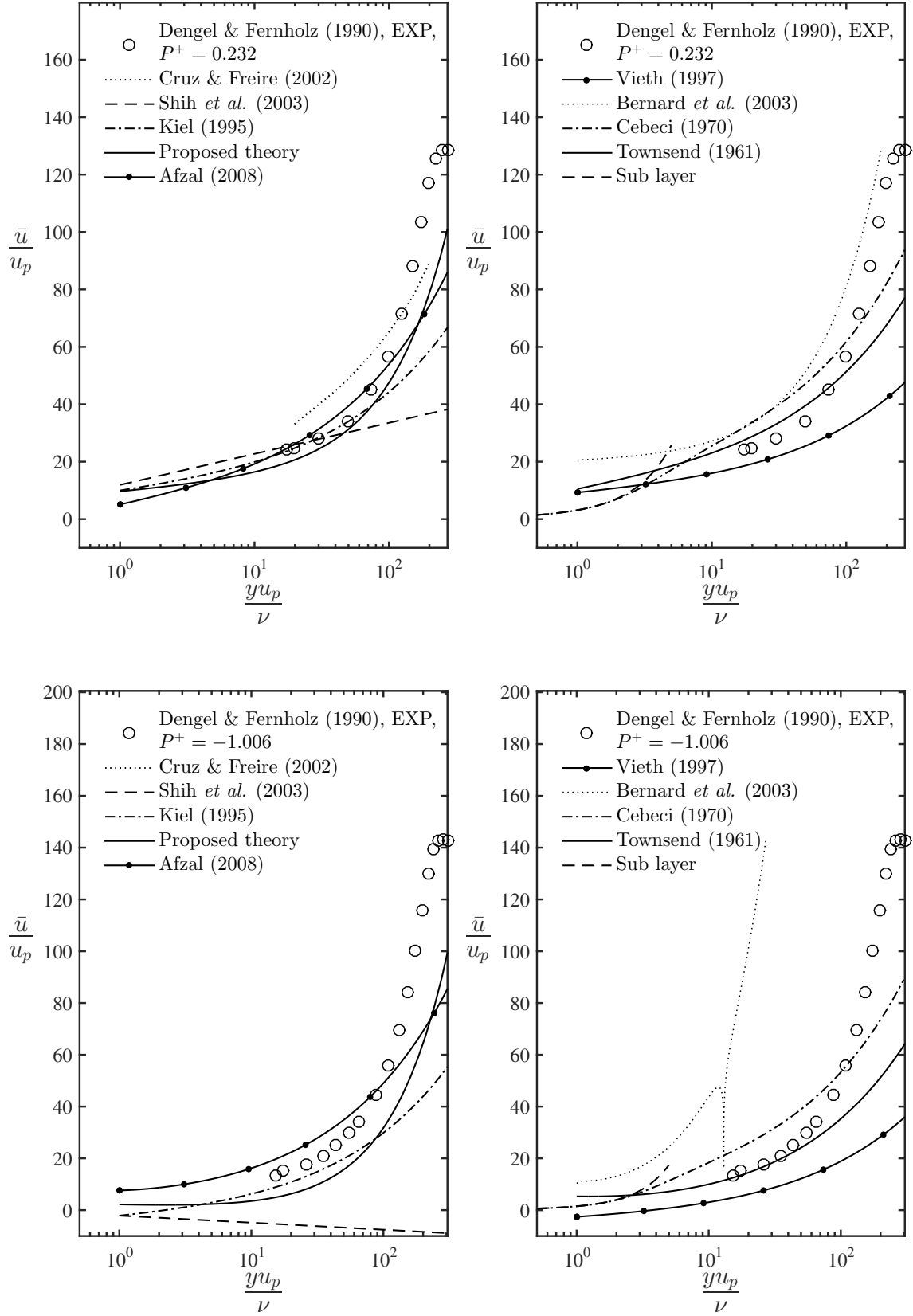


Figure B.83: Mean velocity profiles data compared to different formulations.

Bondary layer flow with separation

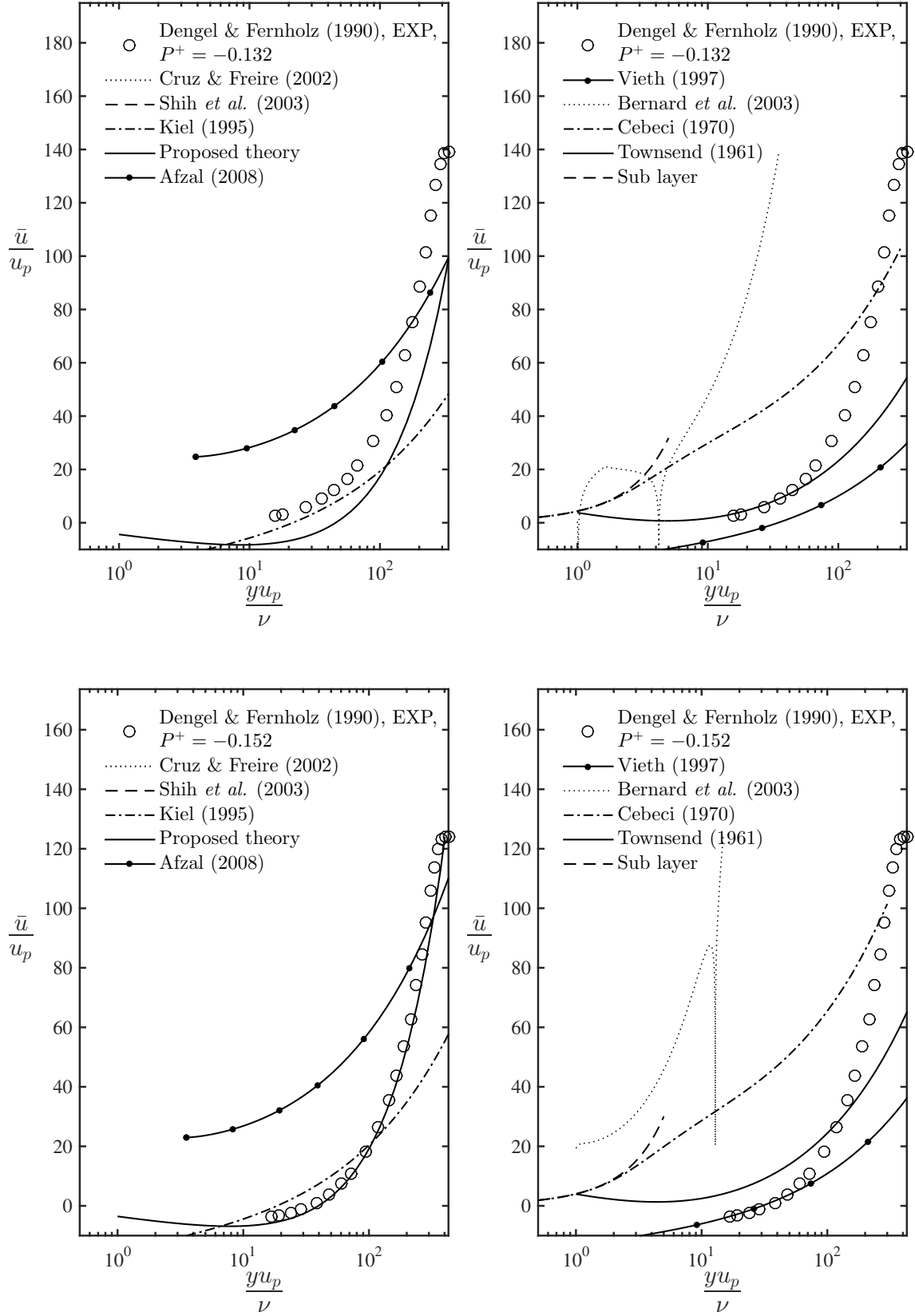


Figure B.84: Mean velocity profiles data compared to different formulations.

Bondary layer flow with separation

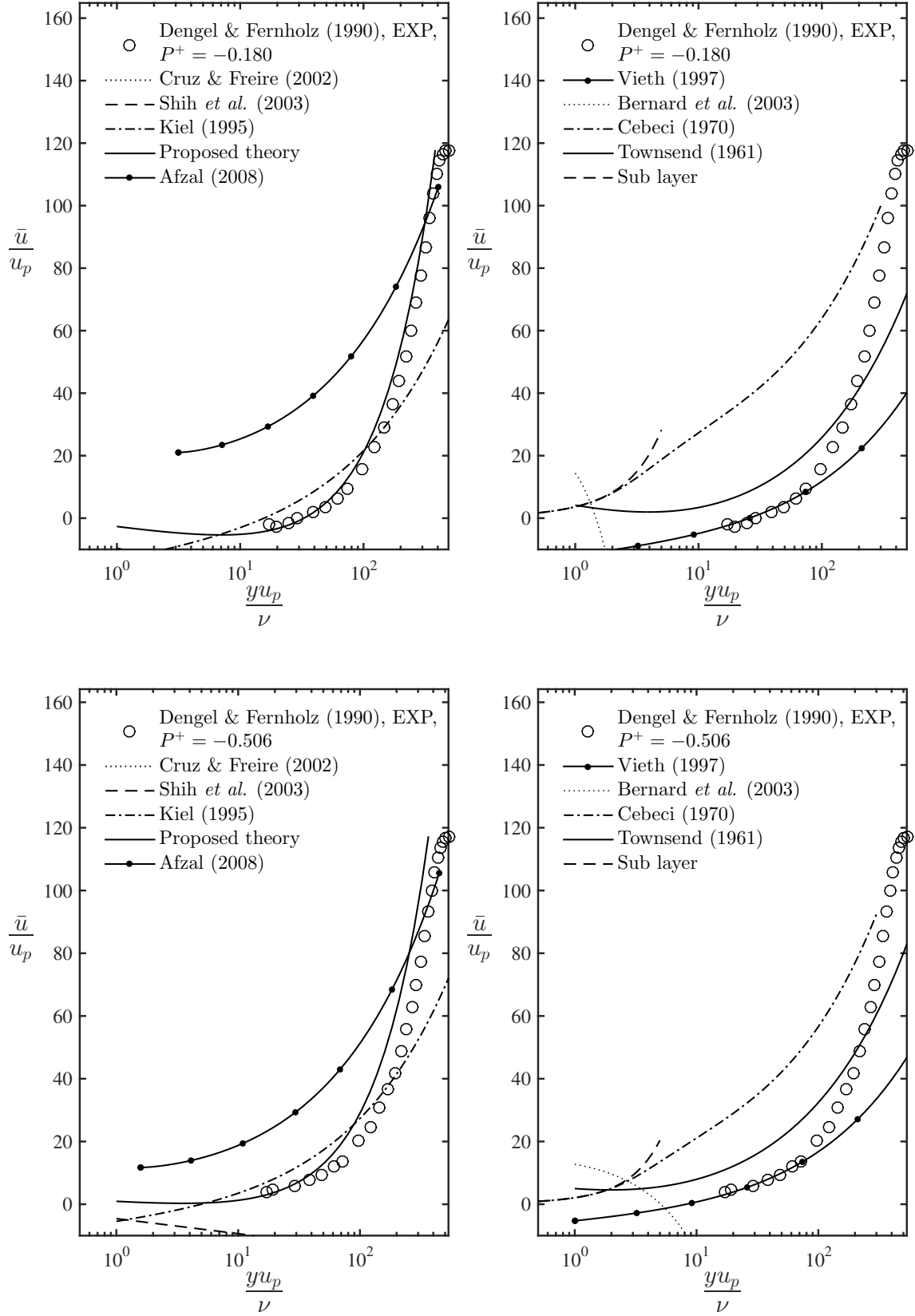


Figure B.85: Mean velocity profiles data compared to different formulations.

Bondary layer flow with separation

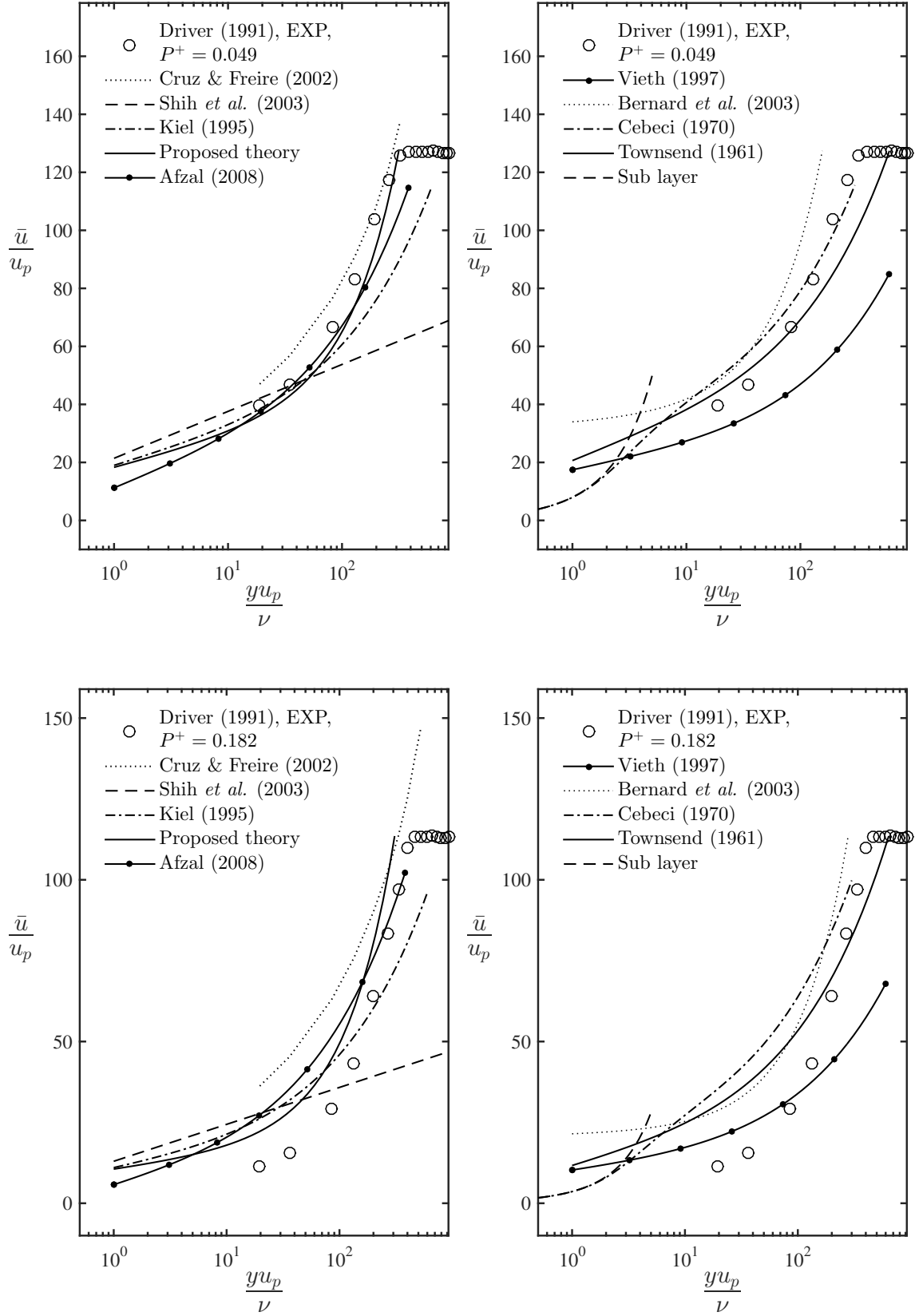


Figure B.86: Mean velocity profiles data compared to different formulations.

Bondary layer flow with separation

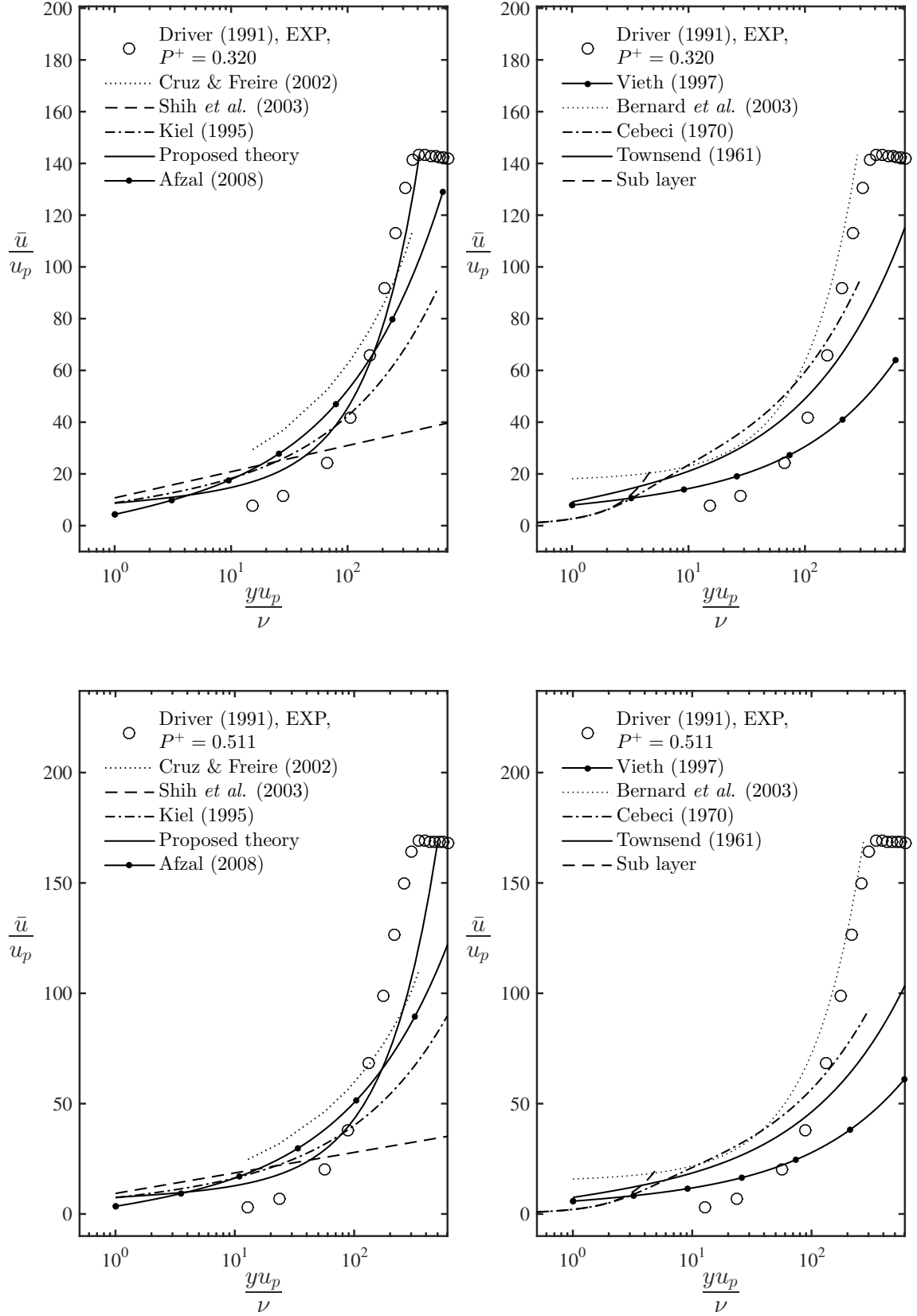


Figure B.87: Mean velocity profiles data compared to different formulations.

Bondary layer flow with separation

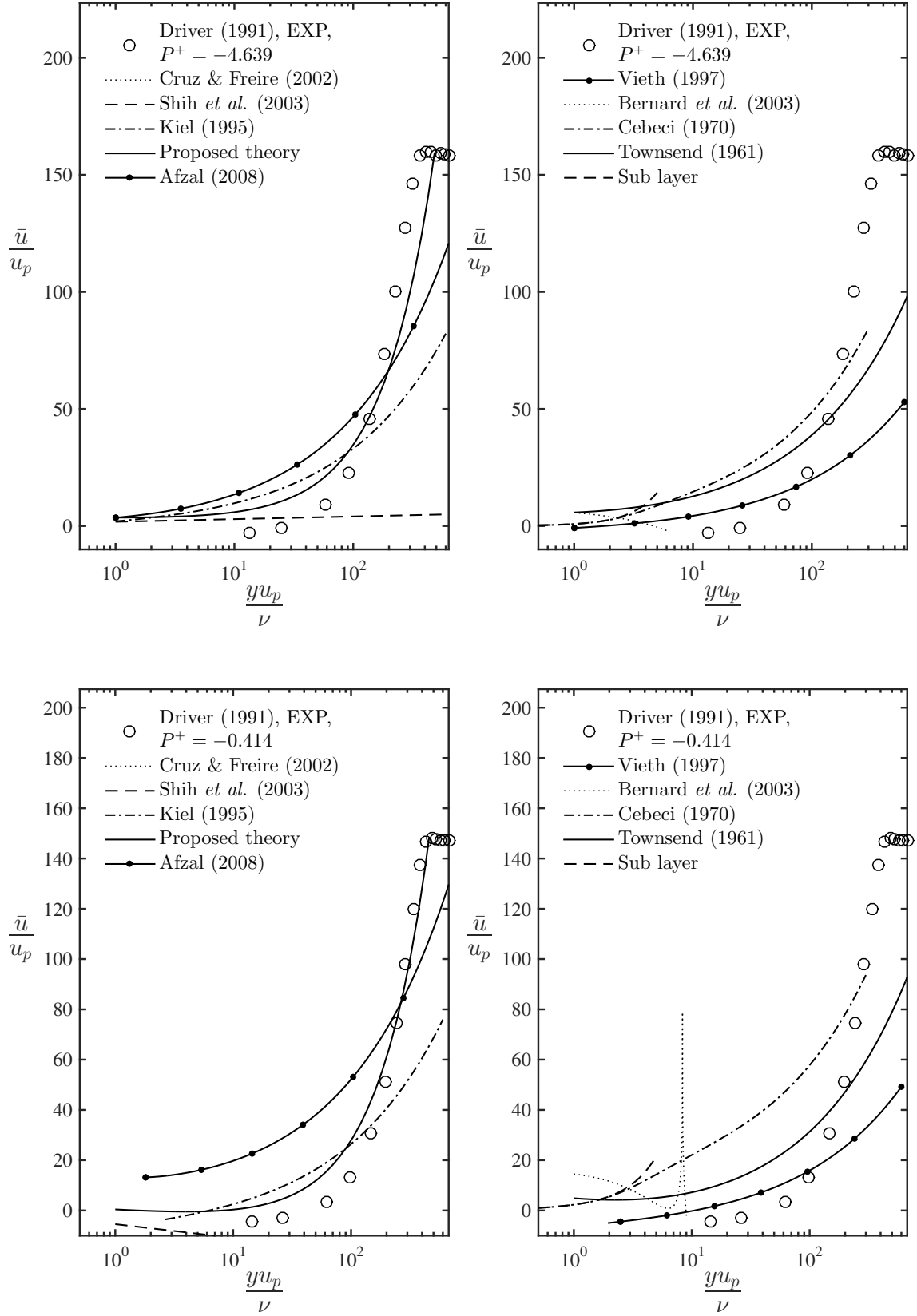


Figure B.88: Mean velocity profiles data compared to different formulations.

Bondary layer flow with separation

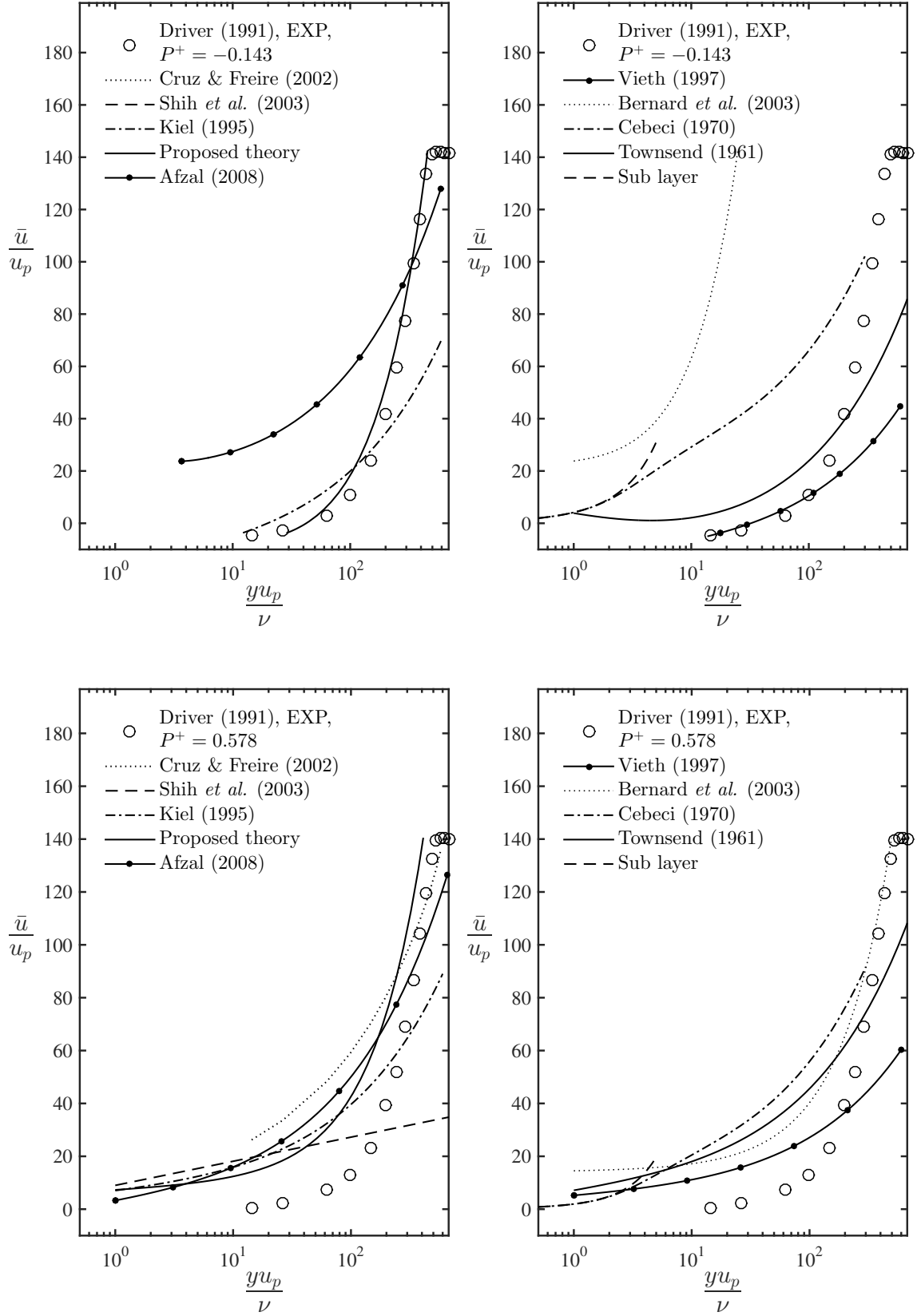


Figure B.89: Mean velocity profiles data compared to different formulations.

Bondary layer flow with separation

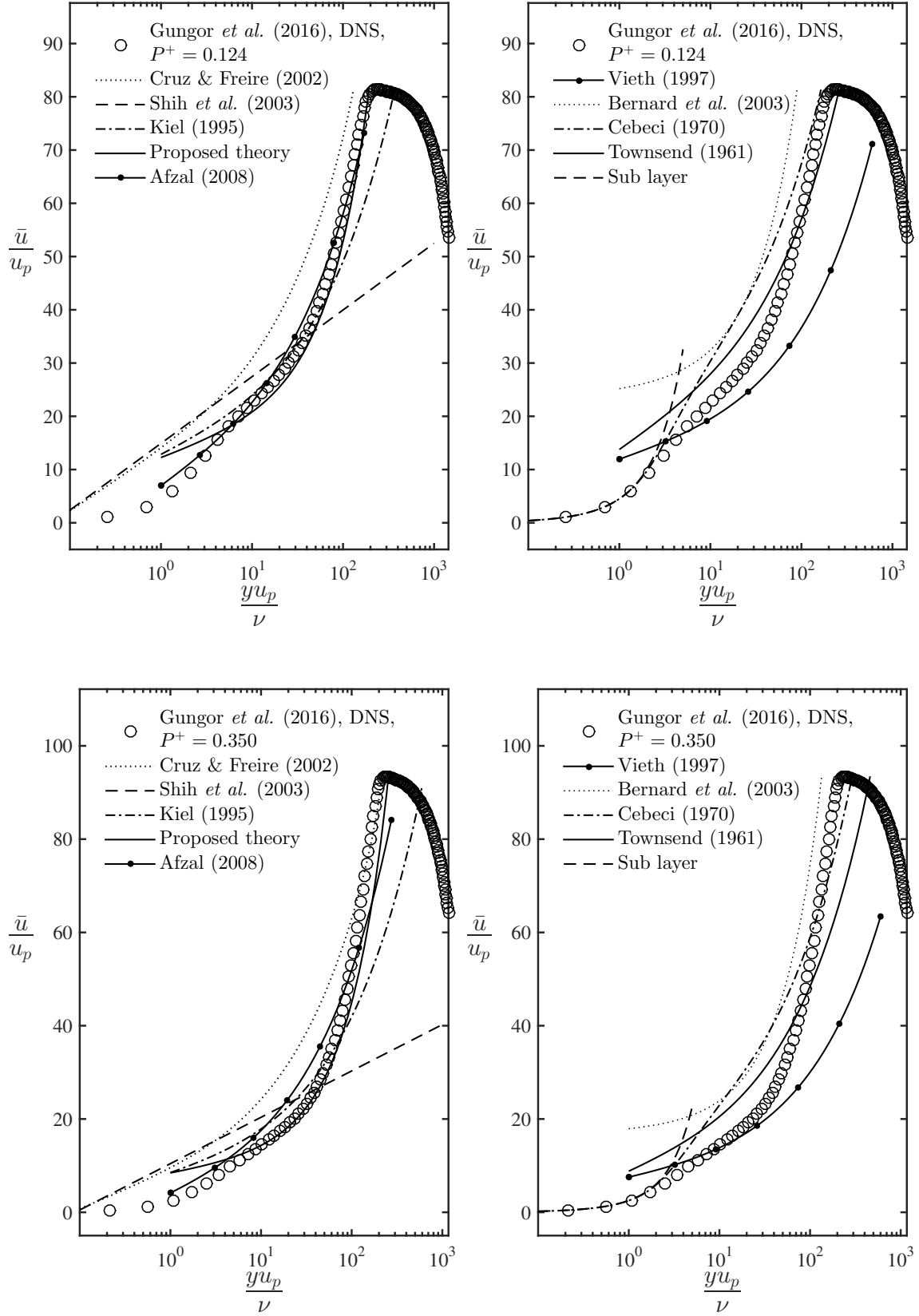


Figure B.90: Mean velocity profiles data compared to different formulations.

Bondary layer flow with separation

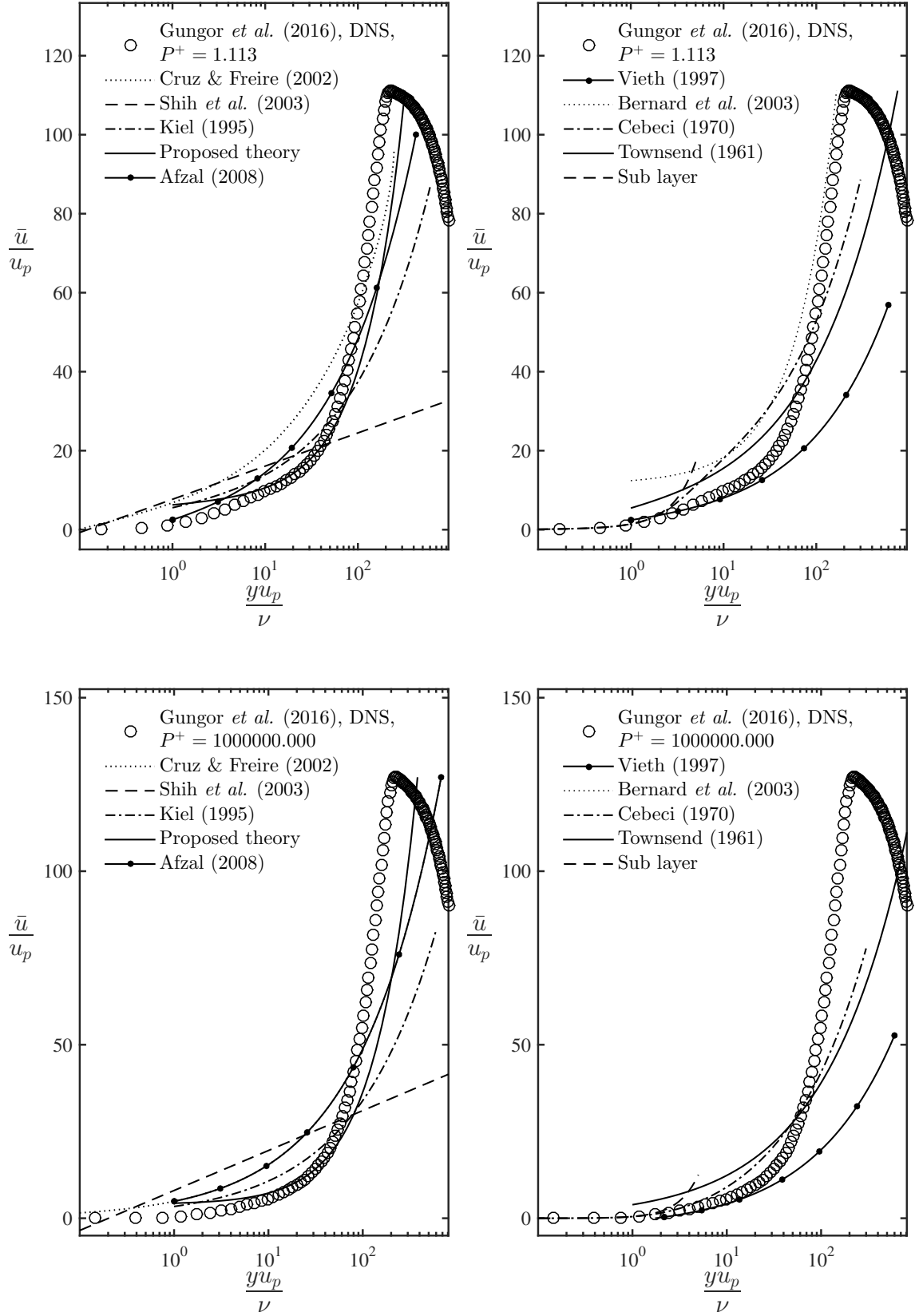


Figure B.91: Mean velocity profiles data compared to different formulations.

Bondary layer flow with separation

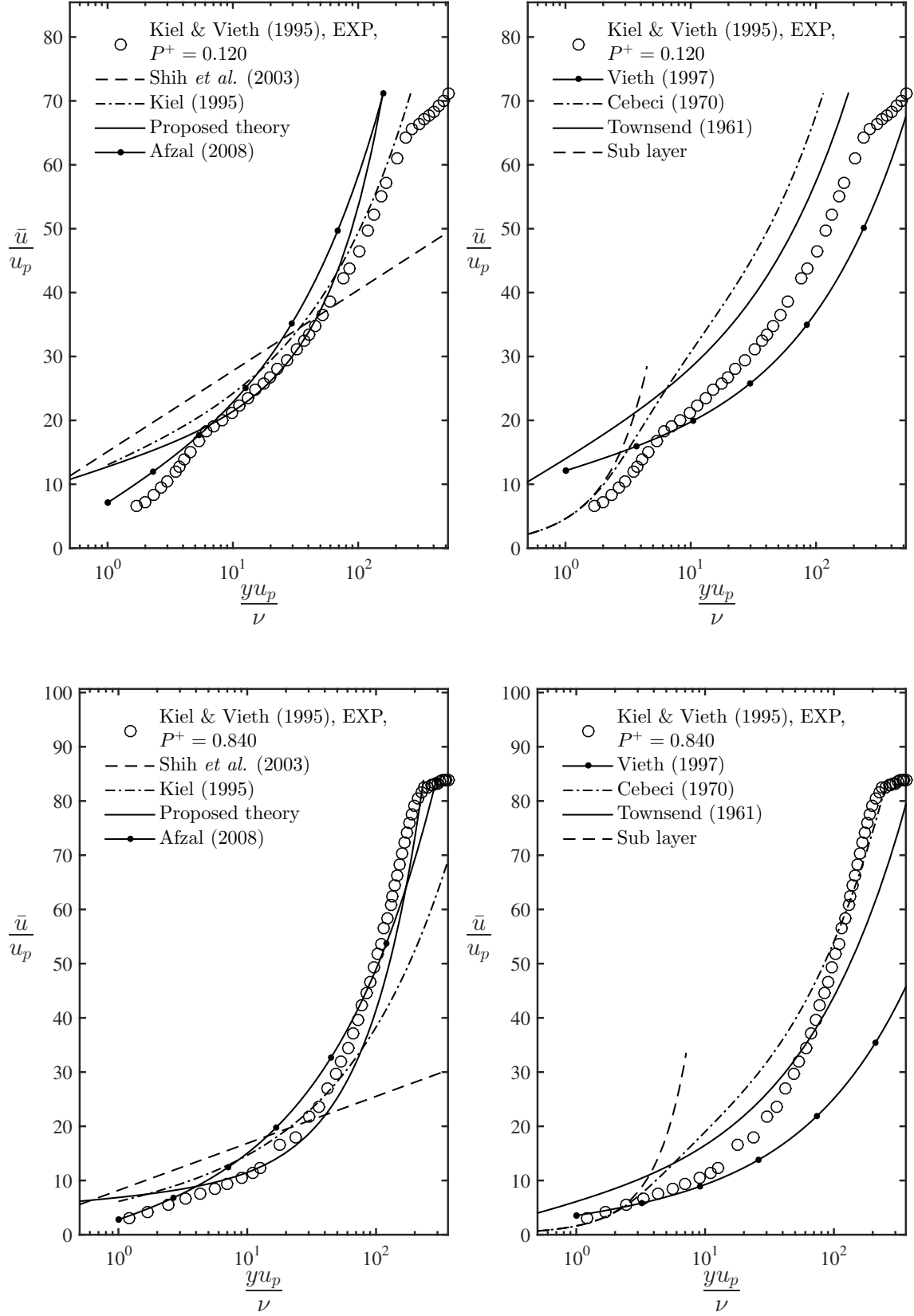


Figure B.92: Mean velocity profiles data compared to different formulations.

Bondary layer flow with separation

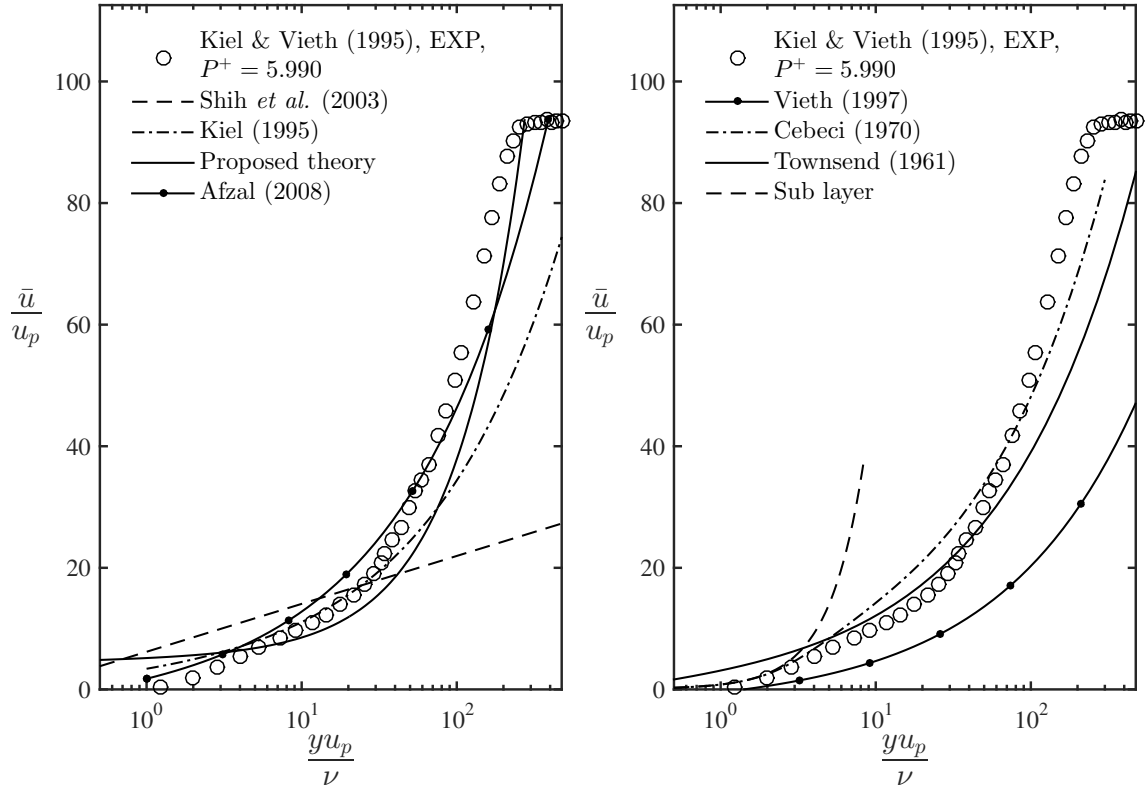


Figure B.93: Mean velocity profiles data compared to different formulations.

Bondary layer flow with separation

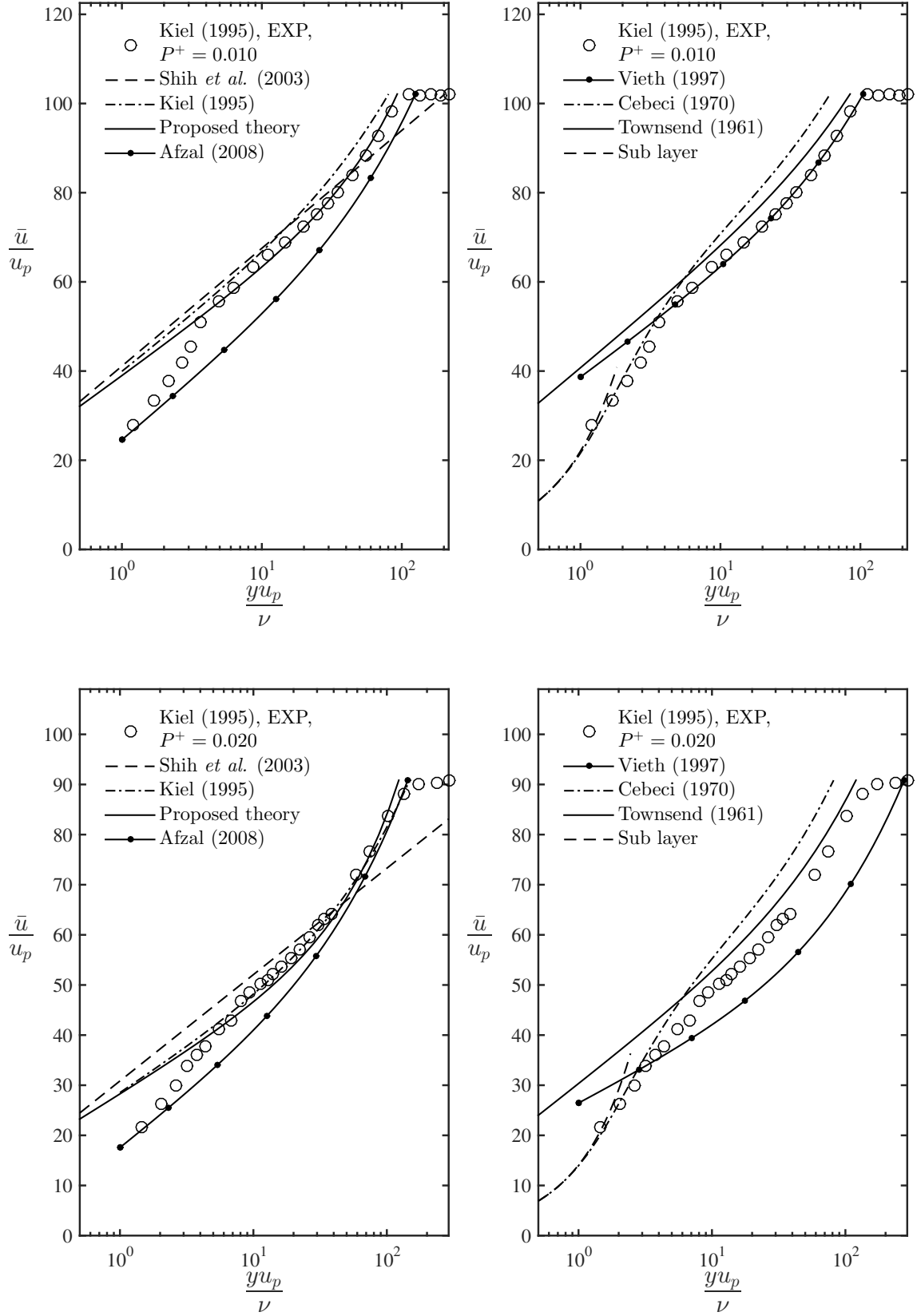


Figure B.94: Mean velocity profiles data compared to different formulations.

Bondary layer flow with separation

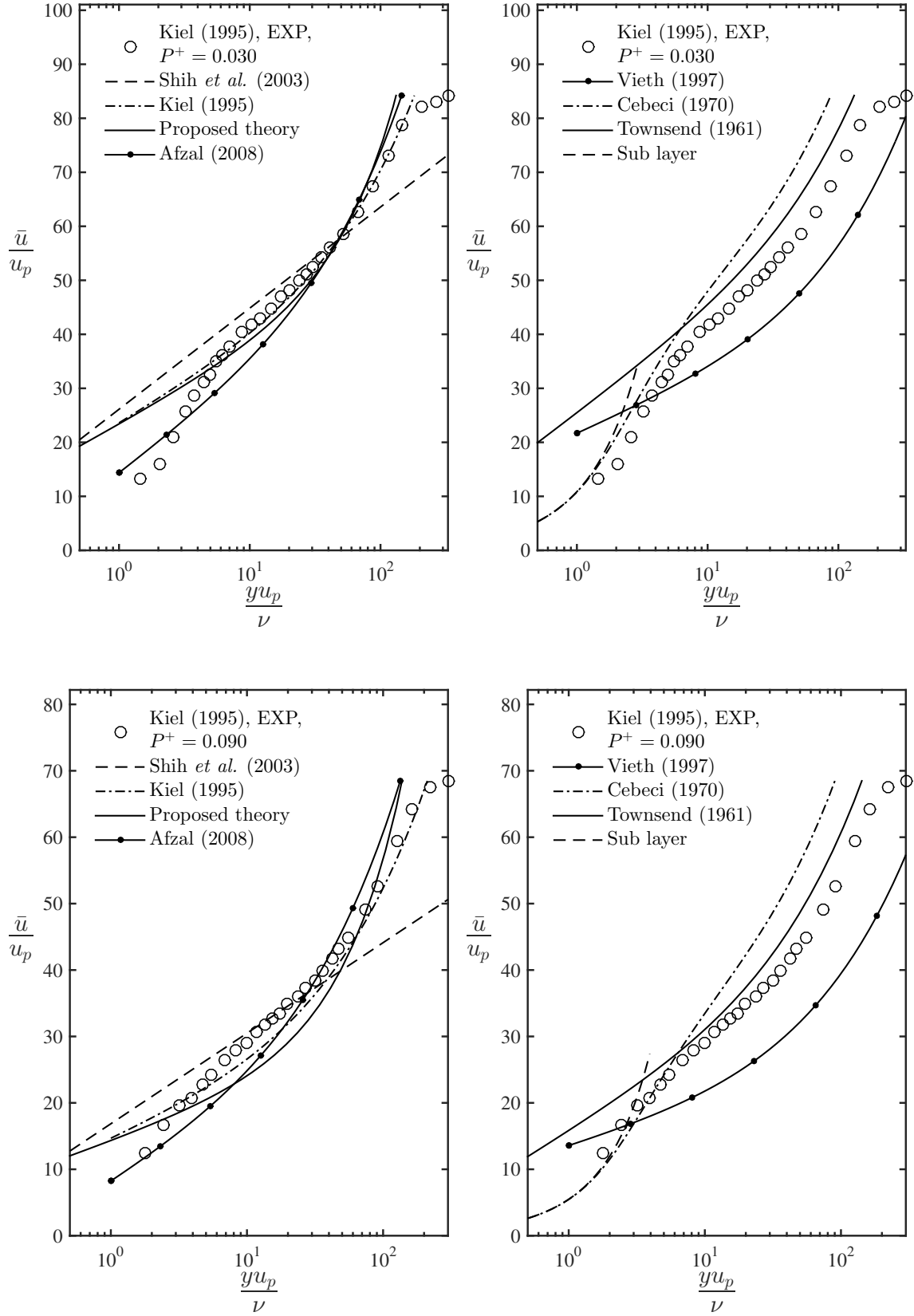


Figure B.95: Mean velocity profiles data compared to different formulations.

Bondary layer flow with separation

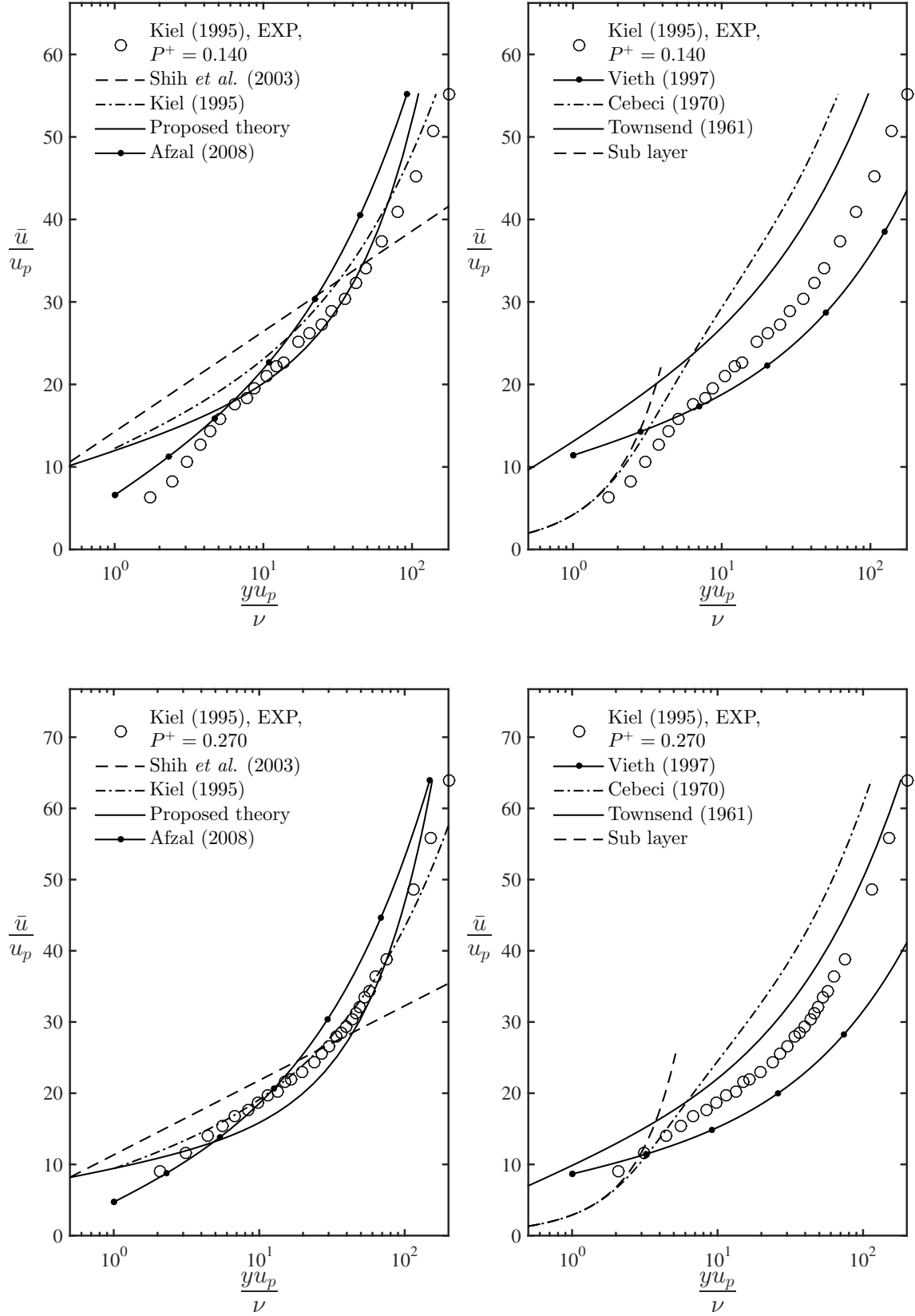


Figure B.96: Mean velocity profiles data compared to different formulations.

Bondary layer flow with separation

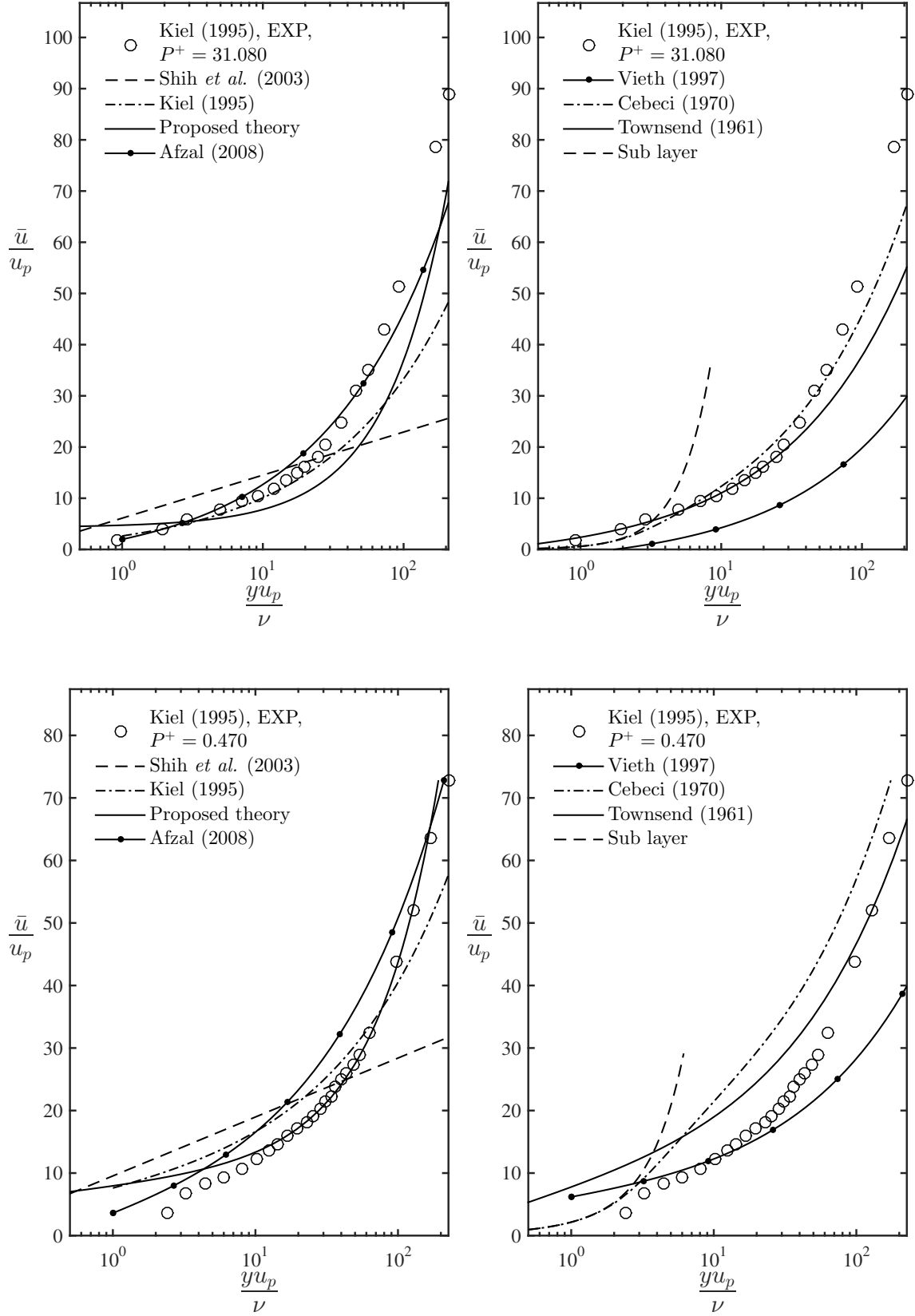


Figure B.97: Mean velocity profiles data compared to different formulations.

Mild APG boundary layer flow

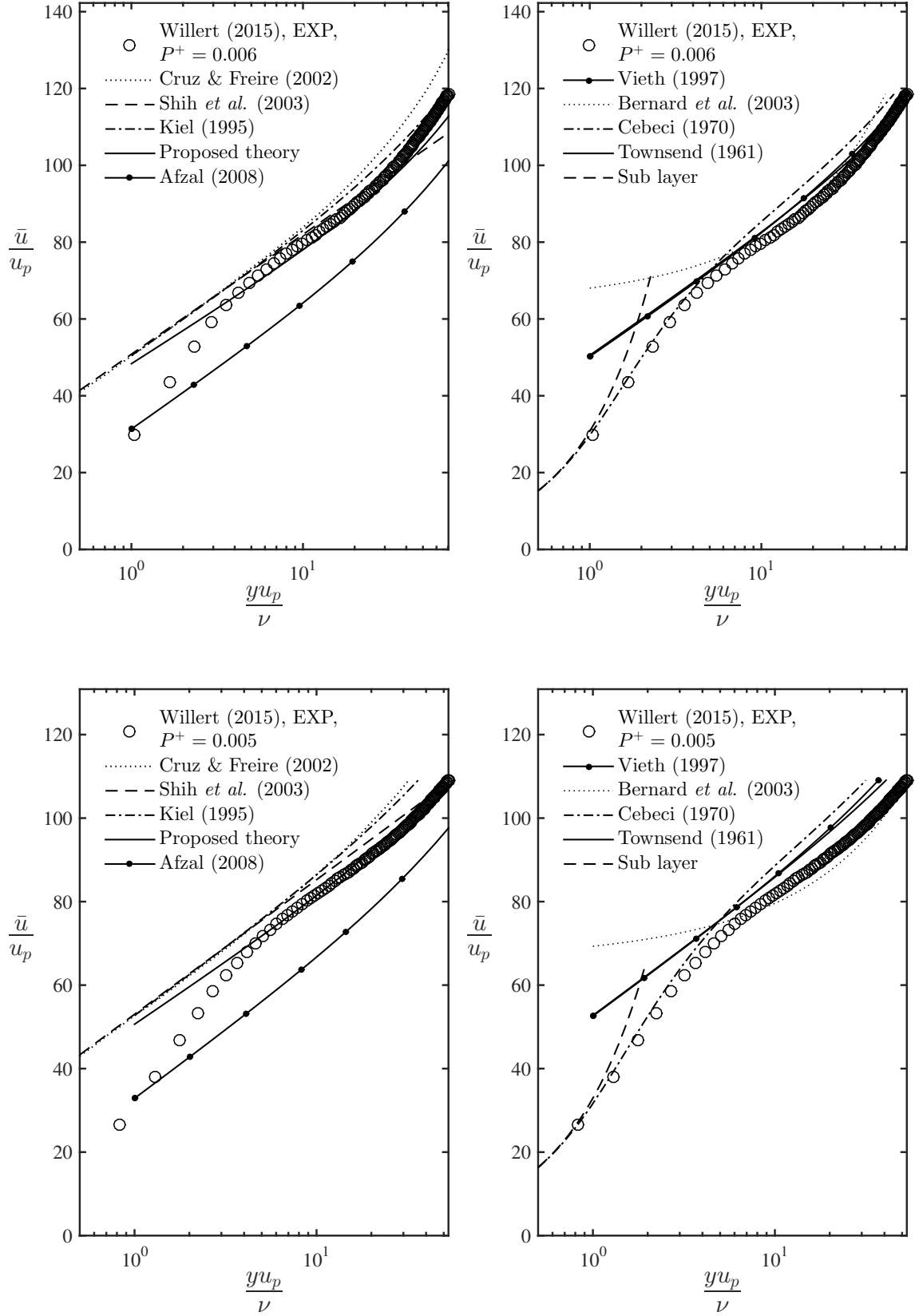


Figure B.98: Mean velocity profiles data compared to different formulations.

Mild APG boundary layer flow

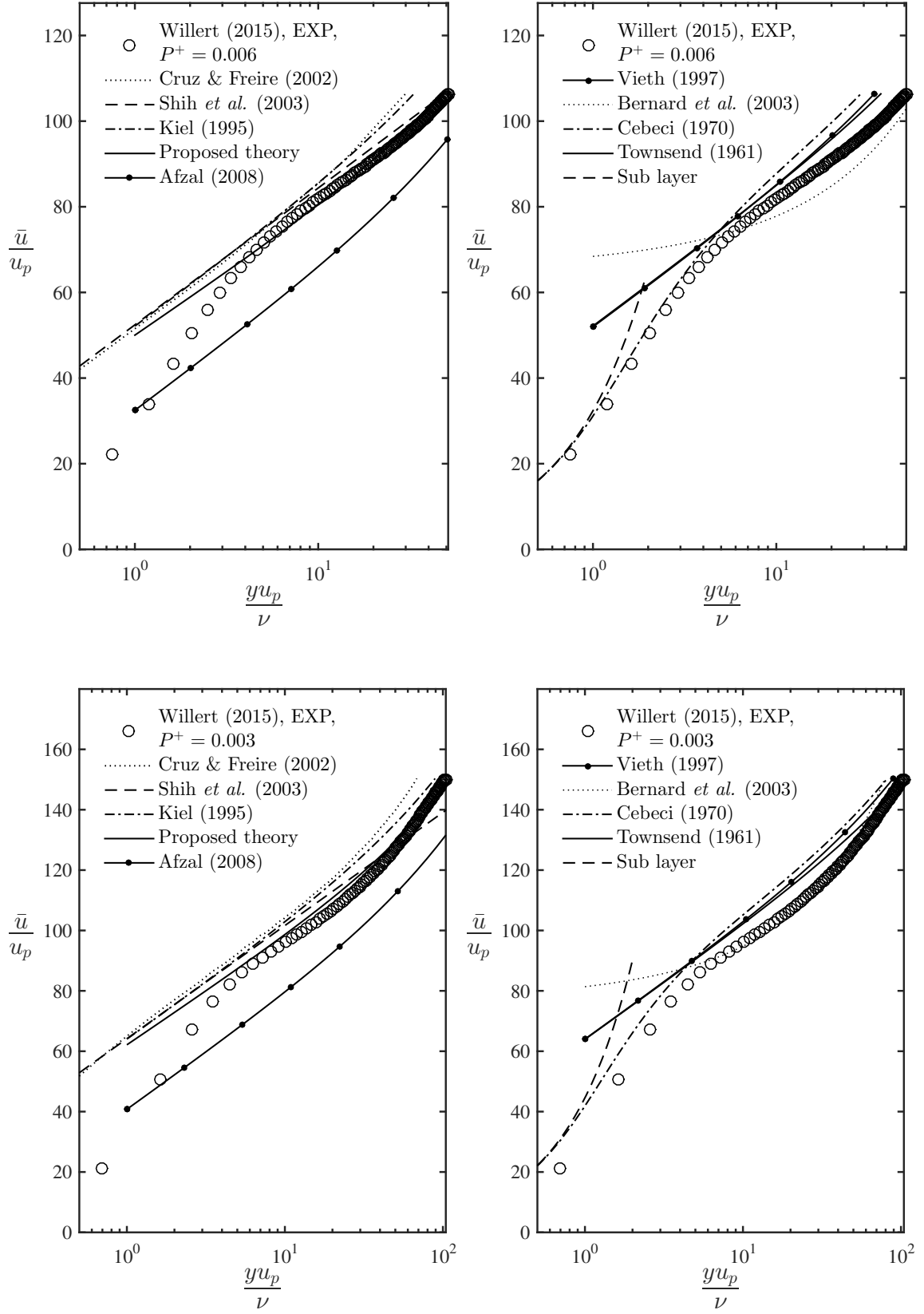


Figure B.99: Mean velocity profiles data compared to different formulations.

Mild APG boundary layer flow

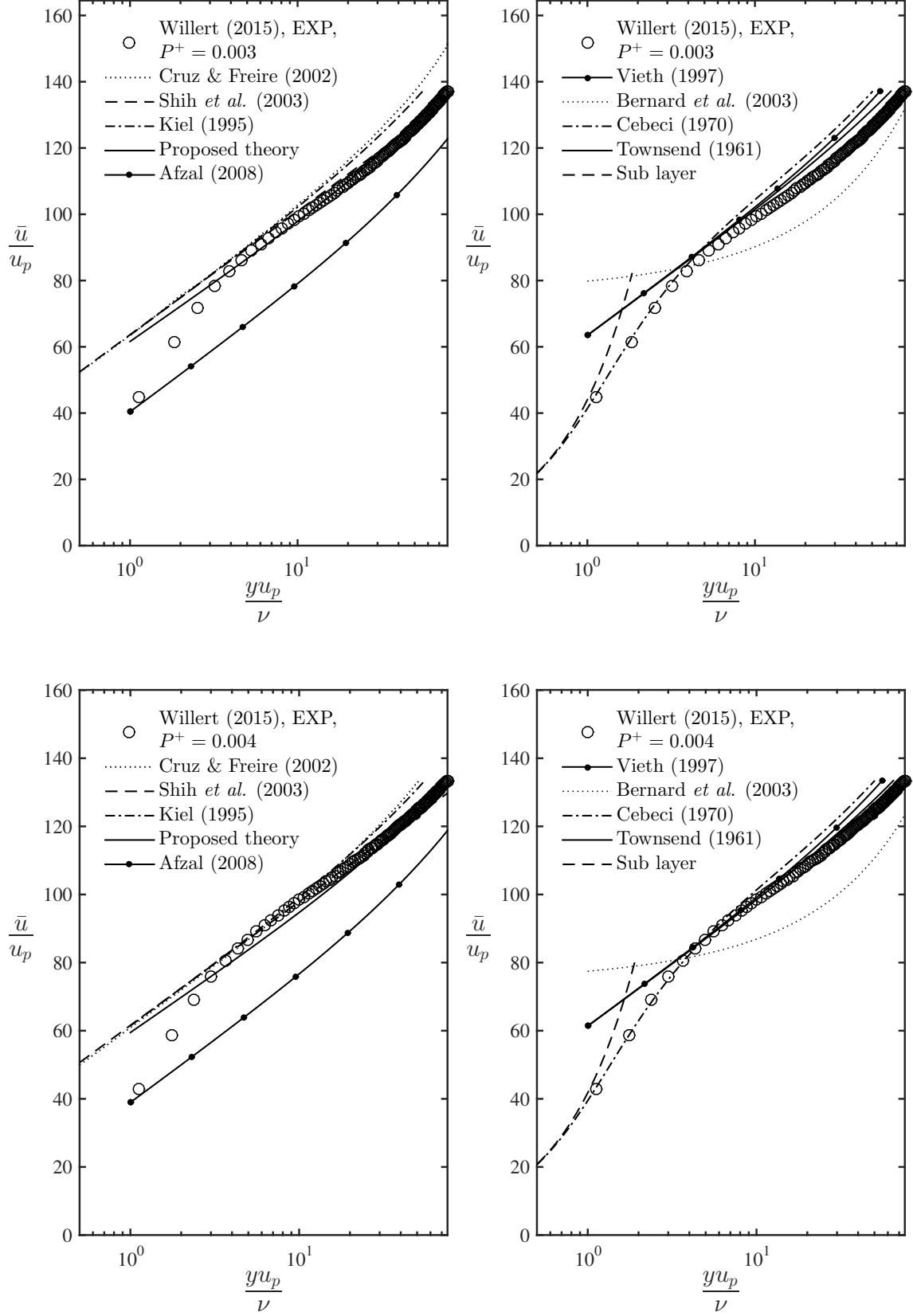


Figure B.100: Mean velocity profiles data compared to different formulations.

Bondary layer flow with separation

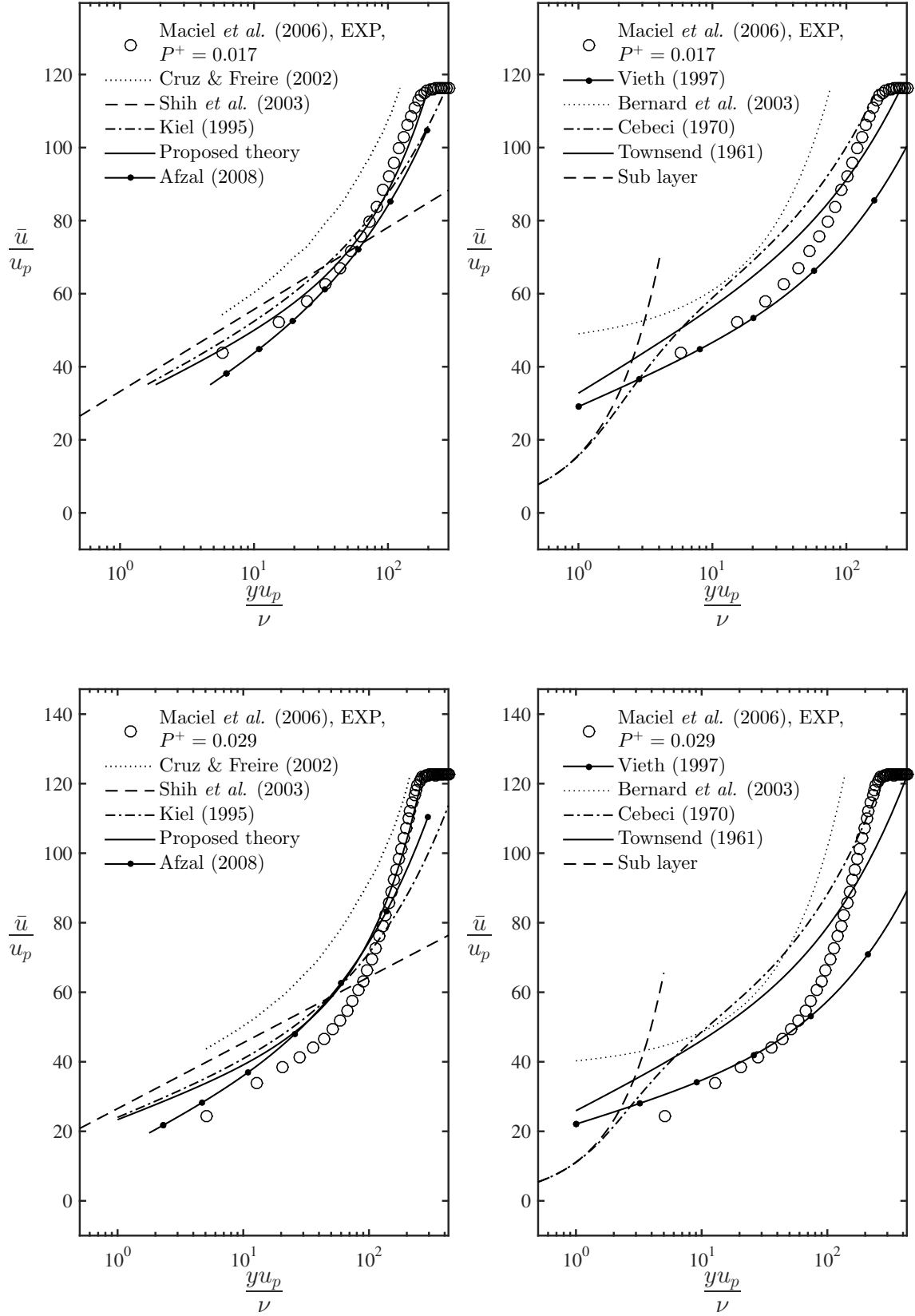


Figure B.101: Mean velocity profiles data compared to different formulations.

Bondary layer flow with separation

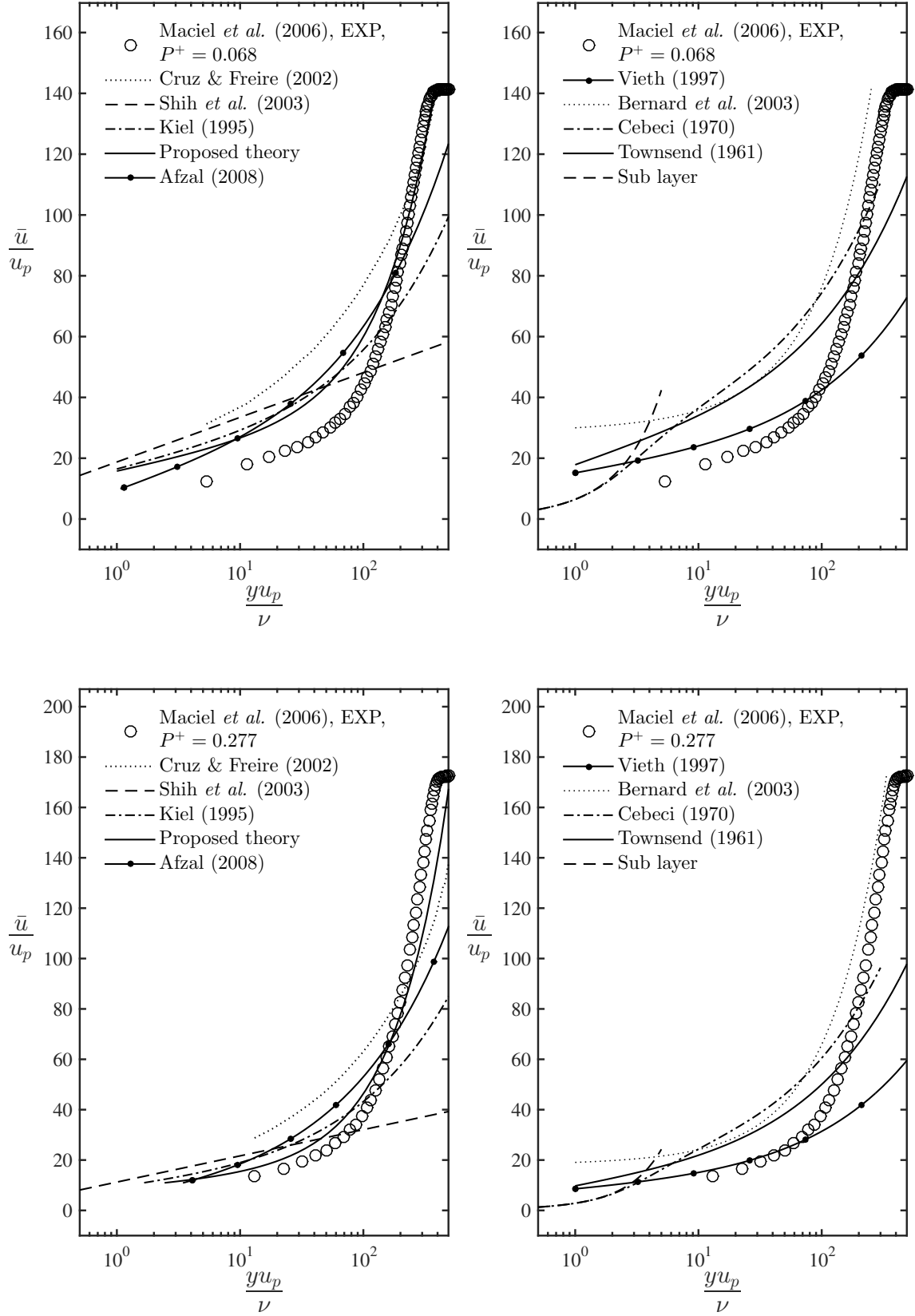


Figure B.102: Mean velocity profiles data compared to different formulations.

Bondary layer flow with separation

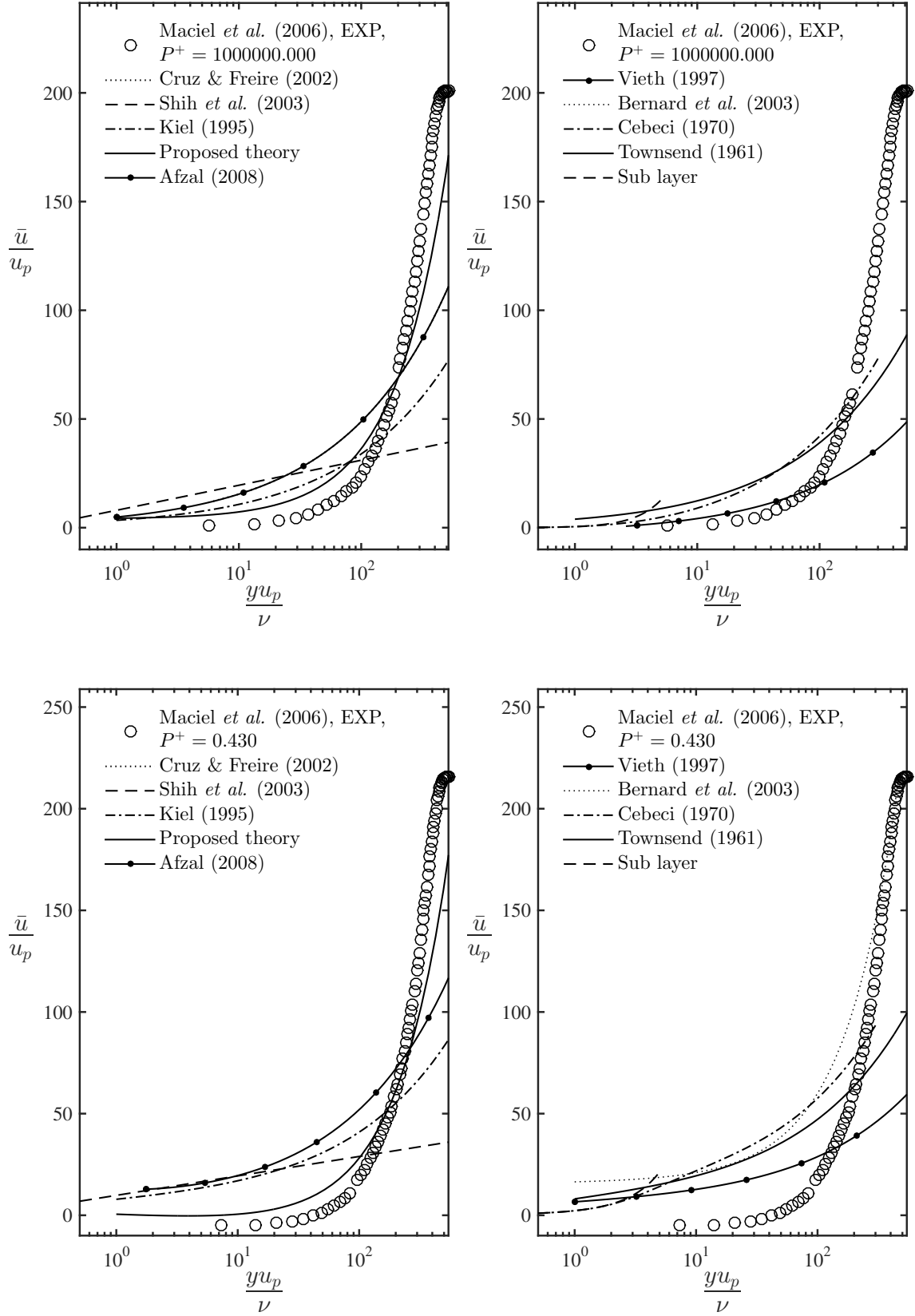


Figure B.103: Mean velocity profiles data compared to different formulations.

Mild APG boundary layer flow

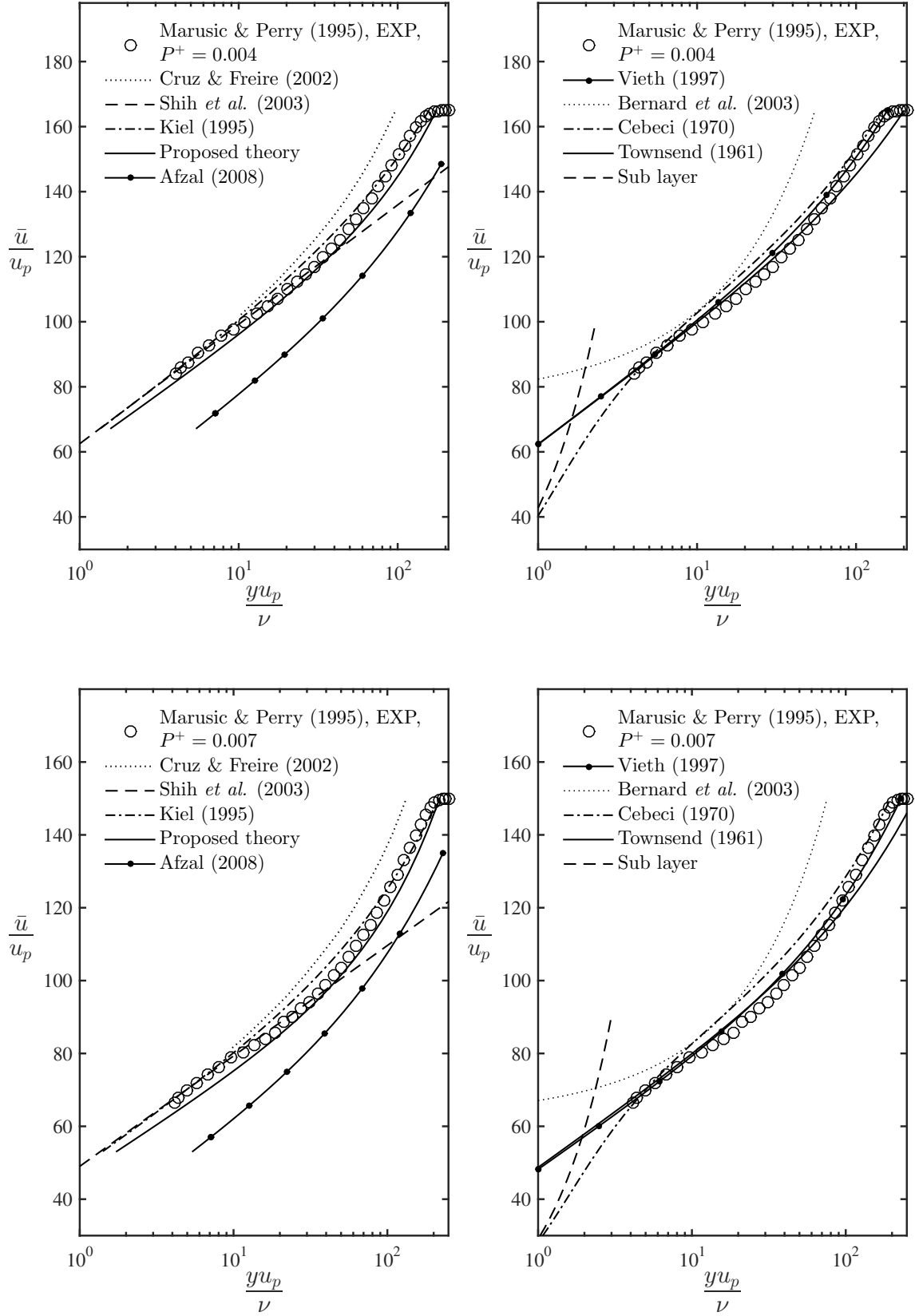


Figure B.104: Mean velocity profiles data compared to different formulations.

Mild APG boundary layer flow

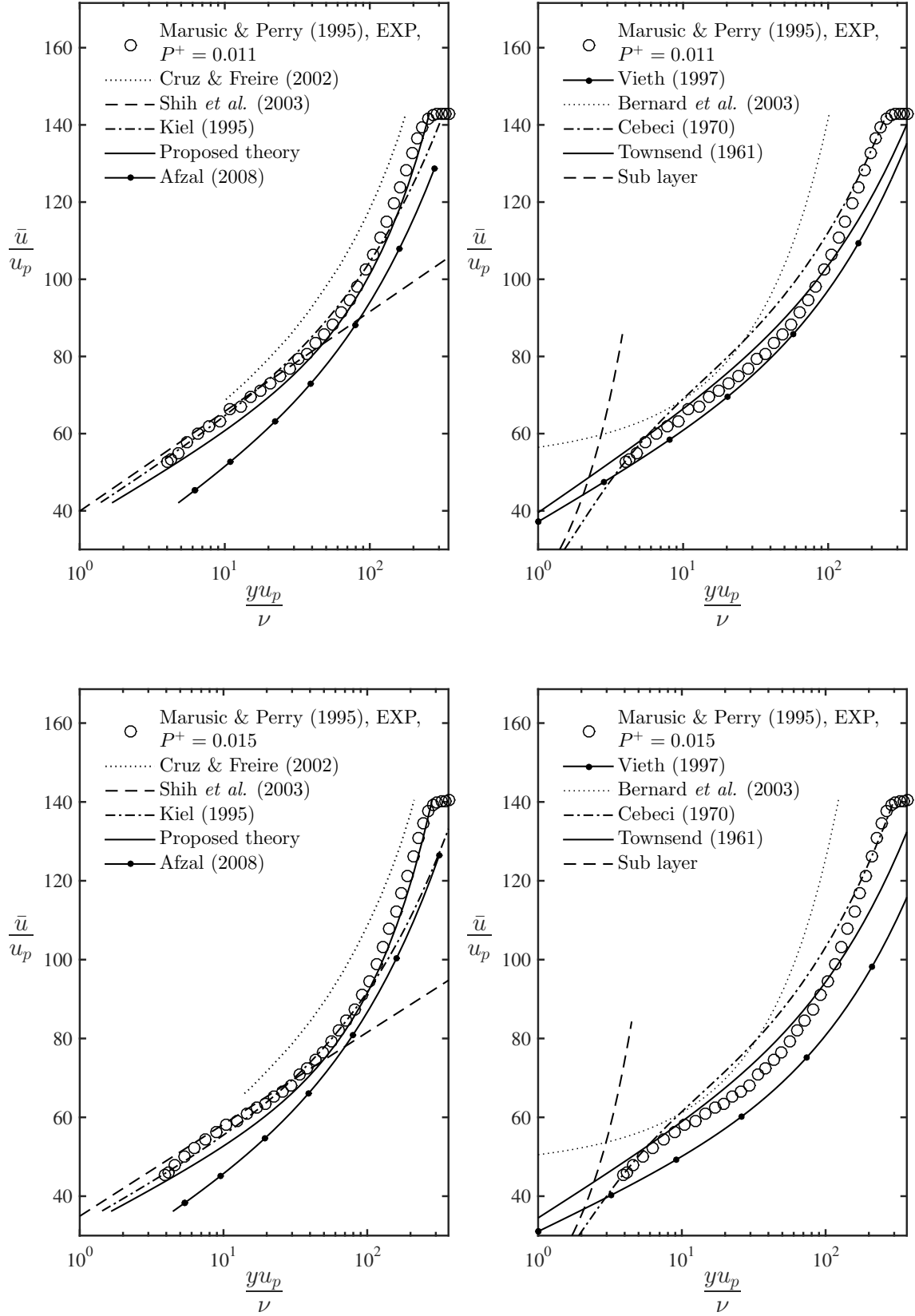


Figure B.105: Mean velocity profiles data compared to different formulations.

Mild APG boundary layer flow

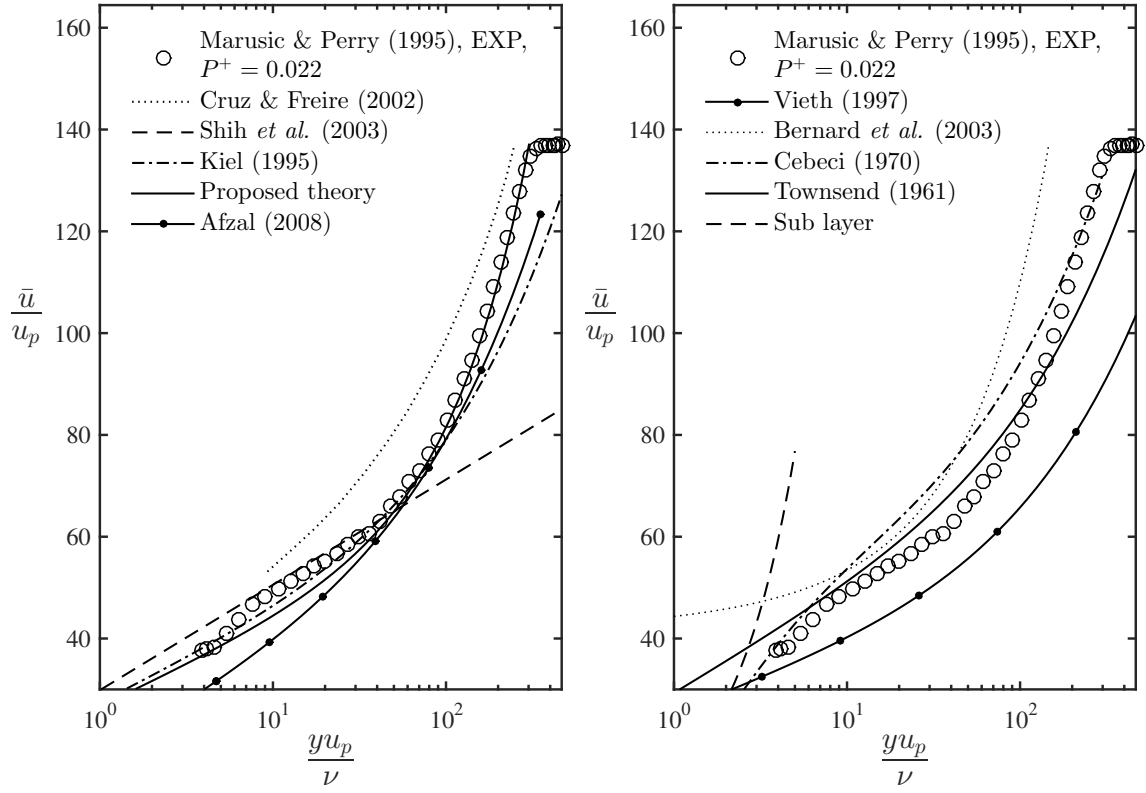


Figure B.106: Mean velocity profiles data compared to different formulations.

Mild APG boundary layer flow

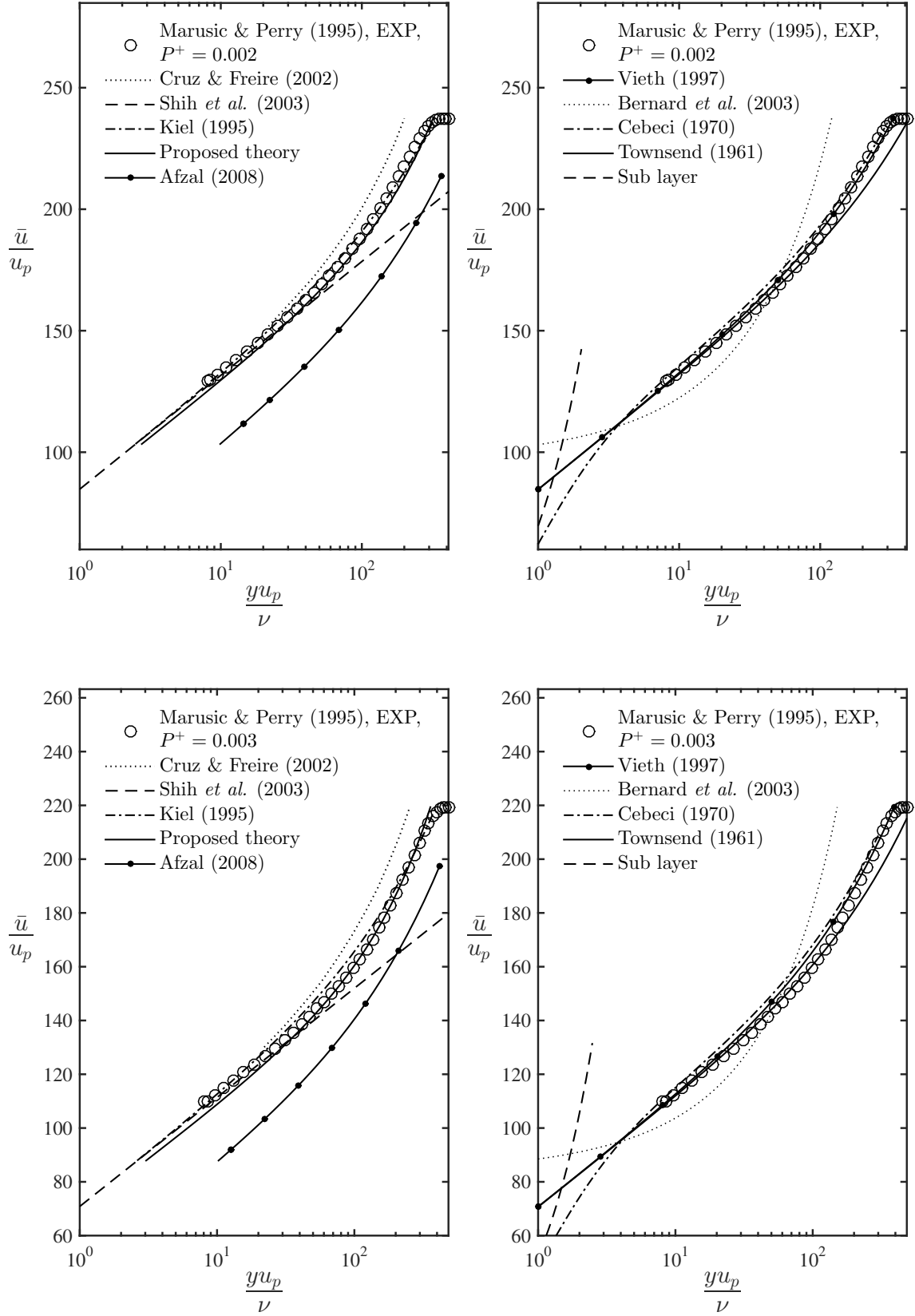


Figure B.107: Mean velocity profiles data compared to different formulations.

Mild APG boundary layer flow

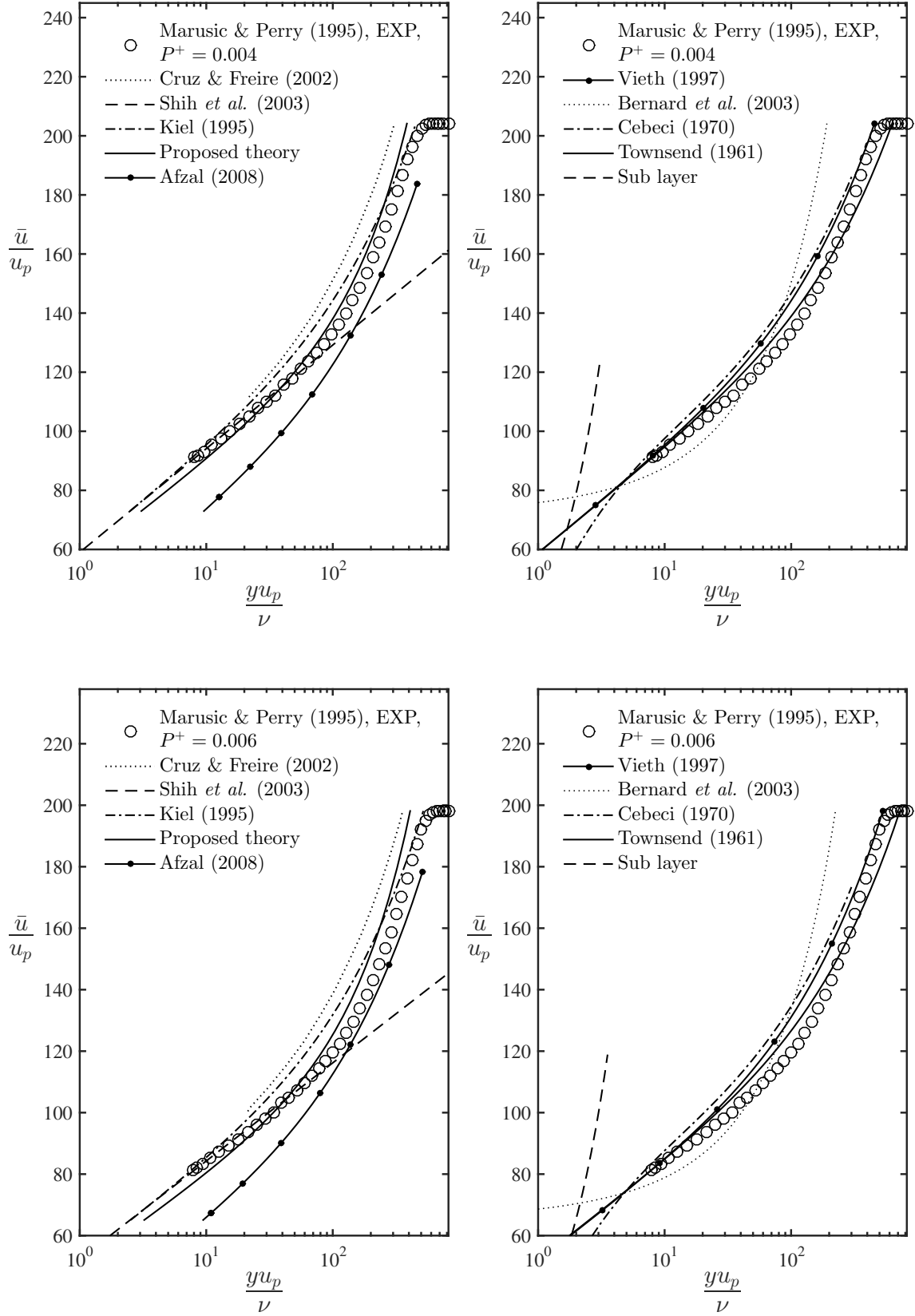


Figure B.108: Mean velocity profiles data compared to different formulations.

Mild APG boundary layer flow

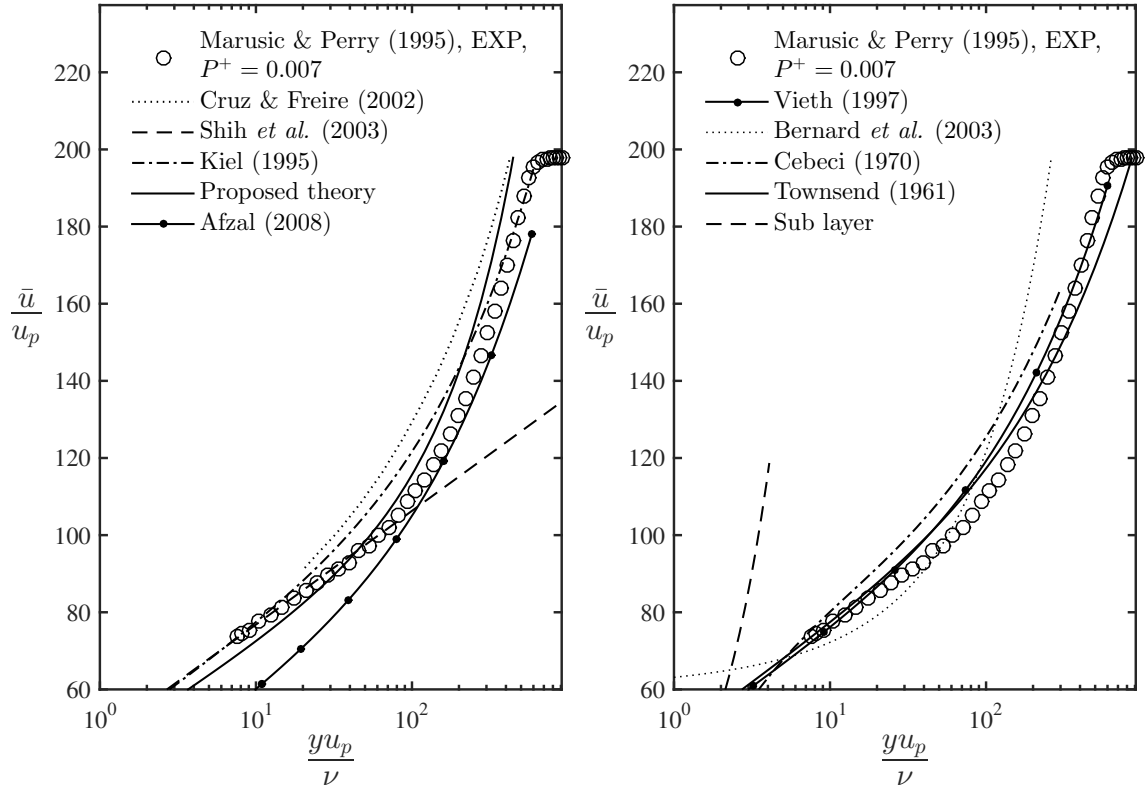


Figure B.109: Mean velocity profiles data compared to different formulations.

High APG boundary layer flow

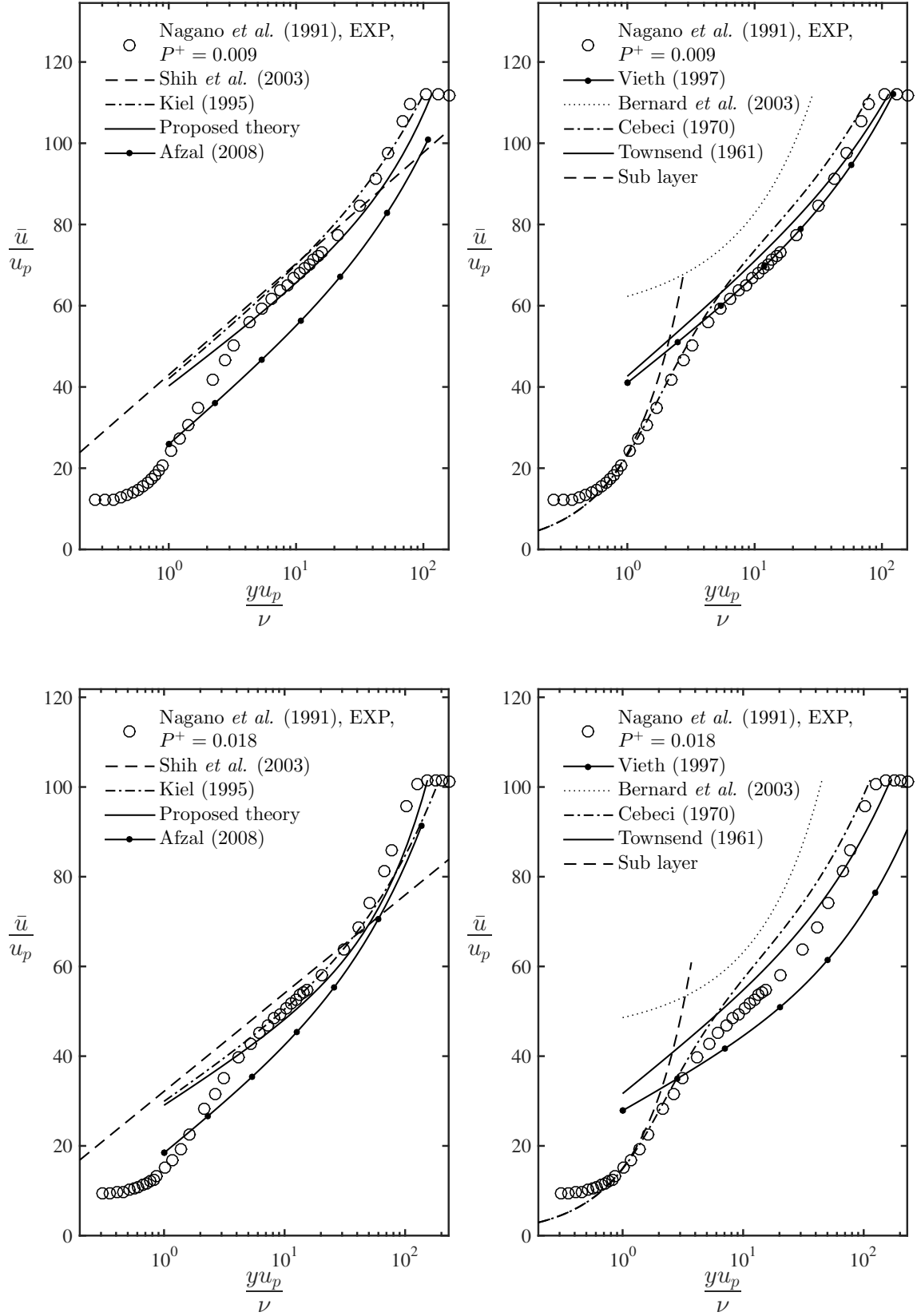


Figure B.110: Mean velocity profiles data compared to different formulations.

High APG boundary layer flow

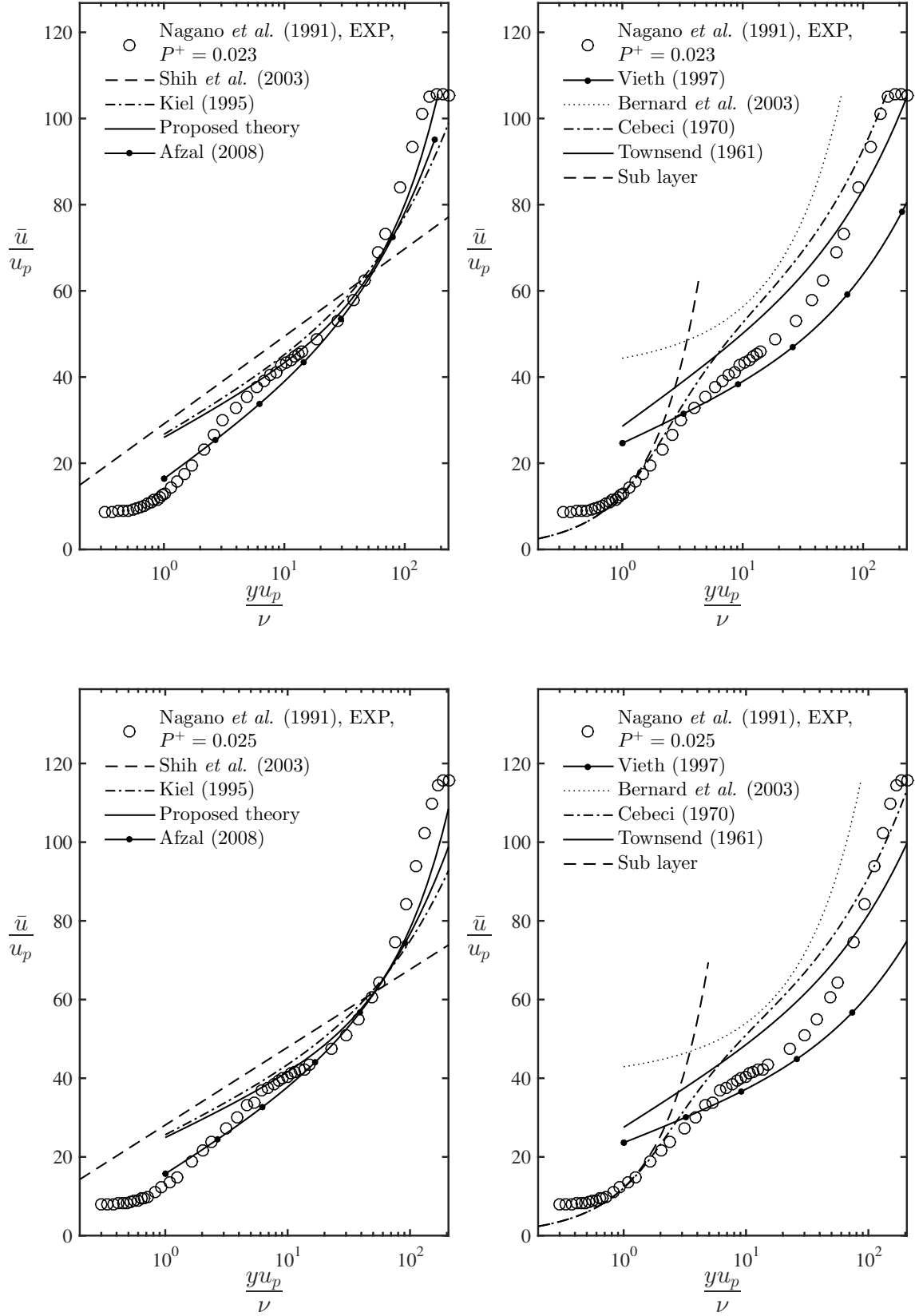


Figure B.111: Mean velocity profiles data compared to different formulations.

High APG boundary layer flow

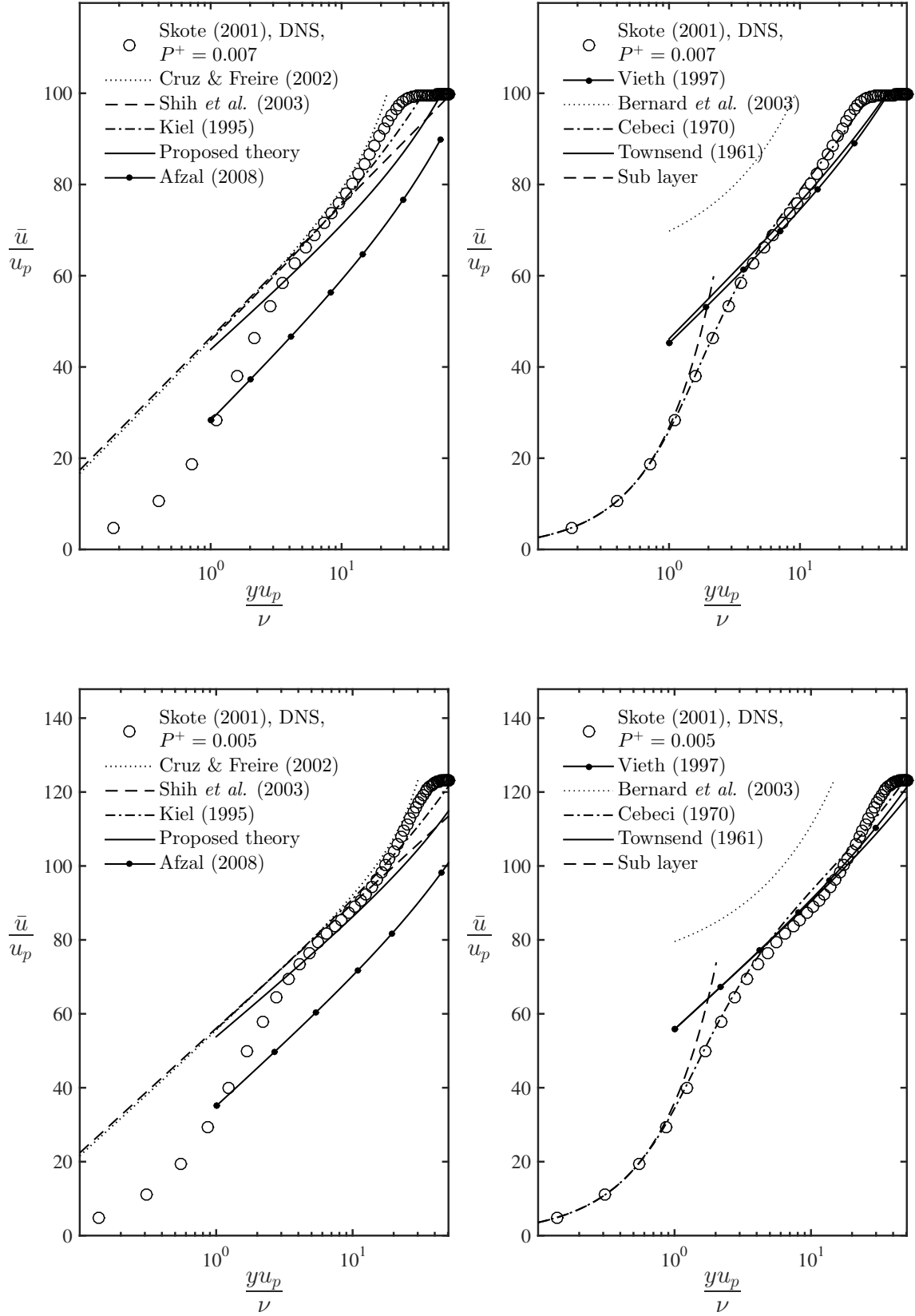


Figure B.112: Mean velocity profiles data compared to different formulations.

High APG boundary layer flow

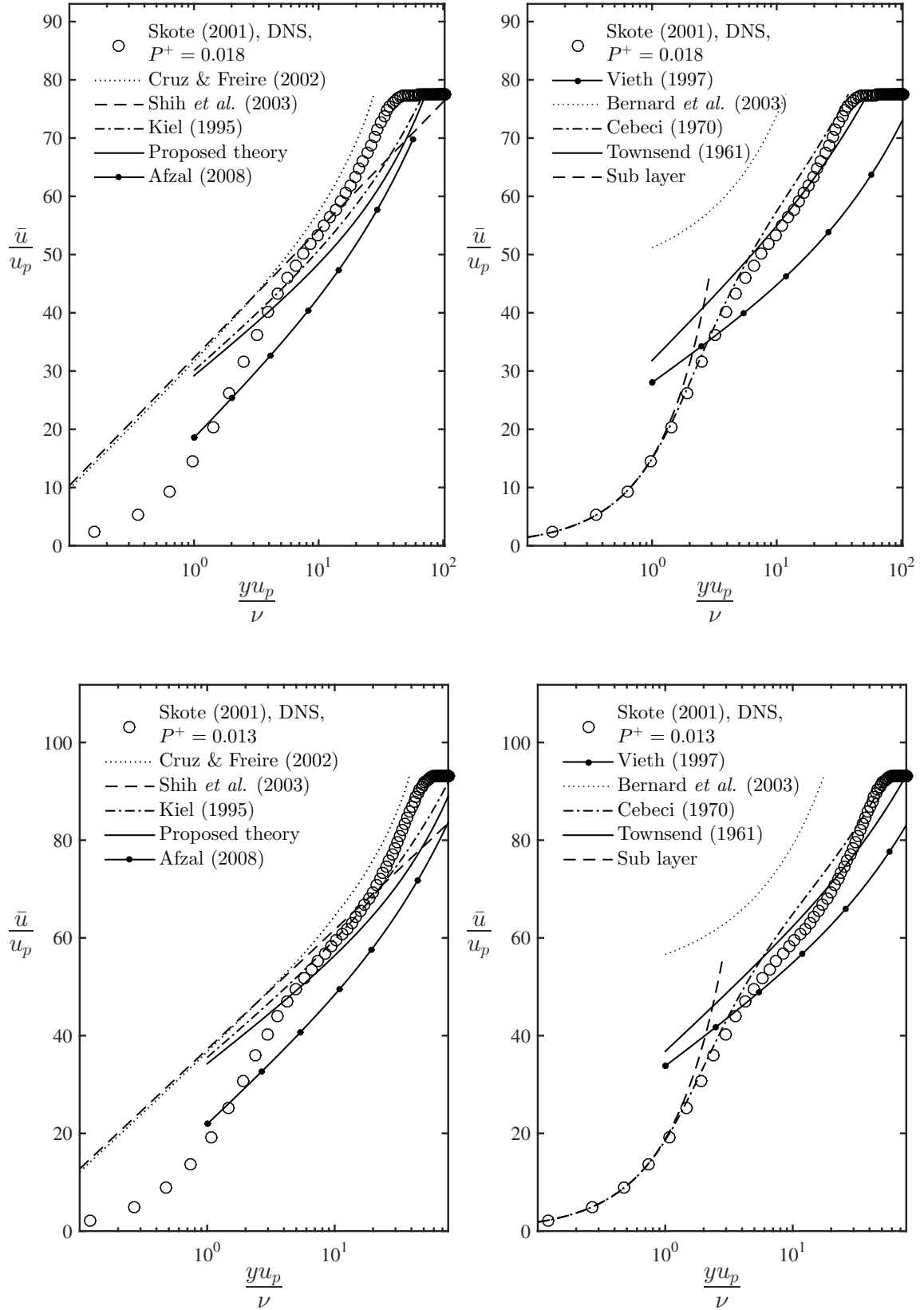


Figure B.113: Mean velocity profiles data compared to different formulations.

High APG boundary layer flow

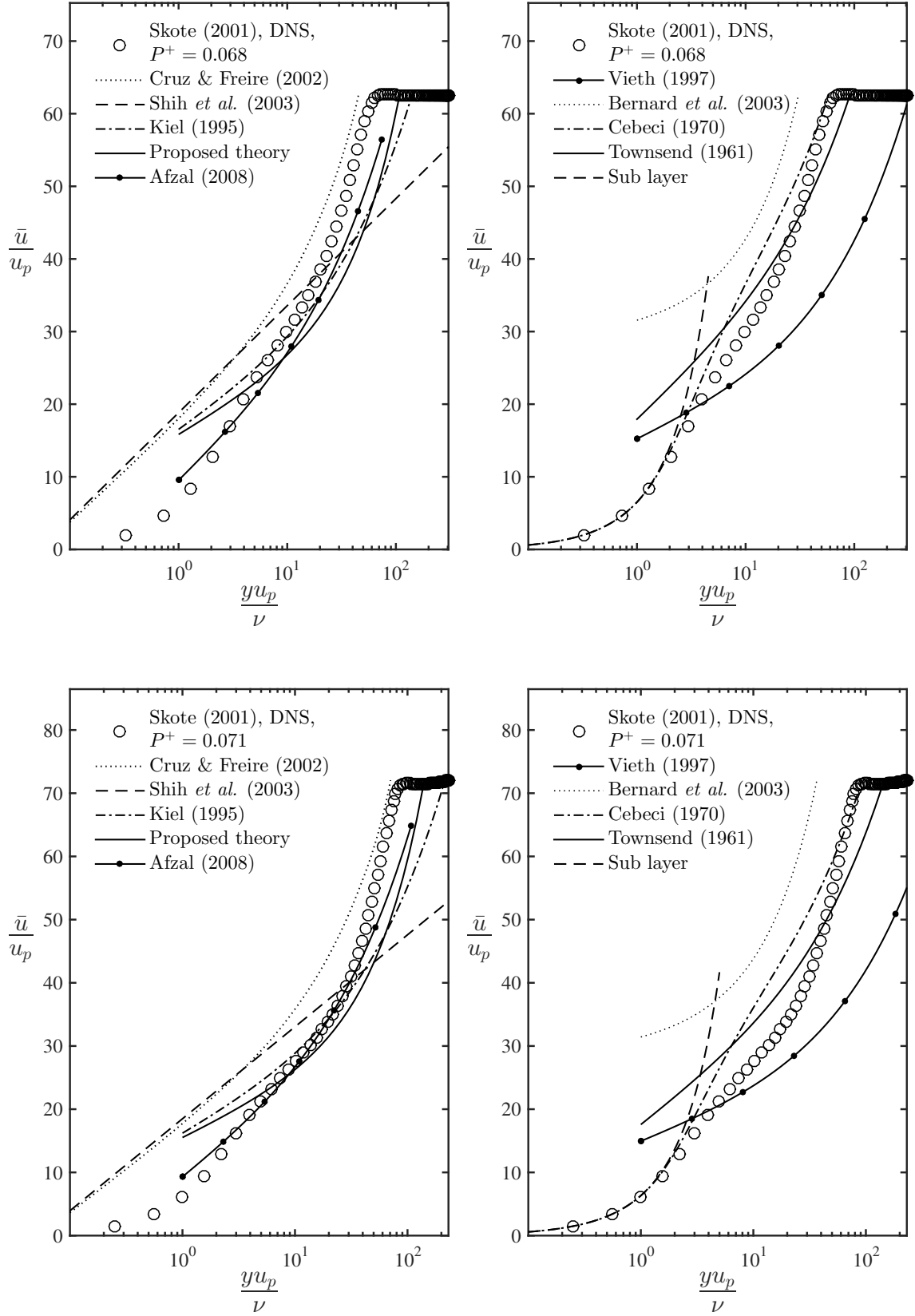


Figure B.114: Mean velocity profiles data compared to different formulations.

High APG boundary layer flow

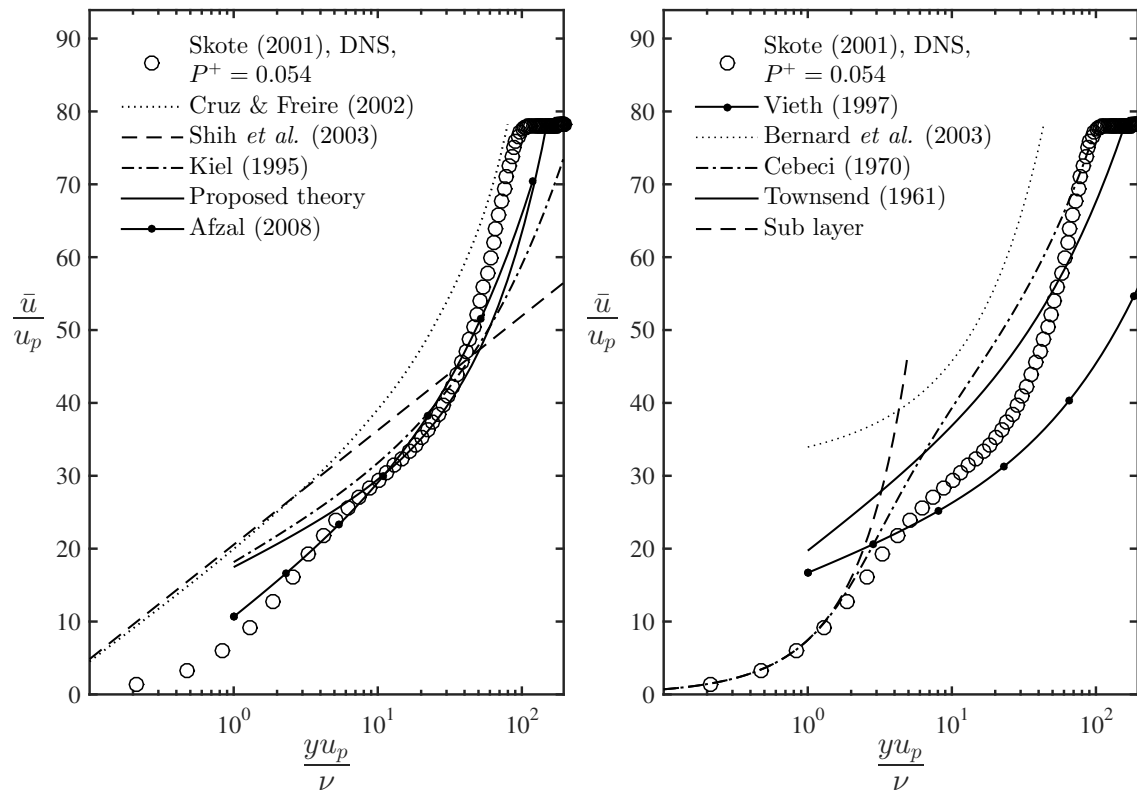


Figure B.115: Mean velocity profiles data compared to different formulations.

Bondary layer flow with separation

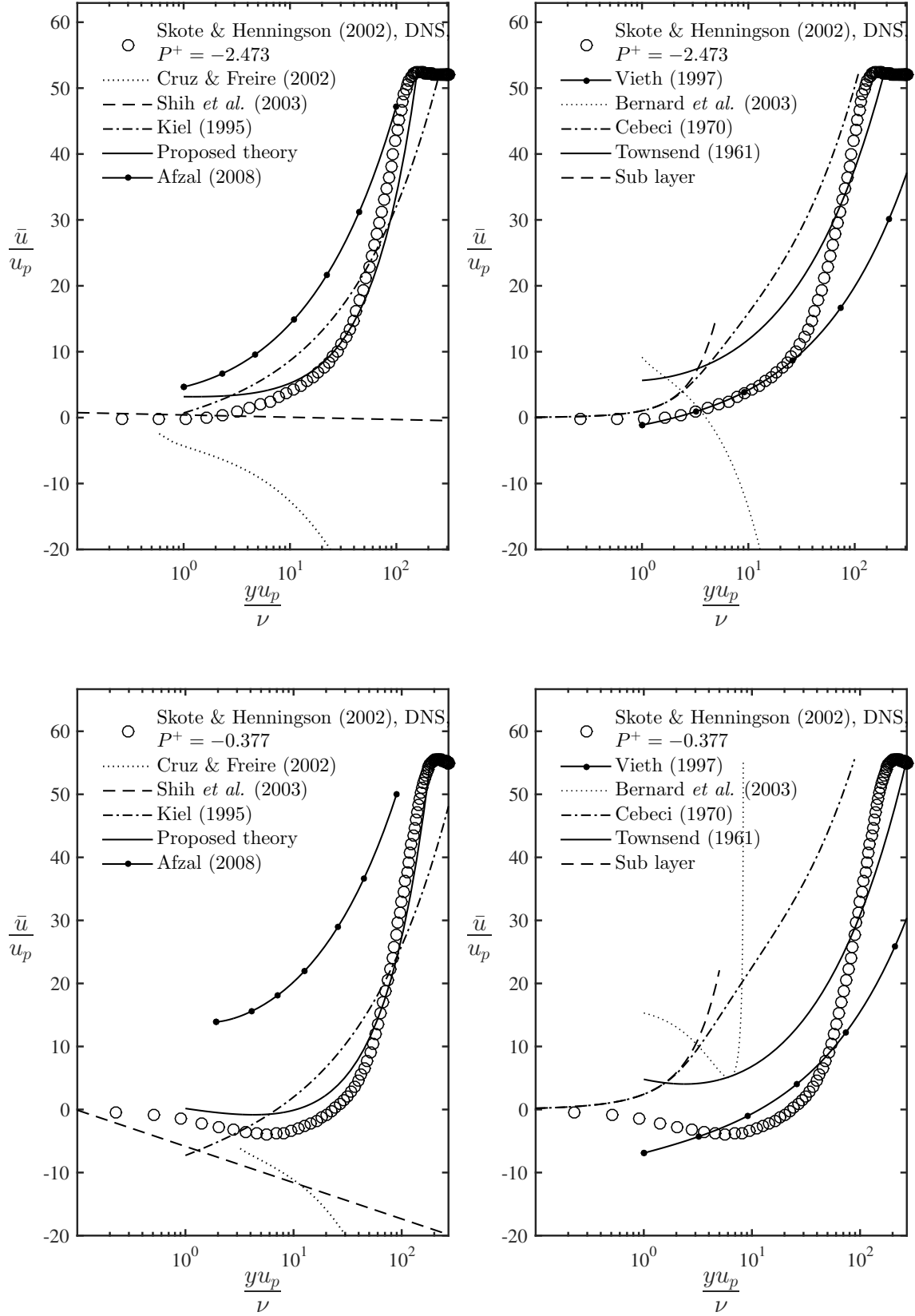


Figure B.116: Mean velocity profiles data compared to different formulations.

Bondary layer flow with separation

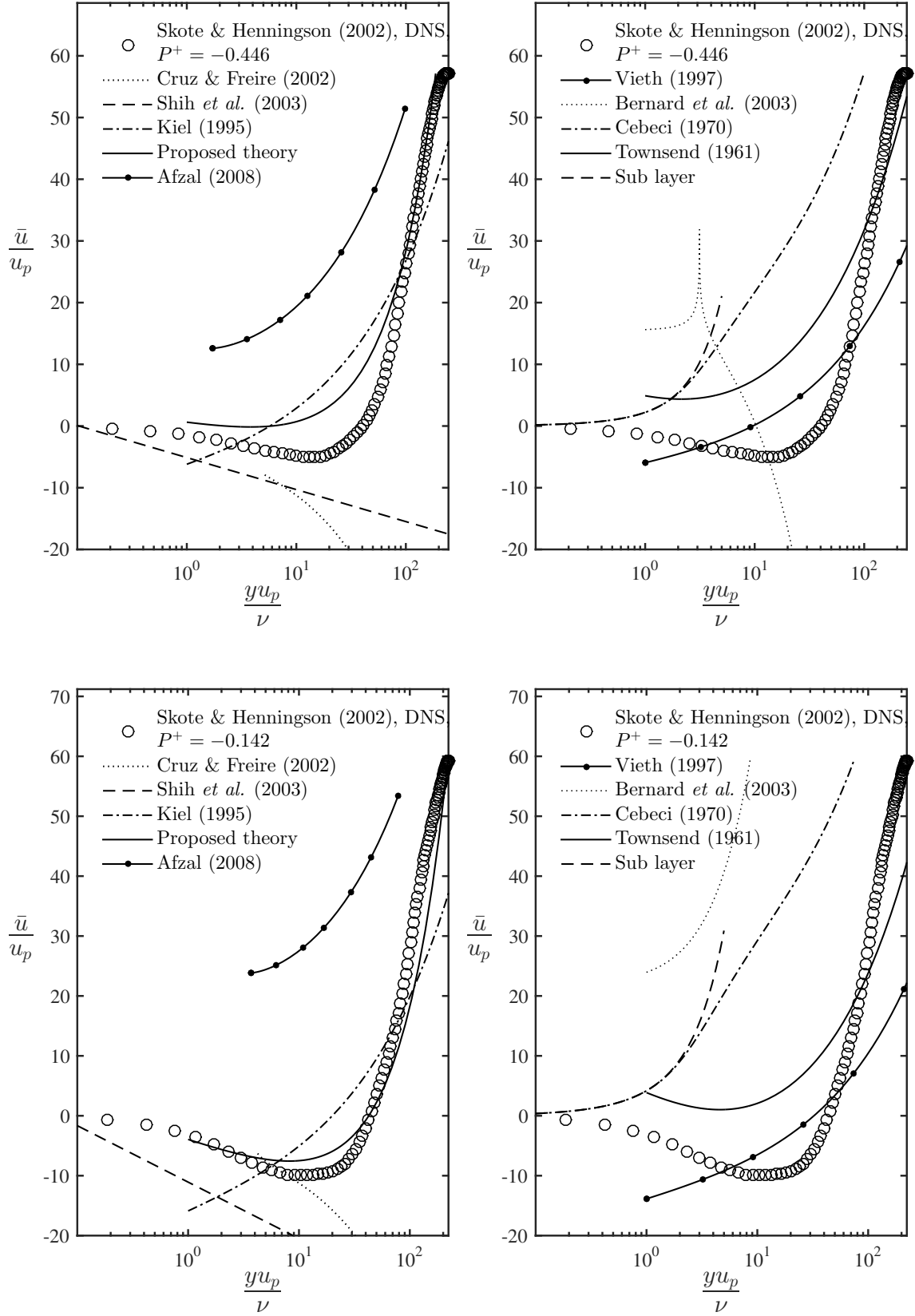


Figure B.117: Mean velocity profiles data compared to different formulations.

Bondary layer flow with separation

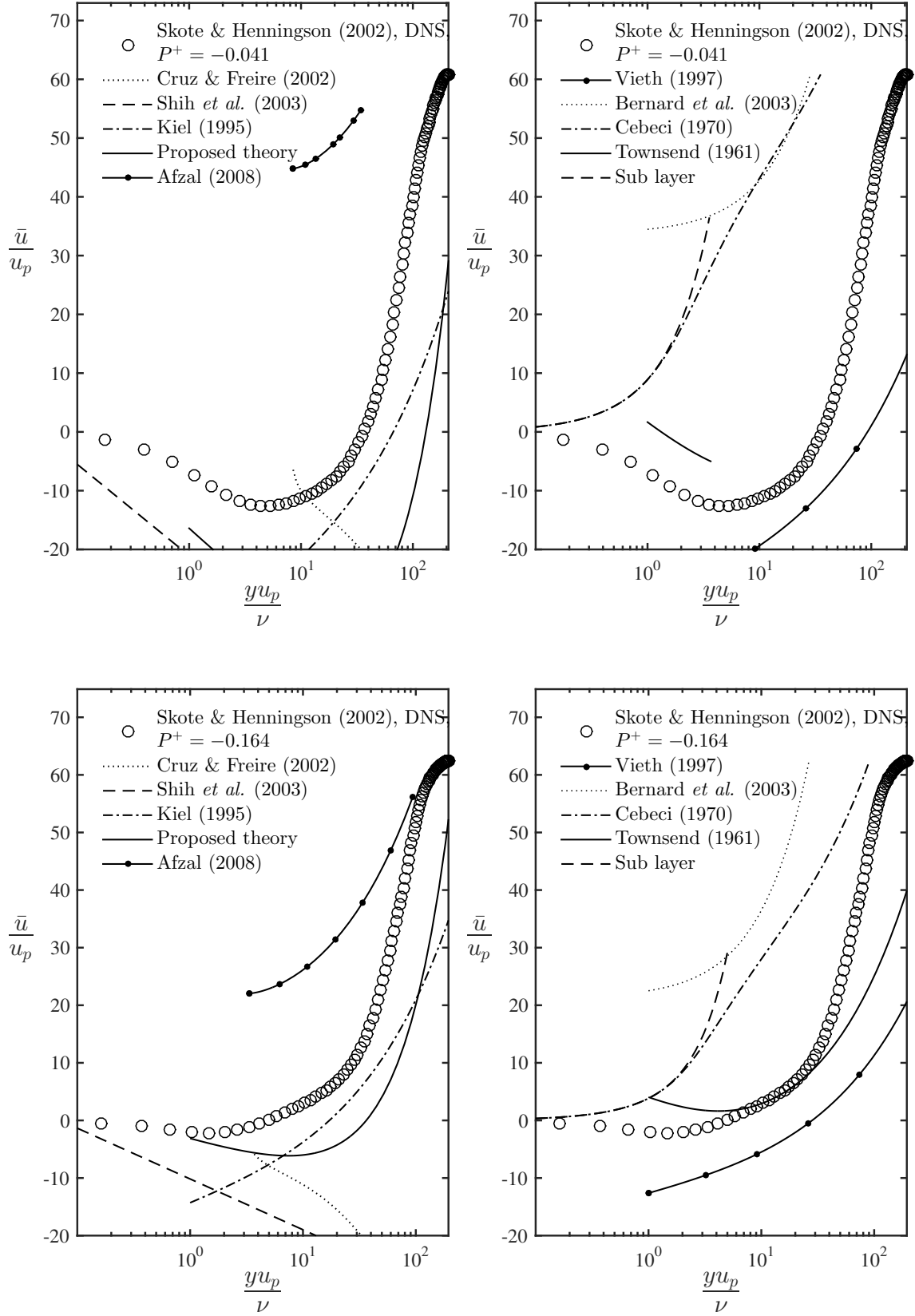


Figure B.118: Mean velocity profiles data compared to different formulations.

Bondary layer flow with separation

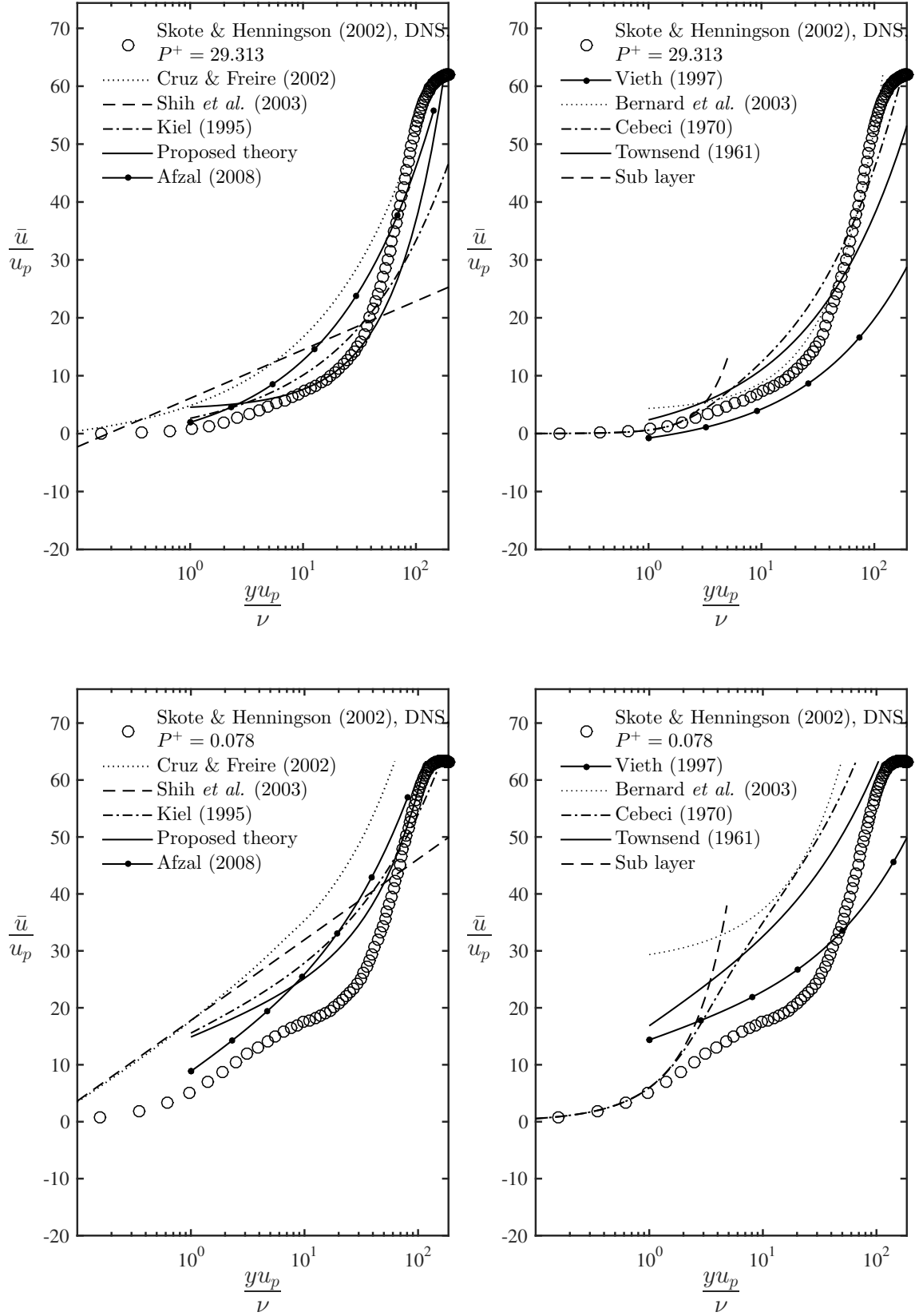


Figure B.119: Mean velocity profiles data compared to different formulations.

Bondary layer flow with separation

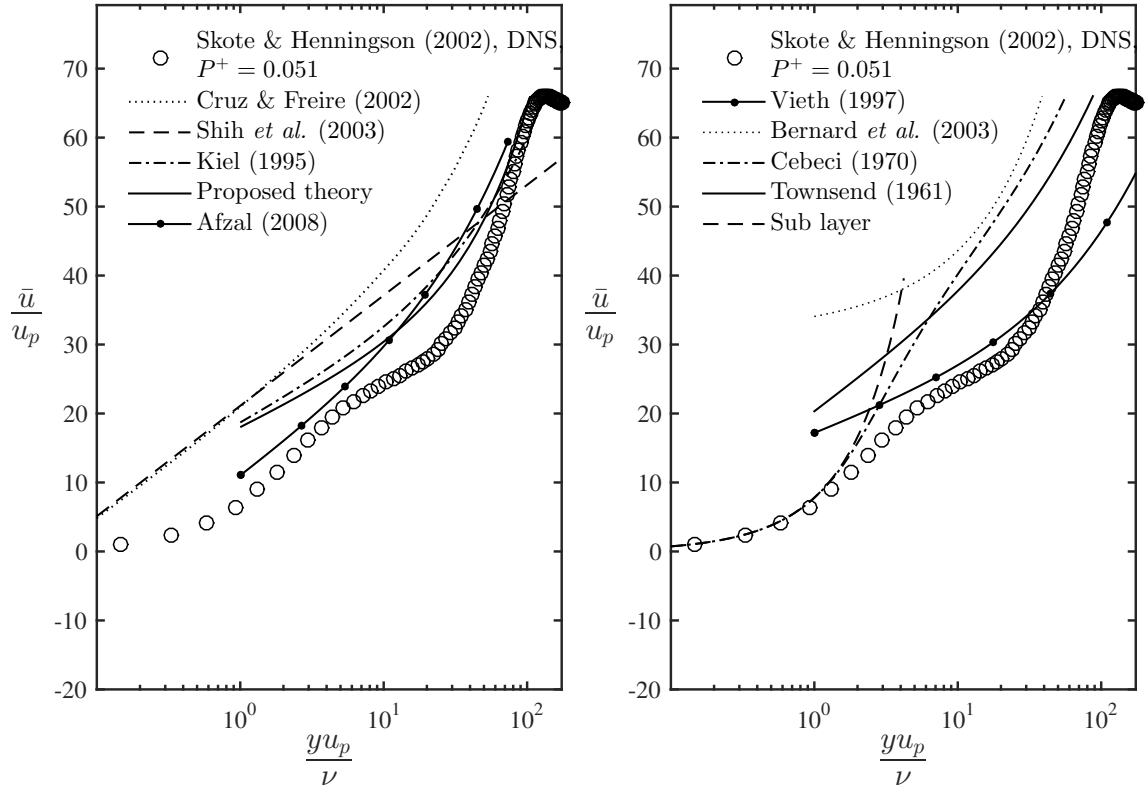


Figure B.120: Mean velocity profiles data compared to different formulations.

Mild APG boundary layer flow

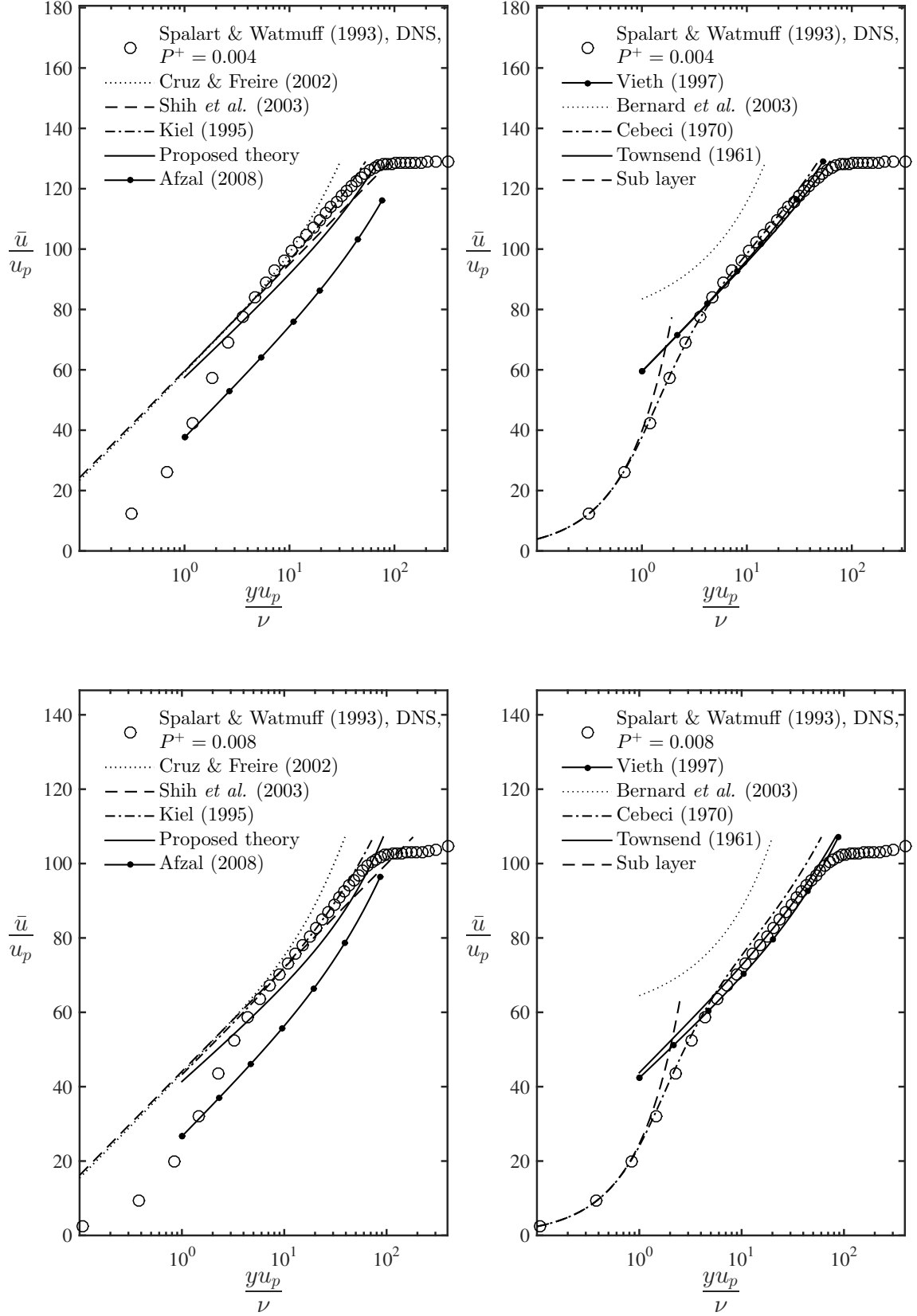


Figure B.121: Mean velocity profiles data compared to different formulations.

Mild APG boundary layer flow

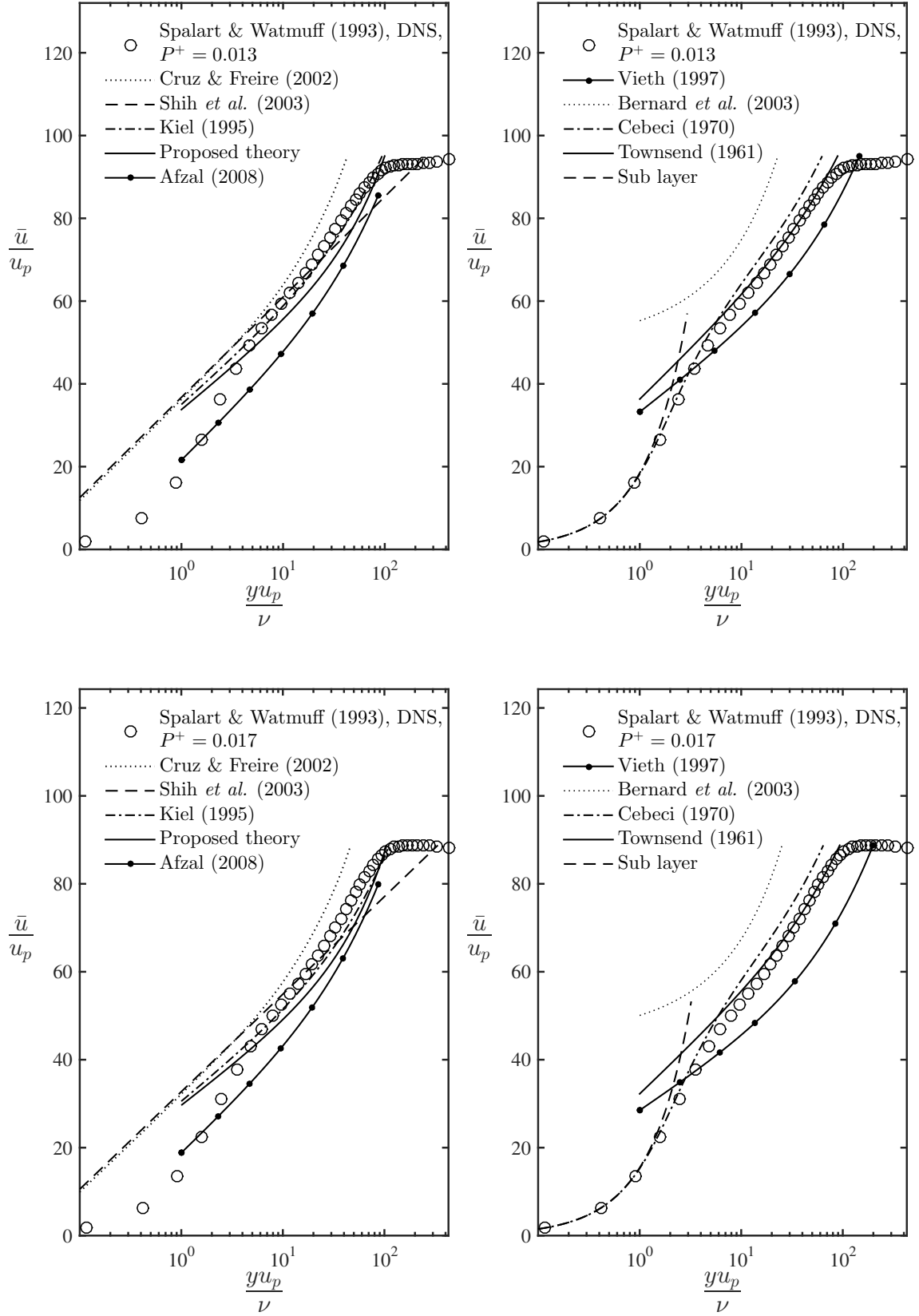


Figure B.122: Mean velocity profiles data compared to different formulations.

Mild APG boundary layer flow

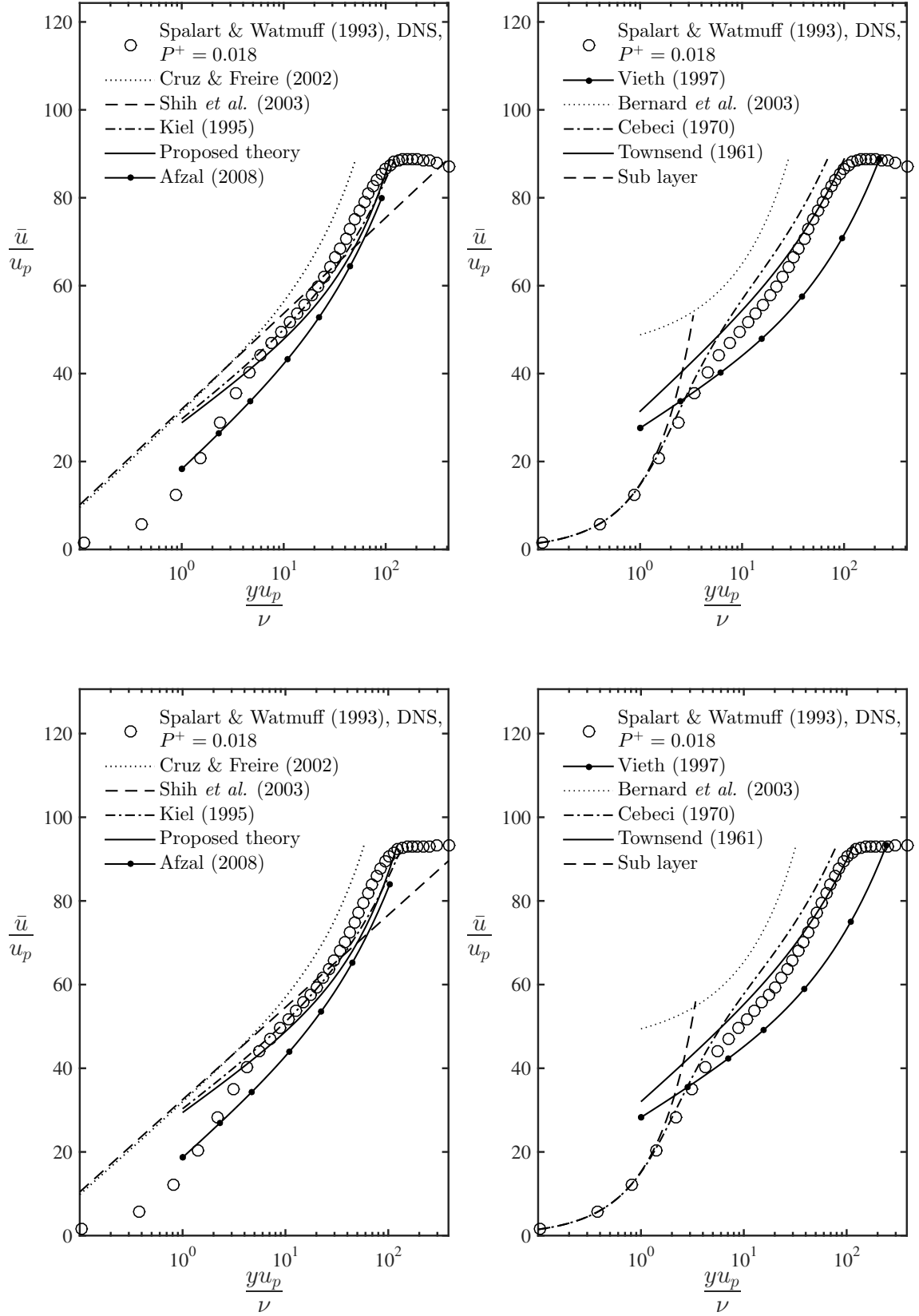


Figure B.123: Mean velocity profiles data compared to different formulations.

Mild APG boundary layer flow

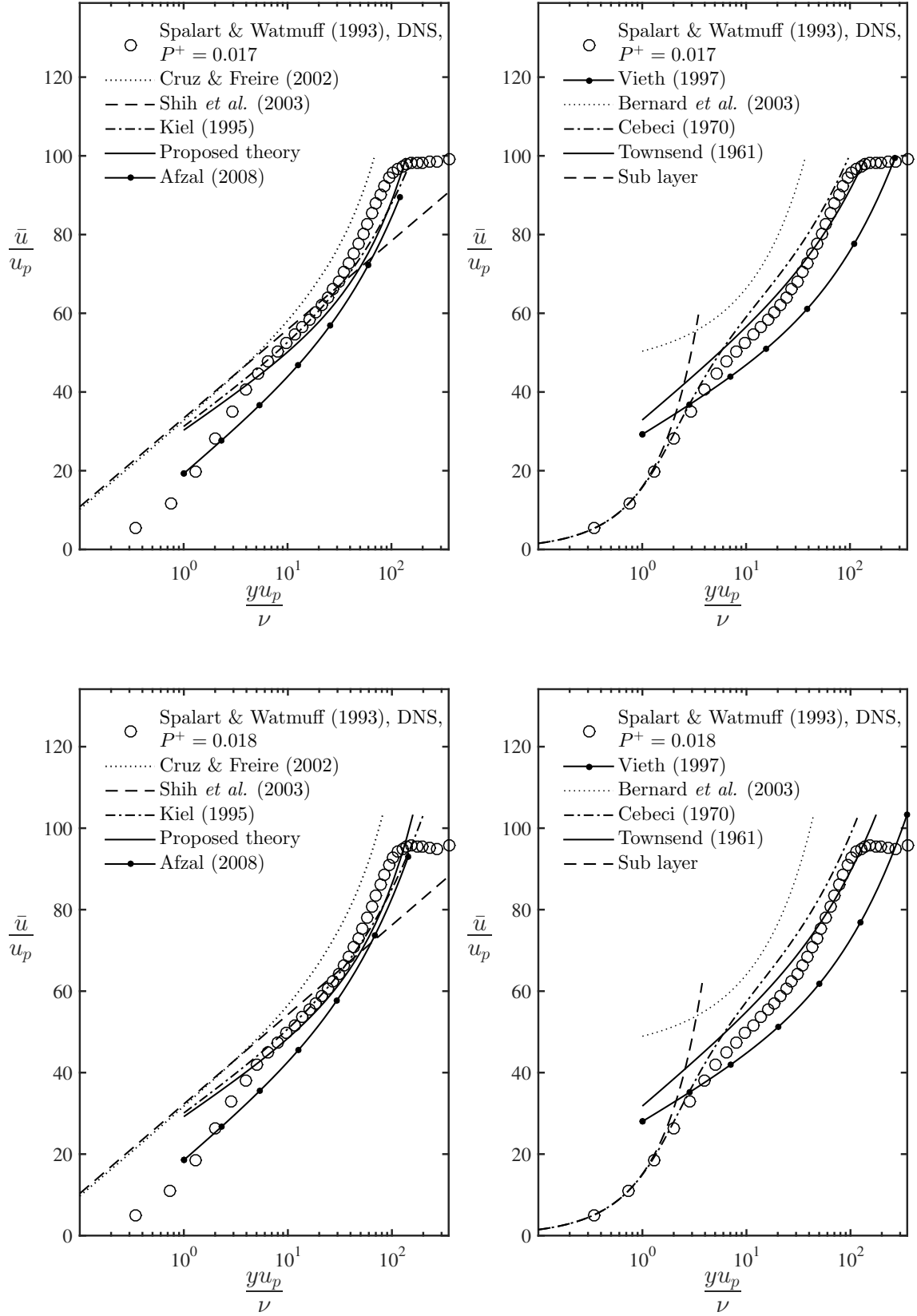


Figure B.124: Mean velocity profiles data compared to different formulations.

Bondary layer flow with separation

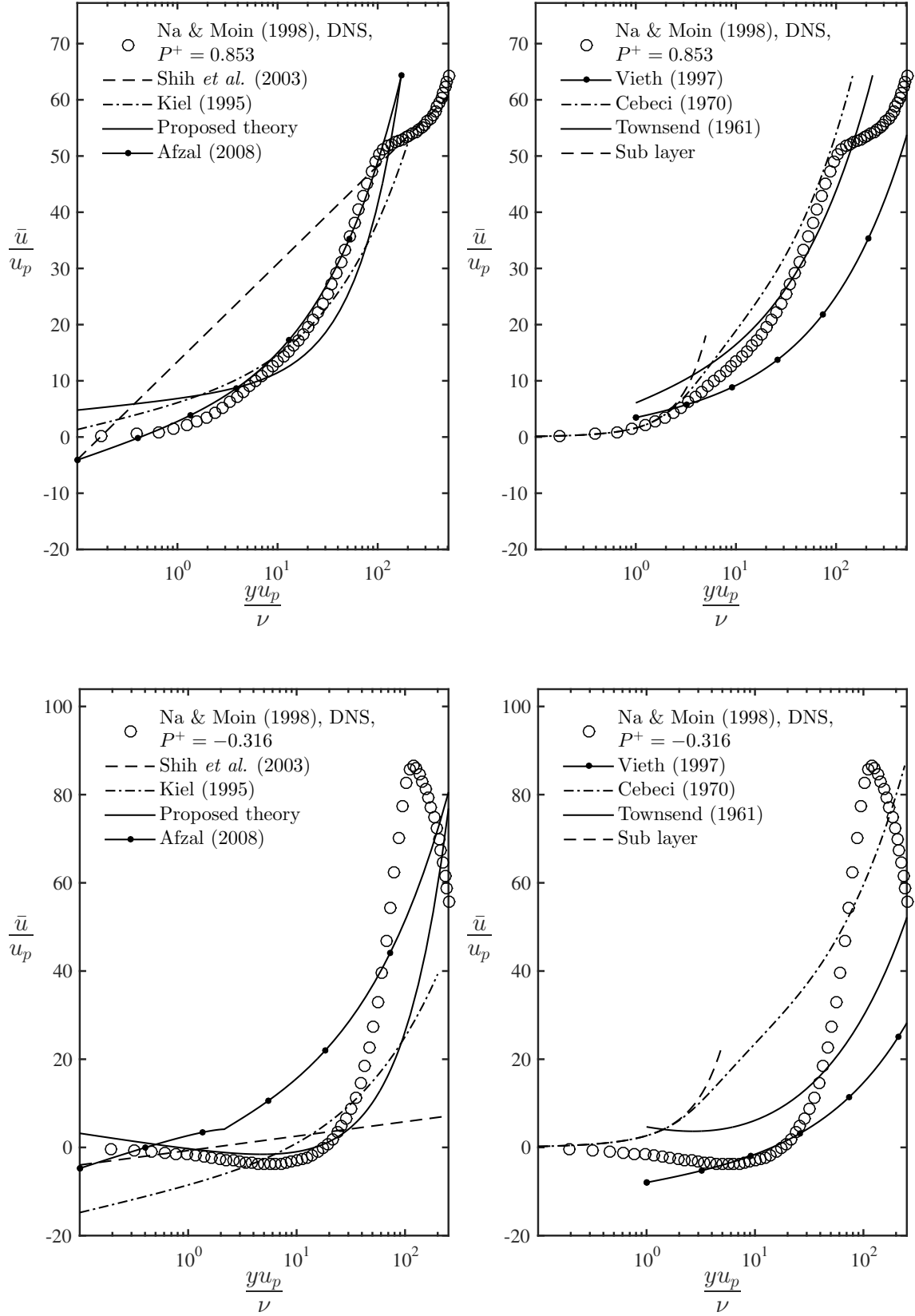


Figure B.125: Mean velocity profiles data compared to different formulations.

Bondary layer flow with separation

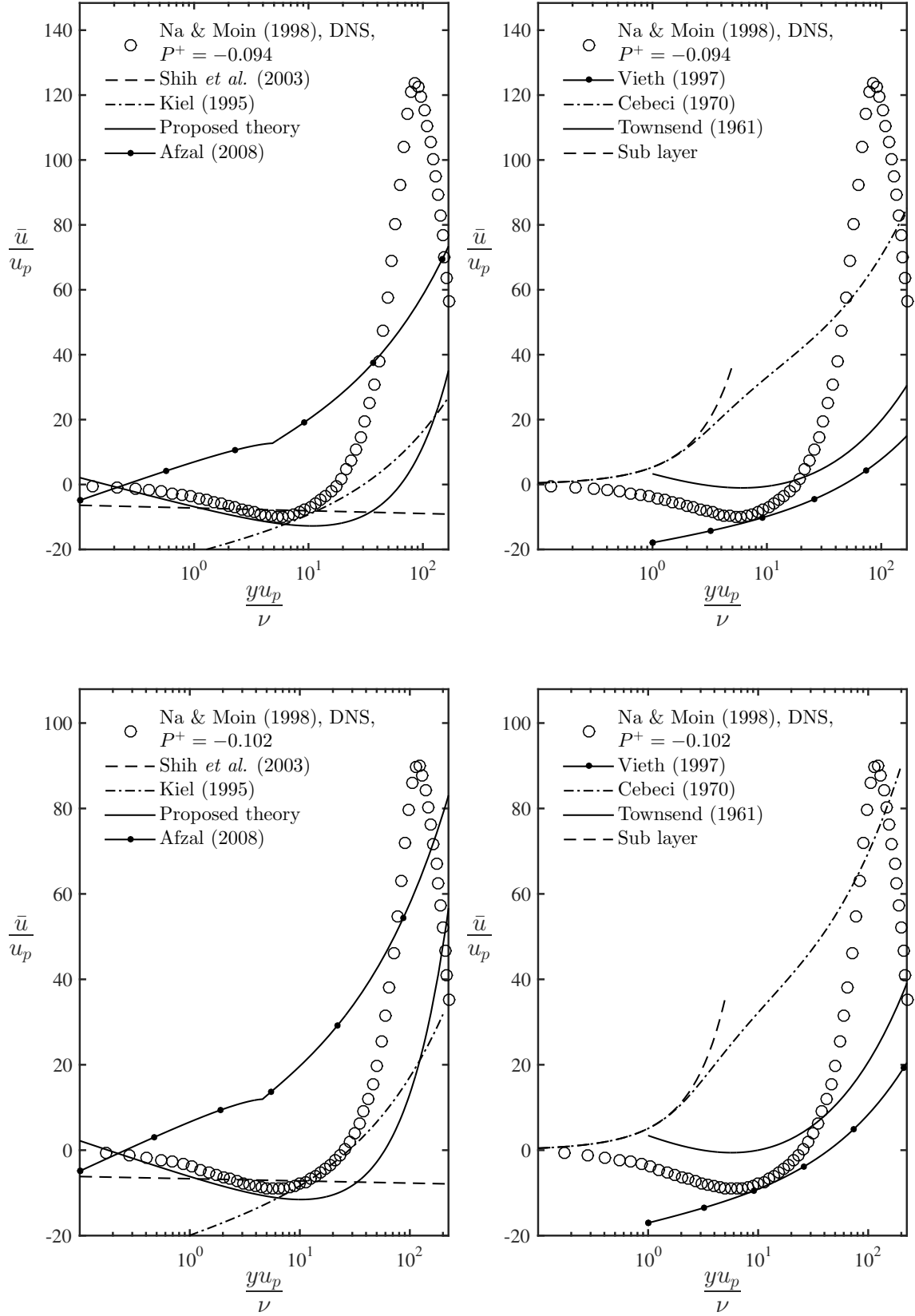


Figure B.126: Mean velocity profiles data compared to different formulations.

Bondary layer flow with separation

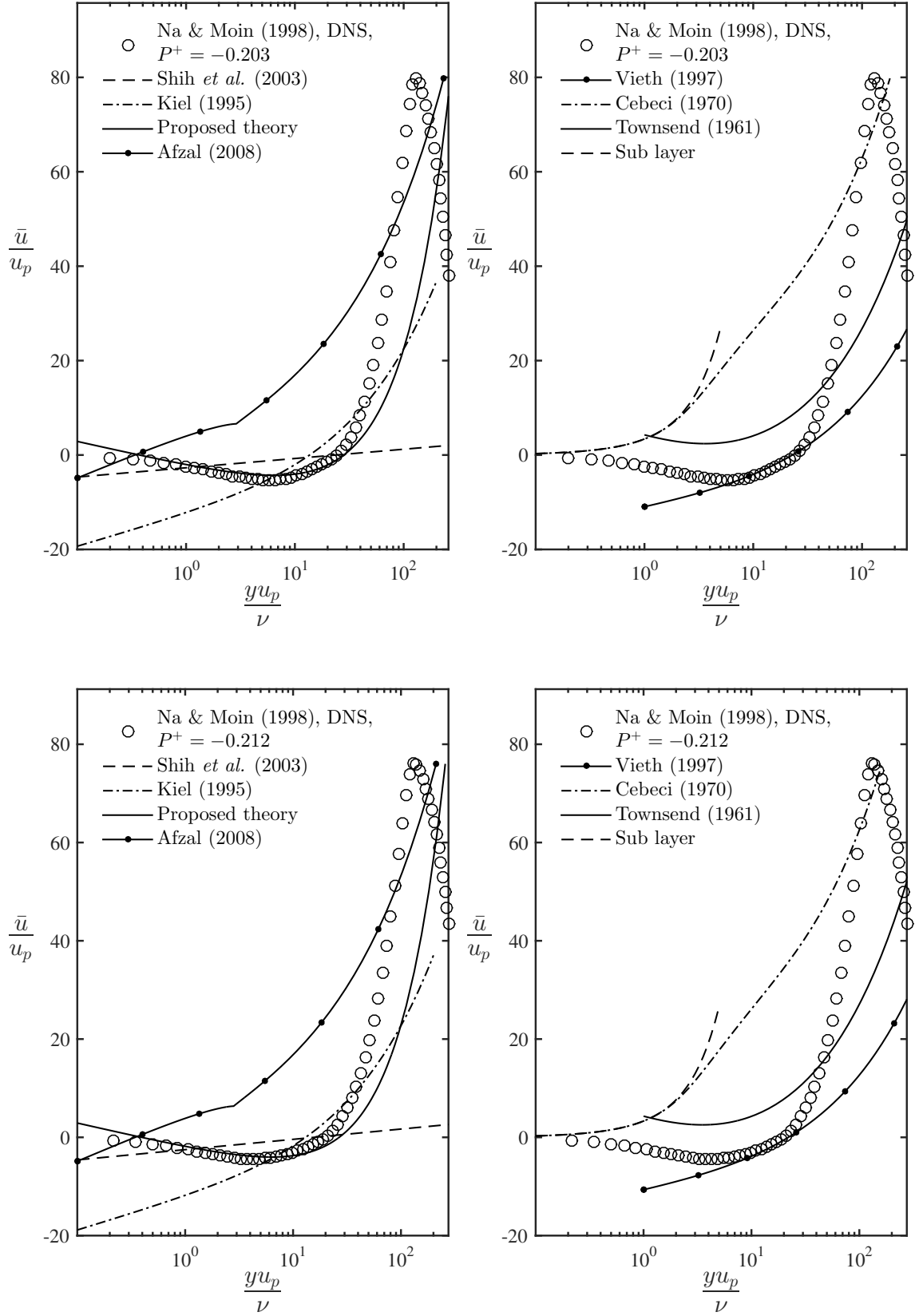


Figure B.127: Mean velocity profiles data compared to different formulations.

Bondary layer flow with separation

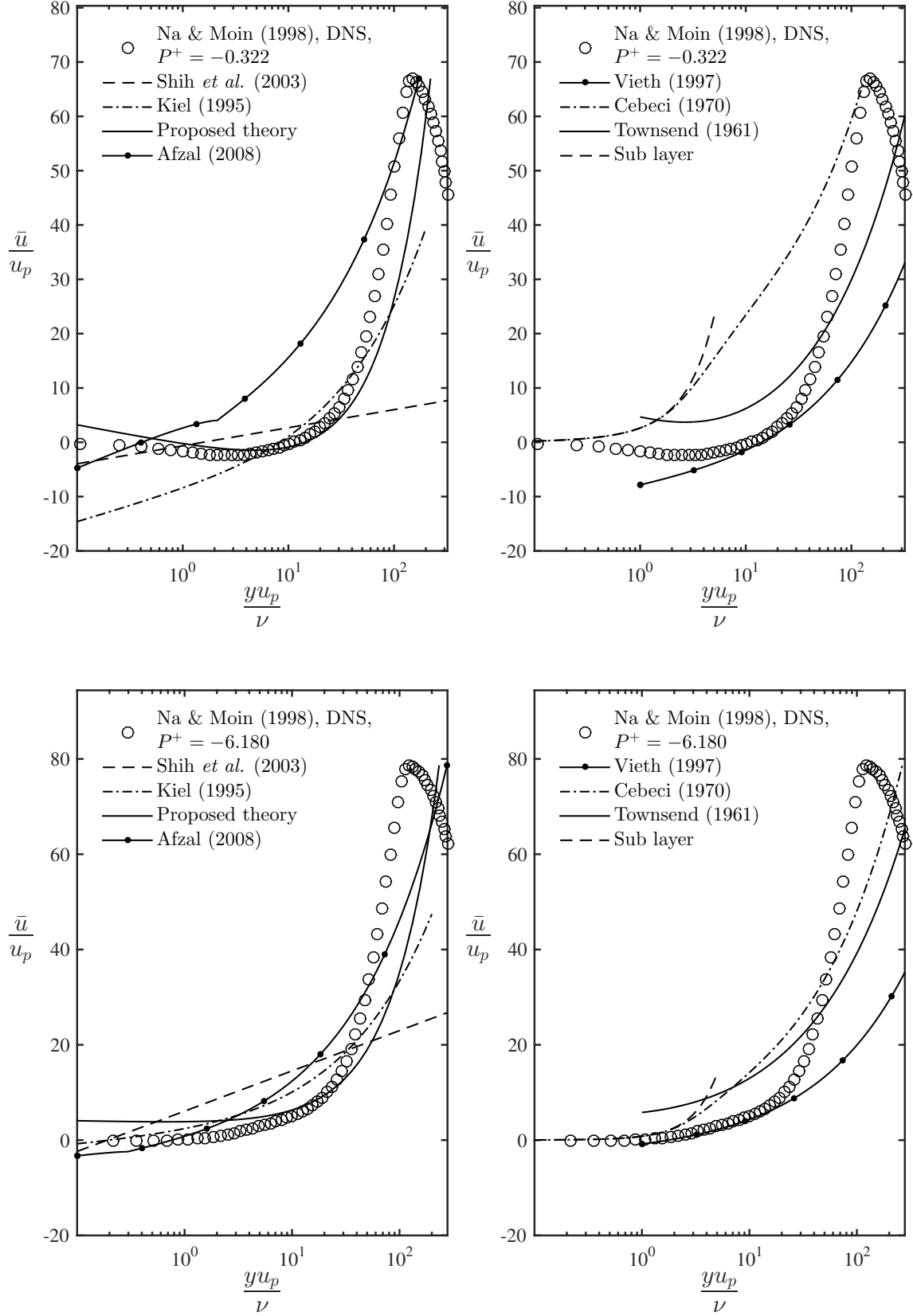


Figure B.128: Mean velocity profiles data compared to different formulations.

Bondary layer flow with separation

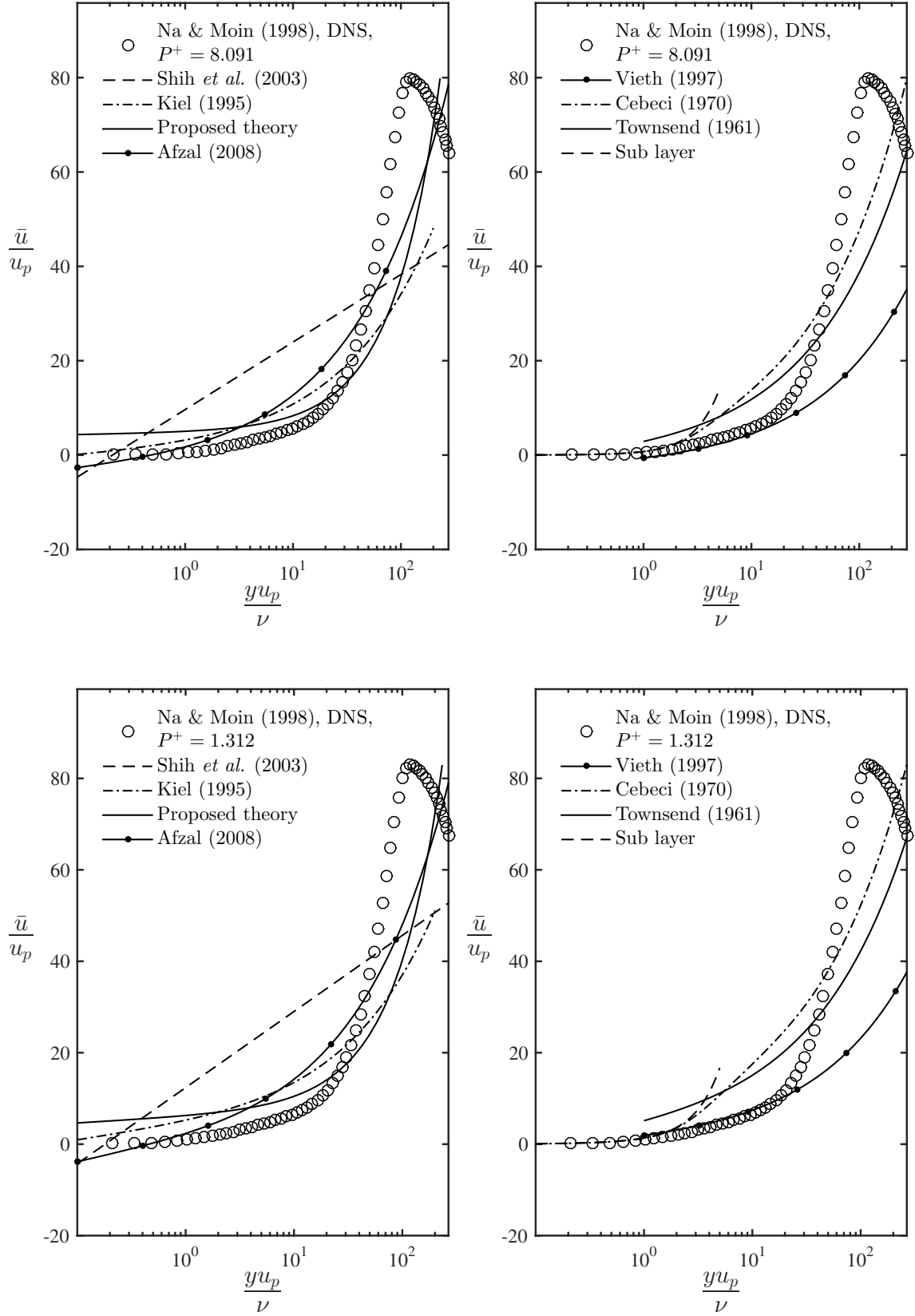


Figure B.129: Mean velocity profiles data compared to different formulations.

Bondary layer flow with separation

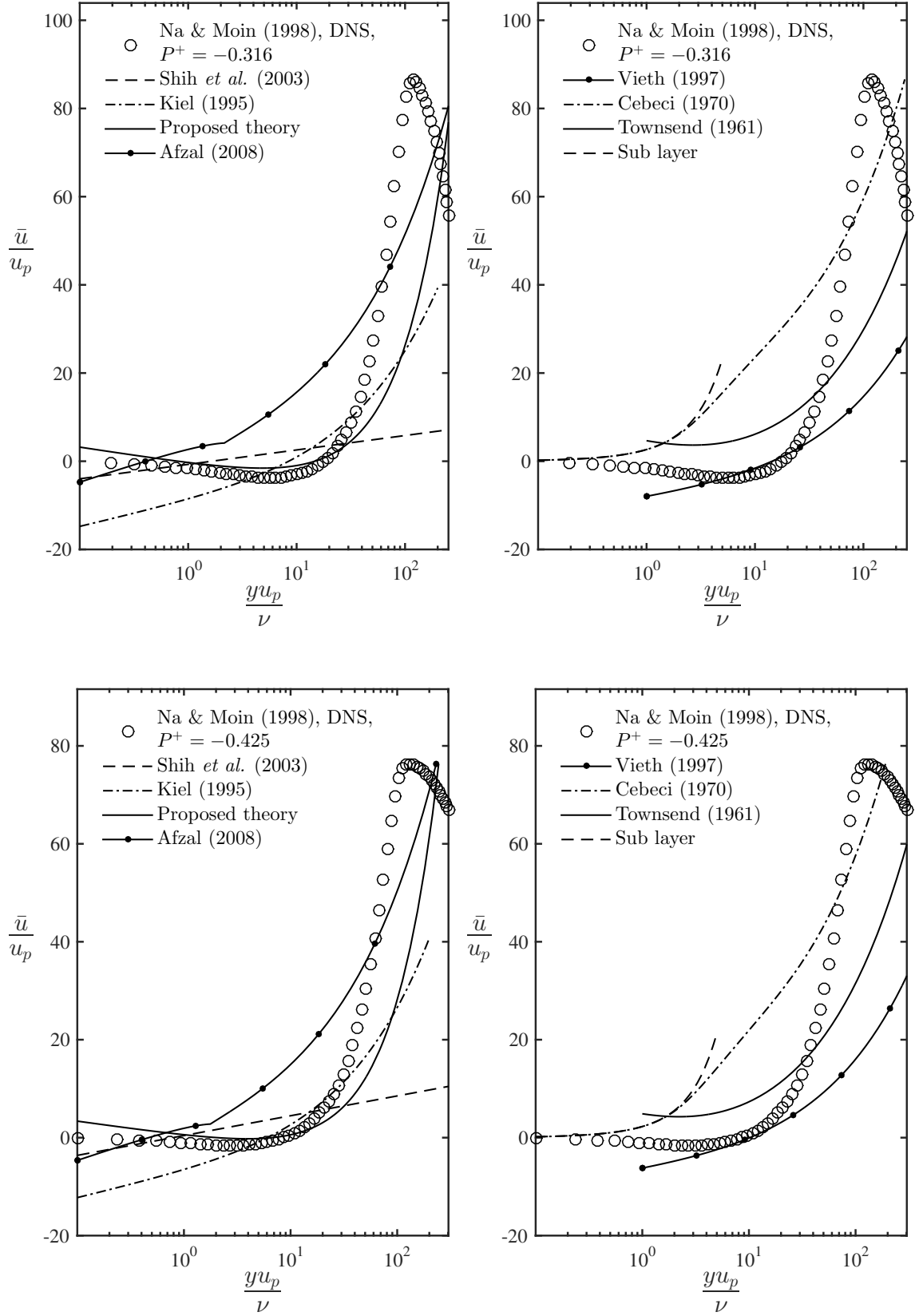


Figure B.130: Mean velocity profiles data compared to different formulations.